

Copyright
by
Faiz Koyassan Veedu
2010

**The Thesis Committee for Faiz Koyassan Veedu
Certifies that this is the approved version of the following thesis:**

Scale-up Methodology for Chemical Flooding

**APPROVED BY
SUPERVISING COMMITTEE:**

Supervisor: _____
Gary A. Pope

Co-Supervisor: _____
Mojdeh Delshad

Scale-up Methodology for Chemical Flooding

by

Faiz Koyassan Veedu, B.E.

Thesis

Presented to the Faculty of the Graduate School of

The University of Texas at Austin

in Partial Fulfillment

of the Requirements

for the Degree of

Master of Science in Engineering

The University of Texas at Austin

December 2010

Dedication

To my parents and my fiancé

Acknowledgements

I am deeply grateful to my supervisors, Dr. Gary A. Pope and Dr. Mojdeh Delshad, for their invaluable guidance. Working under them was a great learning experience.

I would like to thank Dr. Quoc Nguyen, Dr. Sanjay Srinivasan, Dr. Maghsood Abbaszadeh, Dr. Ekwere Peters and Dr. Martin Chenevert for their excellent teaching skills. The courses I learned under them gave a good foundation and insight into various important aspects of petroleum engineering.

I would like to acknowledge the financial support of the UT-Chevron Alliance for EOR provided by Chevron and also the sponsors of the Chemical EOR Industrial Affiliates Program in the Center for Petroleum and Geosystems Engineering at the University of Texas at Austin.

I would like to thank Hourshad Mohammadi, Dr. Do Hoon Kim, Chris Britton, Dr. Chrissi King, Dr. Ali Farhadania, Ahra Lee, Hyun Tae Yang, Heesong Koh, Ester Berrientes and Joanna Castillo who directly or indirectly contributed toward the success of this research.

I would like to thank some of my good friends for their good company during good and bad times- Abhinav Sharma, Vikram Chandrasekar, Nitish Koduru, Vinay Sahni, Raushan Kumar, Syed Furqan Gilani, Naveed Arsalan, Farrukh Hamza, Abdul Khan, Abhishek Kumar, Suleen Bhagat, Lokendra Jain, Sahil Malhotra, Abhishek Goyal and Hariharan Ramachandran.

Abstract

Scale-up Methodology for Chemical Flooding

Faiz Koyassan Veedu. M.S.E.

The University of Texas at Austin, 2010

Supervisor: Gary A. Pope

Co-supervisor: Mojdeh Delshad

Accurate simulation of chemical flooding requires a detailed understanding of numerous complex mechanisms and model parameters where grid size has a substantial impact upon results. In this research we show the effect of grid size on parameters such as phase behavior, interfacial tension, surfactant dilution and salinity gradient for chemical flooding of a very heterogeneous oil reservoir. The effective propagation of the surfactant slug in the reservoir is of paramount importance and the salinity gradient is a key factor in ensuring the process effectiveness. The larger the grid block size, the greater the surfactant dilution, which in turn erroneously reduces the effectiveness of the process indicated with low simulated oil recoveries. We show that the salinity gradient is not adequately captured by coarse grid simulations of heterogeneous reservoirs and this leads to performance predictions with lower recovery compared to fine grid simulations. Due to the highly coupled, nonlinear interactions of the many chemical and physical

processes involved in chemical flooding, it is better to use fine-grid simulations rather than coarse grids with upscaled physical properties whenever feasible. However, the upscaling methodology for chemical flooding presented in this work accounts approximately for some of the more important effects, as demonstrated by comparison of fine grid and coarse grid results and is very different than the way other enhanced oil recovery methods are upscaled. This is a step towards making better performance predictions of chemical flooding for large field projects where it is not currently feasible to perform the large number of simulations required to properly consider different designs, optimization, risk and uncertainty using fine-grid simulations.

Table of Contents

List of Tables	xi
List of Figures	xiii
List of Figures	xiii
Chapter 1: Introduction and Literature Review	1
Description of Reservoir Simulator, UTCHEM	6
Chapter 2: Effect of grid size on chemical flooding simulations	7
2.1 Simulation model	8
2.2 Scale up simulations with chemical formulation A	9
2.2.1 Surfactant data	9
2.2.1.1 Aqueous Stability Test	10
2.2.1.2 Phase Behavior Experiment	10
2.2.2 Polymer data and modeling	11
2.2.3. History match of coreflood M9	11
2.2.4 Field scale simulations using chemical formulation A:	13
2.2.4.1 Water flood simulations	14
2.2.4.2 Alkaline-Surfactant-Polymer (ASP) flood simulations ..	14
2.2.5 Parameters studied for upscaling	16
2.2.5.1 Salinity Gradient	17
Normal Salinity Gradient:	18
2.2.5.2 Surfactant Dilution	19
2.2.5.3 Dispersion	19
2.2.5.4 Critical Micelle Concentration	21
2.2.5.5 Capillary Desaturation Curve	21
2.2.6 Upscaling methodologies	23
2.3 Scale up simulations with chemical formulation B	24
2.3.1 Field scale simulations using chemical formulation B:	25
2.3.1.1 Water flood simulations	26

2.3.1.2 ASP flood simulations	26
2.3.2 Parameters studied for upscaling	27
2.3.2.1 Salinity Gradient	27
2.3.2.2 Surfactant Dilution	28
2.3.2.3 Dispersion	29
2.3.2.4 Critical Micelle Concentration	29
2.3.2.5 Capillary Desaturation Curve	30
2.3.3 Upscaling methodology	30
2.4 Summary	31
Chapter 3: Scale-up of ASP flooding simulations with acidic crude	94
3.1 Introduction	94
3.2 UTCHEM Simplified ASP model	95
3.2.1 Soap Generation	95
3.2.2 Phase behavior in the presence of soap and surfactant	96
3.2.2.1 Effect of soap on salinity window (CSEL and CSEU)...	97
3.2.2.2 Effect of soap on height of binodal curve (HBNC)	97
3.2.3 Alkali consumption	98
3.2.4 Surfactant adsorption at high pH	99
3.3 Phase behavior modeling and coreflood history matching	100
3.4 Field scale simulations of ASP flooding using UTCHEM SASP model	100
3.4.1 Water flood simulations	101
3.4.2 Alkaline-Surfactant-Polymer (ASP) flood simulations	101
3.4.2.1 Effect of dilution on salinity	103
3.4.3 Upscaling methodology	103
3.5 Summary	104
Chapter 4: Conclusions and Recommendations	121
4.1 Conclusions	121
4.2 Recommendations	122

Appendix A: Average layer permeabilities of all the grid block models.....	123
Appendix B: Hand's model for binodal curve	128
Appendix C: Guidelines for Selection of phase behavior parameters for Alkaline/Surfactant/Polymer (ASP) flooding.	132
Phase Behavior.....	132
Phase Behavior data from laboratory	133
Background salinity.....	134
Phase Behavior Match.....	134
1) Phase Behavior Match using UTCHEM in Batch Mode	134
2) Phase Behavior Match using spreadsheet	140
Appendix D: UTCHEM INPUT FILES.....	149
D1: Input file for 43 X 47 X 19 model for the case describe in chapter 2:	149
D2: Input file for 43 X 47 X 19 model for the case describe in chapter 3:	166
D3: Input file for phase behavior match using UTCHEM in batch mode:	185
References.....	192
Vitae.	195

List of Tables

Table 2.1: Grid descriptions.....	33
Table 2.2: Phase behavior parameters for formulation A.....	34
Table 2.3: Core and fluid properties for core flood M9	34
Table 2.4: Brine composition for core flood M9	35
Table 2.5: Residual saturations and endpoint relative permeabilities measured in the laboratory during M9 core flood.....	35
Table 2.6: Injection scheme for the coreflood M9	36
Table 2.7: Residual saturations and endpoint relative permeabilities adjusted to match the coreflood	36
Table 2.8: Polymer parameters used in the coreflood M9 simulation	37
Table 2.9: Microemulsion viscosity parameters used in the coreflood M9 simulation	37
Table 2.10: Adsorption parameters used in the coreflood M9 simulation	37
Table 2.11: Oil recovery after ASP flooding with chemical formulation A.....	38
Table 2.12: Average oil saturation in each layer in 43 X 47 X 19 grid (Average oil recovery from each layer in also shown)	39
Table 2.13: Injection scheme for simulations with a normal salinity gradient	40
Table 2.14: Injection scheme for simulations with a normal salinity gradient	40
Table 2.15: Pseudo CSEL values and recoveries for different grids	41
Table 2.16: Pseudo IFT parameters and recoveries for different grids.....	41
Table 2.17: Core and fluid properties for coreflood with chemical formulation B	42
Table 2.18: Phase behavior parameters for simulations with chemical formulation B	43

Table 2.19: Injection scheme for simulations with chemical formulation B	44
Table 2.20: Oil recovery after ASP flooding simulations with chemical formulation B	45
Table 2.21: Pseudo CSEL values and recoveries for different grids (Formulation B)	45
Table 3.1: Phase behavior parameters used to match the phase behavior data shown in figures 3.1, 3.2 and 3.3	105
Table 3.2: Reservoir core and fluid properties	105
Table 3.3: Brine composition.	106
Table 3.4: Injection scheme for the core flood simulation (Mohammadi, 2008)	106
Table 3.5: Input parameters used for core flood simulation	107
Table 3.6: Grid descriptions.....	108
Table 3.7: Input parameters for included to model simplified ASP flooding described in section 3.2	109
Table A1: Average permeability of all the layers of 43 X 47 X 19 grid.	123
Table A2: Average permeability of all layers of 22 X 24 X 19 grid.....	124
Table A3: Average permeability of all the layers of 11 X 12 X 19 grid.	125
Table A4: Average permeability of all the layers of 43 X 47 X 10 grid.	126
Table A5: Average permeability of all the layers of 43 X 47 X 5 grid.....	126
Table A6: Average permeability of all the layers of 22 X 24 X 10 grid.	127
Table C1: Phase behavior parameters used to match the phase behavior data shown in figure C3.....	141

List of Figures

Figure 2.1: Areal view of 11 X 12 X 19 grid.....	46
Figure 2.2: Areal view of 22 X 24 X 19 grid.....	47
Figure 2.3: Areal view of 43 X 47 X 19 grid.....	48
Figure 2.4: 3-D view of the reservoir showing the depth from the surface, ft	49
Figure 2.5: Areal view of 43 X 47 X 19 grid showing the cross sectional plane used for Figure 2.6	50
Figure 2.6: Permeability field of 43 X 47 X 19 grid (cross section), md	51
Figure 2.7: Permeability field of 22 X 24 X 19 grid (cross section), md	52
Figure 2.8: Permeability field of 11 X 12 X 19 grid (cross section), md	53
Figure 2.9: Porosity distribution of 43 X 47 X 19 grid (cross section).....	54
Figure 2.10: Initial oil saturation in layer 19 of 43 X 47 X 19 (inactive area around the model shown).....	55
Figure 2.11: Comparison of model with experimental solubilization ratio data ...	56
Figure 2.12: Comparison of lab data of salinity dependence on polymer viscosity with UTCHEM model	56
Figure 2.13: Comparison of model with experimental polymer viscosity as a function of polymer concentration	57
Figure 2.14: Comparison of model with experimental polymer viscosity data.....	57
Figure 2.15: Cumulative oil recovery measured from the coreflood M9.	58
Figure 2.16: Capillary desaturation curve for coreflood M9 simulation	58
Figure 2.17: Oil-Water relative permeability curves for the reservoir rock used in coreflood M9.....	59

Figure 2.18: Fractional flow plot for water and ASP coreflood M9 neglecting adsorption.....	59
Figure 2.19: Surfactant adsorption value measured in the coreflood M9 matched Langmuir type adsorption model in UTCHEM.	60
Figure 2.20: Polymer adsorption using Langmuir type adsorption model in UTCHEM.	60
Figure 2.21: Oil recovery match of coreflood M9 using UTCHEM.	61
Figure 2.22: Match of pressure drop from coreflood M9 experiment using UTCHEM.	61
Figure 2.23: Cumulative oil recovery for all the models during Waterflooding...	62
Figure 2.24: Average reservoir pressure for all the models during water flooding	62
Figure 2.25: Change in average oil saturation of all the models during waterflooding	63
Figure 2.26: Cumulative oil recovery in terms of percentage remaining oil in place (% ROIP) for ASP flood simulations for all the grid block models.	64
Figure 2.27: Cumulative oil recovery in terms of percentage original oil in place (% OOIP) for ASP flood simulations for all the grid block models.	65
Figure 2.28: Oil rate for ASP flood simulations of grids with areal coarsening. ..	66
Figure 2.29: Oil rate for ASP flood simulations of grids with vertical coarsening.	66
Figure 2.30: Surfactant concentration of 43 X 47 X 19 grid after 0.1 PV, volume fraction	67
Figure 2.31: Surfactant concentration of 43 X 47 X 19 grid after 0.5 PV, volume fraction	67
Figure 2.32: Surfactant concentration of 43 X 47 X 19 grid after 2.3 PV, volume fraction	67

Figure 2.33: Polymer concentration of 43 X 47 X 19 grid after 0.1 PV, % weight	68
Figure 2.34: Polymer concentration of 43 X 47 X 19 grid after 0.5 PV, % weight	68
Figure 2.35: Polymer concentration of 43 X 47 X 19 grid after 2.3 PV, % weight	68
Figure 2.36: Oil saturation of 43 X 47 X 19 grid after 0.1 PV, volume fraction ..	69
Figure 2.37: Oil saturation of 43 X 47 X 19 grid after 0.5 PV, volume fraction ..	69
Figure 2.38: Oil saturation of 43 X 47 X 19 grid after 2.3 PV, volume fraction ..	69
Figure 2.39: Surfactant concentration profile for layer 19 of 43 X 47 X 19 grid after 0.1 PV ASP slug injection, volume fraction.	70
Figure 2.40: Profile for layer 19 of the 43 X 47 X 19 grid after 0.1 PV	71
Figure 2.41: Profile for layer 19 of the 43 X 47 X 19 grid after 0.4 PV	71
Figure 2.42: Profile for layer 19 of the 43 X 47 X 19 grid after 1 PV	72
Figure 2.43: Salinity profile comparison (after 0.1 PV) for layer 19 of 11 X 12 X 19 and 43 X 47 X 19 grids	72
Figure 2.44: Salinity profile comparison (after 0.5 PV) for layer 19 of 11 X 12 X 19 and 43 X 47 X 19 grids	73
Figure 2.45: Cumulative oil recovery (% ROIP) for ASP flood simulations with a normal salinity gradient.....	74
Figure 2.46: Profile for layer 19 of the 43 X 47 X 19 grid after 0.2 PV	75
Figure 2.47: Profile for layer 19 of the 43 X 47 X 19 grid after 0.4 PV	75
Figure 2.48: Comparison of salinity and surfactant concentration profiles for layer 19 of 43 X 47 X 19 and 11 X 12 X 19 grids after 0.4 PV	76
Figure 2.49: Surfactant concentration in injection grid block after 0.1 PV for one of the injectors using the 11 X 12 X 19 and 43 X 47 X 19 grids	77
Figure 2.50: Sensitivity of physical dispersion on oil recovery of 11 X 12 X 19 grid.	78

Figure 2.51: Oil capillary desaturation curves for three values of trapping parameter	78
Figure 2.52: Sensitivity of capillary desaturation parameter on oil recovery for 11 X 12 X 19 grid	79
Figure 2.53: Salinity profile comparison (0.5 PV) of coarse grid with the fine grid showing the change in CSEL.....	80
Figure 2.54: Oil recovery with CSEL adjusted for coarser grids.	81
Figure 2.55: Interfacial tension between oil and microemulsion for each grid	82
Figure 2.56: Oil recovery with IFT parameters adjusted for coarser grids.....	83
Figure 2.57: Phase behavior data and the match using UTCHEM (Dwarakanath et al., 2008).....	84
Figure 2.58: History match of core flood results using UTCHEM (Dwarakanath et al. 2008).....	84
Figure 2.59: Sensitivity of grid block numbers to oil recovery.	85
Figure 2.60: Cumulative oil recovery in terms of percentage original oil in place (% OOIP) for ASP flood simulations with chemical formulation B for all the grid block models.	85
Figure 2.61: Cumulative oil recovery in terms of percentage remaining oil in place (% ROIP) for ASP flood simulations with chemical formulation B for all the grid block models.	86
Figure 2.62: Profile for layer 19 of the 43 X 47 X 19 grid after 0.1 PV (simulation with formulation B).	87
Figure 2.63: Profile for layer 19 of the 43 X 47 X 19 grid after 0.3 PV (simulation with formulation B).	87

Figure 2.64: Salinity profile comparison of layer 19 of 11 X 12 X 19 and 43 X 47 X 19 grids after 0.1 PV injection (simulation with formulation B).....	88
Figure 2.65: Salinity profile comparison of layer 19 of 11 X 12 X 19 and 43 X 47 X 19 grids after 0.3 PV injection (simulation with formulation B).....	88
Figure 2.66: Salinity profile comparison of layer 19 of 11 X 12 X 19 and 43 X 47 X 19 grids after 0.7 PV injection (simulation with formulation B).....	89
Figure 2.67: Surfactant concentration in injection grid block of one of the injectors of 11 X 12 X 19 and 43 X 47 X 19 grids after 0.1 PV injection (simulation with formulation B).	90
Figure 2.68: Sensitivity of physical dispersion on oil recovery of 11 X 12 X 19 grid (simulation with formulation B).	91
Figure 2.69: Sensitivity of capillary desaturation parameter on oil recovery for 11 X 12 X 19 grid (simulation with formulation B).	91
Figure 2.70: Salinity profile comparison (0.1 PV) of coarse grid with the fine grid showing the change in CSEL.....	92
Figure 2.71: Oil recovery with CSEL adjusted for coarser grids (simulations with formulation B).....	93
Figure 3.1: Phase behavior match for 50 % oil concentration (Mohammadi, 2008)	110
Figure 3.2: Phase behavior match for 30 % oil concentration (Mohammadi, 2008)	110
Figure 3.3: Activity map match, lines are the limits of Winsor's type III calculated from UTCHEM (Mohammadi, 2008)	111
Figure 3.4: Core flood match of the laboratory data with UTCHEM with simplified ASP (SASP) model.....	112
Figure 3.5: Cumulative oil recovery during water flooding for all the models ...	113
Figure 3.6: Average oil saturation during water flooding for all the models	113

Figure 3.7: Cumulative oil recovery in terms of % remaining oil in place (% ROIP) for ASP flood simulations.....	114
Figure 3.8: Cumulative oil recovery in terms of % original oil in place (% OOIP) for ASP flood simulations.....	115
Figure 3.9: Profile for layer 19 of the 43 X 47 X 19 grid after 0.1 PV	116
Figure 3.10: Profile for layer 19 of the 43 X 47 X 19 grid after 0.2 PV injection	116
Figure 3.11: Profile for layer 19 of the 11 X 12 X 19 grid after 0.1 PV injection	117
Figure 3.12: Salinity profile comparison for layer 19 of 11 X 12 X 19 and 43 X 47 X 19 grid after 0.1 PV injection.....	117
Figure 3.13: Salinity profile comparison for 11 X 12 X 19 and 43 X 47 X 19 after 0.1 PV along with the type III window for both the models.....	118
Figure 3.14: Profile for layer 19 of the 11 X 12 X 19 model after 0.2 PV injection	119
Figure 3.15: Cumulative oil recovery in terms of % original oil in place (% OOIP) for ASP flood simulations with salinity window (soap) adjusted for coarser models.	120
Figure B1: Ternary diagrams for surfactant-water-oil mixture at different salinities	131
Figure C1: The effect of salinity on microemulsion phase behavior. Winsor type regions are also marked.....	142
Figure C2: Phase behavior laboratory data	143
Figure C3: Data which are entered in the injection details of the input file to match the laboratory phase behavior data	143
Figure C4: Phase behavior match with laboratory data using UTCHEM in batch mode	144

Figure C5: Input parameters entered in the spreadsheet to match the phase behavior data 145

Figure C6: A screen shot of the spreadsheet which was developed to match the phase behavior data. The picture shows the input salinity values and solubilization ratios from lab and also from the spreadsheet..... 146

Figure C7: Phase behavior match with laboratory data using the spreadsheet developed 147

Figure C8: Phase behavior match with laboratory data using UTCHEM in batch mode as well as spreadsheet developed..... 148

Chapter 1: Introduction and Literature Review

Geological models with more than one million gridblocks are sometimes necessary to capture important geological features associated with an oil reservoir. However, the field scale flow simulations using similar resolution are computationally intensive and still challenging even with more advanced compositional reservoir simulators and current computing power and this is especially true for mechanistic chemical flooding simulators. The stochastic nature of geological data also demands uncertainty analysis using different geological realizations. It is computationally intensive or even prohibitive in some cases to perform these multiple simulations with large fine-grid models. This is also true for the large number of simulations required for design and economic optimization studies typically conducted in field studies. Thus, there is an incentive in such cases to upscale the fine grid model to a much coarser grid. The methodology to calibrate the coarse grid results to those of accurate fine grid simulations is referred to here as upscaling of properties or just upscaling for short. The upscaling refers to either upscaling of the static reservoir properties of permeability and porosity or dynamic properties such as relative permeability and viscosity among many others related to chemical flooding processes. Static properties are commonly upscaled using an averaging scheme or based on single-phase flow simulations. The upscaling of dynamic properties is more complicated and will depend on the recovery process such as miscible gas flooding, water flooding and chemical flooding.

The importance of upscaling has been identified by many researchers and there exists a rich literature on upscaling of different processes such as water flooding, miscible gas flooding, polymer flooding, etc. Durlofsky (2003) published a review of recent progress on upscaling of geocellular models for reservoir flow simulations. An extensive

amount of research has been done in upscaling miscible gas flooding. Such displacement processes demand accurate capturing of fluid flow paths in the reservoir. Various factors such as mixing, relative permeability and fluid viscosity play important roles in the performance of the recovery process. One of the ways to upscale these parameters is through the use of effective properties or pseudo properties for coarse grids. Christie et al. (1995) discuss the use of pseudo fractional flow curves as an upscaling technique for water alternating gas (WAG) floods. Jakupsstovu et al. (2001) developed a procedure for upscaling miscible processes using grid block specific pseudo relative permeability curves. Garmeh and Johns (2009) show the importance of mixing in miscible processes and explain a procedure to incorporate a mixing coefficient in upscaling.

Several groups have studied the impact of grid size on polymer flood simulations. Leung et al. (2010) provide a framework for generating apparent viscosity scaling relationships that account for reservoir heterogeneities. Recent simulations presented by Yuan et al. (2010) indicated that the grid sensitivity is greater for a water flood than a polymer flood. The recoveries were insensitive to the grid block sizes since polymer solution was injected for a relatively long time of the order of 1 PV. In such cases, the polymer rheology and injection well operating conditions have much greater impact on the simulation results than the grid size. However, when the polymer is followed by water injection, fingering occurs. Fingering will affect the results more when less polymer is injected. Very small gridblocks are needed to accurately simulate fingers. Thus, even for polymer flooding, one needs to be very careful about grid block size since it is case dependent.

Scaleup of recovery processes such as miscible flooding and polymer flooding has been presented by several authors, but little work has been published on the scaleup of surfactant-polymer flooding. Upscaling chemical flooding requires a thorough

understanding and appropriate modeling of key parameters such as microemulsion phase behavior, interfacial tension, surfactant concentration, polymer rheology, salinity gradient and dispersion. Winsor (1954) showed the effect of salinity on phase behavior and he classified the microemulsion as Type I, Type II and Type III. The Type III region is the most favorable region which provides ultra low interfacial tension (IFT). The strong dependence of phase behavior on salinity for anionic surfactants and the relationship between phase behavior and interfacial tension and its dependence on various parameters were shown in Healy and Reed (1973) and in Healy et al. (1975). Huh (1979) theoretically substantiated the correlation of phase behavior and IFT originally proposed by Healy and Reed (1974). Many other studies such as Nelson and Pope (1977) and Hirasaki et al. (1983) also show the extreme importance of salinity on phase behavior and interfacial tension as well as the importance of salinity gradient and other factors affecting the design of chemical floods.

Critical micelle concentration (CMC) is an important parameter which affects the activity of a surfactant. One of the objectives of chemical flood is to maintain the surfactant concentration well above the CMC in the reservoir such that the solubilization of oil is maximized. The interfacial tension increases sharply when the surfactant concentration falls below the CMC (Green and Willhite, 2008). Rosen (2004) presented a list of CMC values for commonly used surfactants.

Trapping of fluid in the porous media is experimentally observed through a relationship between residual saturation and capillary number which is named as capillary desaturation curve. The idea of capillary number was proposed originally by Brownell and Katz (1947), where they defined it as the ratio of viscous and interfacial forces. Delshad et al. (1986) report capillary desaturation curves for two and three phase brine/oil/surfactant mixtures and show how such curves can be modeled in terms of

capillary number and how they affect the process by directly controlling the residual oil saturation. Jin (1995) derived a relationship which combined capillary number with bond number and named it as trapping number. The relationship between the trapping number and the residual saturation is shown in Pope et al. (2000). These curves are dependent on interfacial tension, which depends on phase behavior, which depends on salinity, so it is essential to include the effects of salinity in any chemical flooding simulator.

One of the most important aspects of Alkaline-Surfactant-Polymer flooding is the generation of in-situ surfactant or soap due to reaction between injected alkali and acidic components present in crude oil. Alkaline flooding was a much researched topic which started from 1920's. The first patent on the use of caustic for enhanced oil recovery was issued in United States in 1927 (Atkinson, 1927). A rich and extensive literature exists since then on the topic of alkaline flooding. Most of the researchers (Reisberg and Doscher, 1956; Jennings, 1975; Radke and Somerton, 1977) reported that the lowest interfacial tension occurs at very low alkali concentrations. On the other hand the alkali consumption in the reservoir demands injection of higher alkali concentration. This problem was resolved by Nelson et al. (1984) where he introduced the concept of co-surfactant enhanced oil recovery. He proposed a method to increase the low IFT window and thereby the optimum salinity by combining the alkali with a co-surfactant which is more hydrophilic than the in-situ generated soap. This started a new arena of research on types and uses of various surfactants which can be combined with alkali to mobilize trapped oil. The soap generation and other alkali consumption reactions and its effects on phase behavior and other process variables makes the process highly sophisticated and modeling such process becomes complex. Bhuyan (1989) developed a model to account for the geochemical reactions involved in ASP processes including the soap generation and added this model to UTCHEM. Mohammadi (2008) verified the model where she

matched many ASP core flooding and phase behavior experiments using UTCHEM. Zhang et al. (2006) developed a one dimensional simulator which has the capability to model the in-situ soap generation and track its movement. Other chemical reactions which may occur during the ASP flooding such as cation exchange and precipitation or dissolution reactions were not considered in their model. One of the main assumptions in their model was that all the naphthenic acid present in the crude oil will be converted to soap in the presence of alkali. Wang (1994) generalized the UTCHEM geochemical model initially developed by Bhuyan (1989) for any number of elements and reactions. This model (UTCHEM Technical Documentation, 2000) is the most comprehensive for modeling Alkaline-Surfactant-Polymer (ASP) flooding.

Green and Willhite (1998) include material from these and many other sources in their description of chemical flooding and how salinity affects both the surfactant and polymer properties. Various studies have been performed to understand the complexity of field scale chemical flooding simulations. Wu (1996) and Anderson et al. (2006) analyzed important factors in designing field-scale chemical floods.

There are many successful field tests of surfactant EOR reported in the literature. SP field test of Big Muddy reservoir in Wyoming reported by Gilliland and Conley (1976) is one of them. Bragg et al. (1982) reported a successful pilot test conducted at Exxon's Loudon field in Illinois. Another SP field test was conducted at Chevron's Glen Pool field in Oklahoma and the results are reported by Bae (1995). All of them reported the importance of low-IFT and mobility control for a successful surfactant enhanced oil recovery technique. Pandey et al. (2008) showed a detailed review of laboratory evaluations and simulation studies done in the design of an ASP pilot for Mangala field. Some of the important aspects of field pilot design are outlined in the paper. Pratap and

Gauma (2004) reported a successful pilot test of ASP flooding performed in Viraj oil field in India.

The importance of critical parameters on the performance of chemical flooding is shown in this study. The importance of accurately modeling various physical and chemical phenomenon related to chemical flooding are also explained. The impact of grid size on chemical flooding simulations and methodologies for upscaling field scale chemical flooding simulation are discussed.

Description of Reservoir Simulator, UTCHEM

The University of Texas Chemical Compositional Simulator, UTCHEM (Delshad *et al.*, 1996; UTCHEM, 2000) is used for modeling the ASP process. The simulator is a 3D multicomponent chemical flooding simulator. The solution scheme is an IMPEC formulation, where water pressure is solved implicitly and species concentrations are solved explicitly. Various physical and chemical phenomena modeled include microemulsion phase behavior and interfacial tension models, compositional phase viscosity models, phase trapping models, three-phase relative permeability models that depend on trapping number, chemical adsorption models, and polymer rheological models and how all of these depend directly or indirectly on salinity (and divalent cation concentration) and other variables such as co-solvent concentration.

Chapter 2: Effect of grid size on chemical flooding simulations

Accurate simulation of chemical flooding requires a detailed understanding of numerous complex mechanisms and model parameters where the grid size has a substantial impact upon the results. This chapter discusses the effect of grid size on parameters such as phase behavior, interfacial tension, surfactant dilution and salinity gradient for chemical flooding of a very heterogeneous oil reservoir. The ultimate objective of this study is to develop upscaling methodology to correct for the errors generated by using large grid blocks in reservoir simulations. A thorough understanding of various parameters which are critical to the performance of chemical flooding is of paramount importance in developing a strategy for upscaling.

The effective propagation of the surfactant slug in the reservoir is of paramount importance and the salinity gradient is a key factor in ensuring the process effectiveness. The larger the grid block size, the greater the surfactant dilution, which in turn erroneously reduces the effectiveness of the process indicated with low simulated oil recoveries. The best solution to this problem is to use a sufficiently fine grid in the simulations but as discussed in Chapter 1, this is often computationally intensive or may not be even feasible in some cases. Another way to tackle the problem is by using suitable scale up methodology. The chapter also discusses various scale up methodologies used to reduce the error associated with the selection of large grid block sizes.

ASP flooding simulations with two different chemical formulations, formulation A and B, were studied. The geological model and most of the reservoir properties were same for both set of simulations. Section 2.1 describes the simulation model used which is common to all the simulations. Section 2.2 discusses the modeling and simulations

with chemical formulation A. Similarly Section 2.3 discusses the simulations with chemical formulation B. Finally, concluding comments are outlined in Section 2.4.

2.1 SIMULATION MODEL

The effect of grid size on chemical flooding simulations was studied using models with varying grid block sizes. Seven different models were used for this study. Grid configuration and properties are shown in Table 2.1. The finest model studied was 86 X 94 X 19 (grid G) which has 153,596 grid blocks with a grid block size of 19 feet in the areal direction and 2 feet in the vertical direction. The coarsest model was 11 X 12 X 19 (grid A) which has 2508 grid blocks with a grid block size of 150 feet in the areal direction and 2 ft in the vertical direction. Figures 2.1, 2.2 and 2.3 show the areal view of grids A, C and F.

The reservoir is 1915 feet deep, 185 ° F and 37 feet thick. The permeability field, porosity and initial water and oil saturations for the coarser models are upscaled from the finest model which is 86 X 94 X 19. Figure 2.4 shows a three-dimensional view of the reservoir and the property shown in the figure is the depth from the surface. Figure 2.6 shows the permeability field of a cross section of grid F. This figure is a 3D diagonal slice through the central producer and the injectors (Figure 2.5). The figure shows that the reservoir is highly heterogeneous. The permeability varies from 10 md to 10,000 md. The permeability of lower layers (layers 13 - 19) is much higher than top layers (layers 1 - 12). Figures 2.7 and 2.8 show the permeability field of grid A and grid C. The porosity distribution of 43 X 47 X 19 (cross section) is shown in Figure 2.9. The initial water saturation is assumed to be 20% for all the models corresponding to the start of the waterflood. The total model area is simulated with a closed boundary, which was done by placing inactive grid blocks with zero porosity along the boundary. Figure 2.10 shows the

initial oil saturation in layer 19 of 43 X 47 X 19 grid. The boundary with inactive cells, cells with no initial oil, is clearly seen in the figure.

The total pilot area is about 115 acres, consisting of a central regular seven spot pattern, surrounded by partial regular seven spot patterns. The area for the central seven-spot well patterns is 29.25 acres. There are a total of ten injectors and seven producers (Figure 2.3) completed throughout the reservoir thickness of about 37 feet. All the injection wells are rate constrained with a rate of 8000 B/D for water flood and 2500 B/D for chemical flood. All production wells are pressure constrained with a maximum bottomhole pressure of 300 psi.

2.2 SCALE UP SIMULATIONS WITH CHEMICAL FORMULATION A

The input parameters for the field simulations were obtained in part by matching a core flood experiment performed in the laboratory using the reservoir core and crude oil. The surfactants, polymer and other chemicals for this study were selected through various experiments like aqueous stability, phase behavior screening tests and polymer rheology measurements. The parameters for modeling surfactant phase behavior and polymer rheology were obtained by matching phase behavior and polymer data from the laboratory experiments.

2.2.1 Surfactant data

The primary purpose of using surfactant is to lower the interfacial tension (IFT). Apart from low IFT, there are also other requirements that are critical in selection of the best surfactant for a crude oil and a reservoir. The most important requirement is low surfactant retention. Other important requirements are aqueous stability and compatibility

with polymer. Levitt et al., 2006, reported a detailed screening procedure for selecting the best surfactant formulation.

2.2.1.1 Aqueous Stability Test

An aqueous stability test was performed to confirm the stability of surfactant mixture at various conditions. This also helped to verify the homogeneity of the surfactant mixture. The surfactant mixture should be clear at reservoir conditions and at certain salinity ranges of interest. The test was performed by visually inspecting vials containing aqueous solution of the surfactant mixture at various different salinities which was performed by H. Yang (2010). The maximum salinity where the surfactant mixture was clear was noted and the chemicals were injected at salinities lower than this value.

2.2.1.2 Phase Behavior Experiment

The surfactant mixture selected through the screening procedure for the crude oil and reservoir conditions consisted of 0.25 % C32-7PO-6EO-Sulfate and 0.25 % C20-24 IOS. 0.25 % Triethylene glycol monobutyl ether (TEGBE) was added as a co-solvent. 0.4% sodium dihexyl sulfosuccinate was added as a solubilizer to give stability to the surfactant mixture.

The phase behavior plot is matched using Hand's model of binodal curve. A spreadsheet was developed to match the phase behavior data. The procedure to match the phase behavior experiment using the spreadsheet is explained in Appendix C. Figure 2.11 shows the phase behavior match obtained using the spreadsheet. The optimum solubilization ratio is 17 cc/cc at an optimum salinity of 32,000 ppm sodium carbonate. The interfacial tension at optimum salinity calculated from the solubilization ratio of 17 is 0.001 mN/m (Huh, 1979).

2.2.2 Polymer data and modeling

The polymer data was obtained from various laboratory tests such as filtration ratio test and rheology measurements. The polymer used for this study was a high molecular weight hydrolyzed polyacrylamide (SNF's FP 3630S).

Salinity dependence of polymer viscosity was modeled by matching measured viscosities at different salinities (Figure 2.12). The input parameter to UTCHEM for modeling salinity dependence is obtained through this match and is shown in the figure. Polymer viscosities at different polymer concentrations were reported from the laboratory and values were matched using UTCHEM polymer model (UTCHEM Technical documentation, 2000). Figure 2.13 shows the matched graph. The values of the matching parameters, AP1, AP2 and AP3 are also shown. Another important parameter in polymer modeling is the shear dependence of polymer viscosity. Polymer viscosities at various shear rates were measured using a low-shear viscometer in the laboratory. The values of these viscosities were matched using polymer shear thinning model (UTCHEM Technical documentation, 2000). Figure 2.14 shows the match along with the input parameters used to match the curve.

Table 2.2 summarizes the surfactant phase behavior modeling parameters. The procedure to match the data is given in the Appendix C.

3.2.3. History match of coreflood M9

The efficacy of the surfactant formulation and the effect of polymer injection were tested through coreflood experiment (coreflood M9) performed using the reservoir core. The core and fluid properties are given in Table 2.3. The core was first saturated

with 2895 ppm TDS brine. The composition of the brine is given in Table 2.4. The brine saturated core was then flooded with filtered crude oil to residual water saturation. The core was then water flooded to residual oil saturation. The initial saturation, residual saturations and end point relative permeability values for both water and oil are given in Table 2.5. The core was then flooded with an Alkaline-Surfactant-Polymer (ASP) slug with a slug size of 0.3 pore volumes (PV). The surfactant concentration in the ASP slug was 0.5 wt%. The surfactants were described earlier in the surfactant data section (Section 2.2.1) and are also shown in Table 2.6. The polymer concentration in the ASP slug was 2000 ppm. The ASP slug was then followed with a polymer drive for 2 PV. The polymer concentration in the polymer drive was 1150 ppm. The complete injection scheme is given in Table 2.6. The cumulative oil recovery and the oil cut given by the coreflood experiment are shown in Figure 2.15. The oil recovery is about 98% of the residual oil saturation with maximum oil cut in oil bank of about 0.65.

The coreflood experiment was history matched using UTCHEM. The surfactant phase behavior was matched and is shown in Section 2.2.1 (Figure 2.11). The parameters used for matching (Table 2.2) were used in UTCHEM input for coreflood history matching. The residual saturations measured in the laboratory were slightly changed from the measured value in the laboratory to match the breakthrough through time and oil cut in the oil bank. The endpoint relative permeabilities were also slightly changed. Table 2.7 lists the changed values of residual saturations and endpoint relative permeabilities to match the coreflood. The capillary desaturation parameters were also used as matching parameters. Figure 2.16 shows the capillary desaturation curve. The relative permeability and the fractional flow diagram are shown in Figures 2.17 and 2.18. The polymer measurements and modeling were described in Section 2.2.2. The same polymer was used in the coreflood. The polymer parameters used in modeling experimental

measurements were used for the coreflood simulation and are shown in Table 2.8. The microemulsion viscosity measurements were not available thus the parameters for the viscosity of microemulsion are obtained through matching the pressure drop values of simulation with that of the coreflood experiment. The values of microemulsion viscosity parameters obtained are listed in Table 2.9

The adsorption of surfactant measured in the laboratory was 0.01 mg/g. The polymer adsorption value was not available. The polymer adsorption (Figure 2.20) was assumed to be 9 micrograms per gram ($\mu\text{g/g}$) to match cumulative oil recovery and pressure drop measured during the core flood. The values of surfactant and polymer adsorption parameters used in the coreflood simulation are given in Table 2.10. Figure 2.19 shows the adsorption isotherm matched for measured surfactant adsorptions measured during the coreflood. A core flood simulation was performed using the properties and input parameters shown in Tables 2.2 - 2.10. A good agreement was obtained between the simulation and laboratory results. Figure 2.21 shows the oil recovery and oil cut match. The breakthrough time was also matched well. A good match of pressure drop is also obtained as seen in Figure 2.22.

The simulation of coreflood M9 and matching the results increased the confidence in simulating a field scale ASP flooding. The matching of phase behavior experiment, polymer measurements and the coreflood validated the physical and chemical property models used in UTCHEM.

2.2.4 Field scale simulations using chemical formulation A:

One of the most important objectives of matching a laboratory coreflood is to estimate parameters such as surfactant and polymer adsorption parameters, microemulsion viscosity parameters and capillary desaturation curve parameters. The

coreflood data and simulation will not match unless other parameters such as surfactant phase behavior parameters and polymer viscosity parameters based on measured values are also consistent with the performance during the core flood.

The reservoir under study has been under primary and secondary recovery for long time. A water flood simulation was performed to obtain current conditions of the reservoir. ASP flooding was then started after the waterflood. The following sections (Section 2.2.4.1 and 2.2.4.2) discuss in detail about the water flood simulations and ASP flood simulations using various grids described earlier.

2.2.4.1 Water flood simulations

The initial oil in place for the model was about 3.7 million barrels and the reservoir pore volume was about 4.7 million barrels. The initial oil saturation was 80%. A water flood was performed before the ASP flood, for the seven different grids, to determine the pre-ASP oil and water saturations. The water injection was performed at a rate of 8000 barrels per day. The waterflood was ended at an oil recovery of 56 % OOIP, roughly the current condition of the actual field. Figure 2.23 shows the cumulative oil recovery during water flooding.

The average oil saturation after water flooding was about 0.34 (Figure 2.25). The average reservoir pressure during the water flood is shown in Figure 2.24. The remaining oil in place after waterflooding is 1.63 million barrels. The water flooding simulations set up the initial condition for ASP flooding.

2.2.4.2 Alkaline-Surfactant-Polymer (ASP) flood simulations

Seven ASP simulations were performed using different grid block sizes described earlier (Section 2.1). The end of water flood simulations was the initial conditions for

ASP flood. The permeability fields of some of the models are shown in Figures 2.6, 2.7 and 2.8. The permeability fields of the other grid block models and the average permeability of all the layers for all the models are shown in Appendix A. The surfactant phase behavior modeling and polymer modeling were explained in earlier sections (Sections 2.2.1 and 2.2.2). Other parameters were obtained from the coreflood match as discussed in Section 2.2.3. Injectors were designed as rate constrained with an injection rate of 2500 barrels per day for chemical injection. The producers were on pressure constraint with bottomhole pressure of 300 psi. The injection scheme was similar to the coreflooding apart from the polymer injection. The process design consisted of a 0.3 PV ASP slug followed with 1 PV of polymer drive. A post water flood of 1 PV was simulated after the polymer drive.

The fluid properties and injection schemes are identical in all models. Oil recovery results are summarized in Table 2.11 and compared in Figures 2.26 and 2.27 with substantial differences in oil recovery for different grids. The coarsest grid of 11 X 12 X 19 shows a difference in oil recovery of 22 % of the Remaining Oil in Place (ROIP) or 9.6 % Original Oil in Place (OOIP) in comparison with the finer model of 43 X 47 X 5. The oil recovery decreases when the grids are coarsened in the areal direction and a reverse trend is observed in the vertical direction as indicated in Table 2.11. The areal coarsening reduces the oil recovery by 16 % of ROIP whereas the vertical coarsening causes only a 6% ROIP increase. Figures 2.28 and 2.29 show the overall oil rate for areal and vertical coarsening. The thickness of gridblocks selected in these simulations has less impact on oil recovery compared to the grid block areas.

As discussed earlier, the permeabilities of the bottom layers were higher than the top layers. As a result of this permeability contrast, a high permeability path was created in the bottom where most of the injected fluids flow only through these layers. Figures

2.30 - 2.32 show 2-D vertical cross section through two injectors and a producer of the reservoir. Injectors and producer in the cross section are marked. The surfactant concentration at various times of injection is shown in the figure. The movement of surfactant slug from injector to the producer occurs through the high permeability layers as seen in the figures. Figures 2.33-2.35 show the same cross sectional view as in the previous figures and the movement of polymer is shown. The polymer was injected continuously for 1 PV after 0.3 PV surfactant slug injection. The flow through the high permeability zones is more evident in these figures. These factors resulted in a lower recovery of oil from the low permeability layers. Figures 2.36-2.38 show the oil saturation at different times of injection. The oil saturation of the high permeability layers were reduced close to a very low number where a high percentage of oil was recovered from these layers. Table 2.12 lists the percentage of oil recovered from each layers in terms of the remaining oil after water flooding.

One of the main objectives of this study was to find an upscaling methodology which could reduce the error created in ASP simulation due to the large grid block sizes. The most important step to achieve this goal is to study the effects of various parameters on chemical flooding simulations and more importantly the effect of these parameters on grid sizes.

2.2.5 Parameters studied for upscaling

The first and the most important step in upscaling chemical flooding simulations is to identify the key parameters which distinguish the coarse grid and fine grid results. The critical parameters include salinity gradient, phase behavior, dilution, dispersion and capillary desaturation.

2.2.5.1 Salinity Gradient

The salinity gradient is one of the most important design variables that determine chemical flooding performance. In general the salinity of the SP or ASP slug should be less than the formation brine and the salinity of the polymer drive should be less than the slug. This is a normal salinity gradient. The essential idea is that a slug with optimum Type III salinity is followed by a polymer drive with a lower salinity in the Type I region so that no surfactant will be trapped in the middle phase microemulsion that forms near optimum salinity. If the formation salinity is lower than the optimum salinity in the slug, then the salinity gradient is not normal and it is therefore less favorable.

The simulations performed earlier were not with a normal salinity gradient where the formation brine salinity was lower than the salinity of the ASP slug. Thus these simulations were more sensitive to change in grid sizes. Figure 2.39 shows an areal view of the 43 X 47 X 19 grid showing the spread of the chemical slug and its movement in numerical layer 19. Figure 2.40 shows the profile of surfactant concentration, oil saturation, and effective salinity between an injector and a producer in layer 19 of the fine grid after 0.1 PV chemical slug is injected. The plot shows that the effective salinity remains near optimum and in Type III region and the surfactant is extremely effective in mobilizing the oil. Figure 2.41 gives similar results but at later time of 0.4 PV of injection. The chemical slug has moved towards the producer and the polymer drive with a lower salinity has already started as evident with the lower effective salinity near the injector (Figure 2.41). The salinity is Type III in the surfactant slug resulting in very low oil saturation behind the front. Figure 2.42 shows the profile after 1 PV of injection. The chemical slug has already reached the producer. The effective salinity is close to the polymer injection salinity in more than 50 % of the distance between the injector and the

producer. The low oil saturation signifies the effectiveness of the surfactant slug, polymer injection and the salinity gradient designed for this simulation.

The impact of grid size on salinity gradient is studied by comparing the effective salinity profiles for coarse and fine grid models in Figures 2.43 and 2.44. The effective salinities are clearly different for the two grid models. After 0.1 PV slug injection, the effective salinity for the fine grid simulation remains in the Type III region for more than 30% of the distance between the wells in comparison with coarse grid where the effective salinity sharply drops below the lower Type III salinity window (CSEL). The reason behind this difference is the artificially large dilution of the injected sodium carbonate, surfactant and polymer concentrations in the large gridblocks. After 0.5 PV injection, the effective salinity of the coarser model does not even reach the Type III region whereas that of the finer grid model is still in the Type III environment as the surfactant slug moves towards the producer (Figure 2.44). This difference in the effective salinity makes a significant impact on the oil recovery performance as shown in Figs. 2.26 and 2.27.

Normal Salinity Gradient:

A sensitivity study was performed to investigate the effect of the salinity gradient design in which the salinity ahead of the surfactant slug was greater than the optimum salinity (over optimum or Type II) in contrast to the previous cases with initial salinity being under optimum or Type I. The injection scheme referred to normal salinity gradient is summarized in Table 2.13. The oil recoveries with a normal salinity gradient are listed in Table 2.14. The oil recoveries are higher for the normal salinity gradient and also indicate less sensitivity to the grid resolution compared to the original salinity design. The areal grid size sensitivities for the normal salinity gradient design are shown in Fig. 2.45. The profiles of 43 X 47 X 19 after 0.2 PV and 0.4 PV are shown in Figures 2.46

and 2.47. The effect of a normal salinity gradient is seen from these profiles. Figure 2.48 shows a comparison of effective salinity and surfactant concentration profiles of 43 X 47 X19 and 11 X 12 X 19 grids. The effect of dilution, which was seen in the previous cases without a normal salinity gradient, was minimized in this case with the normal salinity gradient. This makes the simulations with a normal salinity gradient less sensitive to grid size. Thus chemical floods should be designed with a normal salinity gradient when that is feasible, but unfortunately it is not always feasible.

2.2.5.2 Surfactant Dilution

The effect of sodium carbonate dilution and its unfavorable effect on the salinity gradient and the performance are explained in the previous section. The effect of surfactant concentration dilution for different grid size is equally important. The surfactant concentration must be above the critical micelle concentration (CMC) for any surfactant to produce low IFT. The IFT discontinuously increases below the CMC, which is typically about 0.01% for high performance surfactants. Figure 2.49 shows the surfactant concentration at one of the central injection gridblocks for the fine and coarse grid simulations. The effect of dilution is clearly shown in this figure. The surfactant concentration of the coarser grid is much less than that of the fine grid. The difference in the surfactant concentration explains the lower recoveries obtained in the coarse scale simulations.

2.2.5.3 Dispersion

Physical dispersion is modeled as follows:

$$\bar{\bar{K}}_{\kappa\ell ij} \equiv \frac{D_{\kappa\ell}}{\tau} \delta_{ij} + \frac{\alpha_{T\ell}}{\phi S_{\ell}} |\bar{u}_{\ell}| \delta_{ij} + \frac{\alpha_{L\ell} - \alpha_{T\ell}}{\phi S_{\ell}} \frac{u_{\ell i} u_{\ell j}}{|\bar{u}_{\ell}|} \dots\dots\dots (2.1)$$

where $\alpha_{L\ell}$ and $\alpha_{T\ell}$ are phase ℓ longitudinal and transverse dispersivities; τ is the tortuosity factor with the definition of being a value greater than one; $u_{\ell i}$ and $u_{\ell j}$ are the components of Darcy flux of phase ℓ in directions i and j ; and δ_{ij} is the Kronecker delta function. The magnitude of vector flux for each phase is computed as

$$|\bar{u}_{\ell}| = \sqrt{u_{x\ell}^2 + u_{y\ell}^2 + u_{z\ell}^2} \dots\dots\dots (2.2)$$

The effect of physical dispersion on chemical flooding performance was studied by varying the dispersivity parameters as shown in Figure 2.50 for the coarse grid of 11x12x19. The default values in base case simulations are $\alpha_{L\ell} = 4$ ft and $\alpha_{T\ell} = 0.4$ ft. The oil recovery decreased from 32% to 27% as the longitudinal dispersivity increased by over two orders of magnitude.

The effect of numerical dispersion was also studied using different numerical schemes of single-point upstream, two-point upstream weighting and a third-order finite-difference method with a flux limiter (UTCHEM, 2000). There is a maximum of 1% difference in oil recoveries between the single point and TVD methods for the simulations of 11x12x19 and 22x24x19. In other cases, the numerical method makes larger differences, but in this case the reservoir is extremely heterogeneous, so that dominates over numerical and physical dispersion.

2.2.5.4 Critical Micelle Concentration

Critical micelle concentration (CMC) is the concentration at which a surfactant forms aggregates called micelles. One of the objectives of chemical flood is to maintain the surfactant concentration well above the CMC in the reservoir such that the solubilization or mobilization of oil is maximized. For a given surfactant this necessitates that either a sufficiently high concentration or alternatively a large slug of surfactant be injected such that the surfactant concentration remains above the CMC after dilution and dispersion in the reservoir. The important modeling implication of this parameter is that for surfactant concentration below CMC, there is no solubility enhancement and no interfacial tension reduction and surfactant resides in the water phase and only slightly affects the viscosity and density of the water phase.

The effect of CMC on the oil recovery was studied by changing the CMC in the range of 10^{-6} to 10^{-4} (volume fraction). The oil recoveries are insensitive to the values of CMC studied with the 11x12x19 grid.

2.2.5.5 Capillary Desaturation Curve

Capillary desaturation curve (CDC) is the relationship between residual phase saturation (oil, aqueous, and microemulsion) and trapping number. The dimensionless trapping number is the ratio of combined viscous and gravitational forces to capillary forces. The residual saturations as a function of trapping number are calculated using the following empirical correlation (Delshad et al., 1986).

$$S_{\ell r} = \min \left(S_{\ell}, S_{\ell r}^{\text{high}} + \frac{S_{\ell r}^{\text{low}} - S_{\ell r}^{\text{high}}}{1 + T_{\ell} N_{T_{\ell}}} \right) \dots\dots\dots (2.3)$$

where $S_{\ell r}^{\text{low}}$ and $S_{\ell r}^{\text{high}}$ are the input residual saturation for phase ℓ at low and high trapping numbers. T_ℓ is the trapping parameter for phase ℓ and N_{T_ℓ} is the trapping number given by

$$N_{T_\ell} = \frac{\left| \vec{k} \cdot \vec{\nabla} \Phi_{\ell'} + \vec{k} \cdot \left[g(\rho_{\ell'} - \rho_\ell) \vec{\nabla} D \right] \right|}{\sigma_{\ell\ell'}} \dots\dots\dots (2.4)$$

where IFT between microemulsion phase and water ($\ell = 1$) or microemulsion phase and oil phase ($\ell = 2$) is given by

$$\sigma_{\ell 3} = \sigma_{ow} e^{-aR_{\ell 3}} + \frac{cF_\ell}{R_{\ell 3}^2} \left(1 - e^{-aR_{\ell 3}^3} \right) \dots\dots\dots (2.5)$$

where $R_{\ell 3}$ is the solubilization ratio (UTCHEM, 2000) and input variables 'a' and 'c' are constants.

At sufficiently high trapping numbers that correspond to an ultra-low IFT, the trapped oil can be completely mobilized. A sensitivity simulation study to CDC is performed by changing the capillary desaturation parameter for the oil phase ($T_\ell = T22$). Increasing the oil trapping parameter shifts the CDC to a lower critical capillary number and is thus more favorable for oil mobilization (Figure 2.51). Figure 2.52 shows the oil recovery sensitivity to different oil CDCs showing that an order of magnitude increase in the oil trapping parameter caused an increase of only 4 % ROIP (1.8 % OOIP).

2.2.6 Upscaling methodologies

The objective of this study was to develop a methodology to match the results of coarse grid chemical flooding simulations to those of the fine grid simulations to aid in better performance predictions of large field projects. The first step was to identify key parameters that are impacted by the grid size, as done in the previous section. After a thorough study, it was concluded that the key phenomenon controlling the oil recovery for different grid sizes is the dilution of both alkali and surfactant concentrations which can severely impact the phase behavior. A coarse grid causes significant smearing of the injected chemicals which may reduce the calculated effective salinity below the optimum region. The under optimum flood increases the IFT and reduces the computed oil recoveries.

One approach to match the coarse grid oil recoveries with those of the finest grid of 43x47x19 was to use the concept of pseudo optimum salinity and widen the Type III salinity region by lowering the CSEL (effective salinity where the Type III first forms). The idea was to lower the optimum salinity such that the diluted effective salinity of the coarse grid passes through the Type III region similar to the fine grid. Figure 2.53 shows the salinity profile for the finest and coarsest grid models after 0.5 PV of injection. The three-phase Type III region for the fine grid corresponds to effective salinities of 0.5-0.85 meq/ml compared to 0.15-0.85 meq/ml for the coarse grid of 11x12x19. Coarse-grid simulations were repeated with pseudo CSEL and the oil recoveries became comparable to those of the finest grid (Figure 2.54). Table 2.15 gives the values of pseudo CSEL used in each coarse grid simulation and the resulting oil recoveries. Thus, the key to upscaling this particular case was the salinity. The coarse grid salinities are much too low due to dilution and this one factor not only causes the results to be very inaccurate,

but it makes the simulations artificially insensitive to other normally important factors such as the CMC and the CDC data.

Even though the oil recoveries are similar for different grid sizes, the method is not robust since it requires the change in the most fundamental phase behavior data. Next, an attempt was made to use pseudo IFT by adjusting the input parameters for the IFT model (parameters a and c in equation 2.5). One of the major reasons for the difference in recoveries for different grids is due to the dilution of salinity and surfactant concentration where the salinity of the coarse grids fall below type III which increases the IFT in those models. The idea of using pseudo IFT curves for coarse grid model was to adjust for the increase in IFT created by the dilution of surfactant and salinity by artificially lowering the IFT directly for coarser models by changing the input parameters in the IFT model. Figure 2.55 shows the pseudo IFT curves for coarse grids and the finest grid of 43x47x19. Table 2.16 gives the values ' c ' and ' a ' of the IFT model for different grids. Figure 2.56 shows the oil recoveries after IFT adjustments in coarse grid simulations and its comparison with the finer model 43 X 47 X 19.

Neither of the proposed approaches was a robust upscaling method. However, the research introduced, for the first time, the significance of grid size resolutions in ASP simulations using a mechanistic chemical flooding simulator. The upscaling approaches presented account approximately for some of the more important effects of phase behavior and interfacial tension.

2.3 SCALE UP SIMULATIONS WITH CHEMICAL FORMULATION B

This section describes the effect of grid size on chemical flooding simulations with a different chemical formulation than the previous section (Section 2.2). The objective of this study is to test the effect of grid block sizes on ASP simulations with a

different formulation than the one studied in Section 2.2. The surfactant concentration in the chemical mixture is 2 vol % which is much higher than formulation A. The grid block models were same as those described in Section 2.2. The permeability fields of the areally coarsened grids were shown in Figures 2.6, 2.7, and 2.8. The chemical flood design was based on a coreflood discussed by Dwarakanath et al. (2008). The input parameters for the field scale simulations were obtained by matching the phase behavior and core flood experiments. The phase behavior and core flood match is shown in Figures 2.57 and 2.58 (Dwarakanath et al., 2008). The solubilization ratios are plotted against normalized salinity (Figure 2.57) which is the ratio of salinity and optimum salinity. The optimum solubilization ratio, as seen from Figure 2.57, is 12. The IFT at optimum salinity calculated from the solubilization ratio of 12 is 0.002 mN/m (Chun Huh, 1979).

The input parameters for the field simulations were obtained by matching phase behavior experiments and core floods (Dwarakanath et al. 2008). Table 2.17 shows the core and fluid properties of the core flood experiment. Table 2.18 list the values of input parameters used in ASP flood simulations. The injection scheme is given in Table 2.19.

2.3.1 Field scale simulations using chemical formulation B:

One of the most important objectives of matching the laboratory coreflood is to obtain modeling parameters for field scale simulation such as surfactant and polymer adsorption parameters, microemulsion viscosity parameters and capillary desaturation curve parameters. The coreflood data and simulation will not match unless other parameters such as surfactant phase behavior parameters and polymer viscosity parameters based on measured values are also consistent with the performance during the core flood. The coreflood match was performed by Dwarakanath et al., 2008. The parameters for field scale simulations are listed in Table 2.18.

The reservoir under study has been under primary and secondary recovery methods for a long time. Thus a water flood was simulated to obtain current conditions of saturations and pressure of the reservoir. ASP flood was then started from the condition after the initial waterflooding. The following sections (Sections 2.3.4.1 and 2.3.4.2) discuss in detail about the water flood simulations and ASP flood simulations using various grids described earlier.

2.3.1.1 Water flood simulations

The water flood simulation was similar to what described in Section 2.2.4.1. The water injection was performed at a rate of 8000 barrels per day. The water flood was ended at an oil recovery of 56 % OOIP. Figures 2.23, 2.24 and 2.25 show the waterflood results.

2.3.1.2 ASP flood simulations

Field scale ASP flooding simulations were performed using grid block models described in Section 2.1. The injection design consisted of 0.2 PV surfactant slug with 2 wt% surfactant concentration and 3 wt% cosolvent which is followed with a 0.2 PV polymer drive with 2200 ppm polymer and 9800 ppm TDS salinity. A second polymer drive of size of 1.2 PV was injected with 1800 ppm polymer concentration and 2865 ppm TDS salinity. This is followed with a post water flood for 0.6 PV with a salinity of 2865 ppm TDS. The injection scheme is summarized in Table 2.19.

ASP simulations were performed using seven different grid block models. Table 2.20 shows the oil recoveries for all the models. The oil recovery given by the finest model 86 x 94 x 19 is very close to that given by the finer model 43 x 47 x 19. Figure 2.59 shows the oil recovery difference with grid block sizes. Figure shows that there is

very less difference in oil recovery after 40,000 gridblocks (43 x 47 x 19). As the results converged after 40,000 grid blocks, 43 X 47 X 19 was taken as the finest model to compare the recoveries with other coarser models. The comparison of oil recoveries in terms of % OOIP and % ROIP are shown in Figures 2.60 and 2.61. The coarsest grid of 11 x 12 x 19 shows a difference in oil recovery of 23 % ROIP which is 10 % OOIP in comparison with the finer model of 43 x 47 x 5. The oil recovery decreases when the grids are coarsened in the areal direction and a reverse trend is observed in the vertical direction, similar to results with chemical formulation A (Section 2.2.4.2). The areal coarsening reduces the oil recovery by 17% ROIP whereas the vertical coarsening causes an increase of 7% ROIP. As discussed earlier, the thickness of numerical layers of these simulations has less impact on oil recovery compared to the areas of the grid blocks.

2.3.2 Parameters studied for upscaling

2.3.2.1 Salinity Gradient

The importance of salinity gradient was described previously (Section 2.2.5). Figure 2.62 and 2.63 shows the profile of surfactant concentration, effective salinity and oil saturation after 0.1 PV and 0.3 PV injection for layer 19. The oil saturation before the start of ASP injection is also shown in Figure 2.62. The formation of oil bank in front of ASP slug is also evident from Figure 2.63. These profile plots show the effectiveness of surfactant slug and polymer drive in mobilizing and sweeping the residual oil. As discussed earlier, one of the important aspects of the profile plots is that these plots show the movement of fluids at various times of injection from the injector towards the producer. This will help in understanding the changes, especially in salinity, happening at various fluid fronts because of mixing of the fluids. Salinity is one of the most important

parameters in the design of an efficient ASP flood. The ultralow IFT occurs at salinity within the Type III region. The ASP slug salinity should be maintained within these limits to take advantage of the surfactant's ability to reduce IFT but due to mixing, there are chances that the salinity of the slug reduces below the Type III region with increases in the IFT. Thus profile plots which show the changes in critical parameters such as salinity, will help in designing an effective ASP slug and polymer injection scheme.

The effect of grid sizes on the salinity profiles was studied. Figure 2.64 shows the salinity profile after 0.1 PV injection for the numerical layer 19. The effect of grid size on the salinity is clearly seen in the profile where the salinity of the coarse grid (11 X 12 X 19) falls below Type III sharply, in comparison with the finer grid. The reason, as explained earlier, is the dilution of the injected sodium carbonate in the large grid blocks. This is also evident from salinity profile after 0.3 PV injection where the first polymer drive injection has already started. The first polymer drive in these simulations was injected at salinity close to optimum salinity to keep the salinity in the Type III for a longer time but the effects of sodium carbonate dilution was still dominant in coarser grids as seen in Figure 2.65. Figure 2.66 shows the comparison of salinity profile after 0.7 PV injection where the first polymer drive has already started to produce. The effect of dilution is seen in the profile.

The dilution of the injected sodium carbonate artificially alters the salinity gradient of coarser grid block models and resulted in a poor performance in comparison with the fine grid results.

2.3.2.2 Surfactant Dilution

The effect of sodium carbonate dilution and its unfavorable effect on salinity gradient and the performance were explained in the previous section. It is equally important to study the effect of surfactant dilution for different grid sizes. Surfactant

concentration dilution effects are critical to the performance of the flood since the injected surfactant concentration is very low. Figure 2.67 shows the surfactant concentration at one of the central injection grid blocks for fine and coarser models. The surfactant concentrations in the coarser grids are comparatively much lesser than that of the fine grid because of the surfactant concentration dilution in larger grid block sizes. Thus the surfactant dilution along with the sodium carbonate dilution explains the lower recoveries obtained in coarse scale simulations.

2.3.2.3 Dispersion

The physical dispersion equation model in UTCHEM was discussed in Section 2.2.5.3. The effect of dispersion on chemical flooding was studied by varying the dispersivity parameter in Equation 2.1. The value of longitudinal dispersivity parameter was varied from 0 to 150 ft. The effect of physical dispersion on oil recovery of 11 x 12 x 19 grid is shown in Figure 2.68. The oil recovery decreased from 42.5 to 36 % ROIP as the longitudinal dispersivity was increased by over two orders of magnitude.

2.3.2.4 Critical Micelle Concentration

The definition and the importance of critical micelle concentration (CMC) are explained in Section 2.2.5.4. The value of CMC in simulations with formulation B, Section 2.3.1.2, was 10^{-3} . The effect of CMC on oil recovery was studied by changing the CMC in the range of 10^{-6} to 10^{-4} (volume fraction). The oil recoveries are insensitive to the values of CMC studied with 11 x 12 x 19 grid.

2.3.2.5 Capillary Desaturation Curve

Capillary desaturation curve (CDC) is the relationship between phase saturation (oil, aqueous and microemulsion) and trapping number, as explained in Section 2.2.5.5. A sensitivity study to CDC was performed by changing the capillary desaturation parameter for the oil phase ($T_{\ell} = T22$). Increasing T22 makes the CDC more favorable for oil mobilization. Figure 2.69 shows the sensitivity of oil recovery to T22 for 11 x 12 x 19 grid. An order of increase in trapping parameter caused an increase in oil recovery of only 5.5 % ROIP (2.4 % OOIP).

2.3.3 Upscaling methodology

The objective of this study was to develop a methodology to match the results of coarse grid chemical flooding simulations to those of the fine grid to aid in better performance predictions of large field projects. As discussed earlier, the first step in our study was to identify key parameters that are impacted by the grid size, as done in the previous section. The key phenomenon controlling the oil recovery for different grid sizes is the dilution of both alkali and surfactant concentrations which can severely impact the phase behavior. The surfactant concentration in large grid block is diluted and may go even below the critical micelle concentration. This increases the IFT and impact adversely on the ASP slug effectiveness. A coarse grid causes significant smearing of the injected chemicals which may reduce the calculated effective salinity below the optimum region. The under optimum flood increases the IFT and reduces the computed oil recoveries.

The concept of pseudo optimum salinity (Section 2.2.6) along with a change in CMC for coarse grid simulations is used to match the coarse grid oil recoveries with those of the finest grid of 43x47x19. The idea is to lower the optimum salinity such that

the diluted effective salinity of the coarse grid passes through the Type III region similar to the fine grid. The CMC for the surfactant formulation is 0.001, which is an order of magnitude higher than CMC used for formulation A (Section 2.2). The high value of CMC along with dilution in the large grid blocks artificially creates error in coarse grid simulations. The three-phase Type III region for the fine grid corresponds to effective salinities of 0.1-0.1 meq/ml compared to the adjusted value of 0.06-0.2 meq/ml for the coarse grid of 11x12x19. The CMC was reduced to 0.0001 for all the coarser models from the original value of 0.001. Figure 2.70 shows the salinity profile for the finest and coarsest grid models after 0.1 PV of injection. Coarse-grid simulations were repeated with pseudo CSEL and the oil recoveries became comparable to those of the finest grid (Figure 2.71). Table 2.21 gives the values of pseudo CSEL used in each coarse grid simulation and the resulting oil recoveries. Thus, the key to upscaling this particular case was the salinity and CMC. The coarse grid salinities are much too low due to dilution and this one factor not only causes the results to be very inaccurate, but it makes the simulations artificially insensitive to other normally important factors such as the CMC and the CDC data.

2.4 SUMMARY

This chapter presented a study on the effect of grid sizes on chemical flooding performance and proposed upscaling strategies to the cases studied. Two different chemical formulations were considered. Surfactant and polymer modeling was briefly described. The experimental data for surfactant and polymer were matched with UCHEM model to obtain input parameters for ASP simulations. A core flood experiment was successfully matched using UTCHEM. The simulation of core flood and history

matching the results increased the confidence in performing field scale ASP flood simulations. The effect of grid size on ASP flood simulations were studied with grid models with different grid sizes. A substantial difference in recoveries was observed for simulations with different grid block models. The results were thoroughly analyzed and the effects of critical parameters on ASP flood performance were studied. The salinity and surfactant concentration were diluted in large grid blocks. The salinity of large grid block models goes below the Type III region because of the dilution where the salinity of the fine grid run stays in the Type III region during that time. This caused a significant difference in the performance of simulations with different grid block sizes. Two upscaling strategies were proposed to reduce the error caused because of the difference in grid sizes. The first method proposed was to artificially lower the optimum salinity of coarse grid models by lowering the lower critical salinity window (CSEL) for those models. The coarse grid simulation results were matched with the fine grid results with the adjusted CSEL. Another methodology proposed was to adjust the IFT parameters for coarse grid simulations to artificially decrease the IFT for coarse grid simulations. The recoveries of coarse model simulations were matched with the fine grid by adjusting the IFT parameters. Neither of the proposed methods was robust since the methods described were case dependent and it is not a predictive method for some other cases. However, a systematic study on critical parameters which impact the ASP simulations and also the impact of grid sizes on ASP performance were done. The importance of salinity gradient and dilution effects was shown. The study also introduced, for the first time, the significance of grid size resolutions in ASP simulations using a mechanistic chemical flooding simulator. The upscaling approaches presented account approximately for some of the more important effects of phase behavior and interfacial tension.

Table 2.1: Grid descriptions.

Grid Name	Grid Configuration	Grid Size	Number of Grid Blocks
A	11 X 12 X 19	150 ft X 150 ft X 2ft	2500
B	22 X 24 X 10	75 ft X 75 ft X 4 ft	5300
C	22 X 24 X 19	75 ft X 75 ft X 2 ft	10000
D	43 X 47 X 5	37.5 ft X 37.5 ft X 8 ft	10000
E	43 X 47 X 10	37.5 ft X 37.5 ft X 4 ft	20000
F	43 X 47 X 19	37.5 ft X 37.5 ft X 2 ft	38000
G	87 X 94 X 19	18.75 ft X 18.75 ft X 2 ft	154000

Table 2.2: Phase behavior parameters for formulation A.

Height of binodal curve at zero salinity, HBNC 70	0.055
Height of binodal curve at optimum salinity, HBNC 71	0.035
Height of binodal curve at twice optimum salinity, HBNC 72	0.055
Lower critical salinity window, CSEL, meq/ml	0.5
Upper critical salinity window, CSEU, meq/ml	0.85
Optimum salinity, meq/ml	0.675

Table 2.3: Core and fluid properties for core flood M9

Core Properties	
Porosity	0.2
Permeability, md	356
Temperature, ° F	185
Length, cm	30
Diameter, cm	5.03
Residual water saturation	0.35
Residual oil saturation	0.375
Water end point relative permeability	0.1
Oil endpoint relative permeability	0.5
Fluid Properties	
Water viscosity, cp	0.37
Oil viscosity, cp	3.4

Table 2.4: Brine composition for core flood M9

Composition	Concentration (ppm)
Na	932
Ca	0
Mg	0
K	15
Cl	800
SO ₄	18
HCO ₃	1100
TDS	2865

Table 2.5: Residual saturations and endpoint relative permeabilities measured in the laboratory during M9 core flood

Residual water saturation	0.39
Residual oil saturation	0.335
Water end point relative permeability	0.056
Oil endpoint relative permeability	0.58

Table 2.6: Injection scheme for the coreflood M9

Alkali-Surfactant-Polymer Slug	
Slug size	0.3 PV
Surfactant mixture and concentration	0.25 % C32-7PO-6EO-Sulfate and 0.25 % C20-24 IOS -- total 0.5 % volume with 0.25 % TEGBE and 0.4 % Sodium dihexyl sulfosuccinate
Polymer concentration	2000 ppm
Salinity	32000 ppm sodium carbonate
Flow rate	1 ft/day
Polymer Drive	
Drive size	1 PV
Polymer concentration	1150 ppm
Salinity	2865 ppm TDS
Flow rate	1 ft/day
Post Waterflood	
Post flush	1 PV
Salinity	2865 ppm TDS

Table 2.7: Residual saturations and endpoint relative permeabilities adjusted to match the coreflood

Residual water saturation	0.39
Residual oil saturation	0.335
Water end point relative permeability	0.056
Oil endpoint relative permeability	0.58

Table 2.8: Polymer parameters used in the coreflood M9 simulation

SSLOPE	-0.377
AP1	45
AP2	625
AP3	1000
GAMMAC	4
GAMHF	30
POWN	1.8

Table 2.9: Microemulsion viscosity parameters used in the coreflood M9 simulation

ALPHA1	0.1
ALPHA2	2.2
ALPHA3	0
ALPHA4	0
ALPHA5	0

Table 2.10: Adsorption parameters used in the coreflood M9 simulation

Surfactant adsorption parameters	
AD31	0.125
AD32	0
B3D	1000
Polymer adsorption parameters	
AD41	2
AD42	0
B4D	100

Table 2.11: Oil recovery after ASP flooding with chemical formulation A

Grid	Oil Recovery (% OOIP)	Oil Recovery (% ROIP)
Vertical Refinement		
43 X 47 X 5	23.8	54
43 X 47 X 10	22.4	51.1
43 X 47 X 19	21	47.8
Areal Refinement		
11 X 12 X 19	14.2	32
22 X 24 X 19	17.3	39.3
43 X 47 X 19	21	47.8

Table 2.12: Average oil saturation in each layer in 43 X 47 X 19 grid (Average oil recovery from each layer in also shown)

Layer	Average Oil Saturation After Waterflooding	Average Oil Saturation After ASP flooding	Average Oil Recovery % ROIP
1	0.5849	0.5024	14.10
2	0.5129	0.4142	19.24
3	0.4725	0.3847	18.58
4	0.4287	0.3373	21.32
5	0.4871	0.3453	29.11
6	0.4796	0.3286	31.48
7	0.4460	0.2667	40.20
8	0.3792	0.1593	57.99
9	0.3459	0.1309	62.16
10	0.3262	0.1165	64.29
11	0.2998	0.1007	66.41
12	0.3006	0.1028	65.80
13	0.2757	0.089	67.72
14	0.2777	0.09323	66.43
15	0.2873	0.08573	70.16
16	0.2838	0.06978	75.41
17	0.2267	0.0356	84.30
18	0.1727	0.02096	87.86
19	0.1498	0.01436	90.41

Table 2.13: Injection scheme for simulations with a normal salinity gradient

Injection well constraints	Rate constraint = 2500 bbl/day (chemical slug, polymer drive and post water flood)
	Rate constraint = 8000 bbl/day (initial water flood)
Production well constraint	Pressure constraint = 300 psi
Waterflood salinity	1.25 meq/ml (67,007 ppm) NaCl
Surfactant slug	0.3 PV
	0.5 v% surfactant
	2000 ppm polymer
	0.7116 meq/ml Na ₂ CO ₃
Polymer drive	1 PV
	1800 ppm polymer
	0.35 meq/ml NaCl
Water postflush	1 PV
	0.0513 meq/ml NaCl

Table 2.14: Injection scheme for simulations with a normal salinity gradient

Grid	Normal Salinity Gradient	
	Oil Recovery (% OOIP)	Oil Recovery (% ROIP)
Areal Refinement		
11 X 12 X 19	21.7	48.7
22 X 24 X 19	23.9	54.3
43 X 47 X 19	26.4	59.9

Table 2.15: Pseudo CSEL values and recoveries for different grids

	Recovery (%ROIP)	Pseudo CSEL meq/ml	Recovery (%ROIP) after shift in CSEL
11 X 12 X 19	32.0	0.15	47.32
22 X 24 X 19	39.3	0.35	46.56
43 X 47 X 19	47.8	0.50	47.80
43 X 47 X 10	51.1	0.60	47.90
43 X 47 X 5	54.0	0.65	49.00
22 X 24 X 10	40.9	0.35	47.90

Table 2.16: Pseudo IFT parameters and recoveries for different grids

	Recovery (%ROIP)	C	a	Recovery (%ROIP) after IFT adjustment
11 X 12 X 19	32.0	0.003	100	47.25
22 X 24 X 19	39.3	0.03	100	48.80
43 X 47 X 19	47.8	0.3	10	47.80
43 X 47 X 10	51.1	0.3	1	47.25
43 X 47 X 5	54.0	0.3	1	49.00
22 X 24 X 10	40.9	0.3	100	45.00

Table 2.17: Core and fluid properties for coreflood with chemical formulation B

Core Properties	
Porosity	0.33
Permeability, md	1428
Temperature, ° F	185
Length, cm	30
Diameter, cm	5.12
Residual water saturation	0.35
Residual oil saturation	0.249
Water end point relative permeability	0.082
Oil endpoint relative permeability	0.85
Fluid Properties	
Water viscosity, cp	3.4
Oil viscosity, cp	0.37

Table 2.18: Phase behavior parameters for simulations with chemical formulation B

Phase Behavior Parameters	
Height of binodal curve at zero salinity, HBNC 70	0.045
Height of binodal curve at optimum salinity, HBNC 71	0.019
Height of binodal curve at twice optimum salinity, HBNC 72	0.045
Lower critical salinity window, CSEL	0.1003
Upper critical salinity window	0.1997
Optimum salinity	0.15
Polymer viscosity parameters	
SSLOPE	-0.4
AP1	30
AP2	280
AP3	350
GAMMAC	4
GAMHF	35
POWN	1.55
Microemulsion viscosity parameters	
ALPHA1	0.2
ALPHA2	2.5
ALPHA3	0.1
ALPHA4	0.1
ALPHA5	0.1
Adsorption Parameters	
AD31	3.1
AD32	0.25
B3D	1000
AD41	1
AD42	0
B4D	100

Table 2.19: Injection scheme for simulations with chemical formulation B

Alkali-Surfactant-Polymer Slug	
Slug size	0.2 PV
Surfactant mixture and concentration	2 % Surfactant ; 0.3 % Cosolvent
Polymer concentration	2500 ppm
Salinity	11,500 ppm sodium carbonate
Polymer Drive1	
Drive size	0.2 PV
Polymer concentration	2200 ppm
Salinity	9800 ppm TDS
Polymer Drive2	
Drive size	1.2 PV
Polymer concentration	1800 ppm
Salinity	2865 ppm TDS
Post Waterflood	
Post flush	0.6 PV
Salinity	2865 ppm TDS

Table 2.20: Oil recovery after ASP flooding simulations with chemical formulation B

Grid	Oil Recovery (% OOIP)	Oil Recovery (% ROIP)
Vertical Refinement		
43 X 47 X 5	28.62	65.4
43 X 47 X 10	27.62	62.9
43 X 47 X 19	26.28	58.8
Areal Refinement		
11 X 12 X 19	18.67	42.0
22 X 24 X 19	22.59	51.1
43 X 47 X 19	26.28	58.8
86 X 94 X 19	26.9	61.0

Table 2.21: Pseudo CSEL values and recoveries for different grids (Formulation B)

	Recovery (%ROIP)	Pseudo CSEL meq/ml	Recovery (%ROIP) after shift in CSEL
11 X 12 X 19	42.3809	0.06	59.02
22 X 24 X 19	50.3032	0.085	58.4979
43 X 47 X 19	59.6556	0.10	59.6556
43 X 47 X 10	62.2434	0.105	59.474
43 X 47 X 5	64.9674	0.11	59.02
22 X 24 X 10	52.7094	0.09	59.02

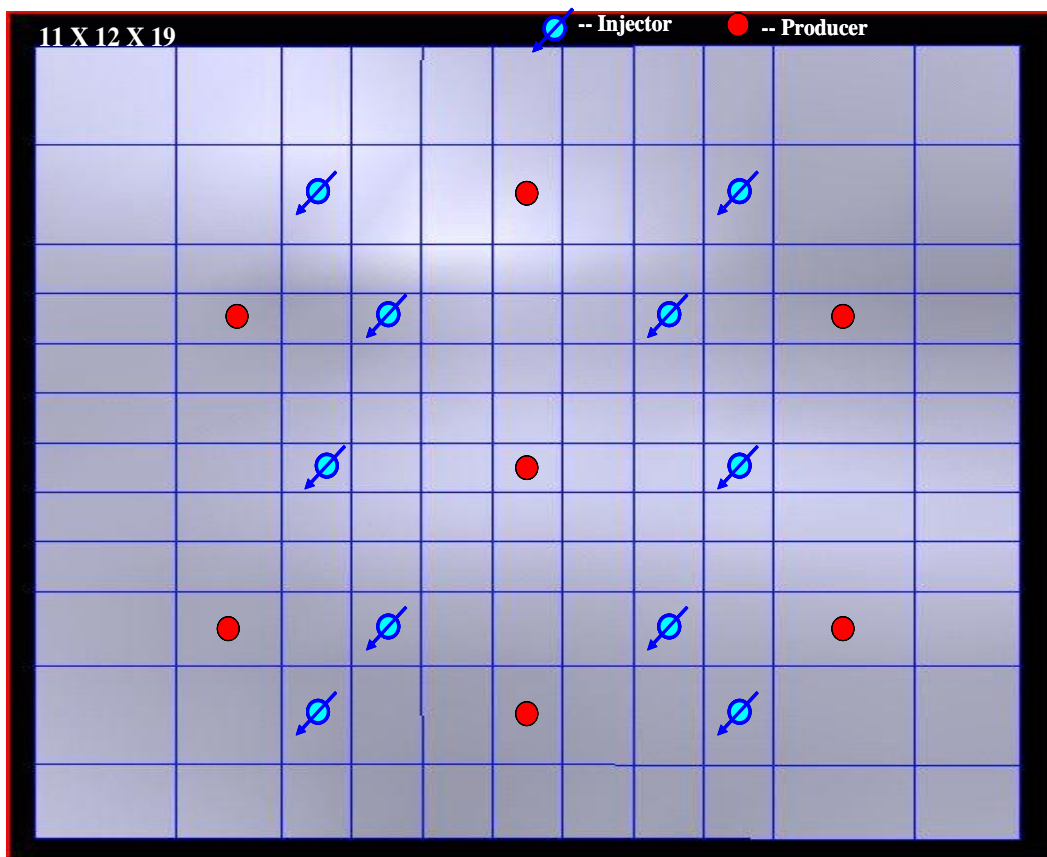


Figure 2.1: Areal view of 11 X 12 X 19 grid.

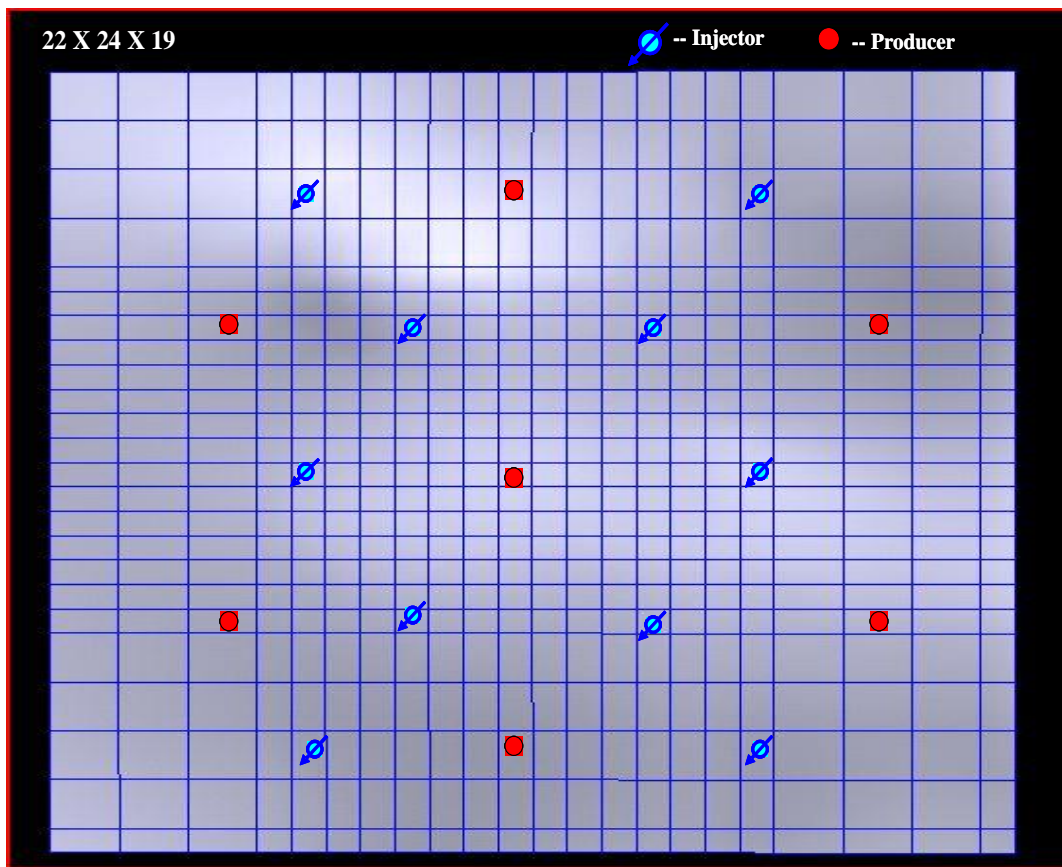


Figure 2.2: Areal view of 22 X 24 X 19 grid.

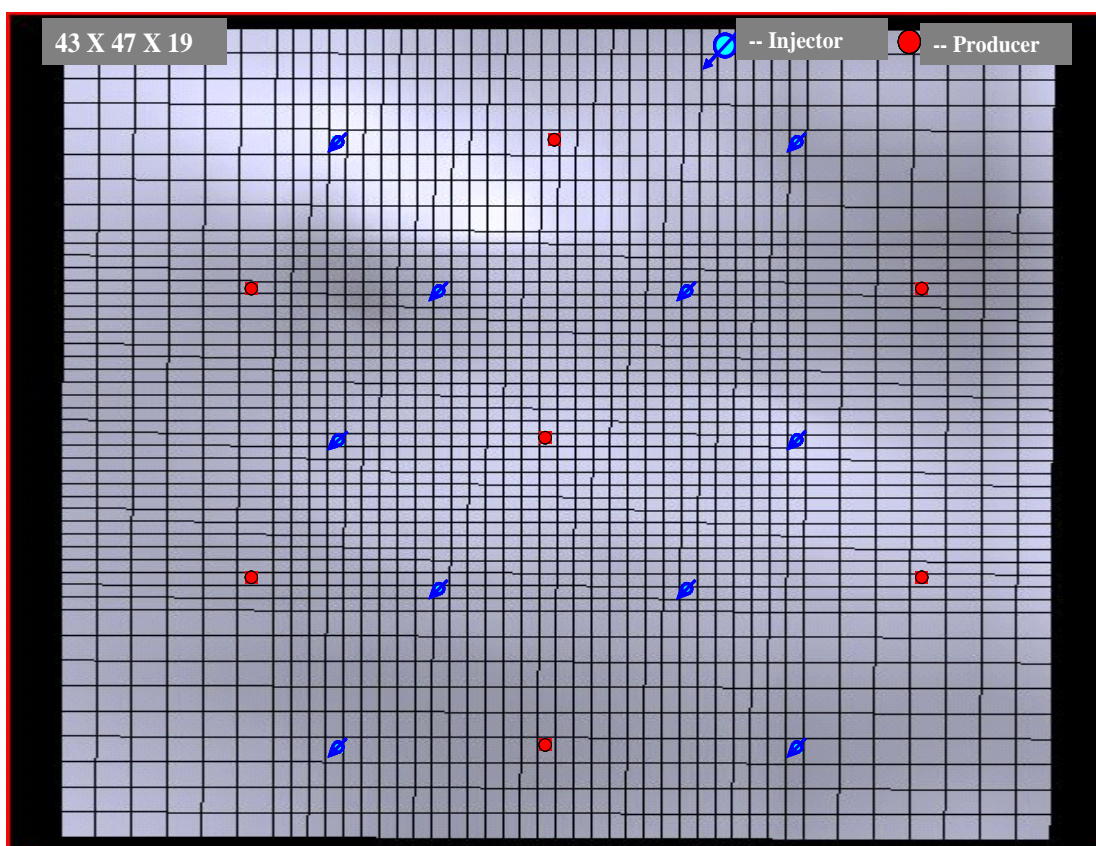


Figure 2.3: Areal view of 43 X 47 X 19 grid.

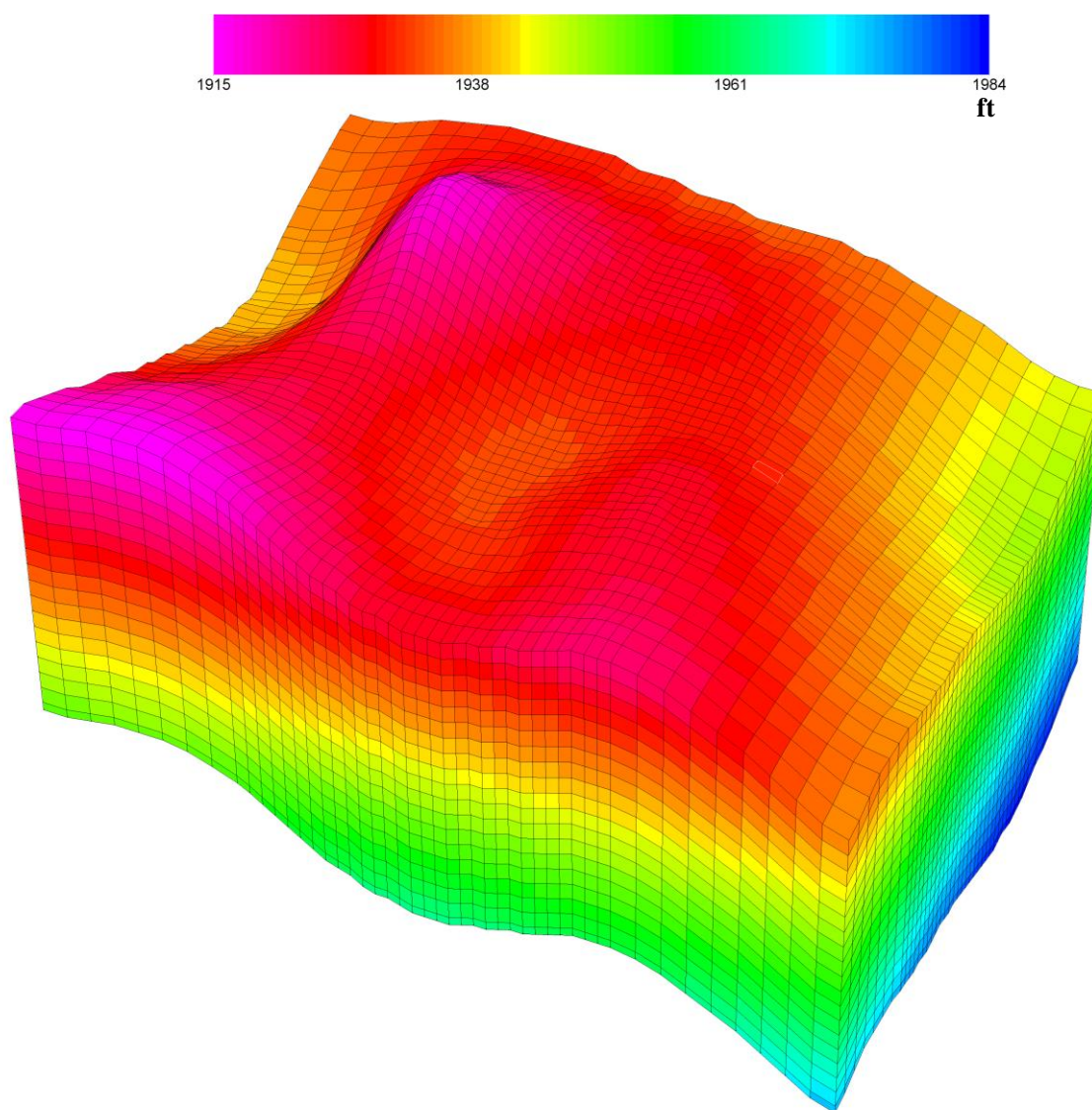


Figure 2.4: 3-D view of the reservoir showing the depth from the surface, ft

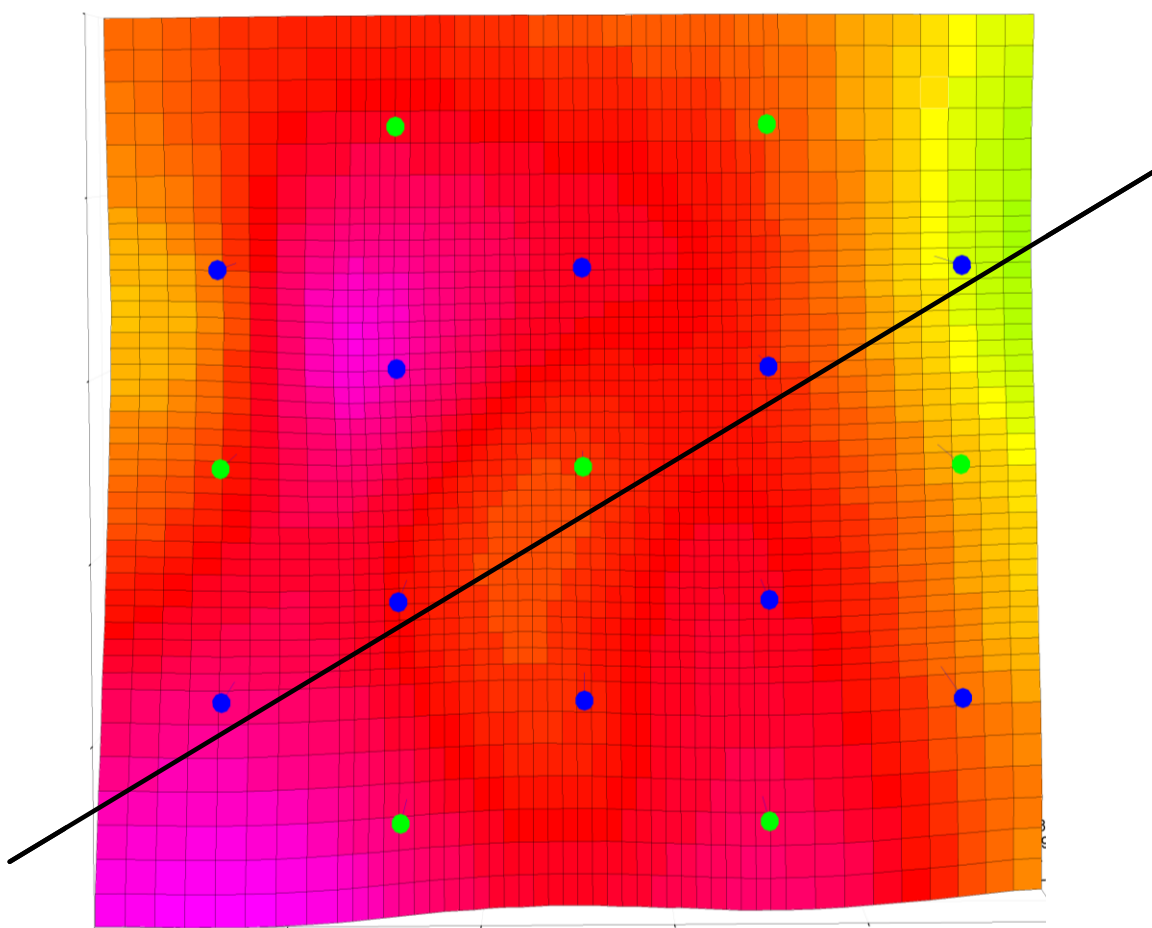


Figure 2.5: Areal view of 43 X 47 X 19 grid showing the cross sectional plane used for Figure 2.6

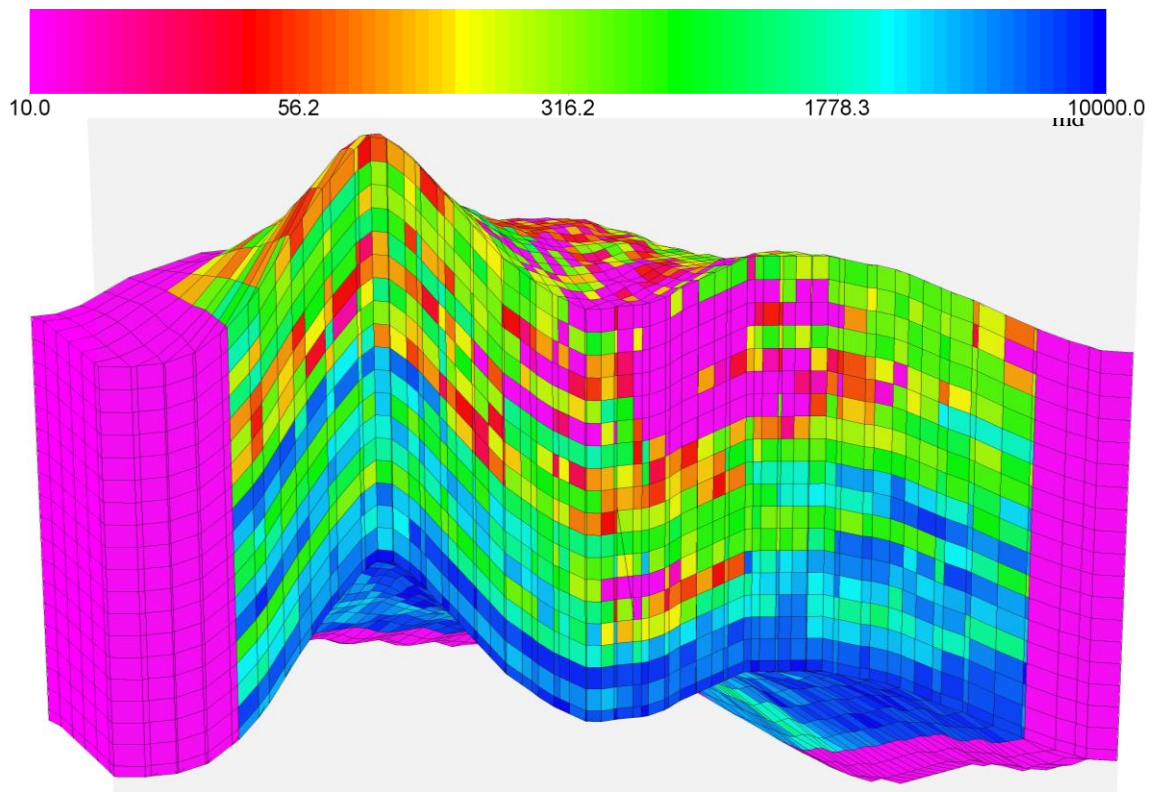


Figure 2.6: Permeability field of 43 X 47 X 19 grid (cross section), md

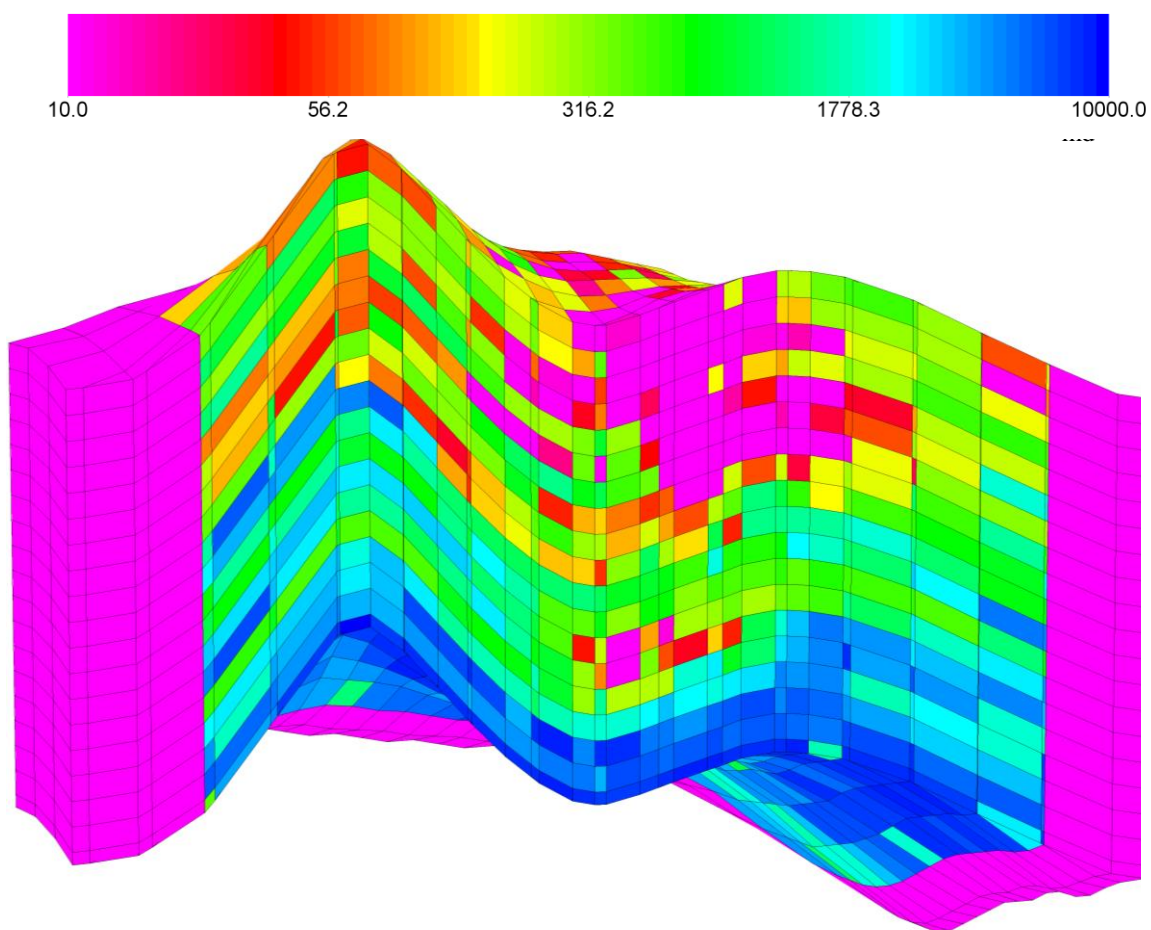


Figure 2.7: Permeability field of 22 X 24 X 19 grid (cross section), md

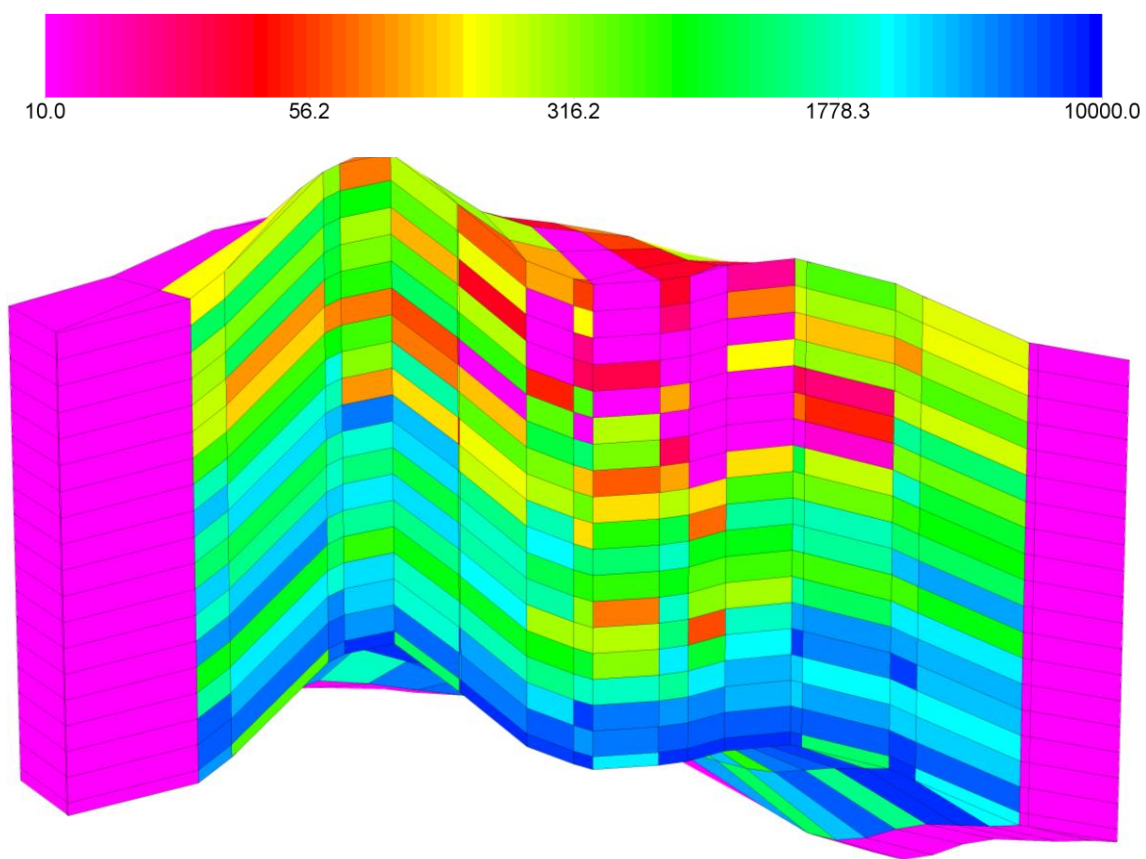


Figure 2.8: Permeability field of 11 X 12 X 19 grid (cross section), md

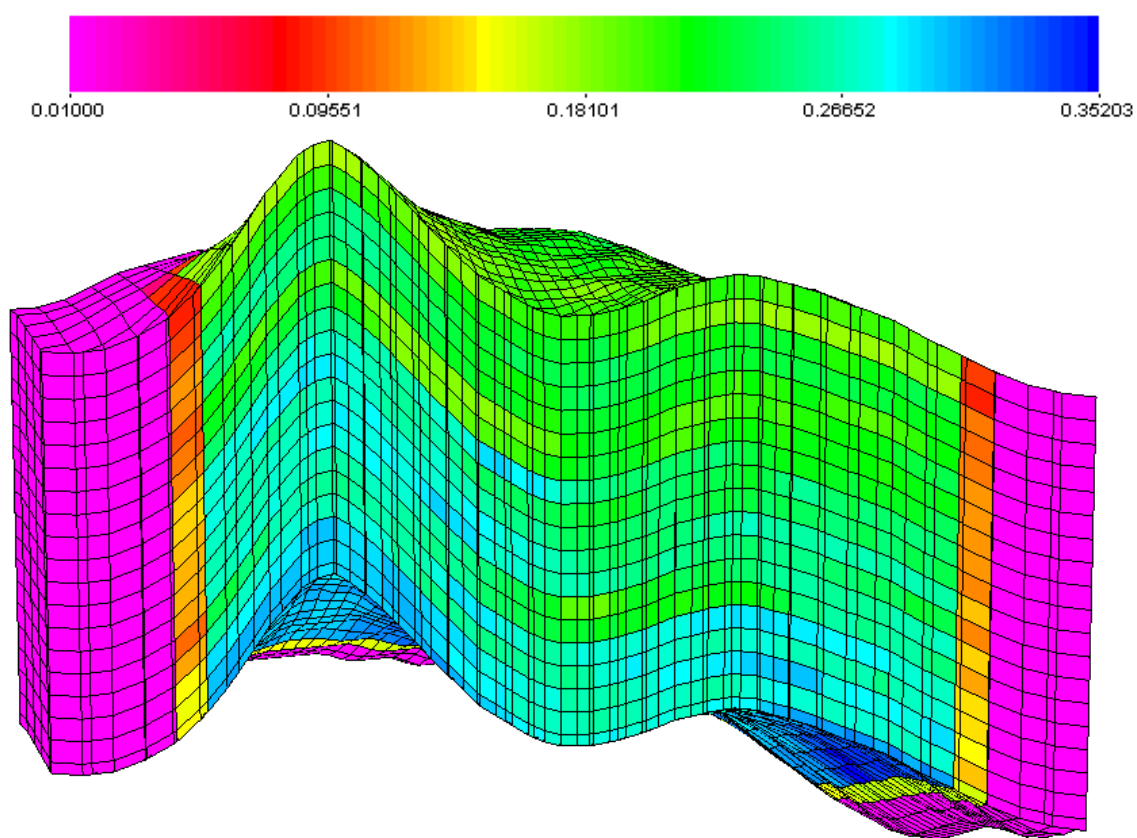


Figure 2.9: Porosity distribution of 43 X 47 X 19 grid (cross section)

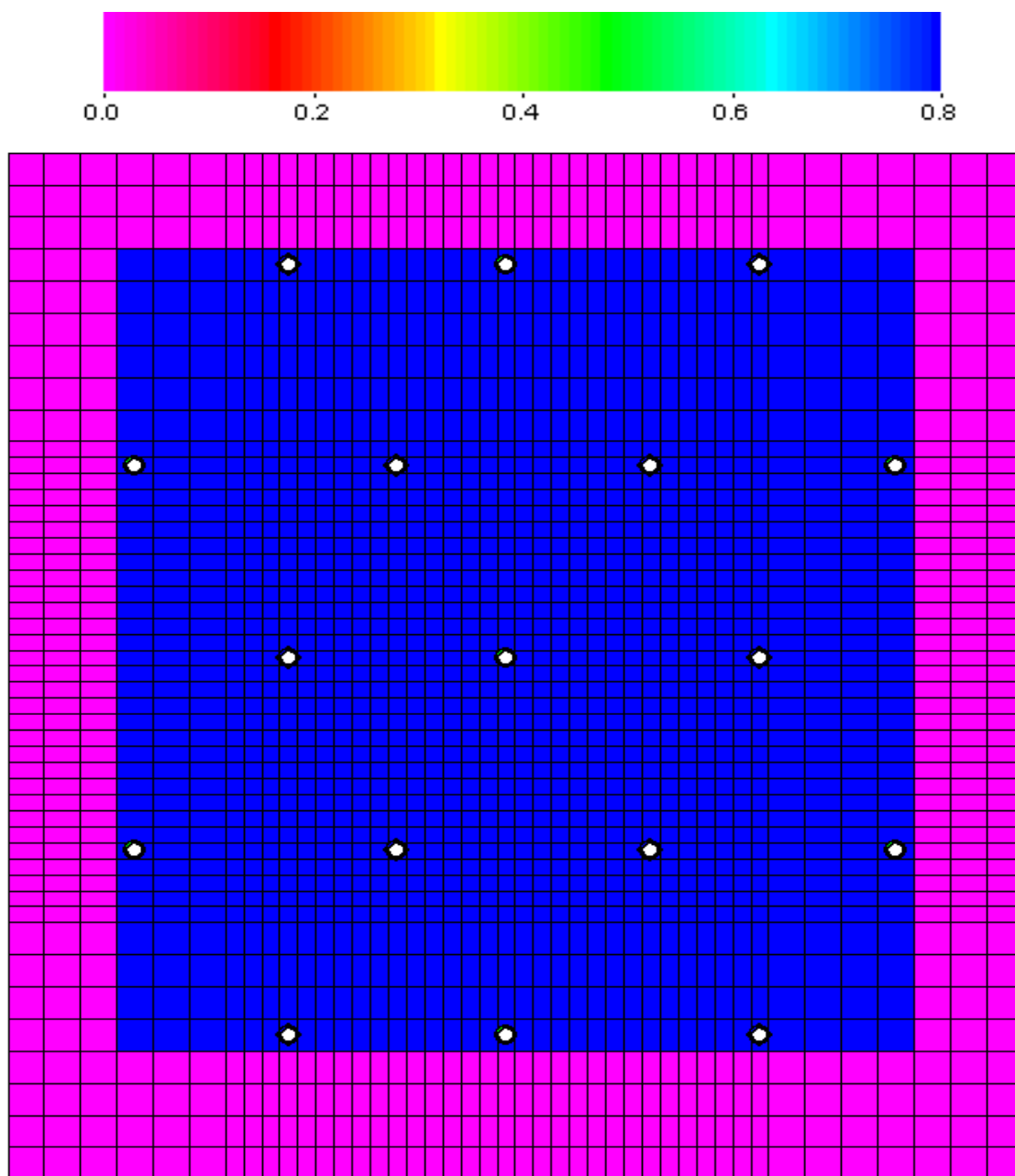


Figure 2.10: Initial oil saturation in layer 19 of 43 X 47 X 19 (inactive area around the model shown).

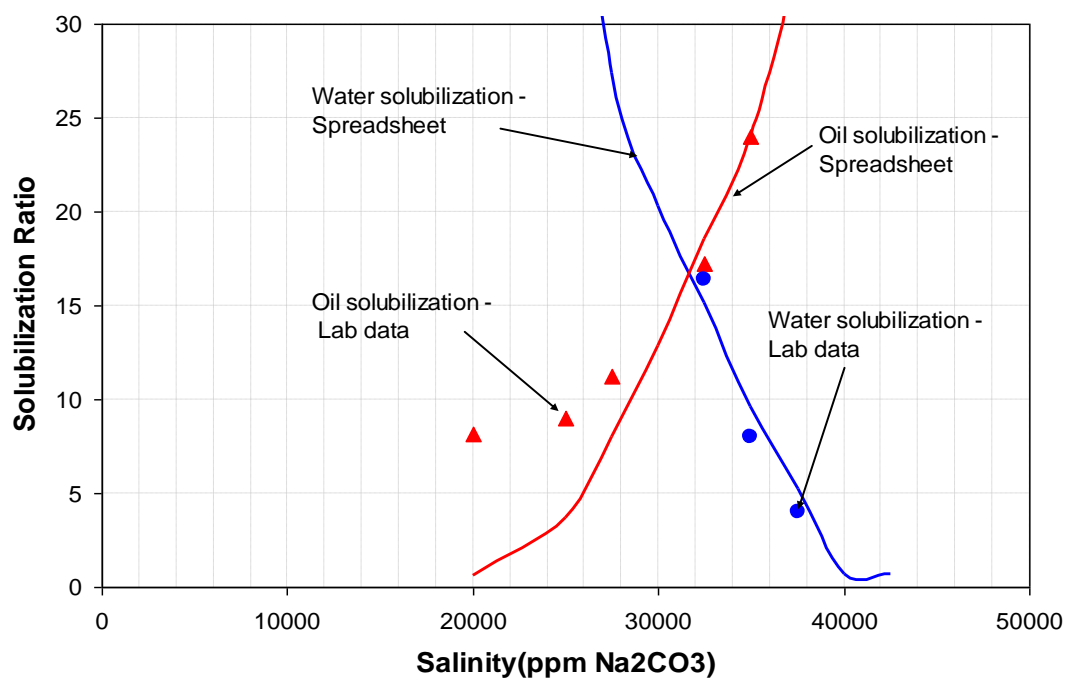


Figure 2.11: Comparison of model with experimental solubilization ratio data

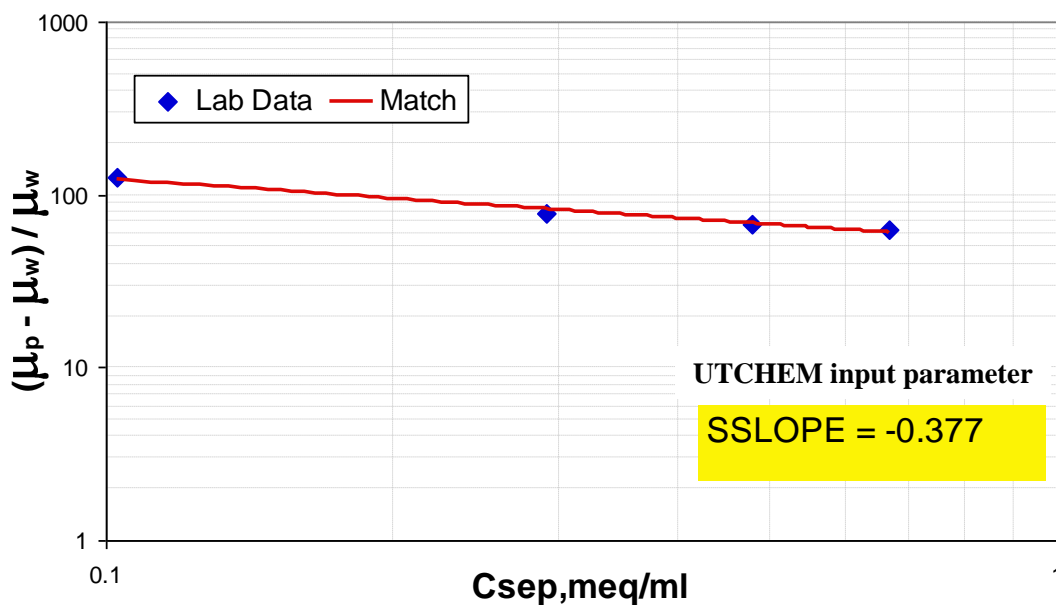


Figure 2.12: Comparison of lab data of salinity dependence on polymer viscosity with UTCHEM model

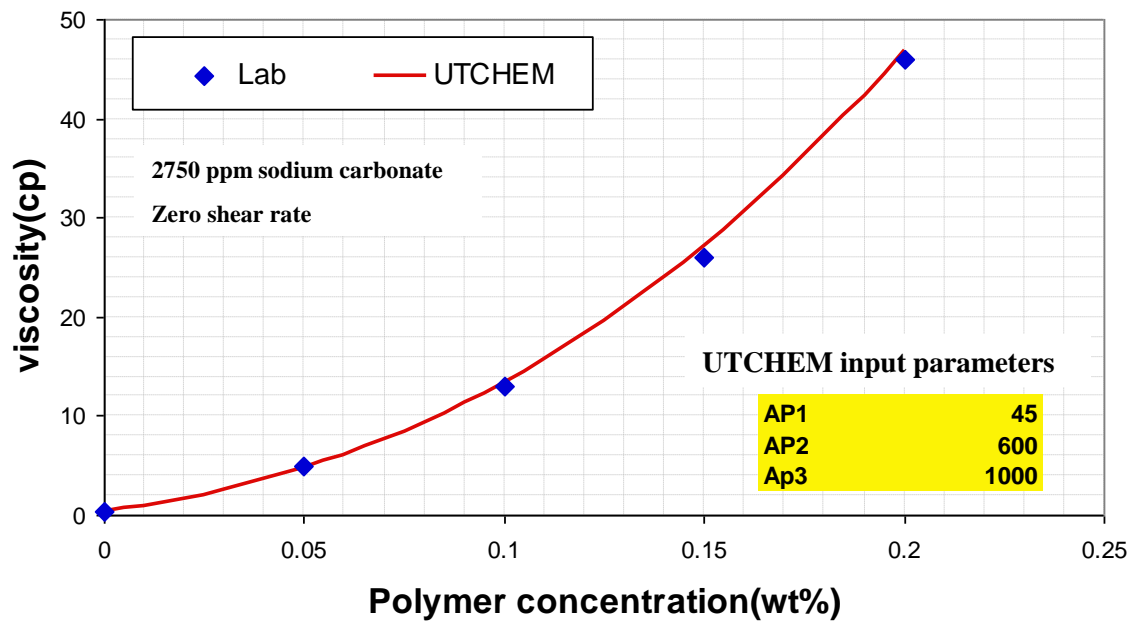


Figure 2.13: Comparison of model with experimental polymer viscosity as a function of polymer concentration

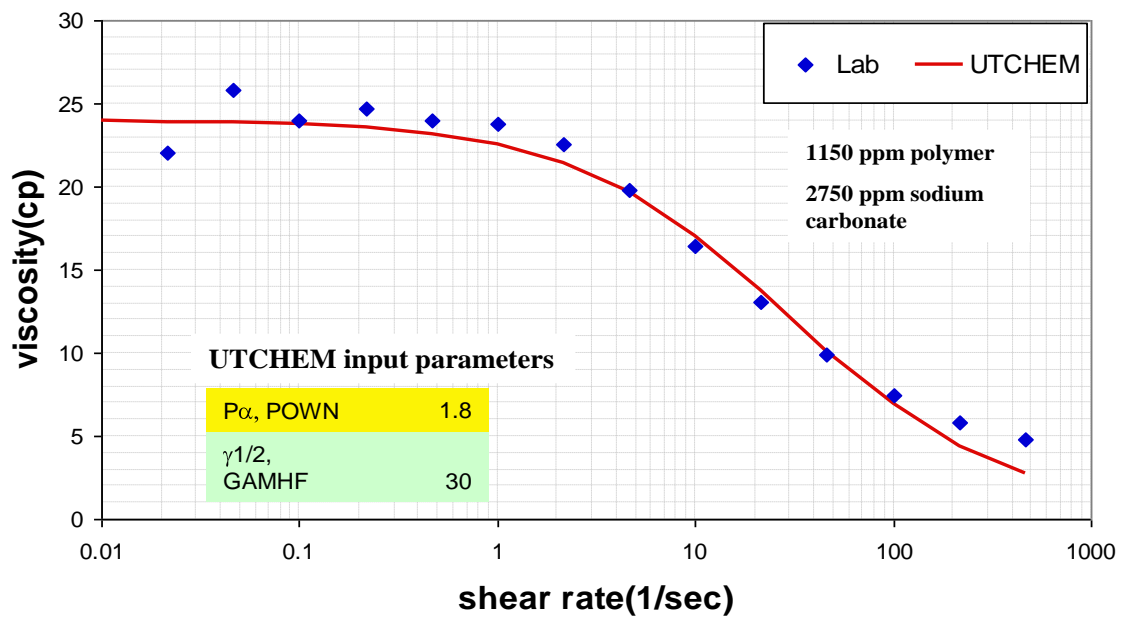


Figure 2.14: Comparison of model with experimental polymer viscosity data

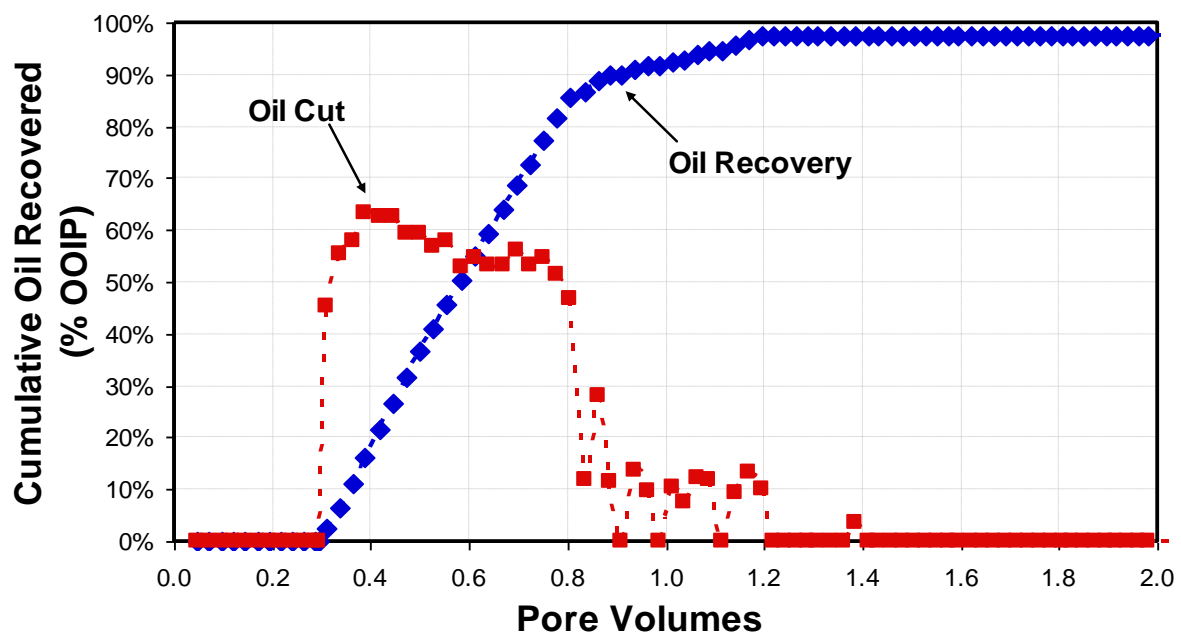


Figure 2.15: Cumulative oil recovery measured from the coreflood M9.

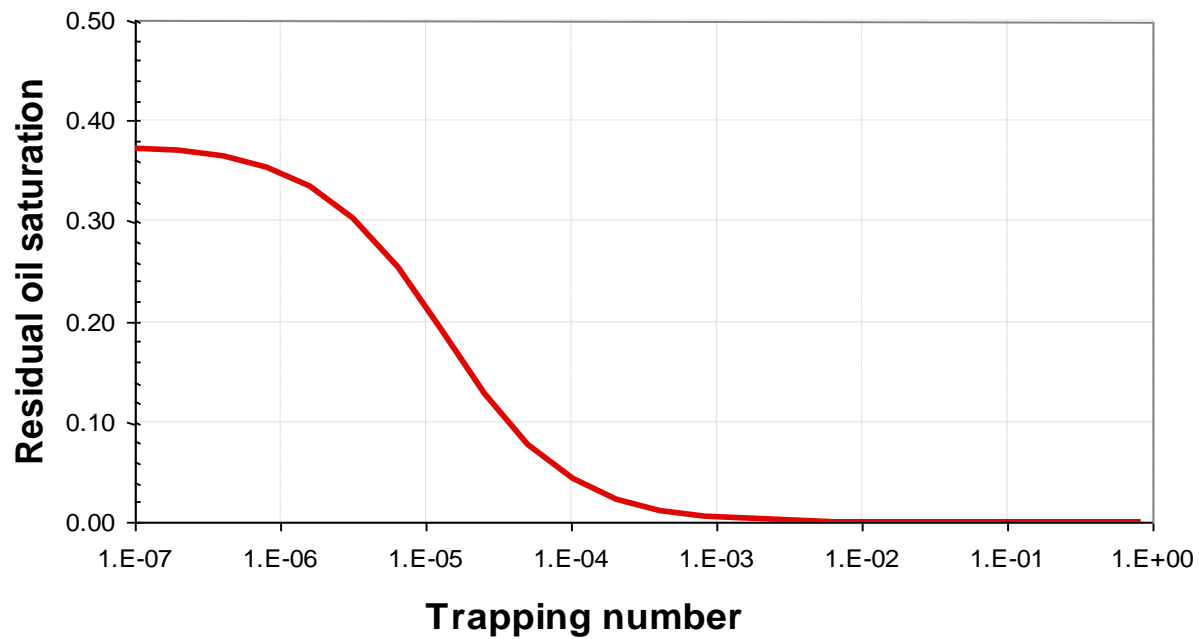


Figure 2.16: Capillary desaturation curve for coreflood M9 simulation

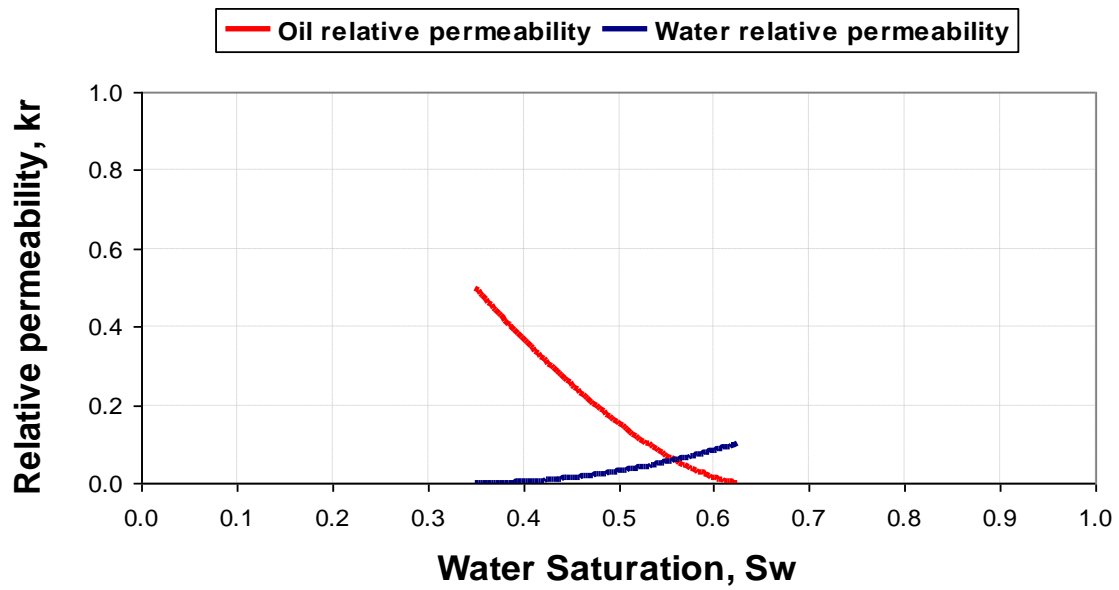


Figure 2.17: Oil-Water relative permeability curves for the reservoir rock used in coreflood M9

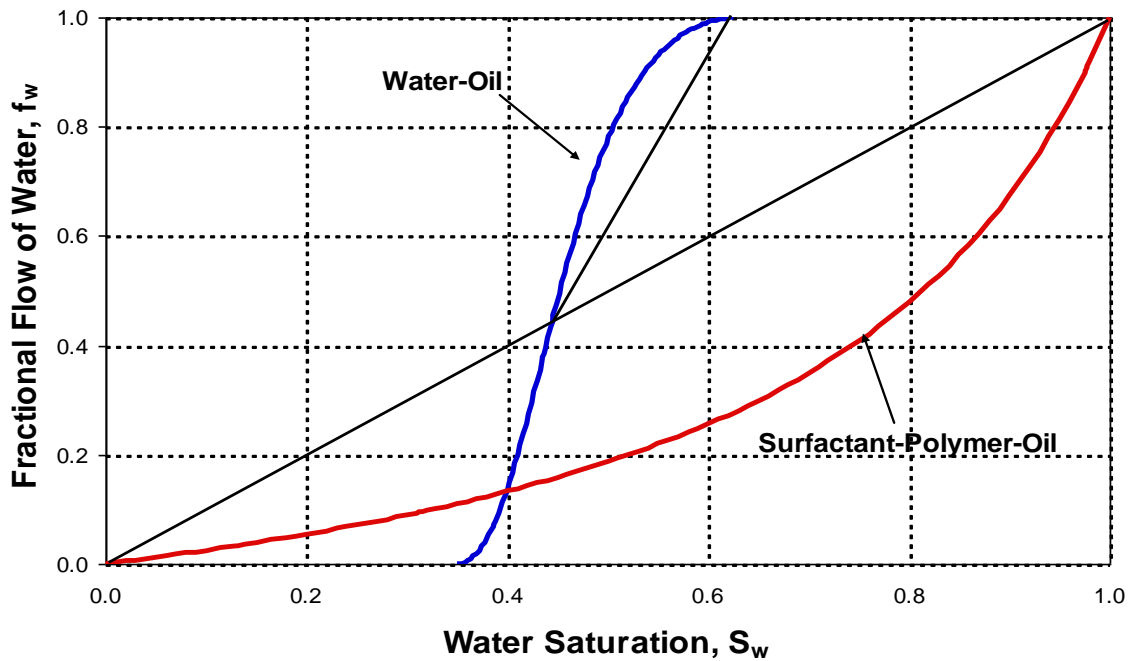


Figure 2.18: Fractional flow plot for water and ASP coreflood M9 neglecting adsorption

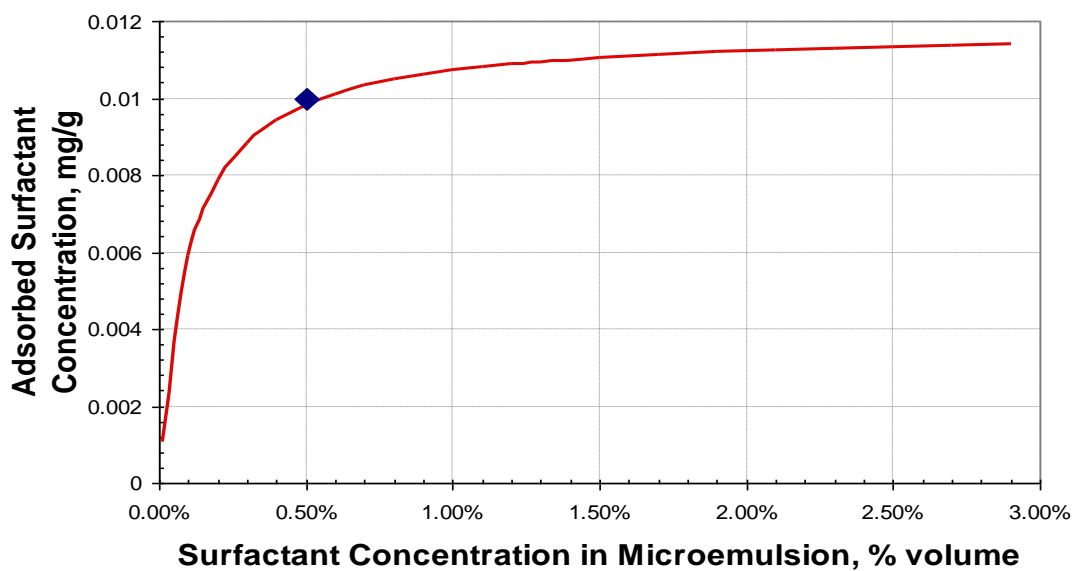


Figure 2.19: Surfactant adsorption value measured in the coreflood M9 matched Langmuir type adsorption model in UTCHEM.

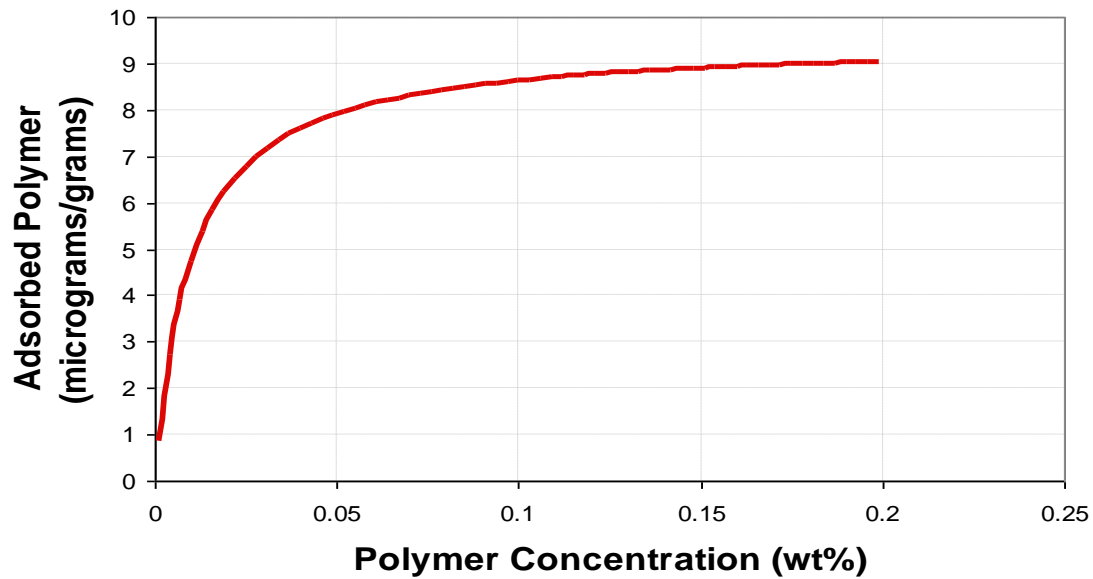


Figure 2.20: Polymer adsorption using Langmuir type adsorption model in UTCHEM.

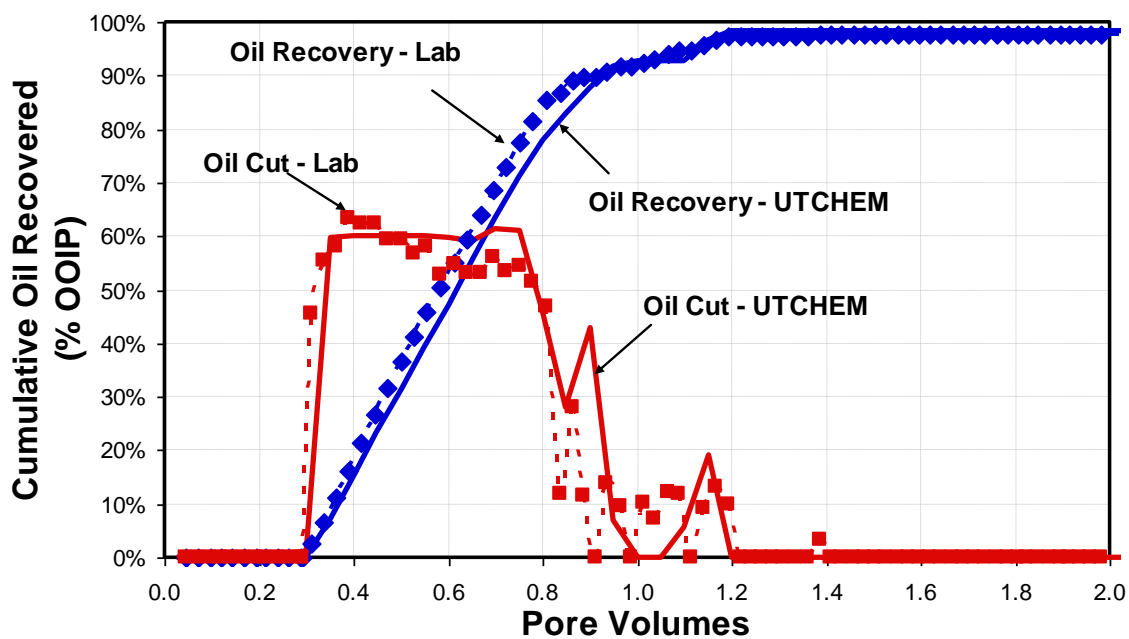


Figure 2.21: Oil recovery match of coreflood M9 using UTCHEM.

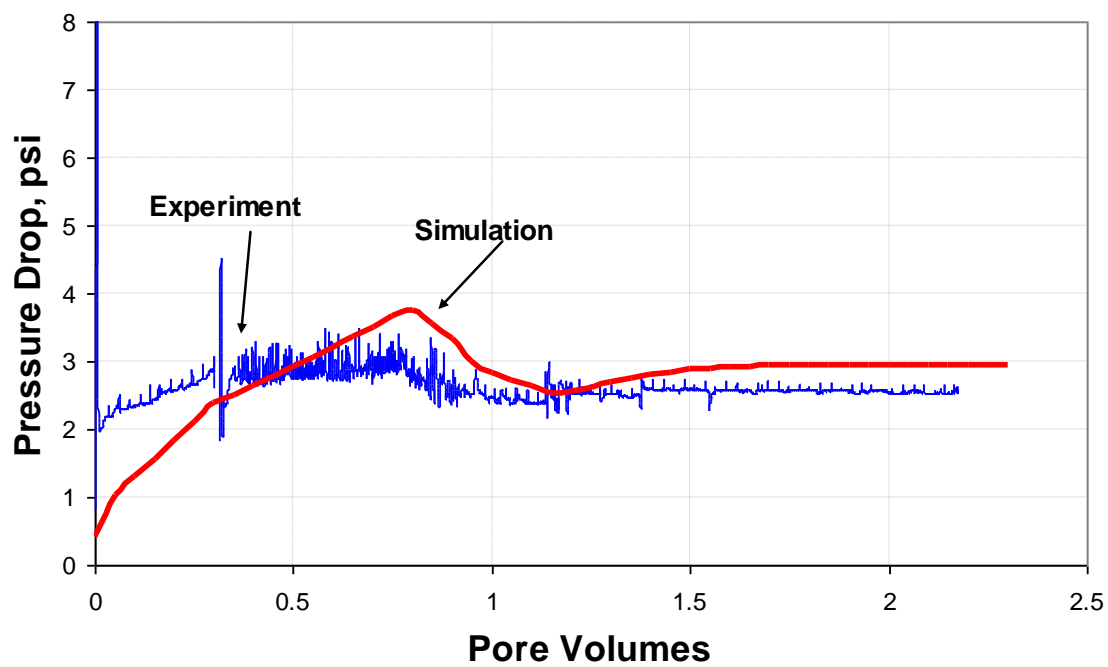


Figure 2.22: Match of pressure drop from coreflood M9 experiment using UTCHEM.

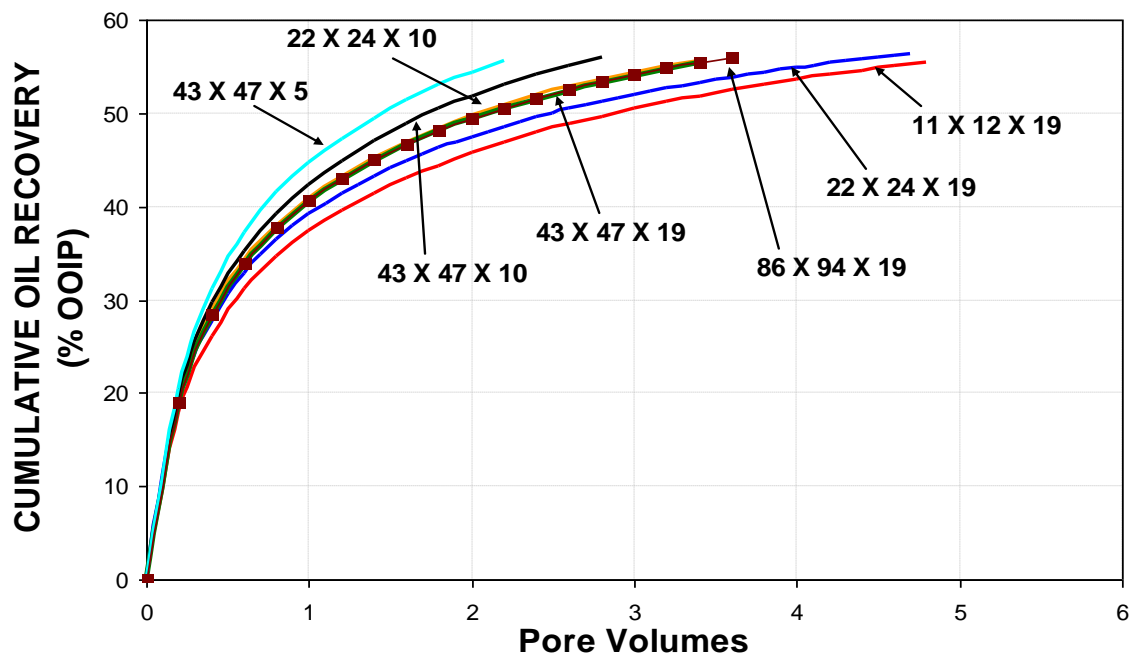


Figure 2.23: Cumulative oil recovery for all the models during Waterflooding

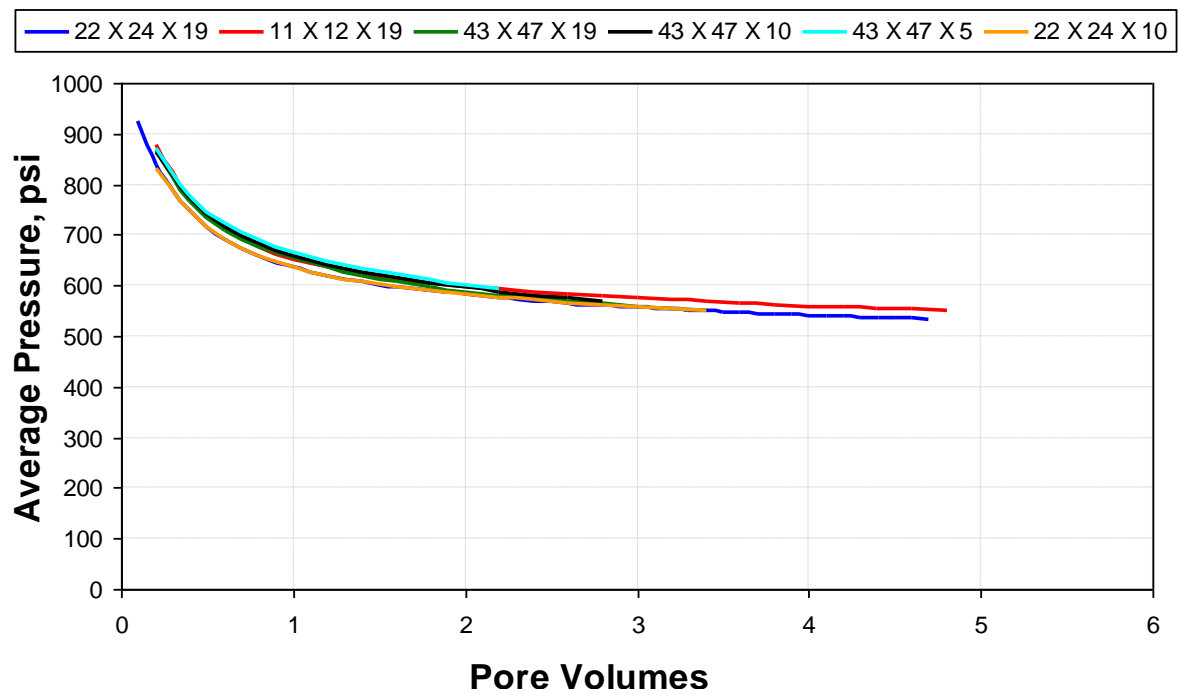


Figure 2.24: Average reservoir pressure for all the models during water flooding

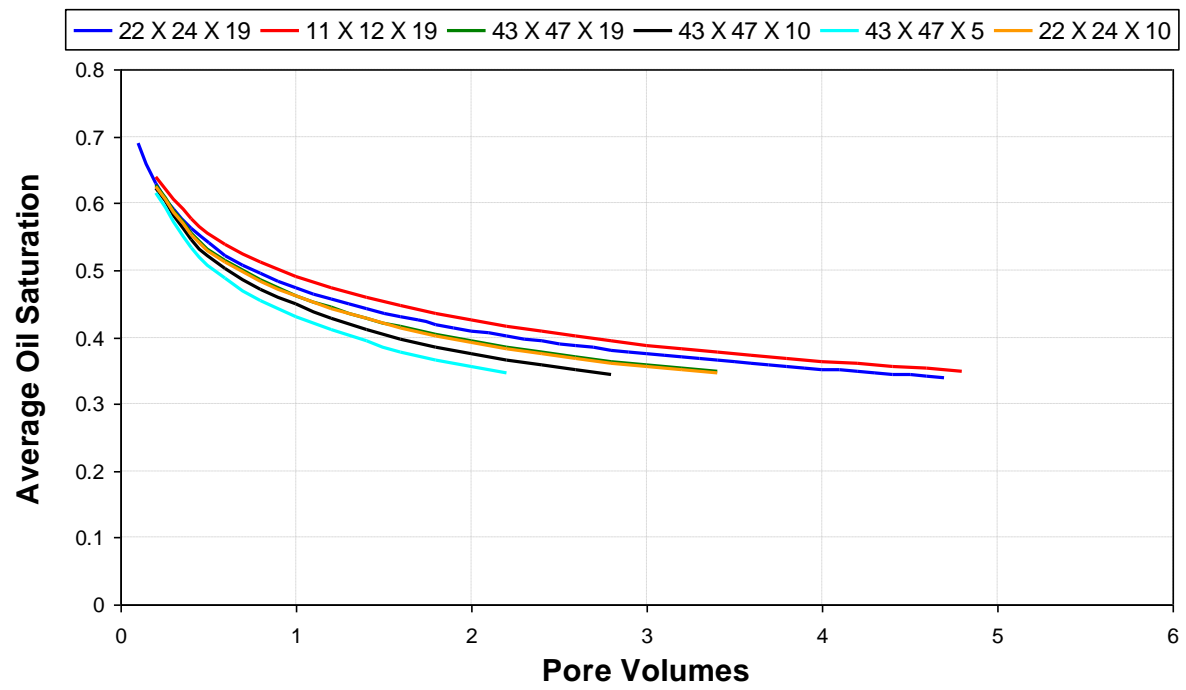


Figure 2.25: Change in average oil saturation of all the models during waterflooding

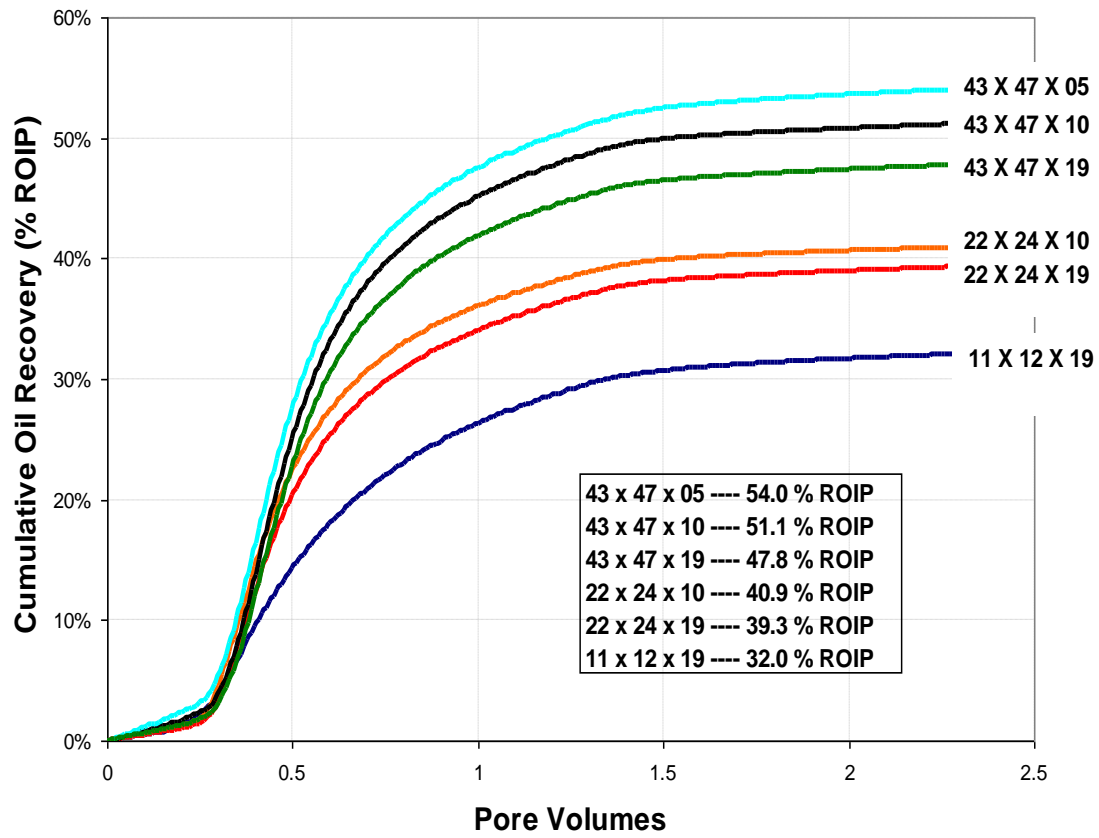


Figure 2.26: Cumulative oil recovery in terms of percentage remaining oil in place (% ROIP) for ASP flood simulations for all the grid block models.

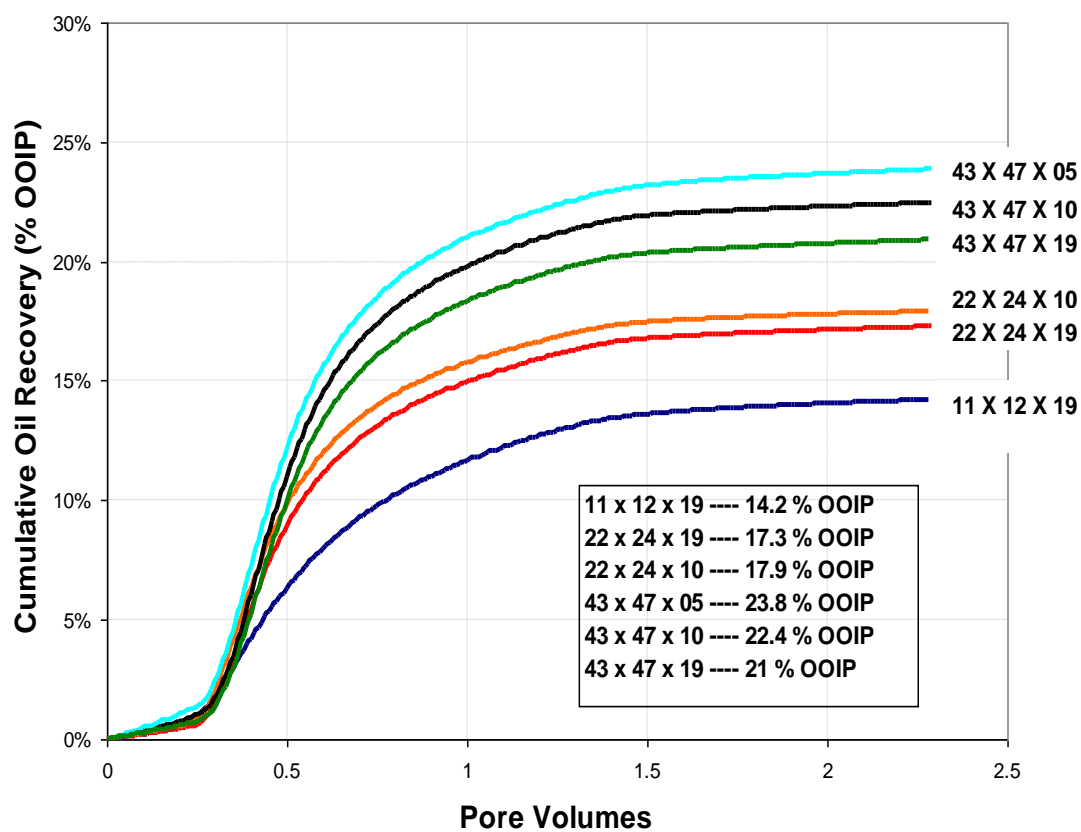


Figure 2.27: Cumulative oil recovery in terms of percentage original oil in place (% OOIP) for ASP flood simulations for all the grid block models.

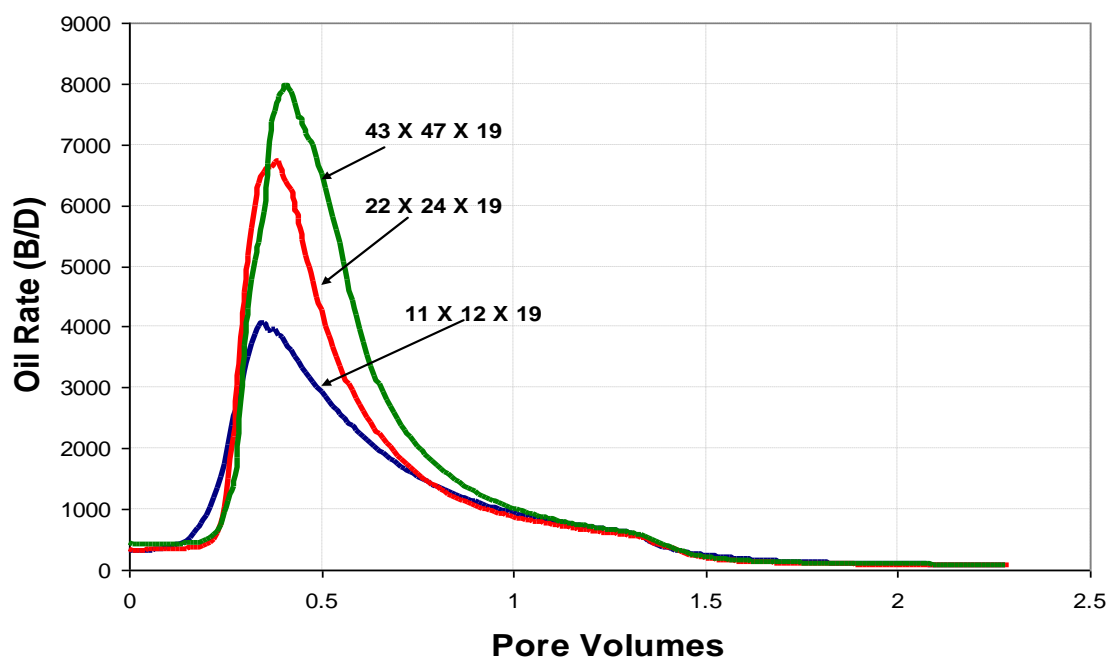


Figure 2.28: Oil rate for ASP flood simulations of grids with areal coarsening.

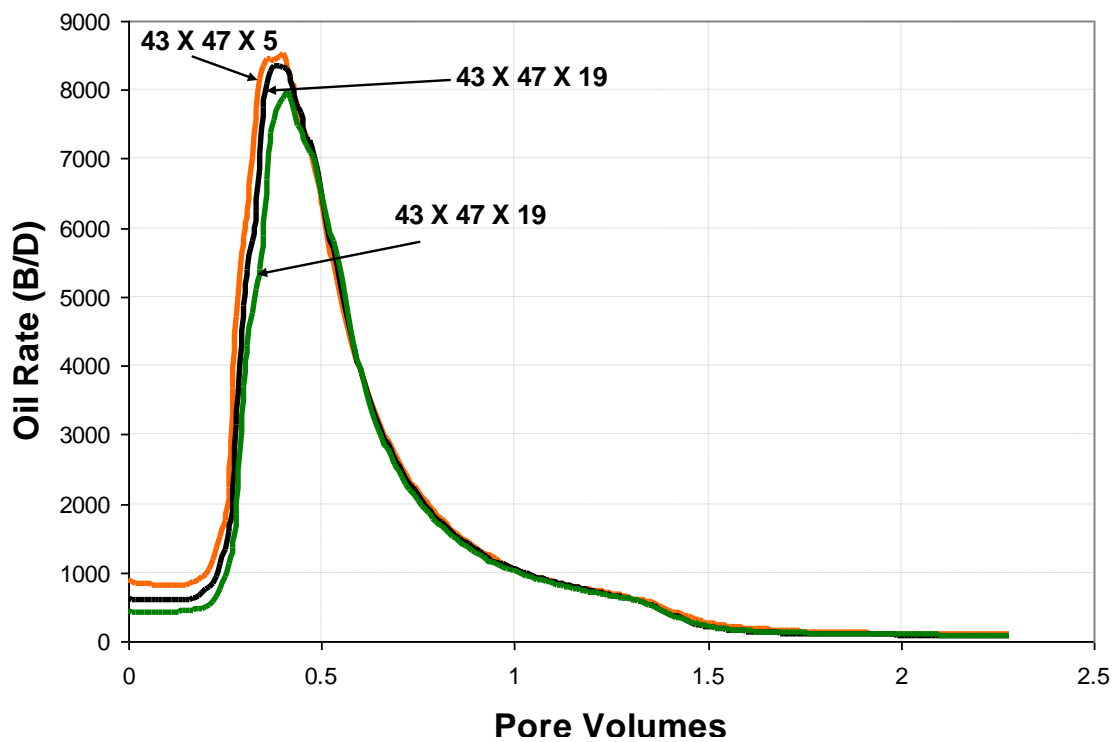


Figure 2.29: Oil rate for ASP flood simulations of grids with vertical coarsening.

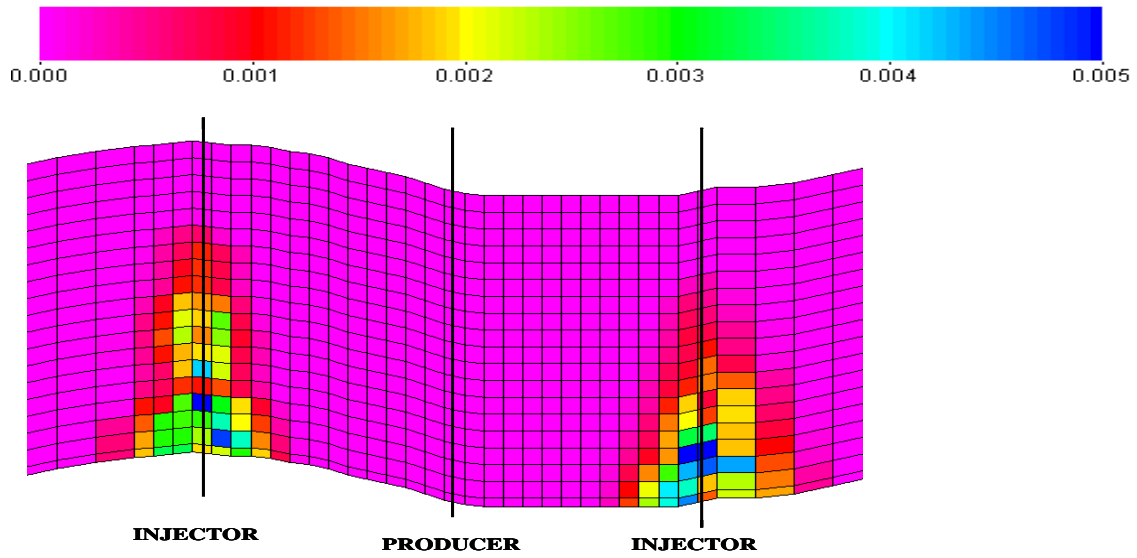


Figure 2.30: Surfactant concentration of 43 X 47 X 19 grid after 0.1 PV, volume fraction

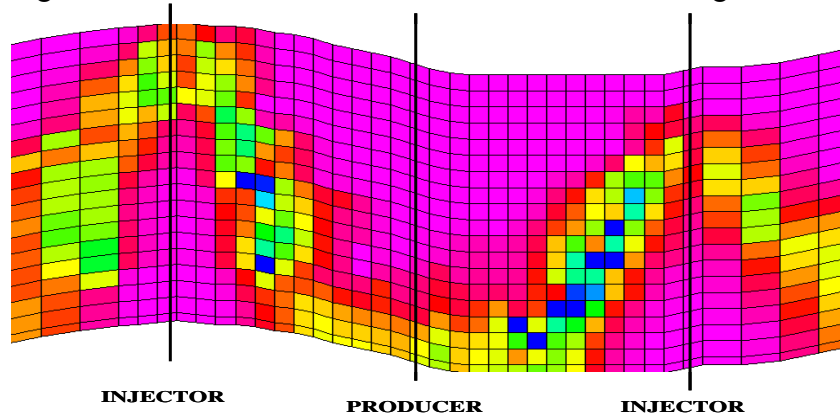


Figure 2.31: Surfactant concentration of 43 X 47 X 19 grid after 0.5 PV, volume fraction

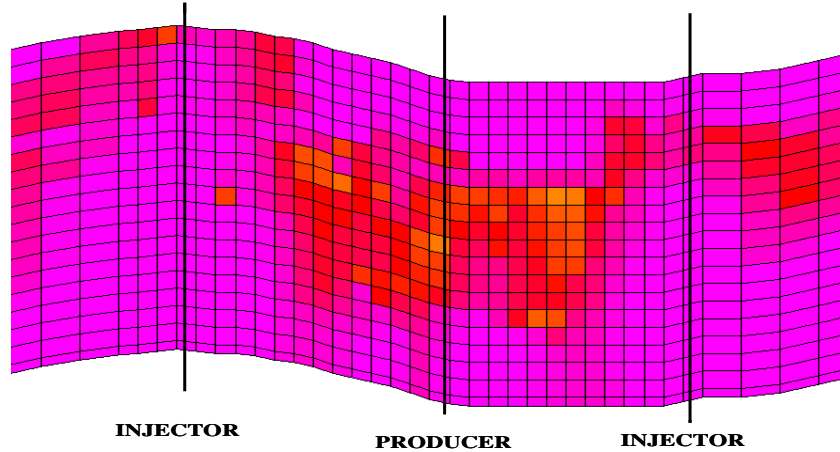


Figure 2.32: Surfactant concentration of 43 X 47 X 19 grid after 2.3 PV, volume fraction

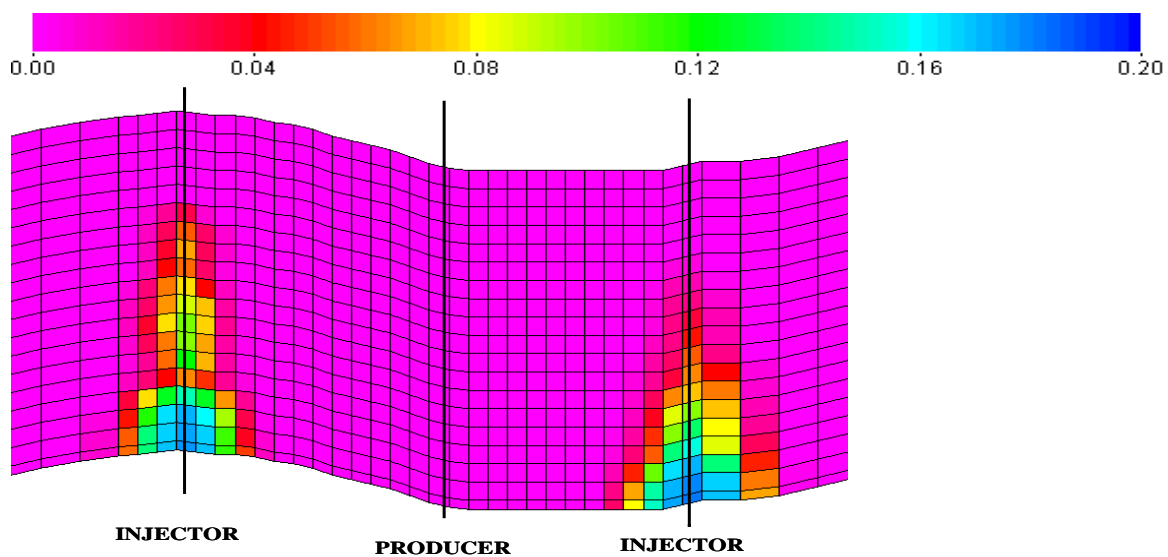


Figure 2.33: Polymer concentration of 43 X 47 X 19 grid after 0.1 PV, % weight

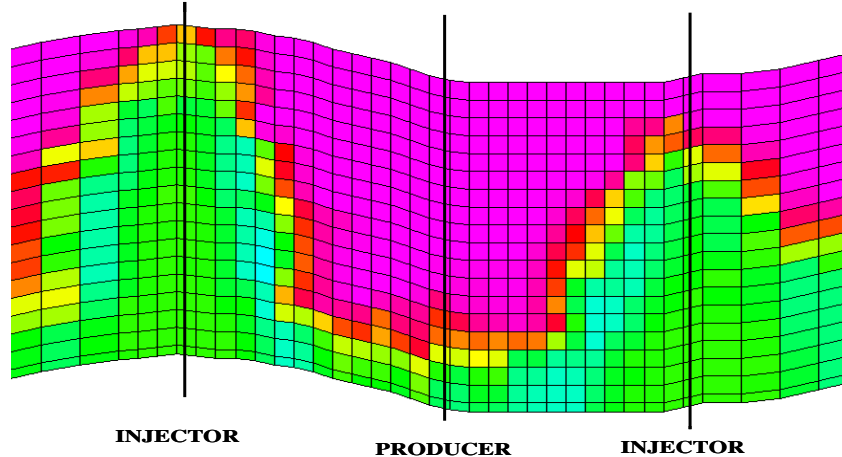


Figure 2.34: Polymer concentration of 43 X 47 X 19 grid after 0.5 PV, % weight

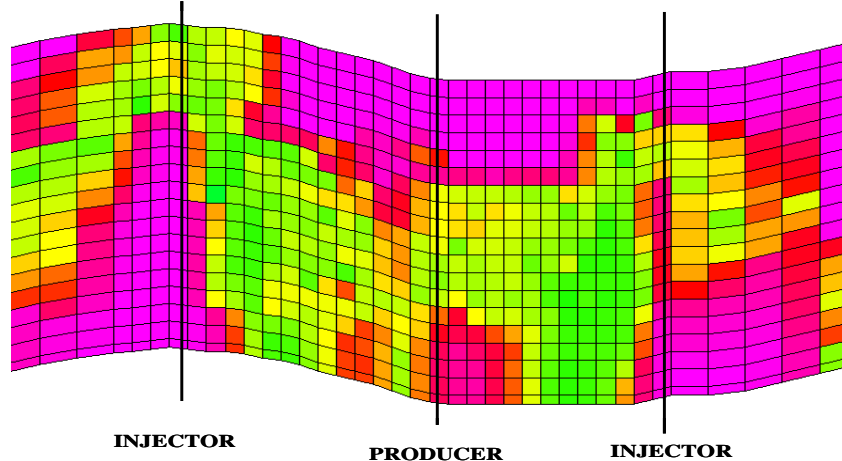


Figure 2.35: Polymer concentration of 43 X 47 X 19 grid after 2.3 PV, % weight

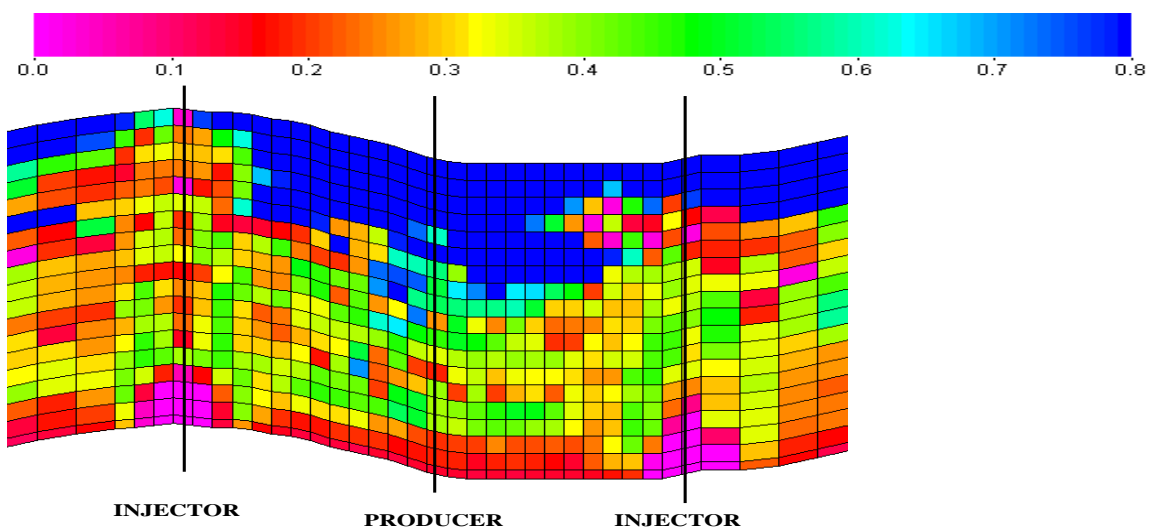


Figure 2.36: Oil saturation of 43 X 47 X 19 grid after 0.1 PV, volume fraction

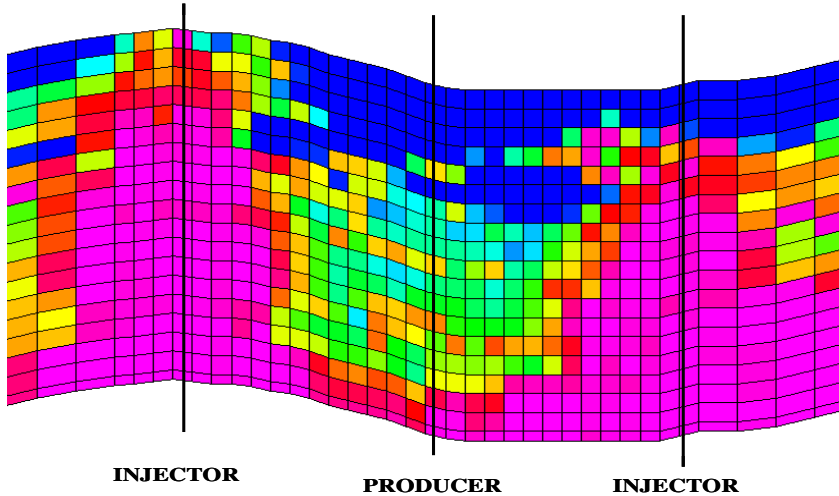


Figure 2.37: Oil saturation of 43 X 47 X 19 grid after 0.5 PV, volume fraction

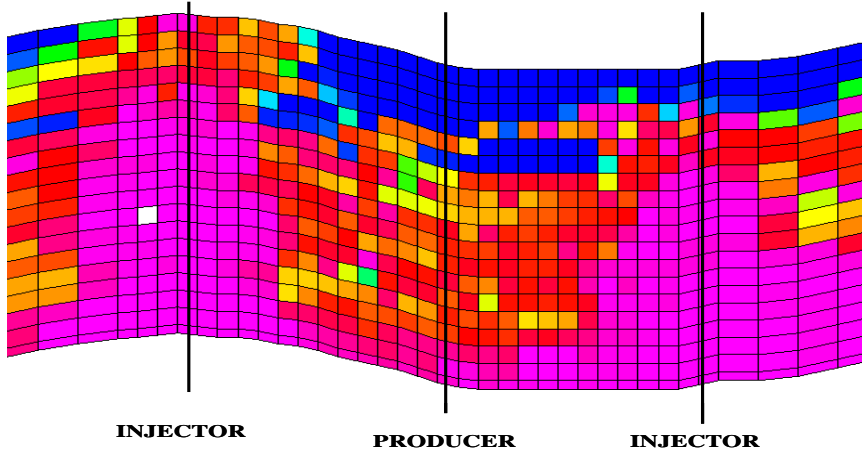


Figure 2.38: Oil saturation of 43 X 47 X 19 grid after 2.3 PV, volume fraction

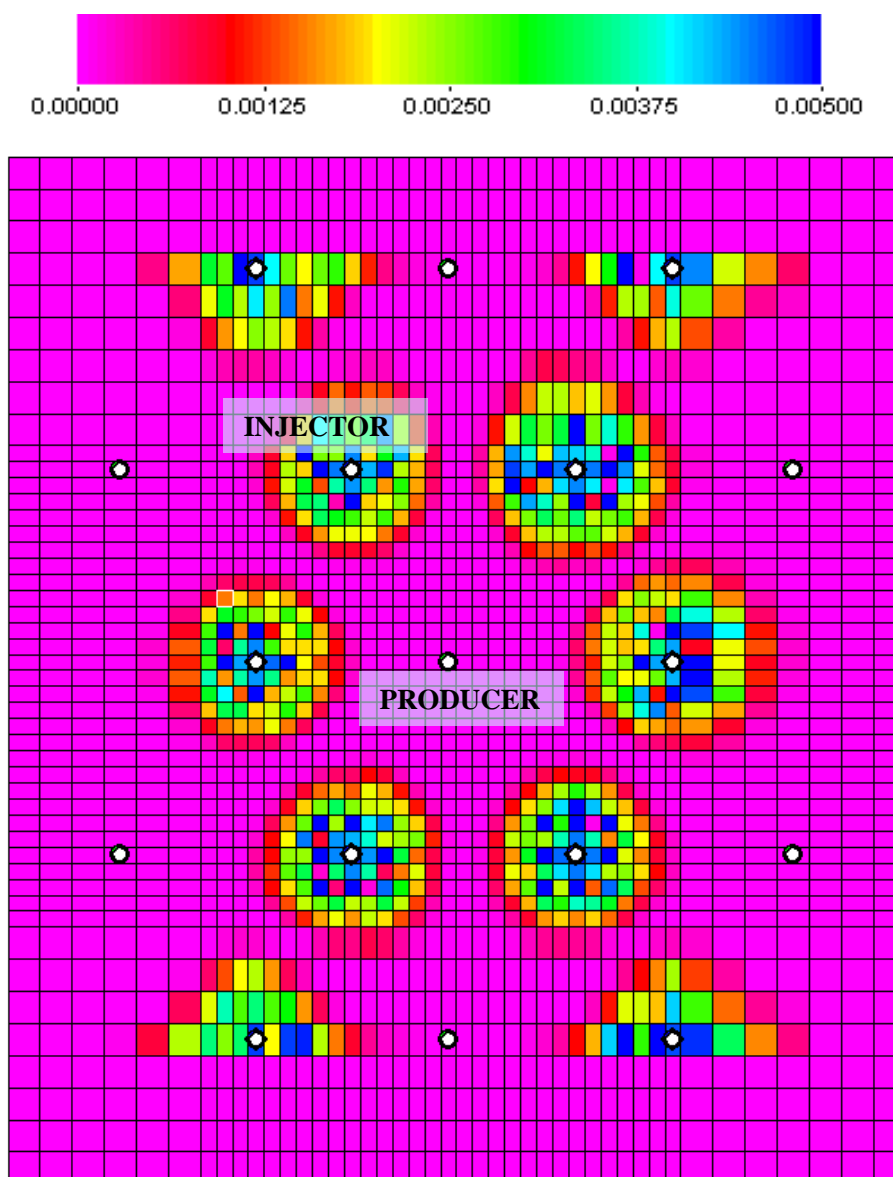


Figure 2.39: Surfactant concentration profile for layer 19 of 43 X 47 X 19 grid after 0.1 PV ASP slug injection, volume fraction.

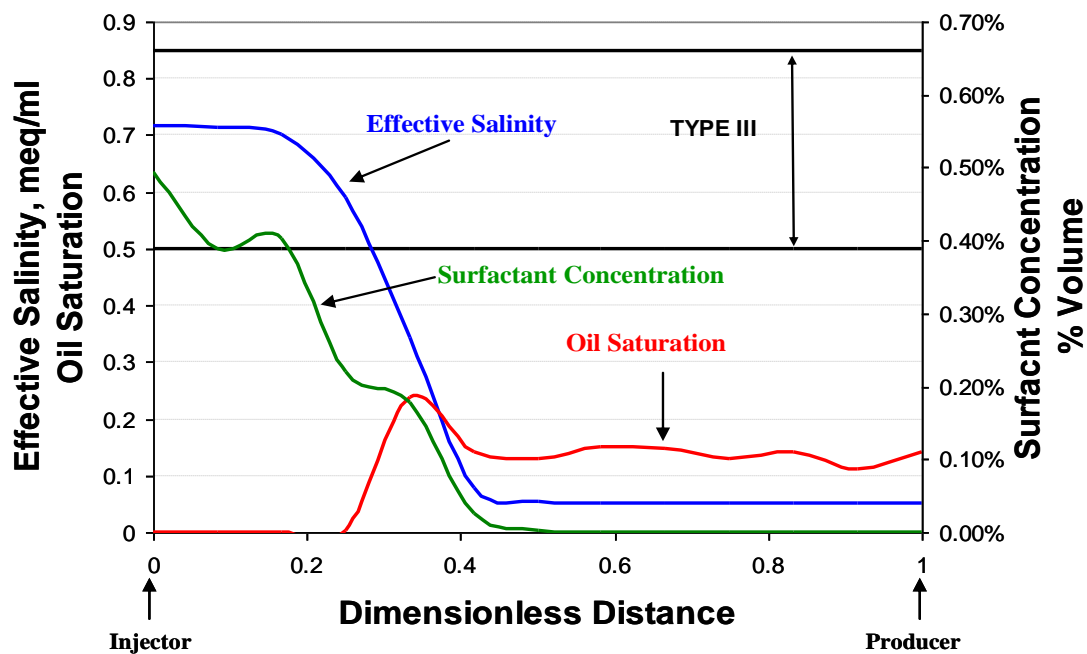


Figure 2.40: Profile for layer 19 of the 43 X 47 X 19 grid after 0.1 PV

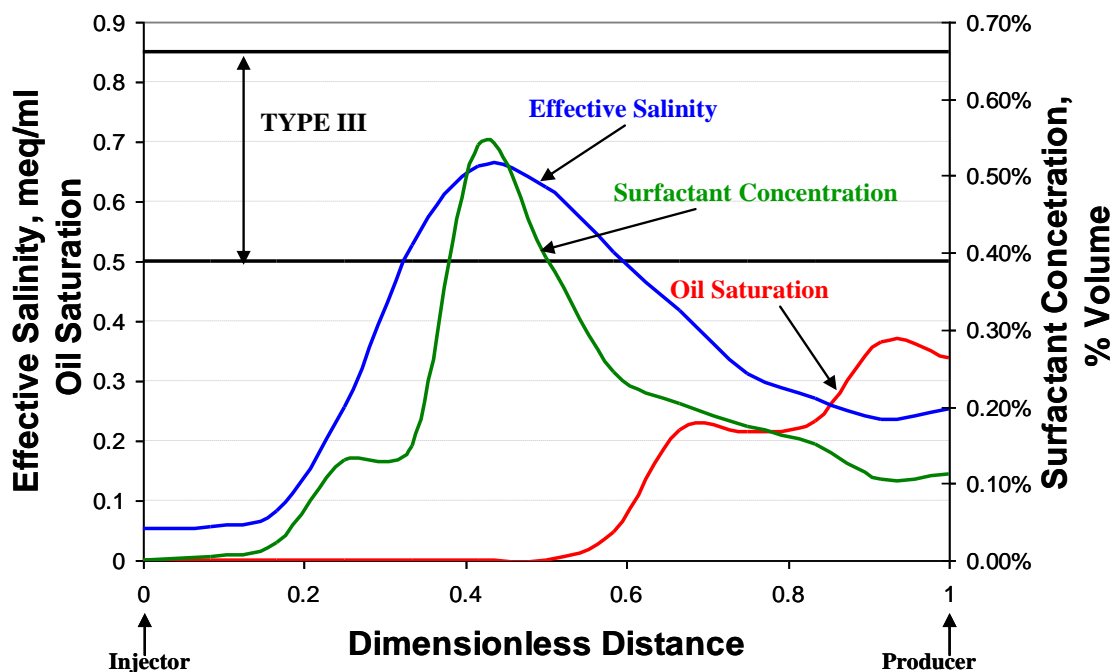


Figure 2.41: Profile for layer 19 of the 43 X 47 X 19 grid after 0.4 PV

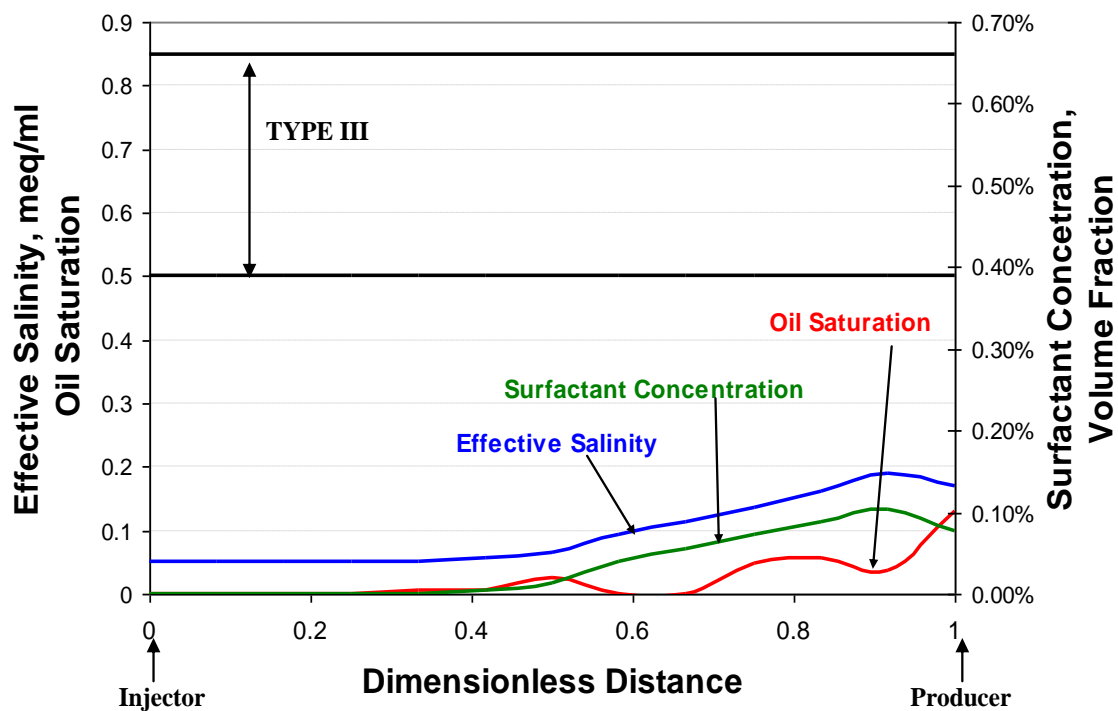


Figure 2.42: Profile for layer 19 of the 43 X 47 X 19 grid after 1 PV

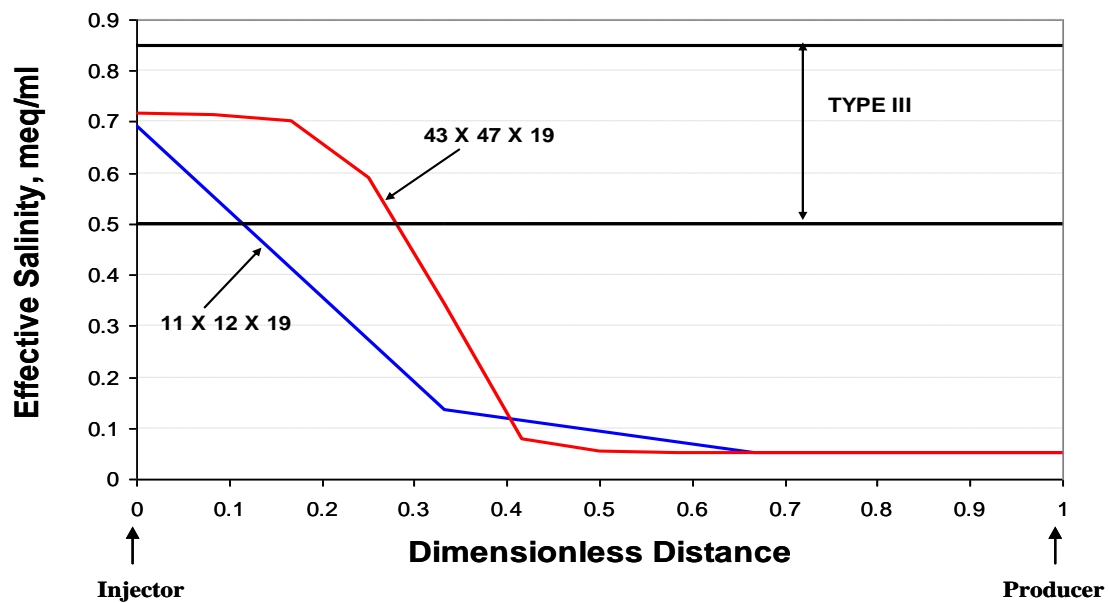


Figure 2.43: Salinity profile comparison (after 0.1 PV) for layer 19 of 11 X 12 X 19 and 43 X 47 X 19 grids

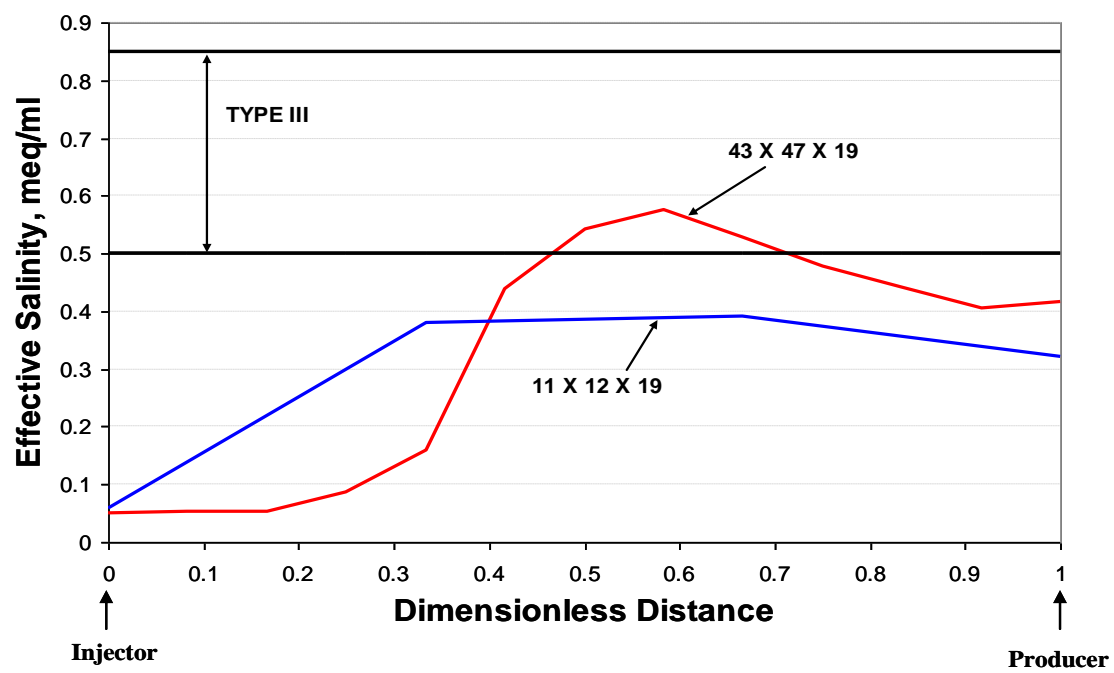


Figure 2.44: Salinity profile comparison (after 0.5 PV) for layer 19 of 11 X 12 X 19 and 43 X 47 X 19 grids

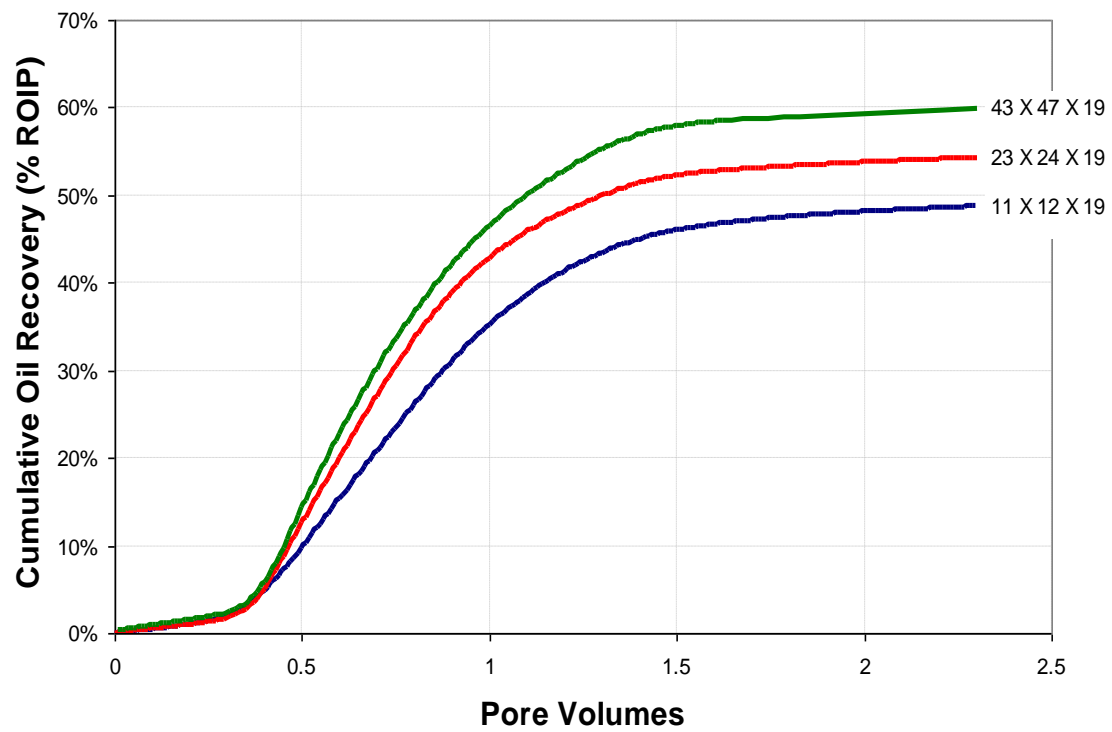


Figure 2.45: Cumulative oil recovery (% ROIP) for ASP flood simulations with a normal salinity gradient.

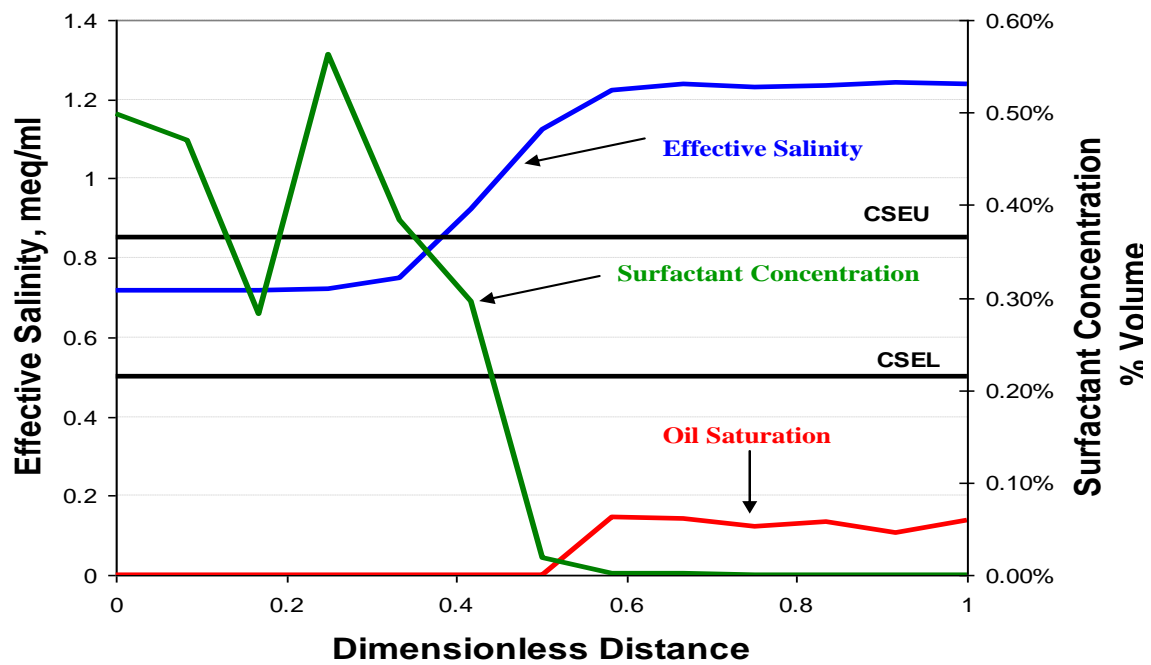


Figure 2.46: Profile for layer 19 of the 43 X 47 X 19 grid after 0.2 PV

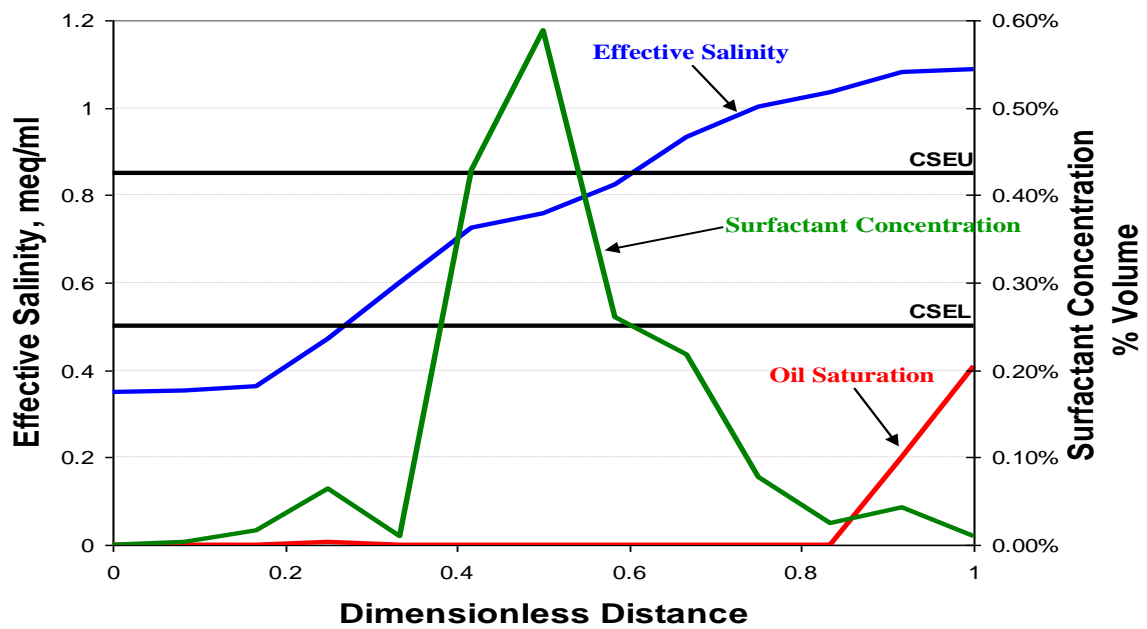


Figure 2.47: Profile for layer 19 of the 43 X 47 X 19 grid after 0.4 PV

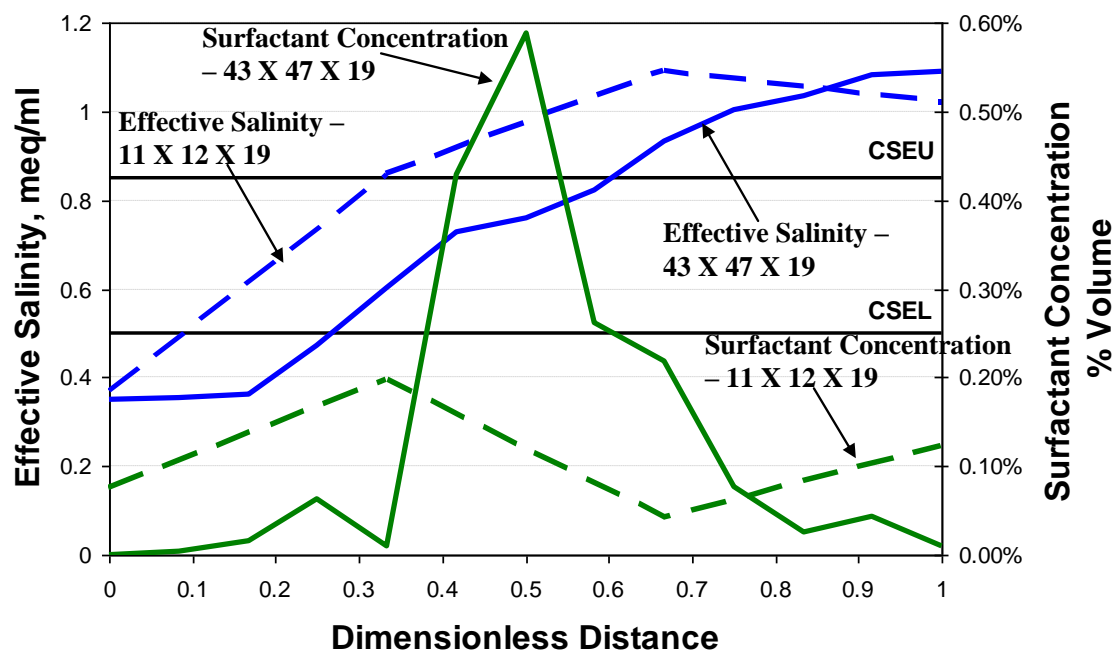


Figure 2.48: Comparison of salinity and surfactant concentration profiles for layer 19 of 43 X 47 X 19 and 11 X 12 X 19 grids after 0.4 PV

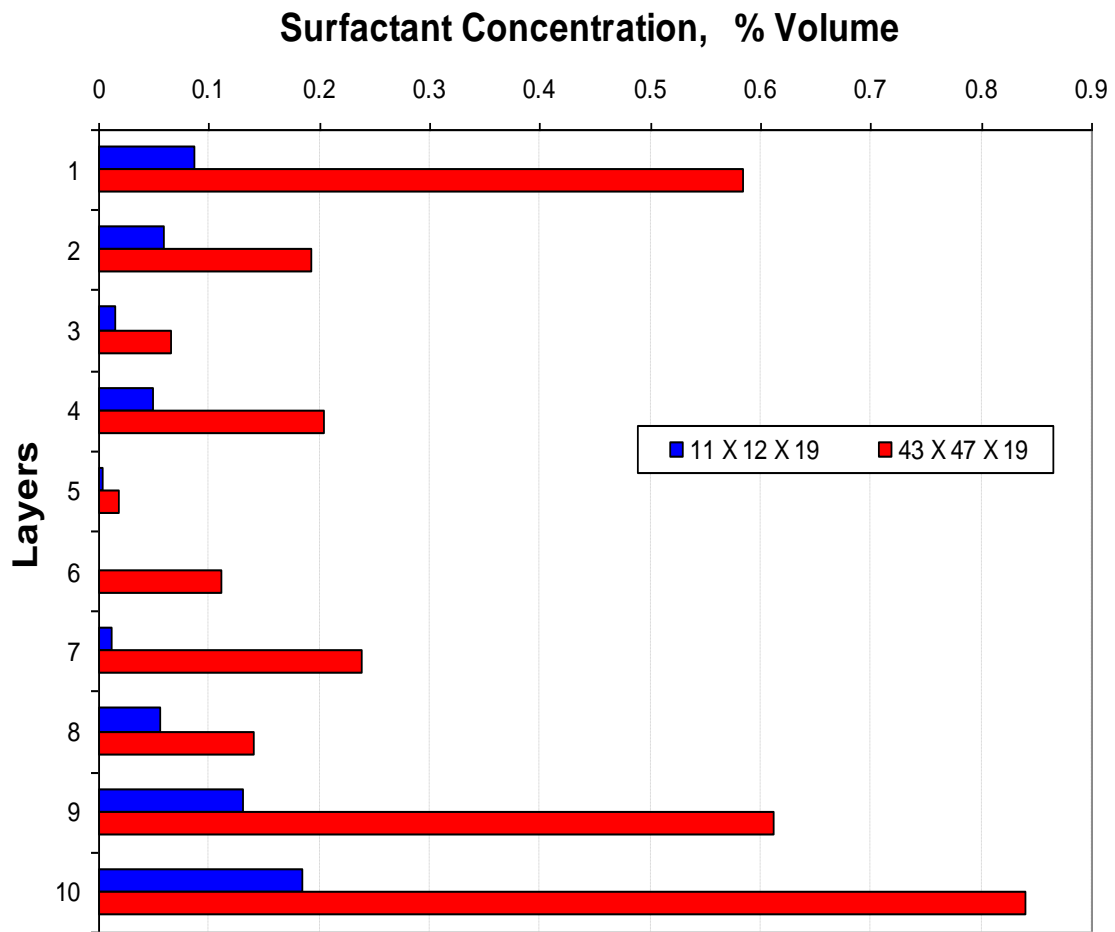


Figure 2.49: Surfactant concentration in injection grid block after 0.1 PV for one of the injectors using the 11 X 12 X 19 and 43 X 47 X 19 grids

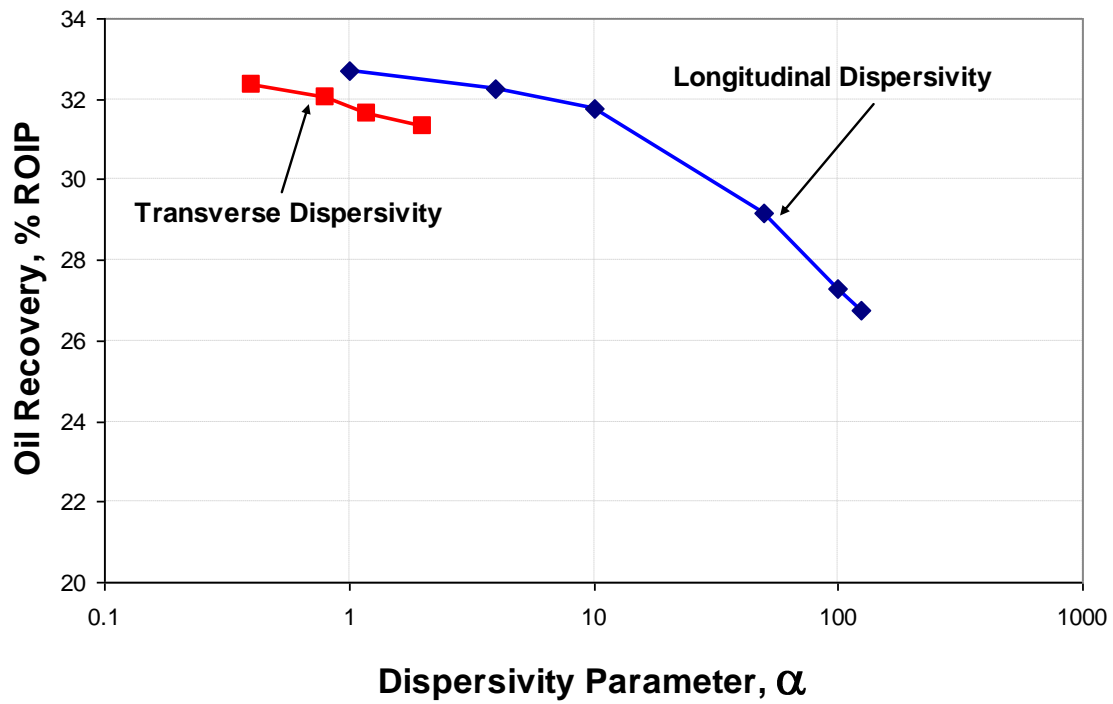


Figure 2.50: Sensitivity of physical dispersion on oil recovery of 11 X 12 X 19 grid.

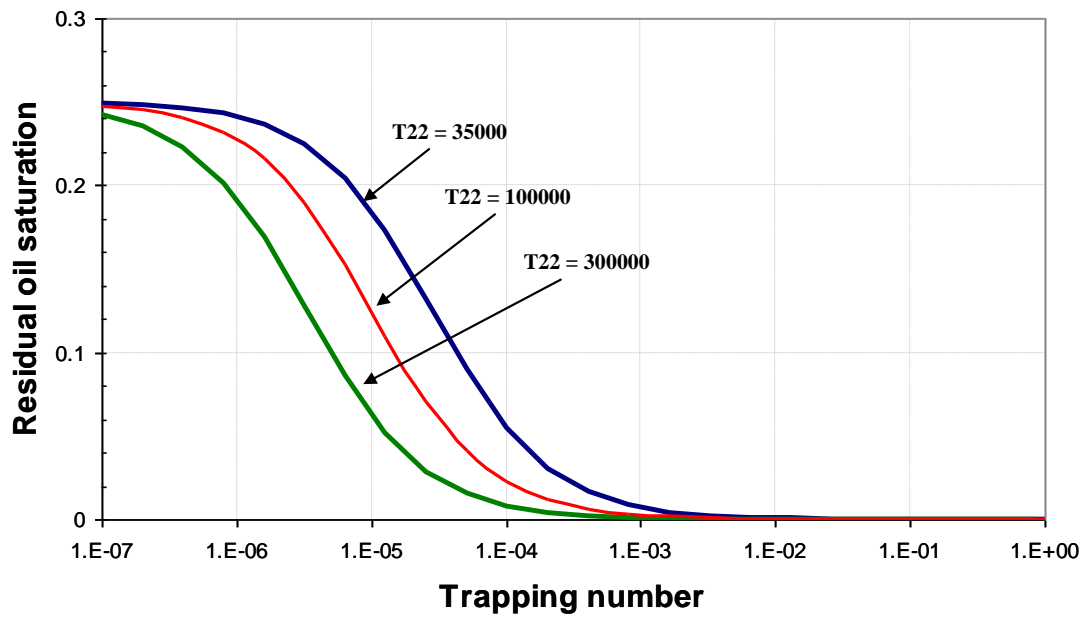


Figure 2.51: Oil capillary desaturation curves for three values of trapping parameter

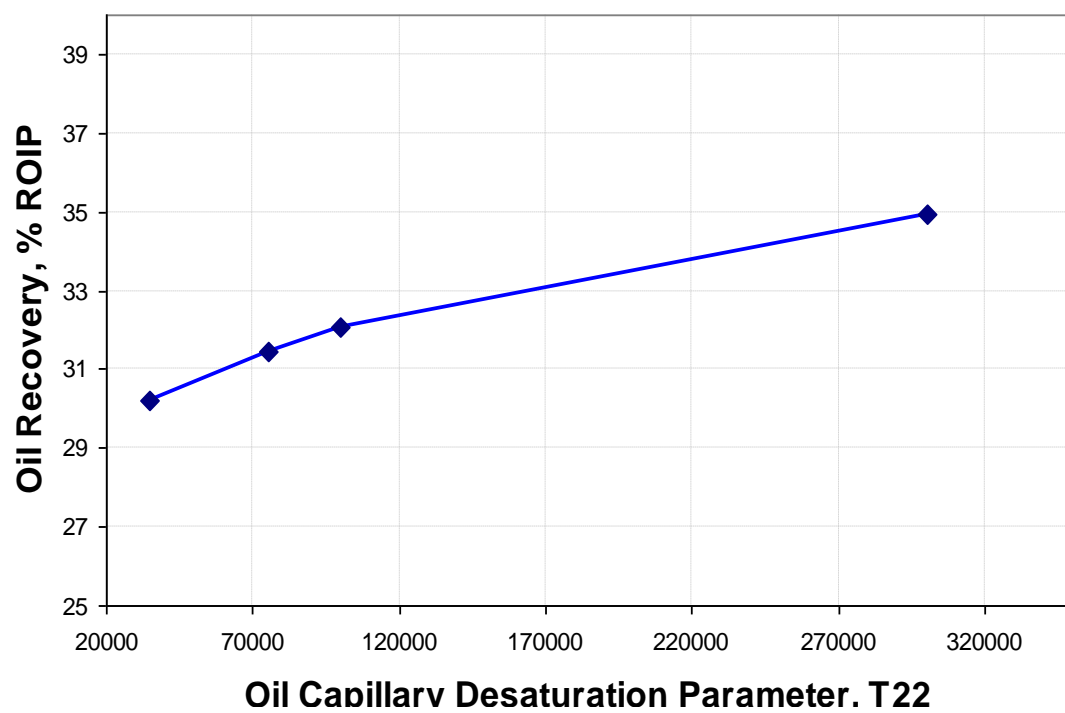


Figure 2.52: Sensitivity of capillary desaturation parameter on oil recovery for 11 X 12 X 19 grid

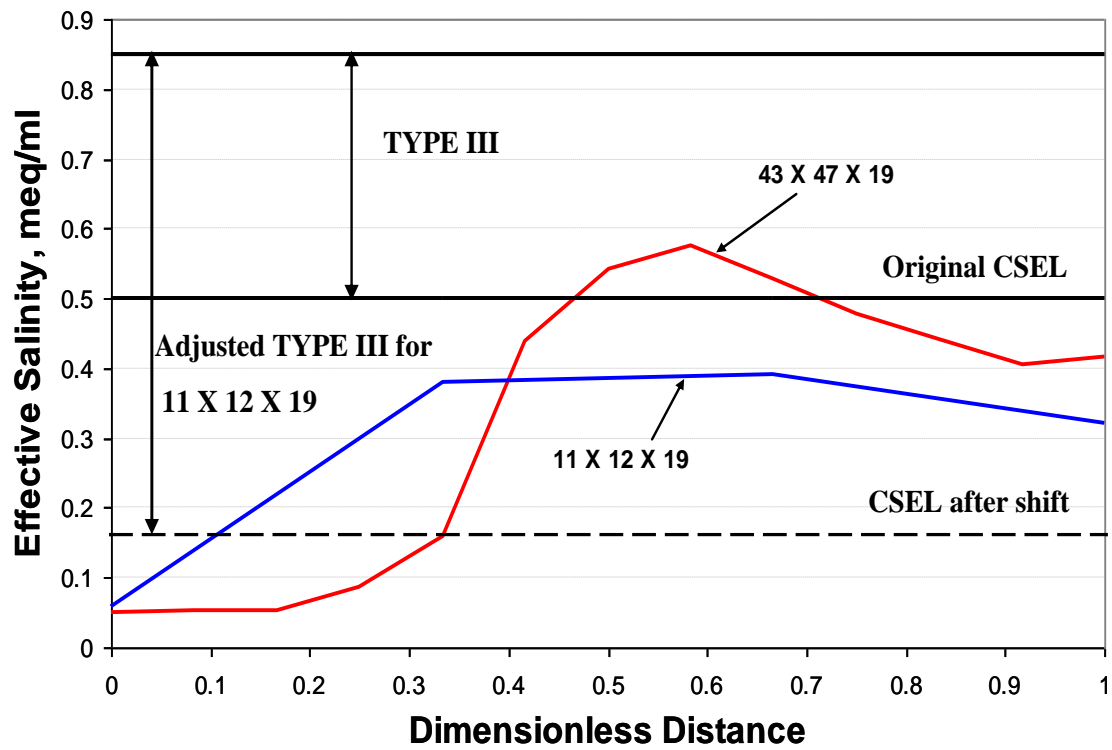


Figure 2.53: Salinity profile comparison (0.5 PV) of coarse grid with the fine grid showing the change in CSEL.

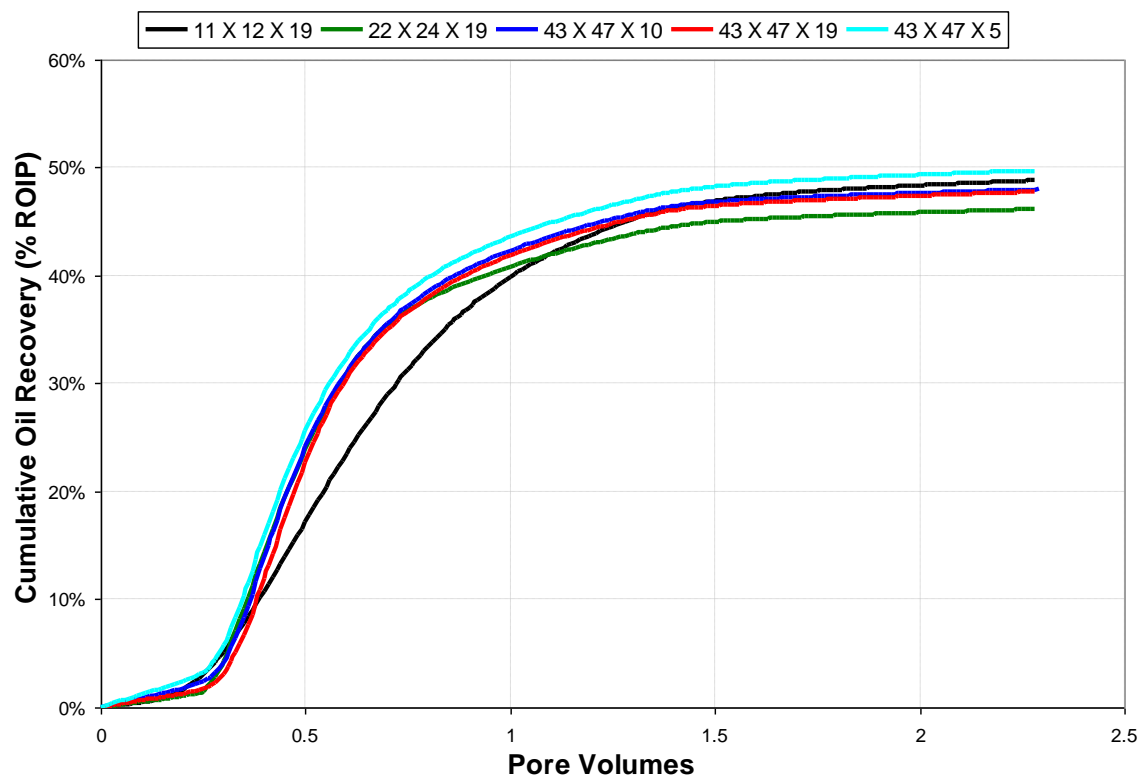


Figure 2.54: Oil recovery with CSEL adjusted for coarser grids.

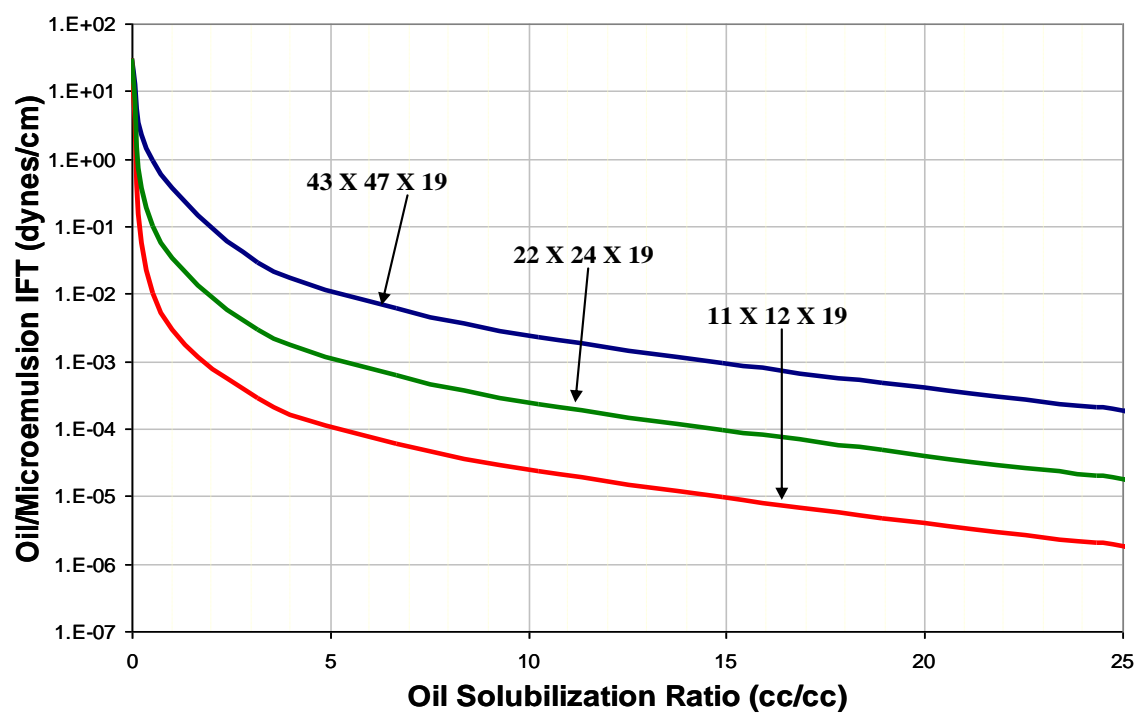


Figure 2.55: Interfacial tension between oil and microemulsion for each grid

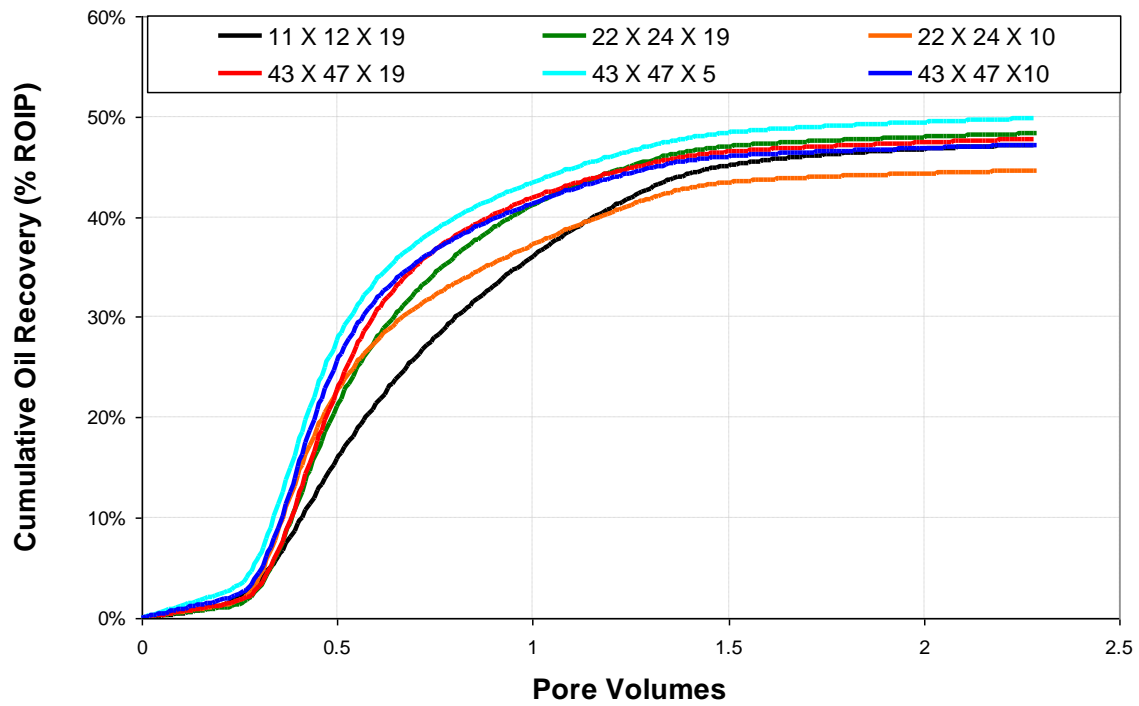


Figure 2.56: Oil recovery with IFT parameters adjusted for coarser grids.

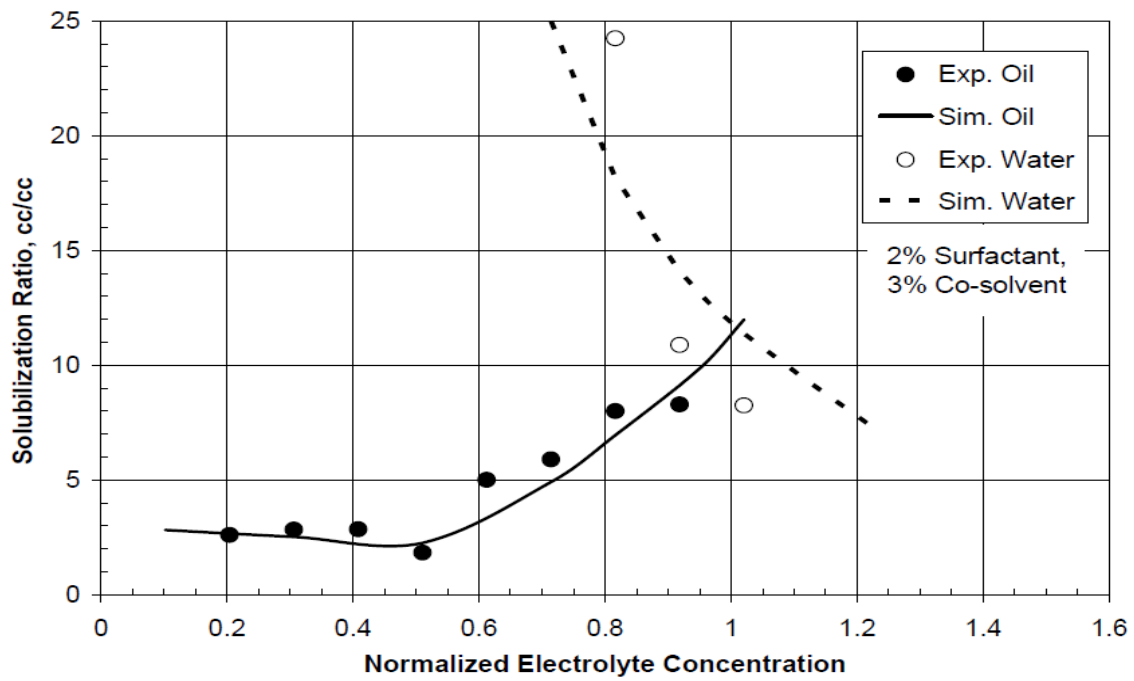


Figure 2.57: Phase behavior data and the match using UTCHEM (Dwarakanath et al., 2008)

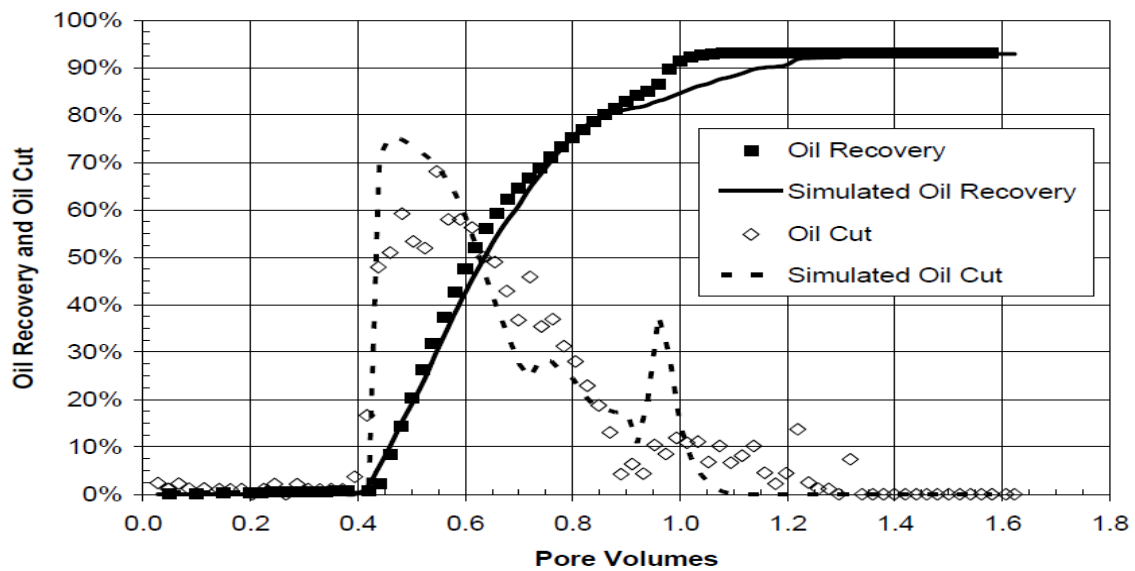


Figure 2.58: History match of core flood results using UTCHEM (Dwarakanath et al., 2008)

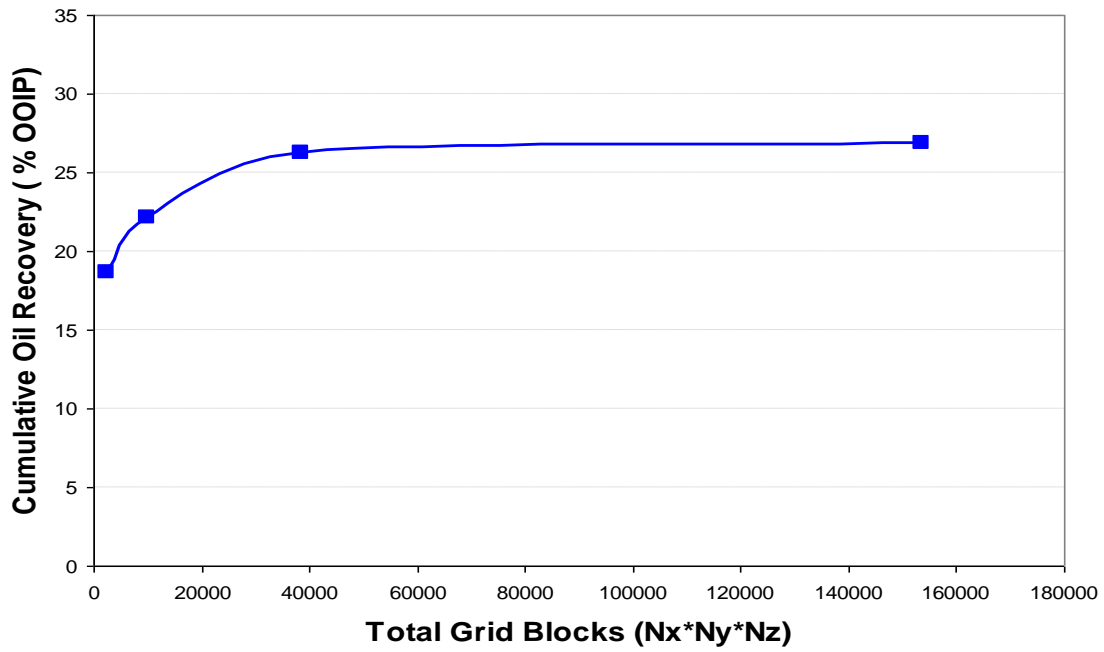


Figure 2.59: Sensitivity of grid block numbers to oil recovery.

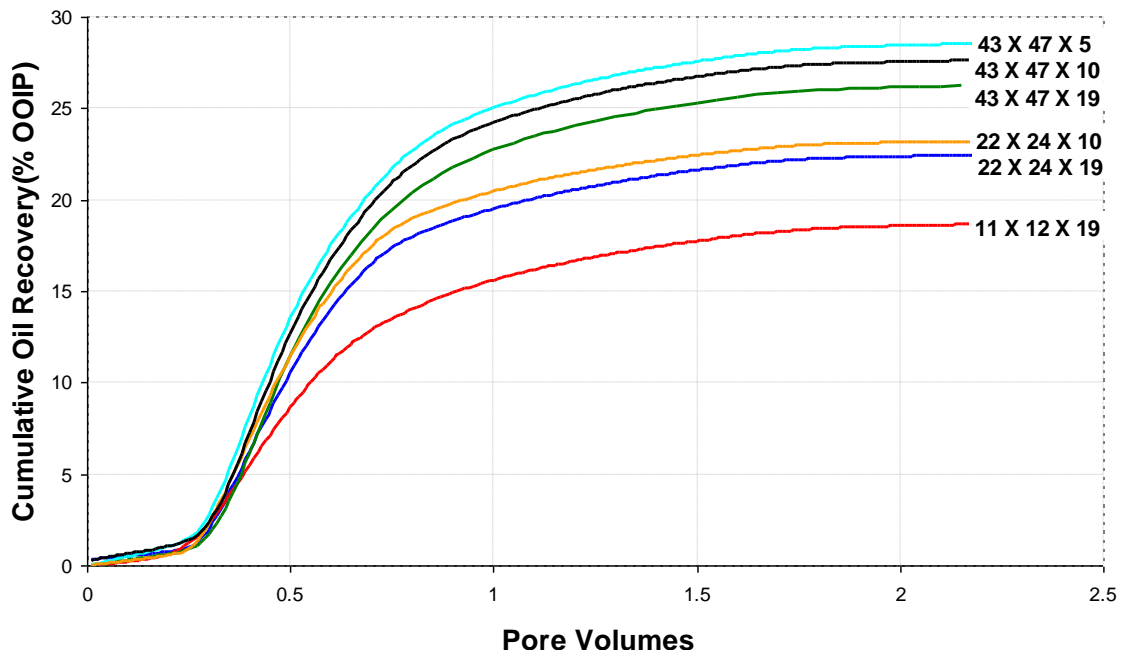


Figure 2.60: Cumulative oil recovery in terms of percentage original oil in place (% OOIP) for ASP flood simulations with chemical formulation B for all the grid block models.

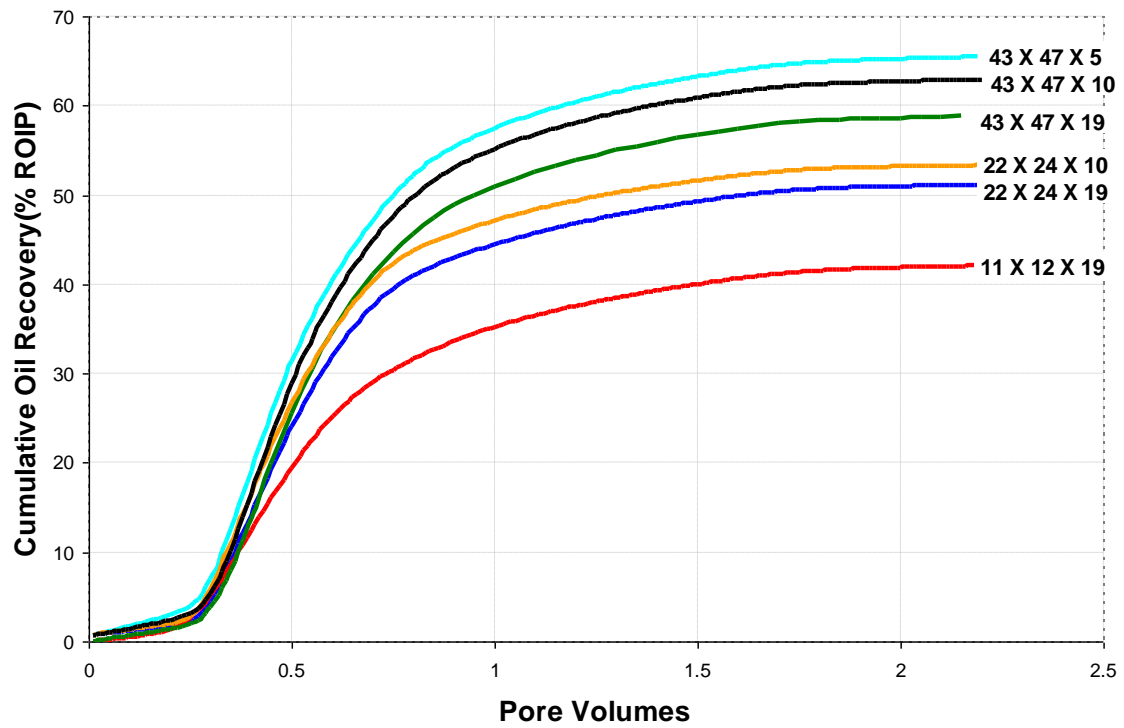


Figure 2.61: Cumulative oil recovery in terms of percentage remaining oil in place (% ROIP) for ASP flood simulations with chemical formulation B for all the grid block models.

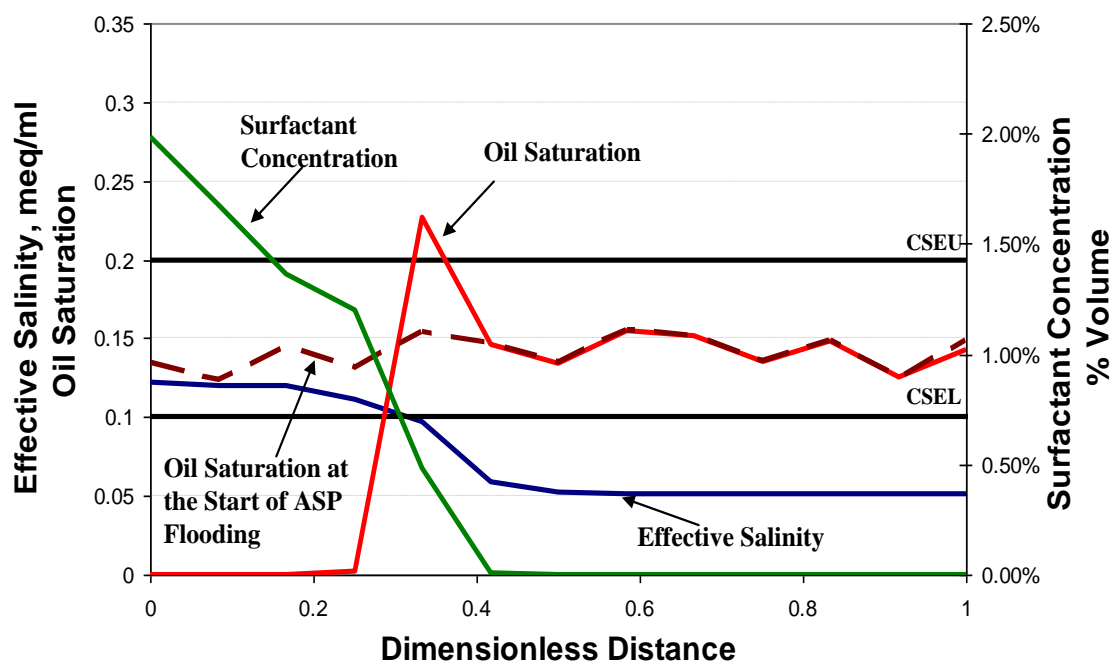


Figure 2.62: Profile for layer 19 of the 43 X 47 X 19 grid after 0.1 PV (simulation with formulation B).

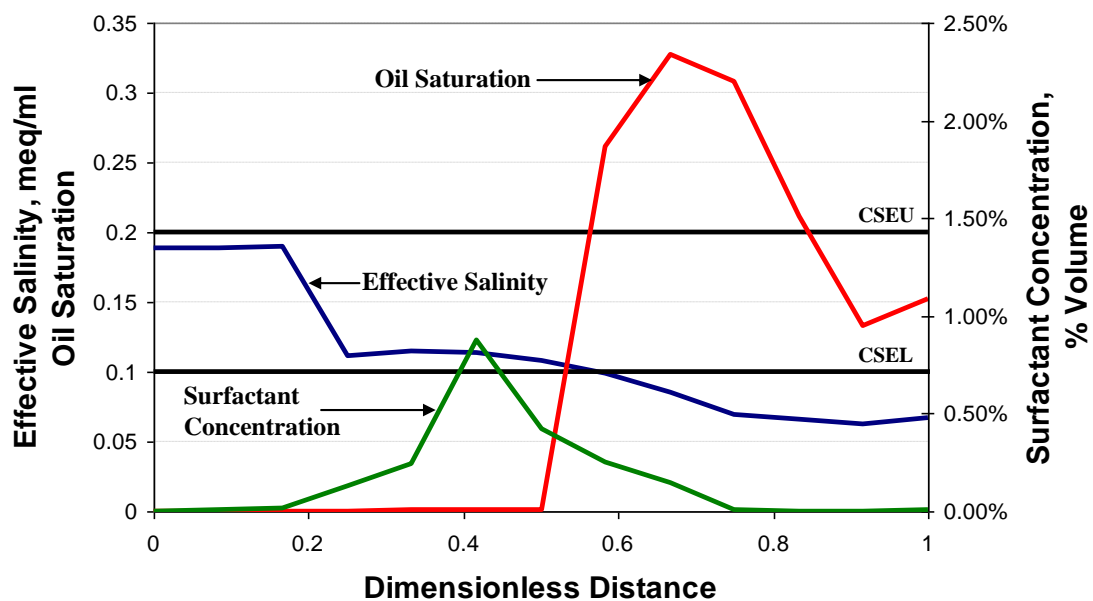


Figure 2.63: Profile for layer 19 of the 43 X 47 X 19 grid after 0.3 PV (simulation with formulation B).

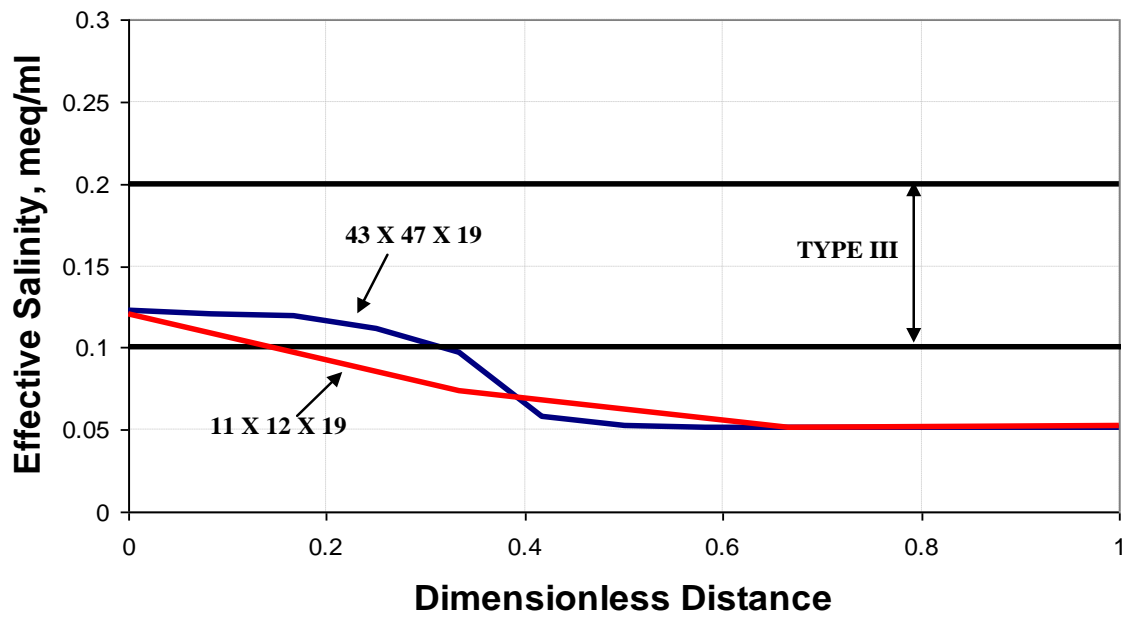


Figure 2.64: Salinity profile comparison of layer 19 of 11 X 12 X 19 and 43 X 47 X 19 grids after 0.1 PV injection (simulation with formulation B).

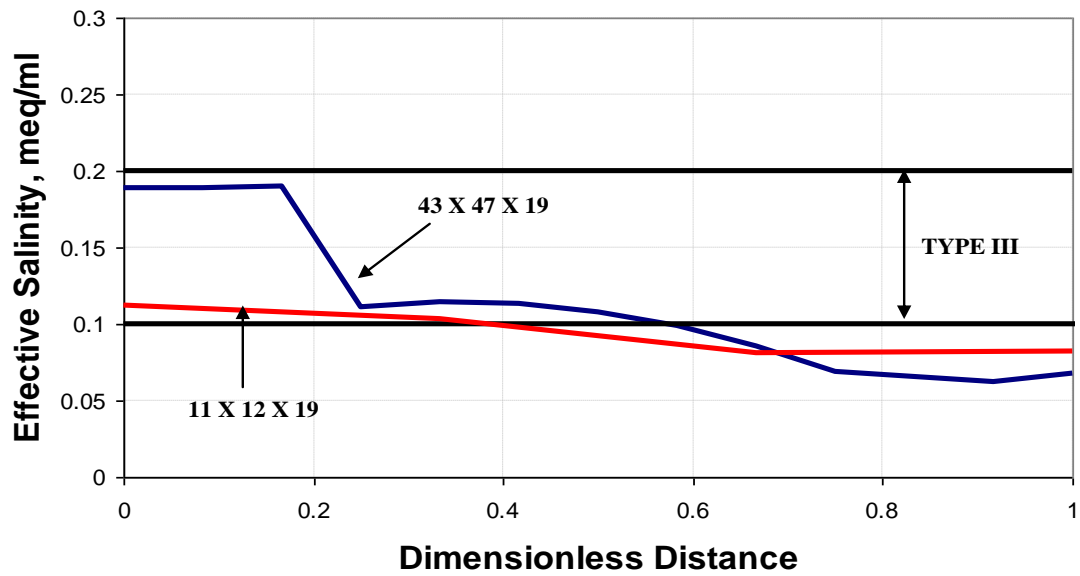


Figure 2.65: Salinity profile comparison of layer 19 of 11 X 12 X 19 and 43 X 47 X 19 grids after 0.3 PV injection (simulation with formulation B).

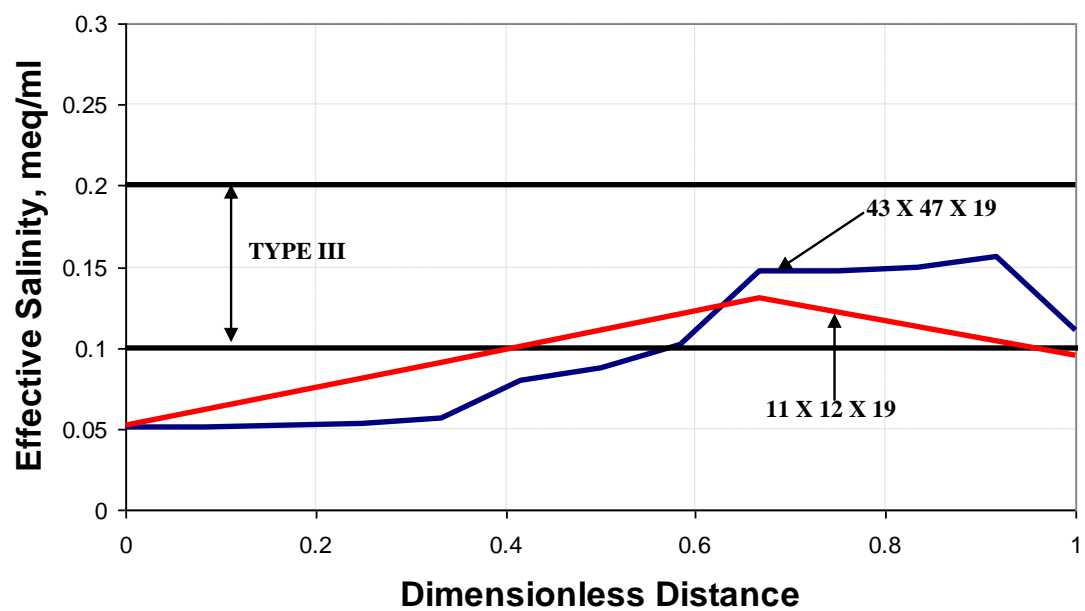


Figure 2.66: Salinity profile comparison of layer 19 of 11 X 12 X 19 and 43 X 47 X 19 grids after 0.7 PV injection (simulation with formulation B).

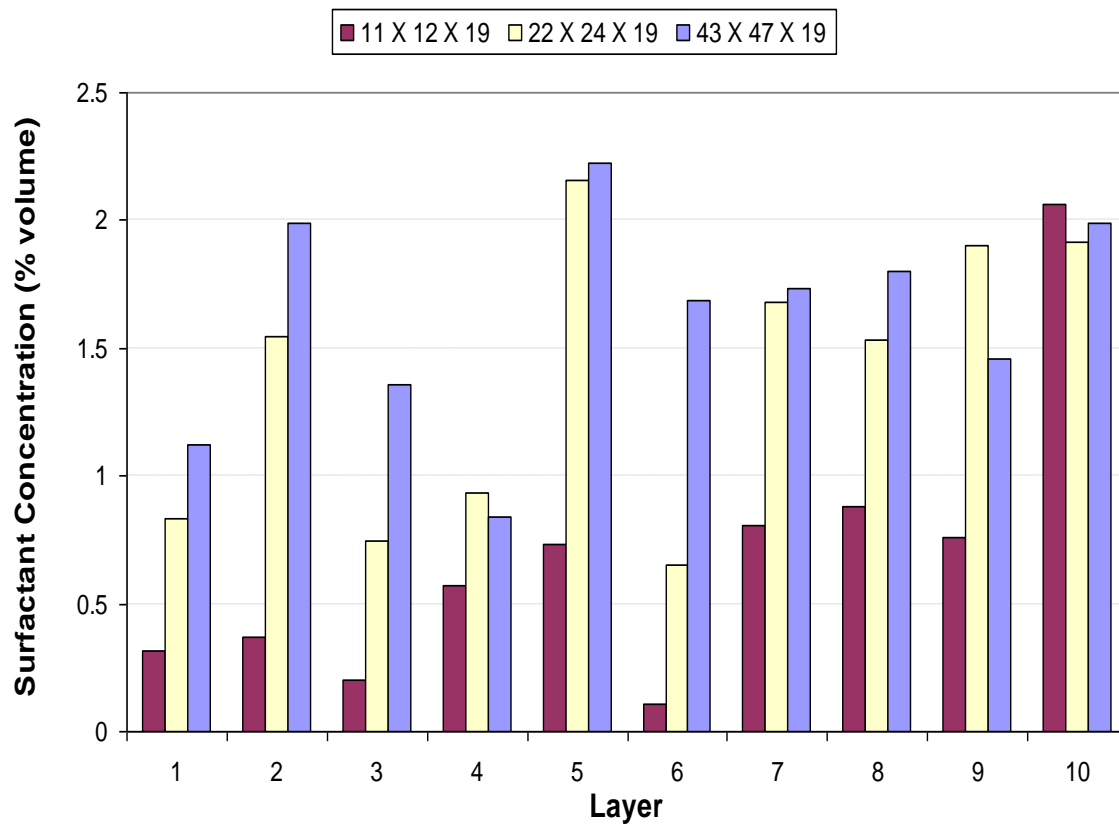


Figure 2.67: Surfactant concentration in injection grid block of one of the injectors of 11 X 12 X 19 and 43 X 47 X 19 grids after 0.1 PV injection (simulation with formulation B).

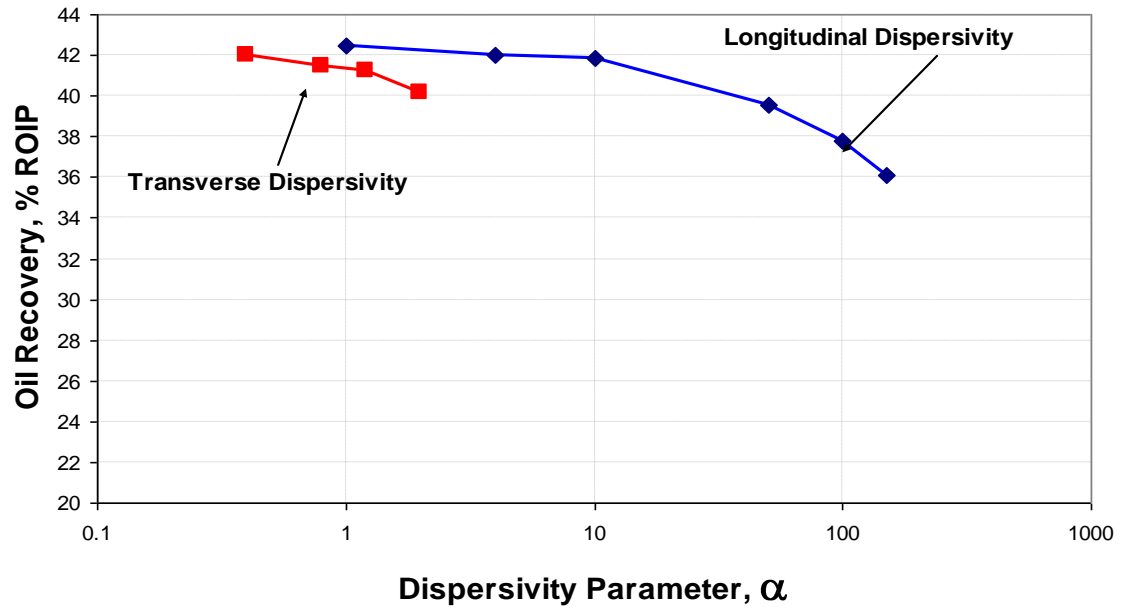


Figure 2.68: Sensitivity of physical dispersion on oil recovery of 11 X 12 X 19 grid (simulation with formulation B).

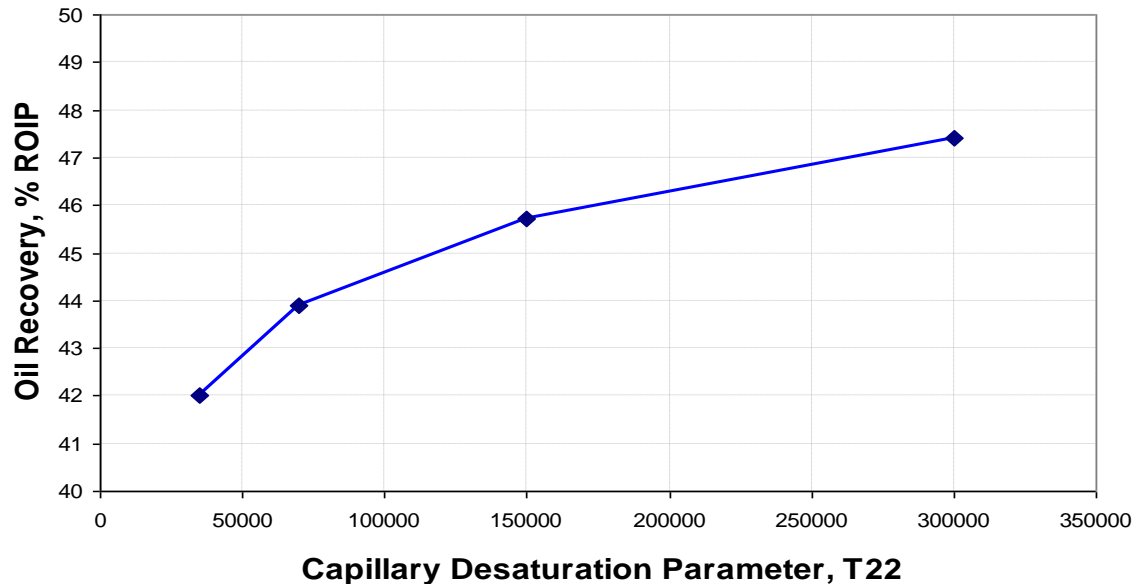


Figure 2.69: Sensitivity of capillary desaturation parameter on oil recovery for 11 X 12 X 19 grid (simulation with formulation B).

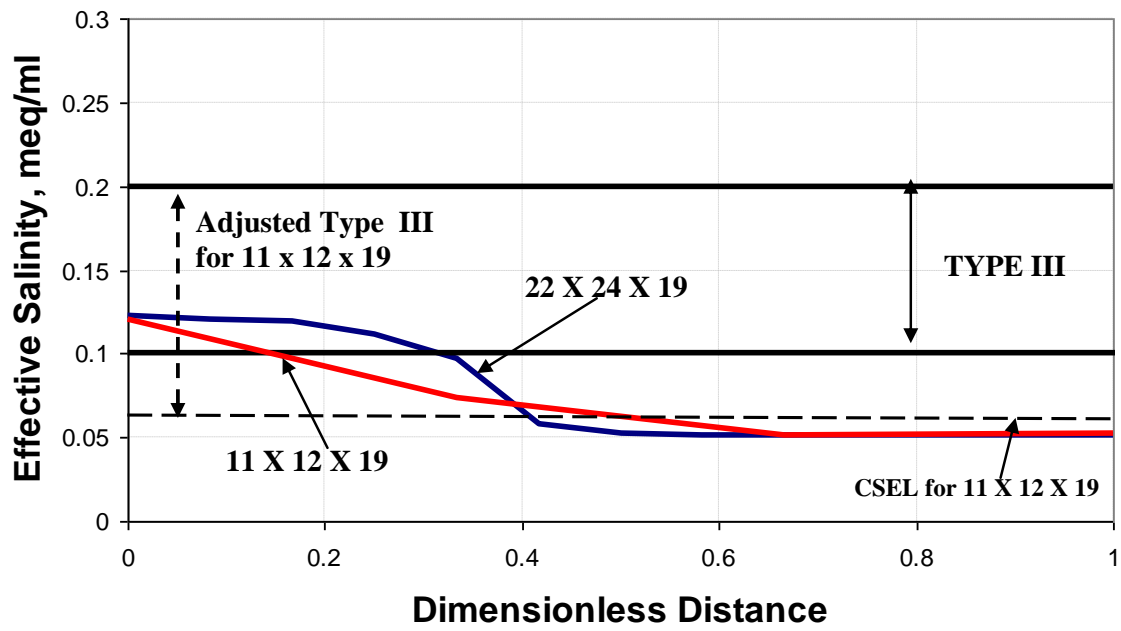


Figure 2.70: Salinity profile comparison (0.1 PV) of coarse grid with the fine grid showing the change in CSEL.

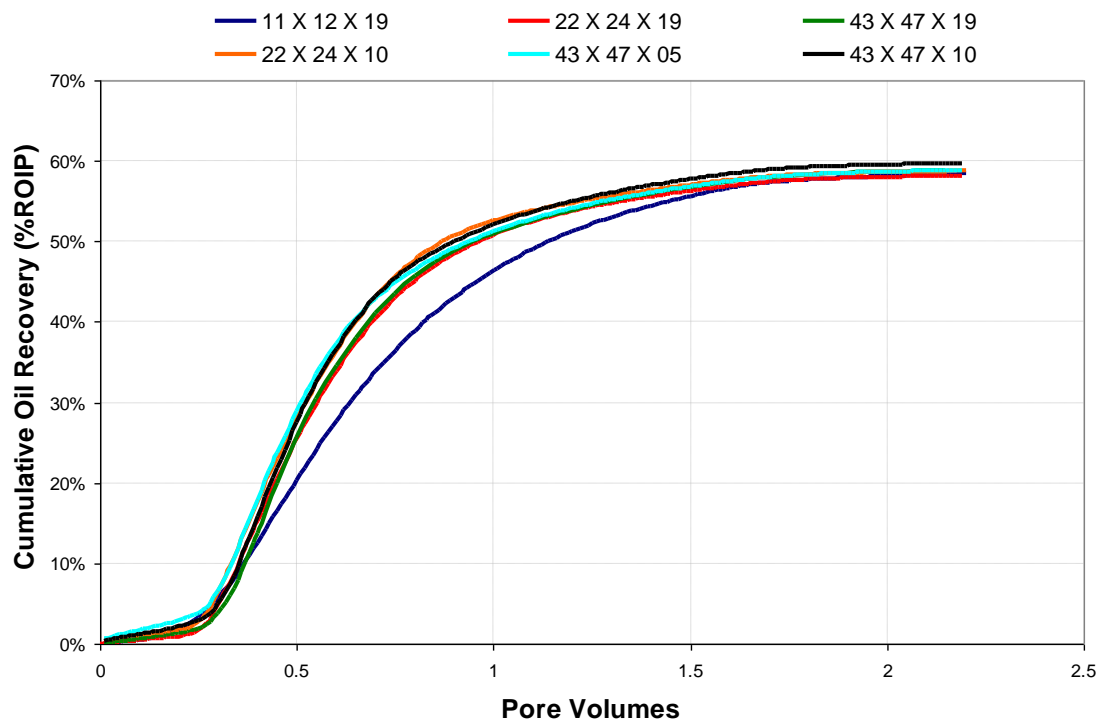


Figure 2.71: Oil recovery with CSEL adjusted for coarser grids (simulations with formulation B).

Chapter 3: Scale-up of ASP flooding simulations with acidic crude

3.1 INTRODUCTION

The previous chapter discussed about the effect of grid sizes on the performance of Alkaline-Surfactant-Polymer (ASP) flooding and proposed methodologies for upscaling for that case. This chapter focuses on the study of the effect of grid sizes on ASP flooding of a reservoir with acidic crude oil. The acidic crude contains certain amount of petroleum acids in the oil composition. The presence of the acidic components makes the crude oil reactive and can undergo saponification reaction when reacted with alkali. This reaction produces in-situ surfactant, described as soap. Thus the generation of the soap reduces the surfactant requirement in the design of ASP flooding. This makes the ASP flooding of reservoirs with acidic crude highly attractive in term of the economics of the process.

The cases studied in chapter 2 were on a reservoir with non acidic crude oil. The use of alkali was to increase the pH there by reduce the surfactant adsorption. The primary use of alkali, in the cases which will be described in this chapter, is to react with the petroleum acids in the crude oil to produce in-situ surfactant or soap. The generation of soap affects the surfactant phase behavior and other parameters. The most important challenge of simulating ASP flooding is to model accurately the generation of soap and its effects on critical parameters like phase behavior. UTCHEM simplified ASP (Delshad et al., 2011) model was developed to model soap generation and its effects on other parameters like phase behavior and salinity. Mohammadi (2008) discussed soap/surfactant phase behavior modeling and matched the various phase behavior experiments using UTCHEM.

The objective of this study is to analyze the effect of grid sizes on ASP flooding simulations of a reservoir with acidic crude oil. As concluded in the earlier chapter, the grid size effects critical parameters like phase behavior and salinity. The chapter first discusses some of the important features of UTCHEM simplified ASP (SASP) model (Section 3.2). The phase behavior modeling of an experiment performed in the laboratory will then be discussed along with polymer modeling. Section 3.3 discusses the history matching of phase behavior and core flooding data. Section 3.4 describes field scale SASP simulation runs with different grid models. The important results will be discussed in this section along with the upscaling methodology used. Section 3.5 lists conclusions on the chapter.

3.2 UTCHEM SIMPLIFIED ASP MODEL

The UTCHEM SASP model is a simplified version of the geochemistry model in UTCHEM which is based on work by Bhuyan (1889) and Bhuyan et al. (1990). The model developed by Bhuyan and others included a comprehensive set of reactions between the injected species and reservoir rock and fluids. The SASP model simplified the comprehensive model by neglecting reactions other than the generation of soap. The important modeling features of SASP model is explained below.

3.2.1 Soap Generation

The acidic component in a crude oil is measured in terms of acid number. The acid number is defined as the milligrams of potassium hydroxide (KOH) required to neutralize one gram of crude oil. The amount of soap generated is calculated based on the

acid number, oil concentration, oil density, and molecular weight of KOH (MW_{KOH}) in the presence of alkali.

$$C_{soap} = \frac{K_{soap} N_{acid} \rho_{oil} C_o}{MW_{KOH}} \quad \text{if } C_o > 0.0001 \text{ and } C_{alk} > C_{alk}^{critical} \dots\dots\dots (3.1)$$

where N_{acid} is in (mg KOH /g oil), ρ_{oil} is in (g/cc), $MW_{KOH} = 56.1$, C_o is in (volume fraction), and C_{soap} is in (mole/L). The critical alkaline concentration, $C_{alk}^{critical}$ (ALKCRIT) is the alkaline concentration above which soap is generated and is an input parameter in meq/ml. The concentration of soap in volume fraction is computed as follows.

$$C_{soap} \text{ vol. fraction} = C_{soap}^m \text{ Mole/L} \times \frac{1000}{Eq_{soap}} \dots\dots\dots (3.2)$$

where, $E_{q_{soap}}$ is the equivalent weight of soap as an input parameter (EQWS).

The input parameters in UTCHEM for modeling the soap generation are ACIDNO which is the acid number (N_{acid} in equation), SOAPK (K_{soap} in equation) and EQW, the equivalent weight of soap. SOAPK is an input parameter which controls the amount of petroleum acid conversion to soap. This is obtained by matching the phase behavior data with UTCHEM run in batch mode (Appendix C).

3.2.2 Phase behavior in the presence of soap and surfactant

The formation of in-situ surfactant or soap affects the phase behavior of a water-oil-surfactant mixture.

3.2.2.1 Effect of soap on salinity window (CSEL and CSEU)

The boundaries of Type III salinity window (CSEL and CSEU) are calculated using a log mixing rule (Salager et al., 1979; Bhuyan et al., 1990) based on mole fractions of the injected and generated (soap) surfactants as follows.

$$\log C_{SEL} = X_{surf} \log C_{SEL}^{Surf} + X_{soap} \log C_{SEL}^{Soap} \dots\dots\dots (3.3)$$

where C_{SEL}^{Surf} and C_{SEL}^{Soap} are lower effective salinity windows where Type III region starts for surfactant and soap respectively. The mole fraction of surfactant and soap are X_{surf}^m and X_{soap}^m . Similarly the upper effective salinity where Type III CSEU is calculated as follows.

$$\log C_{SEU} = X_{surf} \log C_{SEU}^{Surf} + X_{soap} \log C_{SEU}^{Soap} \dots\dots\dots (3.4)$$

where C_{SEU}^{Surf} and C_{SEU}^{Soap} are upper effective salinity windows where Type III region ends for surfactant and soap respectively.

The input parameters for UTCHEM are CSEL7 (C_{SEL}^{Soap}), CSEU7 (C_{SEU}^{Surf}), CSEL8 (C_{SEL}^{Soap}) and CSEU8 (C_{SEU}^{Soap}). These parameters are obtained by matching laboratory phase behavior data using UTCHEM in batch mode.

3.2.2.2 Effect of soap on height of binodal curve (HBNC)

The formation of soap also affects the height of binodal curve. A log mixing rule is used to compute the phase behavior of the mixture of surfactant and soap based on the mole fraction of each component and the respective phase behavior parameters. The

heights of binodal curve at zero, optimum, and twice optimum are input parameters for surfactant and soap.

$$\log HBN_s = X_{surf} \log HBN_s^{Surf} + X_{soap} \log HBN_s^{Soap} \dots\dots\dots (3.5)$$

for s = 0, optimum, twice optimum.

The UTCHEM input parameters are HBNC70, HBNC71 and HBNC72 for surfactant and HBN0, HBN1 and HBN2 for soap at zero salinity, optimum salinity and twice optimum salinity.

The logarithmic mixing rule were validated by Mohammadi et al. (2009) where laboratory measured data for phase behavior were matched using the parameters which are correlated by mixing rule given in Equations 3.3, 3.4, and 3.5.

There are two options for defining the input parameters for the effect of height of soap on height of binodal curve. These options are controlled by an input flag IMIX. The possible values for IMIX are 0 and 1. If IMIX = 1 then the mixing rules are used as given in Equation (5). If IMIX = 0, the height of binodal curves (HBNCs) for soap and surfactant are lumped with input parameters of HBNC70, HBNC71 and HBNC72.

The input parameters (HBNC) are obtained by matching phase behavior experimental data.

3.2.3 Alkali consumption

The consumption of alkaline agent and its retardation is modeled using a Langmuir Type Isotherm.

$$\hat{C}_{alk} = \frac{a_{alk} C_{alk}^f}{1 + b_{alk} C_{alk}^f} \dots\dots\dots (3.6)$$

where a_{alk} (ALKAD) and b_{alk} (ALKBD) are input parameters. C_{alk}^f is the effective concentration of the alkaline agent which is the overall concentration (\tilde{C}_{alk}) minus the adsorbed concentration (\hat{C}_{alk}). The equation can be written as

$$\hat{C}_{alk} = \frac{a_{alk} \tilde{C}_{alk} - \hat{C}_{alk}}{1 + b_{alk} \tilde{C}_{alk} - \hat{C}_{alk}} \dots\dots\dots (3.7)$$

The overall and adsorbed alkali concentrations are expressed in the unit of meq/ml PV. Equation 3.7 can be rearranged resulting in a quadratic equation for adsorbed alkali concentration. The negative root gives the physical solution.

3.2.4 Surfactant adsorption at high pH

One of the benefits of adding alkali is the reduction of injected surfactant adsorption by increasing the solution pH. One of the assumptions in UTCHEM SASP model is that the surfactant adsorption is linearly reduced at high pH or in the presence of alkali.

$$\hat{C}_3 = a_{3d} a_{3PH} \quad \text{if } (C_{alk} - C_{alk}^{ini}) > 0.01 \dots\dots\dots (3.8)$$

where a_{3d} (A3D) is the Langmuir input parameter for surfactant adsorption at low pH and a_{3PH} is the constant input parameter (HPHAD) to reduce the surfactant adsorption at high pH.

3.3 PHASE BEHAVIOR MODELING AND COREFLOOD HISTORY MATCHING

The phase behavior experiment data for the water-oil-surfactant mixture were matched using UTCHEM in batch mode (Chapter 4, Mohammadi, 2008). The oil, surfactant and brine used in this study were the same as those by Mohammadi (2008). Thus the phase behavior parameters were obtained directly from her study. Figures 3.1-3.3 show the phase behavior match (Mohammadi, 2008). Table 3.1 lists the phase behavior parameters.

A core flood was simulated using the phase behavior parameters obtained. The core properties are given in Table 3.2. The reservoir brine composition is given in Table 3.3. The ASP slug with 0.2 wt% surfactant, 3000 ppm polymer (SNF's FP 3630S) and 27,500 ppm Na_2CO_3 was injected for 0.3 PV at a rate of 1.3 ft/day. The slug was followed with 1.5 PV of polymer drive with 2000 ppm polymer concentration. The complete injection scheme is given in Table 3.4. The cumulative oil recovery and the oil cut given by the coreflood are shown in Figure 3.4. The figure also shows the match between experimental core flood and UTCHEM with SASP model. Table 3.5 lists complete set of input parameters used to match the core flood. The input parameters for polymer and surfactant were obtained by matching laboratory polymer measurements and phase behavior experiments.

3.4 FIELD SCALE SIMULATIONS OF ASP FLOODING USING UTCHEM SASP MODEL

The effect of grid size on ASP flooding is studied by running simplified ASP simulations using three grid models with different grid block size. The three grid block models studied in this section were the aerally coarsened grids (11 X 12 X 19 and 22 X 24 X 19) discussed in chapter 3 along with the fine grid block model (43 X 47 X 19). The grid configurations are given in Table 3.6. The areal view of the grid was shown in

Chapter 2 (Figures 2.1 - 2.3). The permeability, porosity and residual saturation distributions were the same as discussed in Chapter 2 (Figures 2.6 - 2.9). The initial water saturation for all the three models was 20 % corresponding to the condition at the beginning of waterflood. The phase behavior data, as explained earlier was taken from Mohammadi (2008). The critical micelle concentration (CMC) for the surfactant studies was 0.001 volume fraction. The parameters for modeling soap generation and other properties explained in Section 3.2 are shown in Table 3.7. The well pattern was the same as those described in Chapter 2 (Section 2. 1).

3.4.1 Water flood simulations

The reservoir pore volume for all the three models was 4.7 million barrels and the initial oil in place was 3.7 million barrels. The reservoir was initially water flooded until 98 % water cut was achieved. The water injection was performed at 8000 barrels per day. The waterflood was simulated until a water cut of 98.5% is reached. Figures 3.5 and 3.6 show the oil recovery and average oil saturation for all the models during water flooding.

The oil recoveries during water flooding for all the models were similar and about 41% OOIP. A difference in 1 % OOIP was observed between 11 X 12 X 19 and the fine model, 43 X 47 X 19. The water flood simulations set the initial condition for ASP flooding.

3.4.2 Alkaline-Surfactant-Polymer (ASP) flood simulations

Three ASP simulations were performed using grid block models described earlier (Table 3.6). As mentioned earlier, the phase behavior parameters and the polymer parameters were obtained from Mohammadi (2008). The injection scheme for the field scale simulations were based on the core flood design explained earlier. The only change

in the injection scheme is the polymer drive size. Polymer drive was injected for 1 pore volume instead of 2.2 PV in the core flood. A post water flood for 1 PV was also injected in the field scale cases after the polymer flood injection. Other input parameters used in the simulations are listed in table 3.5.

The results of the simulations with the three grid models were studied in detail. Figures 3.7 and 3.8 show the cumulative oil recovery during ASP flooding in terms of % remaining oil in place (% ROIP) and % original oil in place (% OOIP) respectively. The coarsest grid of 11 X 12 X 19 shows a difference in oil recovery of 6 % ROIP or 3 % OOIP in comparison with the finer model of 43 X 47 X 19. The oil recovery decreased with the increase in the size of the grid block. The reason for the difference in recovery, as discussed in the previous chapter, was due to the surfactant and sodium carbonate dilution in large grid blocks. The effect of dilution was studied using profile plots.

Figures 3.9 and 3.10 show profile plots of layer 19 of 43 X 47 X 19 model after 0.1 and 0.2 PV injection respectively. As discussed in Section 3.2 the generation of the soap affects the phase behavior. The change in the salinity window is dependent on the amount of soap generated and is modeled using a mixing rule (Equations 3.3 and 3.4). Thus the change in the salinity window (Type III region) seen in Figures 3.9 and 3.10 are due to the presence of soap in that region. The effective salinity of the injected slug is going through the Type III region, where a maximum concentration of soap is observed. As a result, an ultralow IFT zone is created and the oil is mobilized from that region as seen from the figures.

Figure 3.11 shows profile plots of layer 19 of 11 X 12 X 19 model after 0.1 PV injection.

3.4.2.1 Effect of dilution on salinity

The effect of dilution and its effects on salinity were discussed in Chapter 2. The case discussed in Chapter 2 was with non reactive oil, where there was no soap generation. The previous section shows the effect of soap on phase behavior importantly on the salinity window. This section discusses the effect of dilution by comparing the salinity profiles of coarser grid results with that of fine grid.

Figure 3.12 shows the profile of effective salinity of 11 X 12 X 19 and 43 X 47 X 19 after 0.1 PV injection. The effect of dilution is clearly seen. The important thing to note is that the Type III window is not fixed and changes relative to the amount of soap generated. Figure 3.13 shows the comparison of profiles (0.1 PV) of effective salinities of the two models along with the Type III window for those models. The dashed line represents 11 X 12 X 19 and the solid line represents 43 X 47 X 19. The surfactant dilution also affects the salinity window. As discussed in Section 3.2.2.1, the equation for the salinity window (Equations 3.3 and 3.4) includes the concentration of soap generated as well as surfactant injected. When surfactant gets diluted in large grid blocks the salinity window move towards the window for soap which is usually much lower than the surfactant injected. This is seen in Figure 3.13 where the salinity window for coarser model (11 X 12 X 19) is lower than that of the finer model (43 X 47 X 19). The change in salinity window due to the dilution artificially forced the effective salinity to be in the over optimum or Type II region (Figure 3.14). This caused an increase in IFT in those regions and as a result oil was not mobilized.

3.4.3 Upscaling methodology

The sensitivity of grid sizes on ASP flooding simulations with acid crude were much less than those studies for case without acidic crude (Chapter 3). The reason for this was the soap formation as discussed in the earlier sections. The major differences in

recoveries for the cases studied in this chapter were due to the salinity and surfactant dilution. The sensitivity to parameters such as CMC, CDC and dispersivity was studied. The simulation results were not much sensitive to these parameters, as also seen in Chapter 2.

An upscaling method similar to that described in Chapter 2 was tried. The only difference is that the salinity window of soap for the coarser models was adjusted to match the recoveries with that of fine grid model. The idea is to change the upper critical salinity window of soap for coarser models since the change in the salinity window because of the soap formation along with the surfactant and sodium carbonate dilution were the main reasons for the difference in recoveries between the coarser and fine grid models. Figure 3.15 shows comparison of recoveries of fine grid simulations with those of coarser grid with adjusted salinity window which shows comparable results.

3.5 SUMMARY

This chapter presented a study on the effect of grid sizes on ASP flooding in the presence of acidic crude and proposed upscaling strategies to the cases studied. A simplified ASP model developed to account for some of the important effects such as soap generation and its effects on phase behavior was discussed. The effect of grid size on ASP flood simulations were studied with grid models with different grid sizes. The sensitivity to grid sizes for the simulations discussed in this chapter was much less than that described in Chapter 2 (SP flooding with non reactive crude). The grid block models studied were insensitive to parameters such as CDC, CMC and dispersivity. The importance of salinity gradient and dilution effects was shown. An upscaling strategy similar to what used in Chapter 2 was used to match the recoveries of coarse grid model with that of the fine grid model.

Table 3.1: Phase behavior parameters used to match the phase behavior data shown in figures 3.1, 3.2 and 3.3

Phase Behavior Parameters	
Height of binodal curve at zero salinity, HBNC 70	0.03
Height of binodal curve at optimum salinity, HBNC 71	0.015
Height of binodal curve at twice optimum salinity, HBNC 72	0.03

Table 3.2: Reservoir core and fluid properties

Core Properties	
Porosity	0.17
Permeability, md	683
Temperature, ° F	143.5
Length, cm	30
Diameter, cm	5.03
Residual water saturation	0.32
Residual oil saturation	0.43
Water end point relative permeability	0.05
Oil endpoint relative permeability	0.6
Fluid Properties	
Water viscosity, cp	0.5
Oil viscosity, cp	17

Table 3.3: Brine composition.

Composition	Concentration (ppm)
NaCl	4416
NaHCO ₃	348
Na ₂ SO ₄	661
TDS	5425

Table 3.4: Injection scheme for the core flood simulation (Mohammadi, 2008)

Alkali-Surfactant-Polymer Slug	
Slug size	0.3 PV
Surfactant concentration	0.2 vol %
Polymer concentration	3000 ppm (HPAM 3630 S)
Salinity	27,500 ppm sodium carbonate
Flow rate	1 ft/day
Polymer Drive	
Drive size	2.2 PV
Polymer concentration	2000 ppm
Salinity	2865 ppm TDS
Flow rate	1 ft/day

Table 3.5: Input parameters used for core flood simulation

Phase Behavior Parameters	
Height of binodal curve at zero salinity, HBNC 70	0.03
Height of binodal curve at optimum salinity, HBNC 71	0.015
Height of binodal curve at twice optimum salinity, HBNC 72	0.03
Lower critical salinity window for surfactant, CSEL	0.55
Upper critical salinity window for surfactant, CSEU	1.1
Polymer viscosity parameters	
SSLOPE	-0.78
AP1	27.4
AP2	1
AP3	3172
GAMMAC	16
GAMHF	3.1
POWN	1.8
Microemulsion viscosity parameters	
ALPHA1	1
ALPHA2	2
ALPHA3	0.5
ALPHA4	0.5
ALPHA5	0.5
Adsorption Parameters	
AD31	1.7
AD32	0.05
B3D	1000
AD41	2
AD42	0.1
B4D	100

Table 3.6: Grid descriptions

Grid Name	Grid Configuration	Grid Size	Number of Grid Blocks
A	11 X 12 X 19	150 ft X 150 ft X 2ft	2500
C	22 X 24 X 19	75 ft X 75 ft X 2 ft	10000
F	43 X 47 X 19	37.5 ft X 37.5 ft X 2 ft	38000

Table 3.7: Input parameters for included to model simplified ASP flooding described in section 3.2

Acid Number, Nc	0.5
Equivalent weight of surfactant, EQW	400
SOAPK	1
CSEL soap, meq/ml	0.06
CSEU soap, meq/ml	0.12
Equivalent weight of soap, EQWS	500
IMIX	0
Initial hydrogen concentration, C160	8
Constant to reduce surfactant adsorption, HPHAD	0.1
Initial sodium concentration, CNA	0.087
Initial alkaline concentration, CALK	0.002
Alkaline concentration above which soap is generated, ALKCRIT	0.01
Alkaline retention parameter, ALKAD	4
Alkaline retention parameter, ALKBD	100

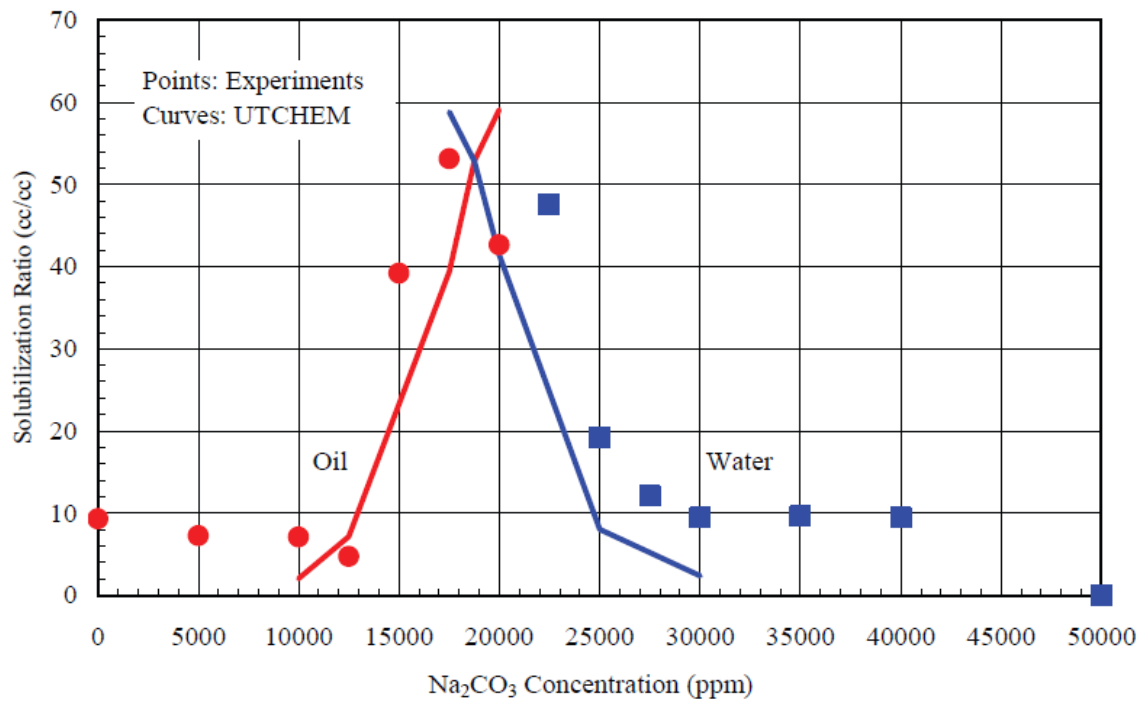


Figure 3.1: Phase behavior match for 50 % oil concentration (Mohammadi, 2008)

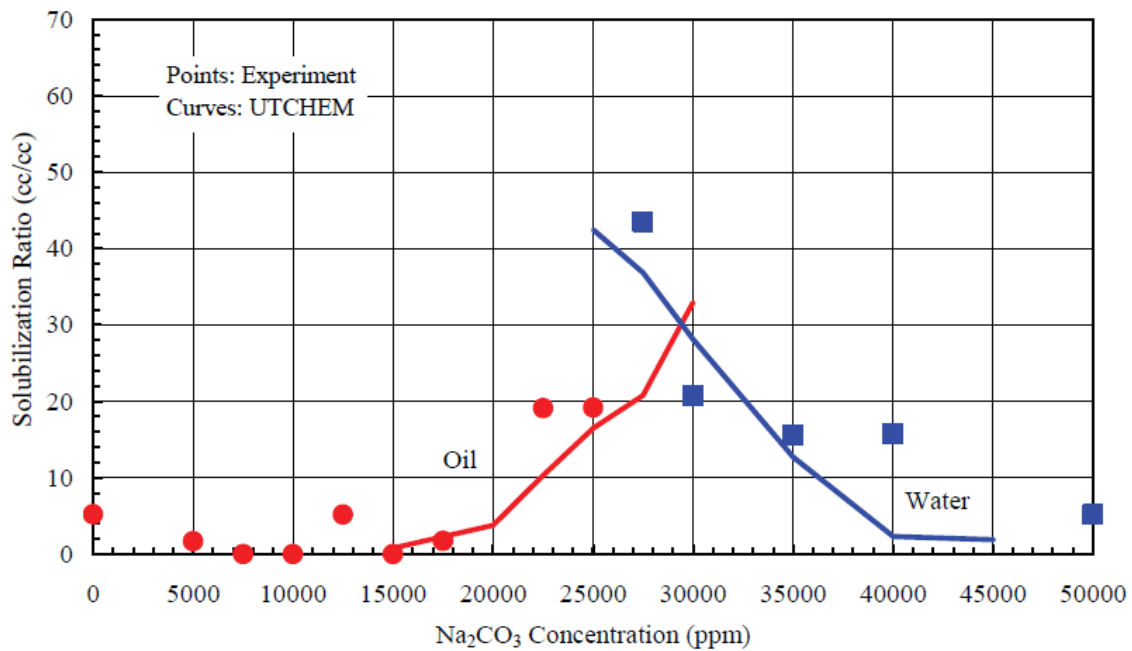


Figure 3.2: Phase behavior match for 30 % oil concentration (Mohammadi, 2008)

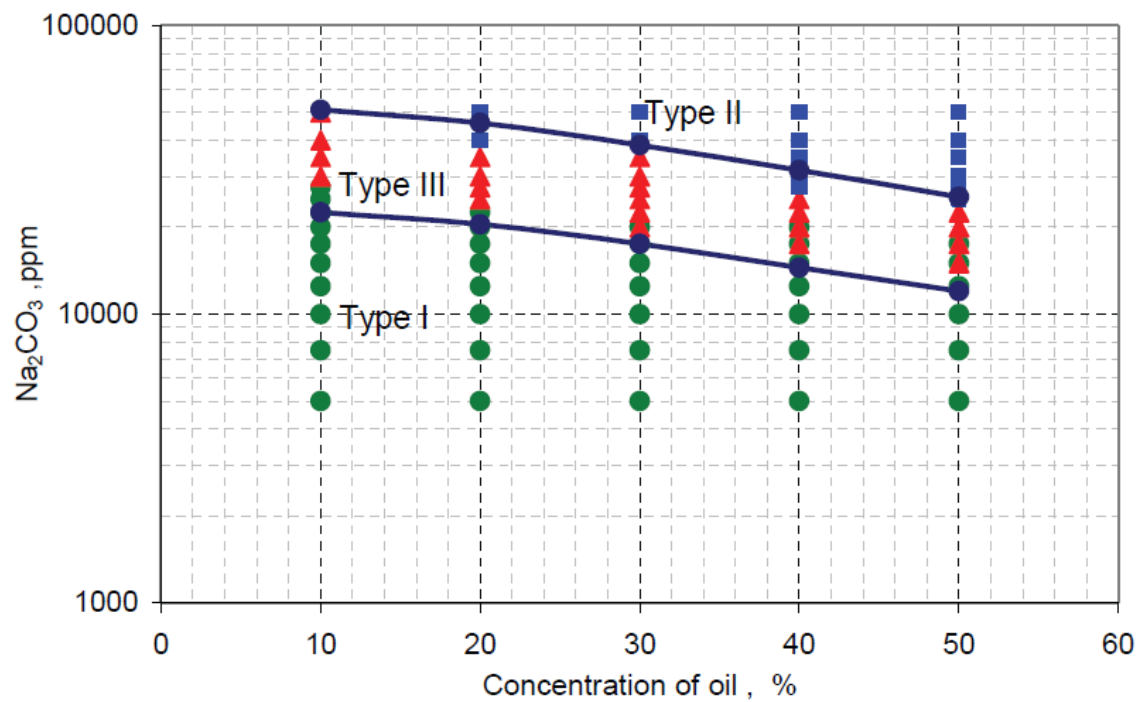


Figure 3.3: Activity map match, lines are the limits of Winsor's type III calculated from UTCHEM (Mohammadi, 2008)

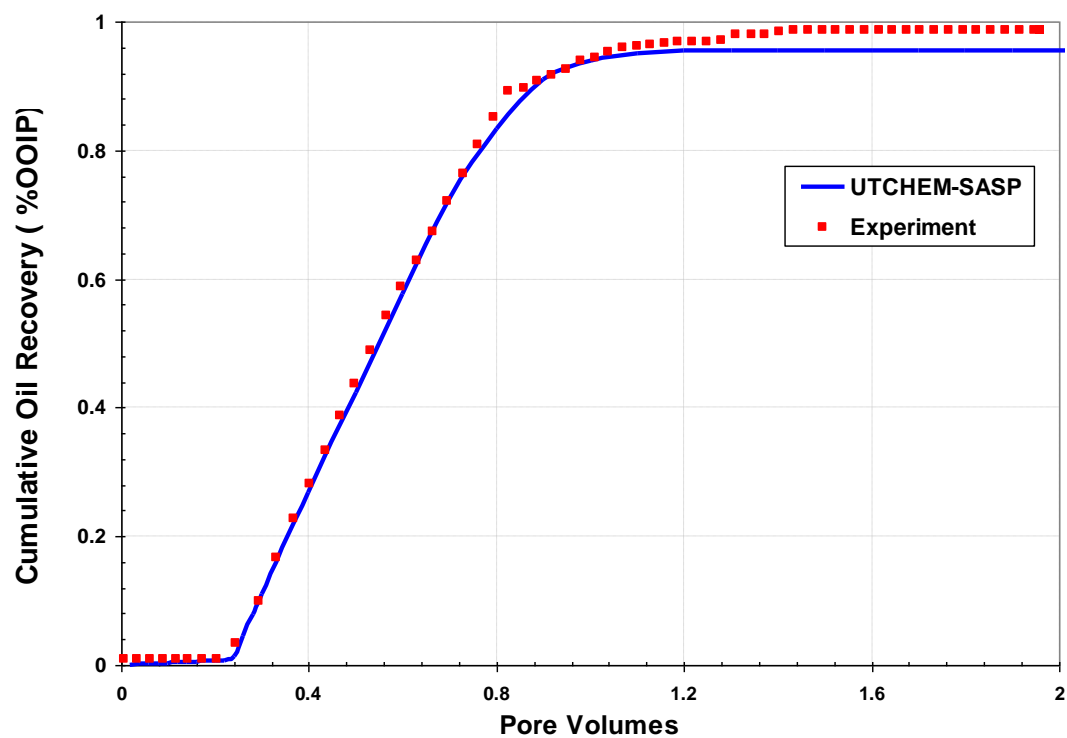


Figure 3.4: Core flood match of the laboratory data with UTCHEM with simplified ASP (SASP) model

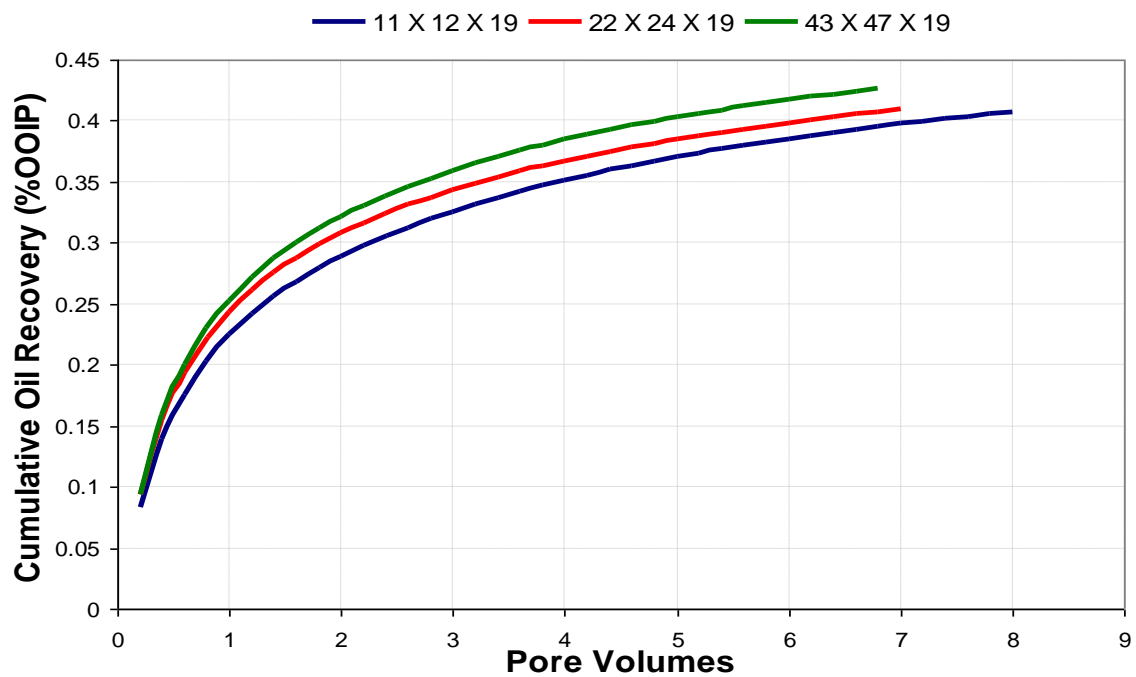


Figure 3.5: Cumulative oil recovery during water flooding for all the models

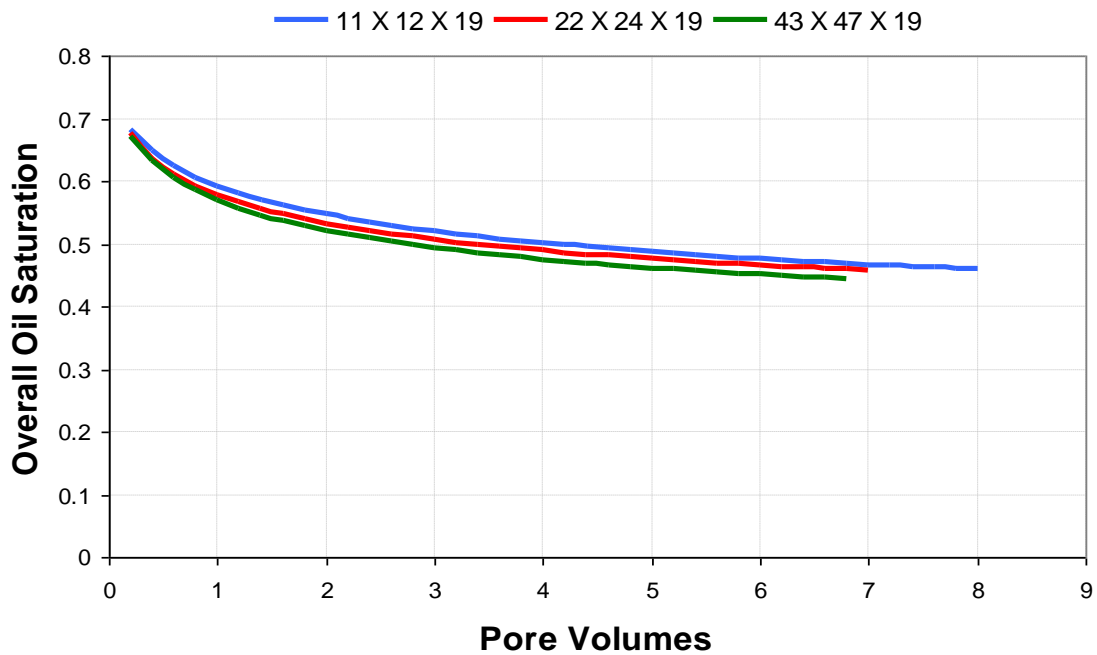


Figure 3.6: Average oil saturation during water flooding for all the models

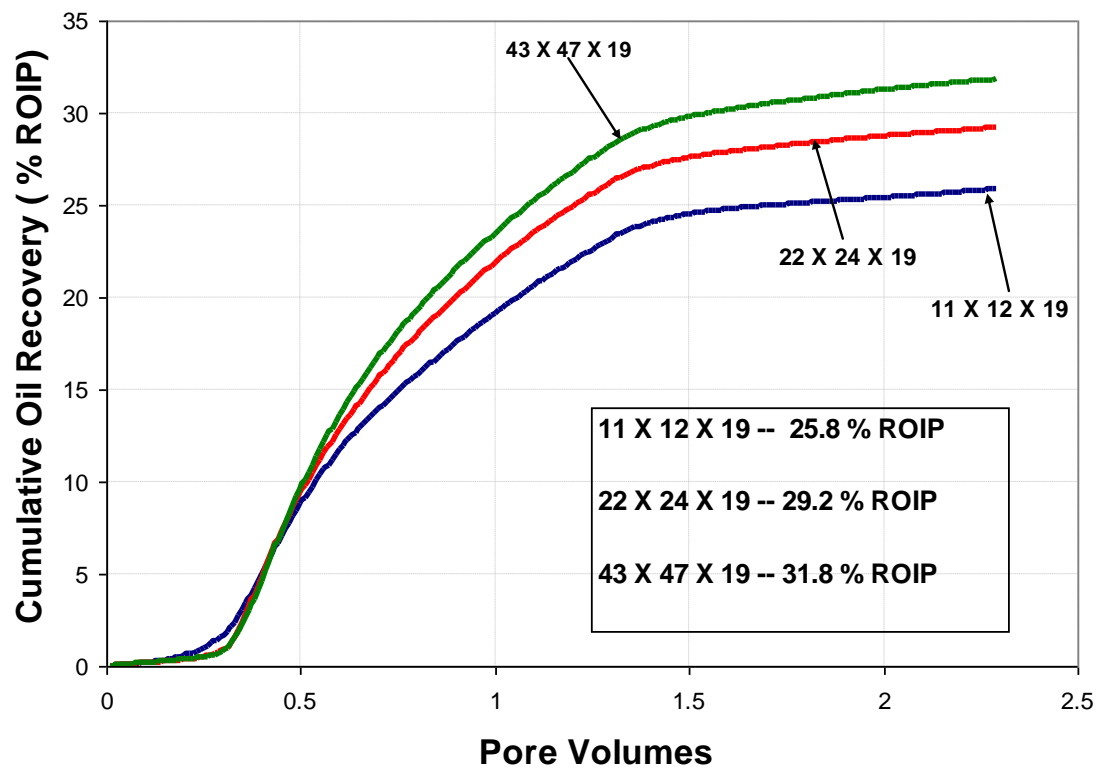


Figure 3.7: Cumulative oil recovery in terms of % remaining oil in place (% ROIP) for ASP flood simulations

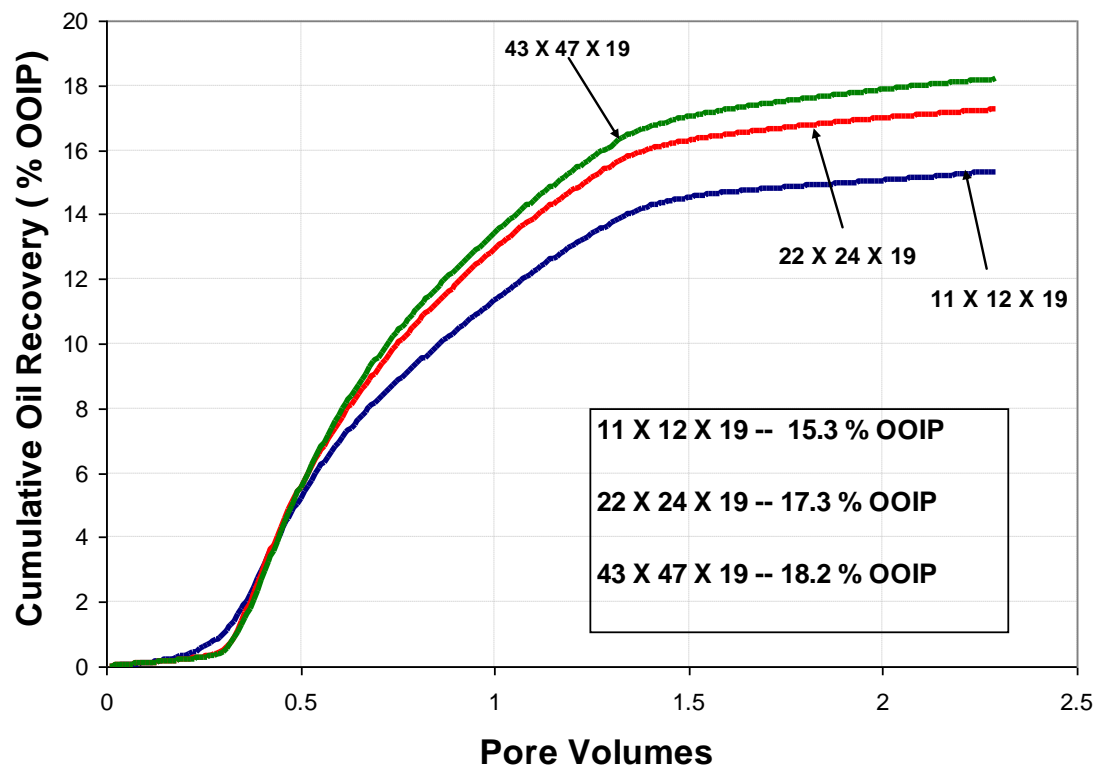


Figure 3.8: Cumulative oil recovery in terms of % original oil in place (% OOIP) for ASP flood simulations

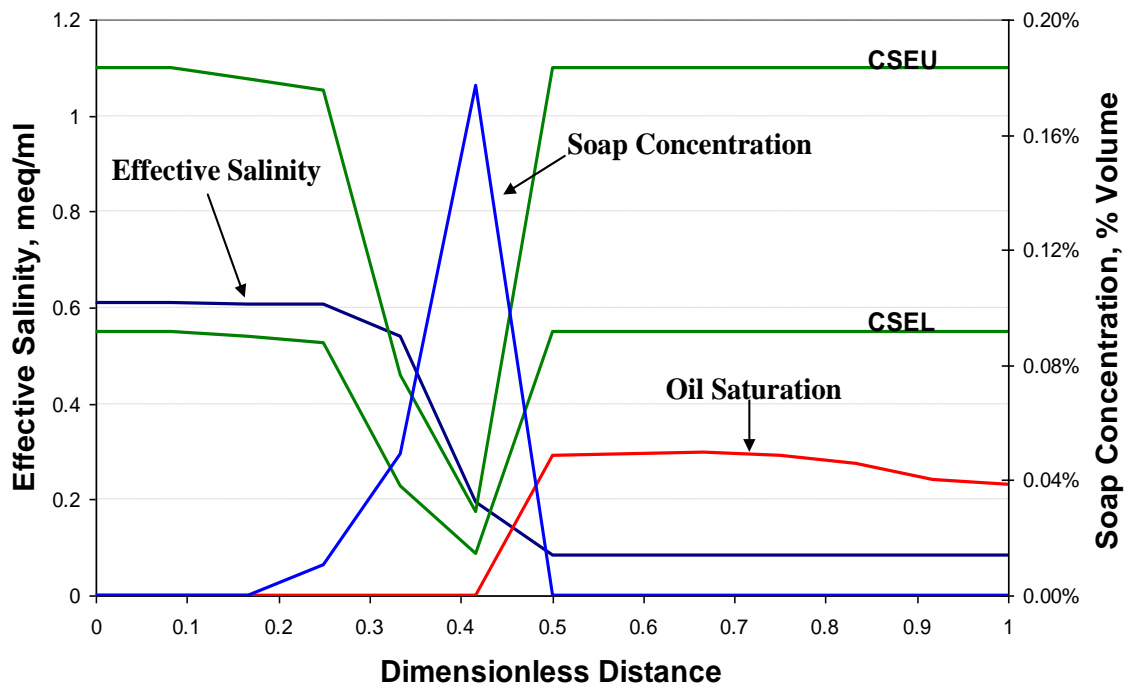


Figure 3.9: Profile for layer 19 of the 43 X 47 X 19 grid after 0.1 PV

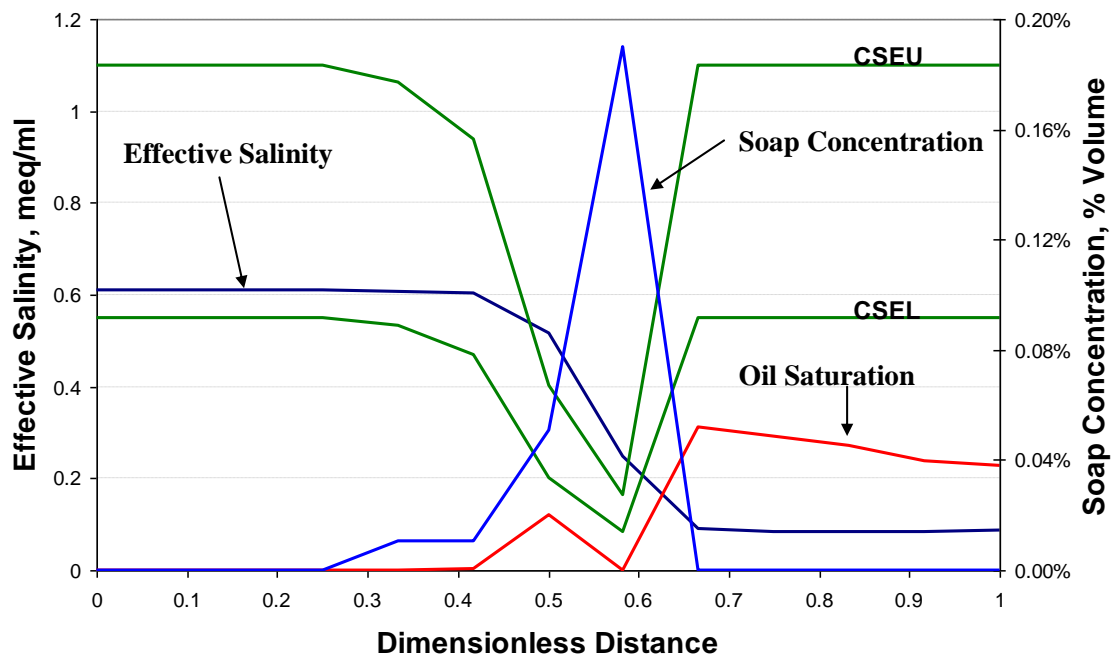


Figure 3.10: Profile for layer 19 of the 43 X 47 X 19 grid after 0.2 PV injection

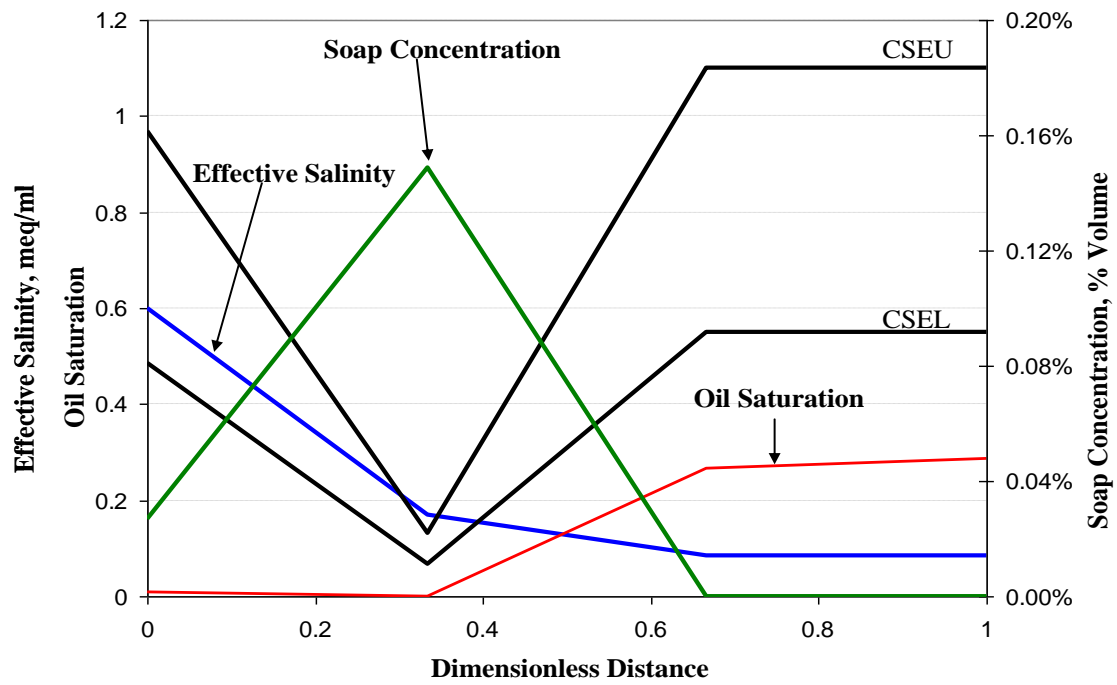


Figure 3.11: Profile for layer 19 of the 11 X 12 X 19 grid after 0.1 PV injection

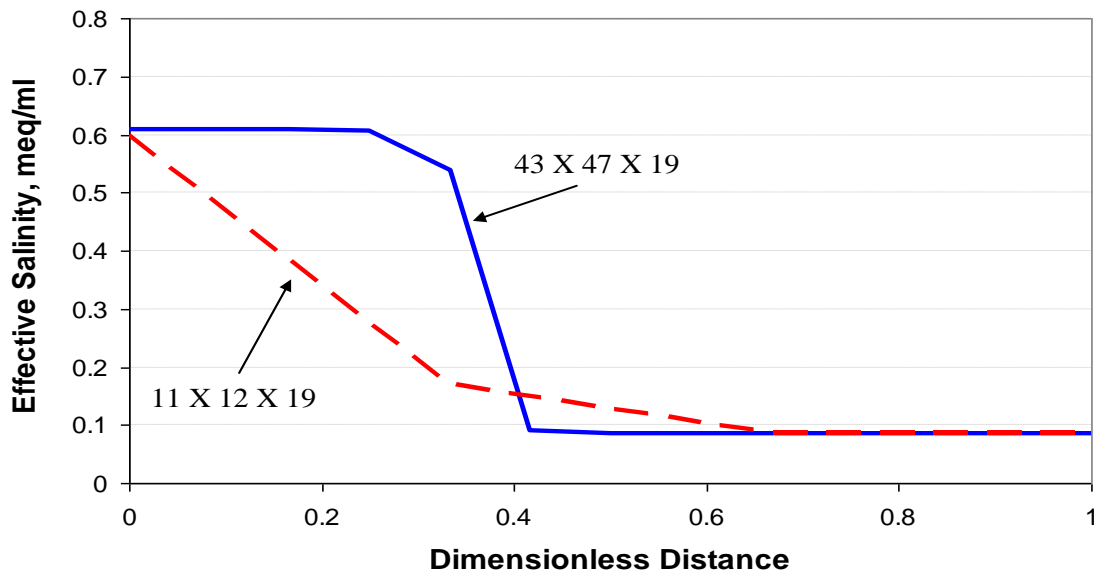


Figure 3.12: Salinity profile comparison for layer 19 of 11 X 12 X 19 and 43 X 47 X 19 grid after 0.1 PV injection

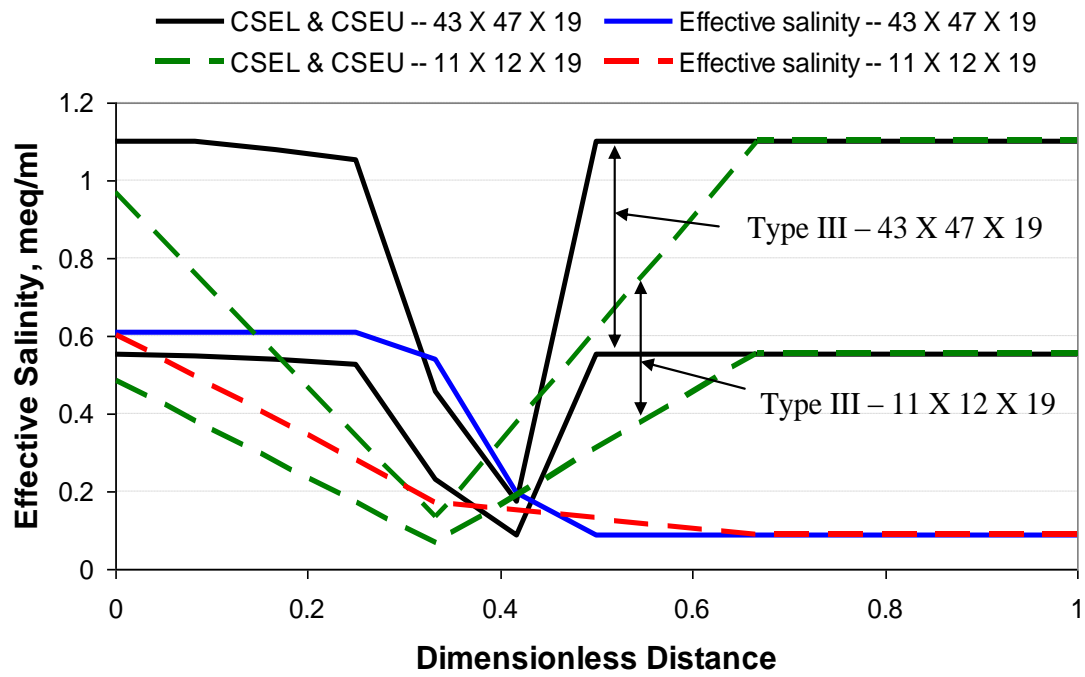


Figure 3.13: Salinity profile comparison for 11 X 12 X 19 and 43 X 47 X 19 after 0.1 PV along with the type III window for both the models

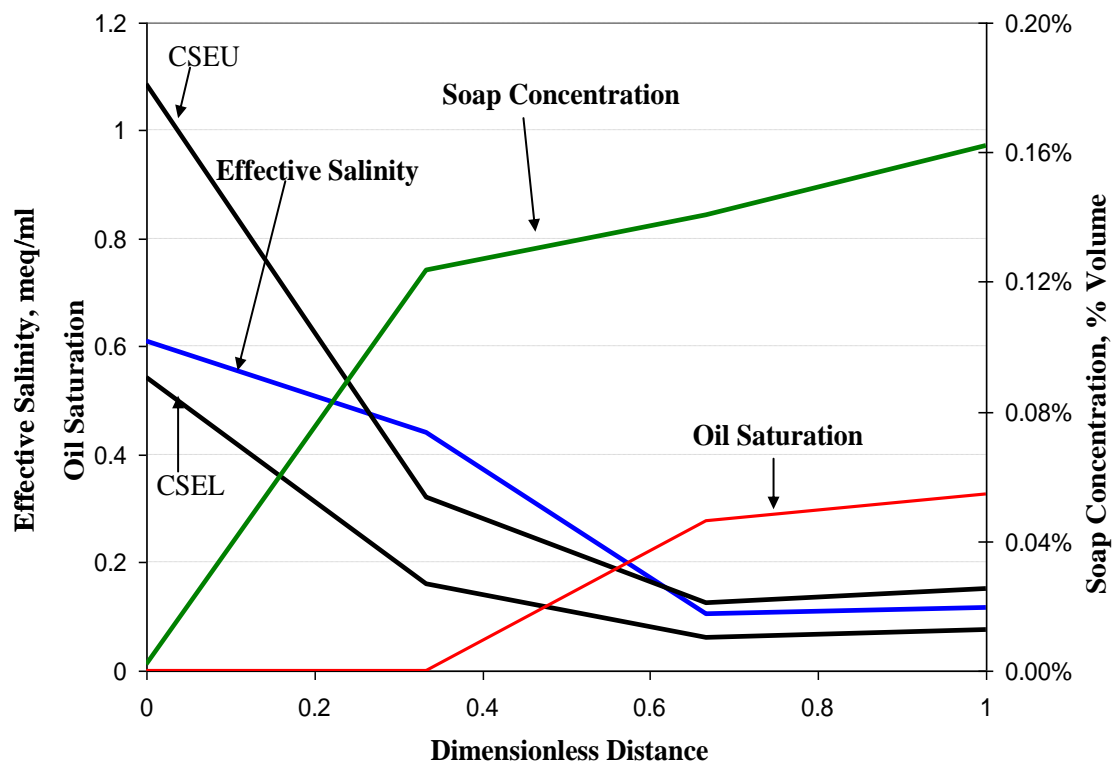


Figure 3.14: Profile for layer 19 of the 11 X 12 X 19 model after 0.2 PV injection

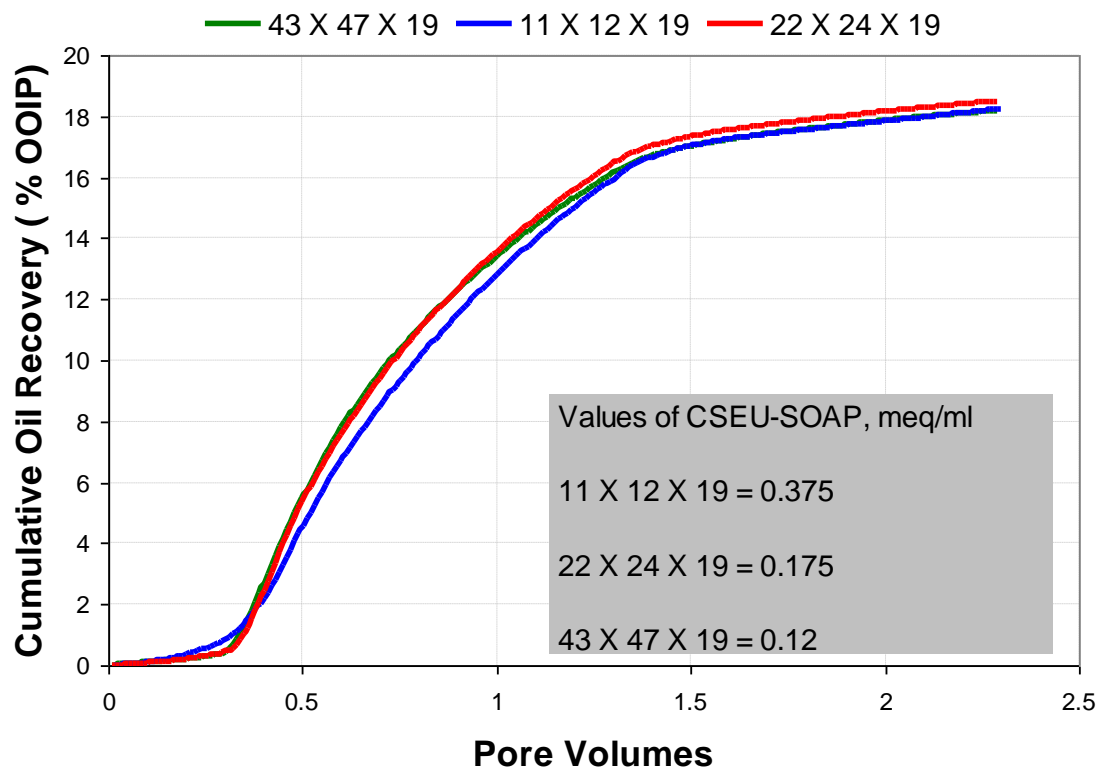


Figure 3.15: Cumulative oil recovery in terms of % original oil in place (% OOIP) for ASP flood simulations with salinity window (soap) adjusted for coarser models.

Chapter 4: Conclusions and Recommendations

4.1 CONCLUSIONS

The effect of grid block size on the simulated performance of a particular chemical flood with an unfavorable salinity gradient in a very heterogeneous reservoir that was the focus of this study can be summarized as follows:

- ✚ The oil recovery decreased when the grid was coarsened in the areal direction and a reverse trend was observed in the vertical direction. The impact of parameters such as salinity gradient, surfactant dilution, interfacial tension, dispersion, critical micelle concentration and capillary desaturation curves were studied.
- ✚ The artificially high dilution of alkali and surfactant concentrations in the coarse grid simulations was identified as the key phenomenon affecting the oil recoveries. The dilution produces computed salinities that are lower than the optimum salinity values and thus the IFT is too high and the oil recovery too low compared to accurate fine-grid results. Coarse grid simulations are biased to oil recoveries that are too low.
- ✚ Coarse grid oil recoveries became similar to the finest grid simulation results when a pseudo optimum salinity or a pseudo IFT curve was used to upscale the results. However, this should not be taken as a general result since other chemical flood designs will be sensitive to different variables that must be carefully studied for each particular case. It is highly desirable to just use a fine grid, but this is not always feasible, so an upscaling strategy such as illustrated may have to be considered in such cases. This example is just the start of the investigation that is needed to determine how to approach upscaling of chemical flooding.

4.2 RECOMMENDATIONS

- ✚ The effect of grid size on ASP simulations discussed was based only on a particular chemical flood with an unfavorable salinity gradient in a very heterogeneous reservoir. The conclusions outlined may not be general and apply to a new case. More simulation runs with different grid sizes and different ASP designs should be studied to analyze the effect of grid sizes on ASP simulation results and should be compared with the studies reported here.
- ✚ More upscaling strategies could be explored other than the ones reported in this work. One of the methods could be the use of a dilution coefficient which could be added to the concentration equation which could negate the effect of dilution. In the simulations discussed here the dilution of surfactant and salinity concentrations was the main reason for the difference in performance of ASP simulations with different grid block models.
- ✚ More ASP simulation design with a normal salinity gradient should be studied. The effect of dilution would be much less sensitive to grid sizes when a normal salinity gradient is maintained in the design.

Appendix A: Average layer permeabilities of all the grid block models

Table A1: Average permeability of all the layers of 43 X 47 X 19 grid.

LAYER 1	178
LAYER 2	477
LAYER 3	351
LAYER 4	558
LAYER 5	378
LAYER 6	513
LAYER 7	784
LAYER 8	1350
LAYER 9	1470
LAYER 10	1798
LAYER 11	2514
LAYER 12	2096
LAYER 13	2253
LAYER 14	2527
LAYER 15	2399
LAYER 16	2449
LAYER 17	4893
LAYER 18	5982
LAYER 19	6651

Table A2: Average permeability of all layers of 22 X 24 X 19 grid.

LAYER 1	178
LAYER 2	477
LAYER 3	351
LAYER 4	558
LAYER 5	378
LAYER 6	514
LAYER 7	784
LAYER 8	1350
LAYER 9	1470
LAYER 10	1798
LAYER 11	2514
LAYER 12	2096
LAYER 13	2253
LAYER 14	2527
LAYER 15	2400
LAYER 16	2450
LAYER 17	4893
LAYER 18	5982
LAYER 19	6651

Table A3: Average permeability of all the layers of 11 X 12 X 19 grid.

LAYER 1	107
LAYER 2	309
LAYER 3	219
LAYER 4	355
LAYER 5	223
LAYER 6	332
LAYER 7	4946
LAYER 8	962
LAYER 9	909
LAYER 10	1301
LAYER 11	1955
LAYER 12	1582
LAYER 13	1741
LAYER 14	1758
LAYER 15	1917
LAYER 16	1963
LAYER 17	3960
LAYER 18	5529
LAYER 19	6035

Table A4: Average permeability of all the layers of 43 X 47 X 10 grid.

LAYER 1	438
LAYER 2	563
LAYER 3	554
LAYER 4	1163.4
LAYER 5	1718.6
LAYER 6	2376
LAYER 7	2460
LAYER 8	2492
LAYER 9	5445
LAYER 10	6651

Table A5: Average permeability of all the layers of 43 X 47 X 5 grid.

LAYER 1	500
LAYER 2	858
LAYER 3	2047
LAYER 4	2476
LAYER 5	5709

Table A6: Average permeability of all the layers of 22 X 24 X 10 grid.

LAYER 1	260
LAYER 2	360
LAYER 3	350
LAYER 4	886
LAYER 5	1356
LAYER 6	2018
LAYER 7	2037
LAYER 8	2168
LAYER 9	4982
LAYER 10	6390

Appendix B: Hand's model for binodal curve

Hand's model for binodal curve is given by the following equation.

$$\frac{C_{3\ell}}{C_{2\ell}} = A \left(\frac{C_{3\ell}}{C_{1\ell}} \right)^B \quad \ell = 1, 2, \text{ or } 3 \dots\dots\dots (B1)$$

$C_{3\ell}$ Concentration of surfactant in phase ℓ

$C_{2\ell}$ Concentration of oil in phase ℓ

$C_{1\ell}$ Concentration of water in phase ℓ

1, 2 and 3 represents aqueous, oleic and microemulsion phases respectively

For symmetrical binodal curve, the parameter B in the equation can be assumed a value of -1. The parameter A is related to the height of binodal curve and is given as

$$A_m = \left(\frac{2C_{3\max,m}}{1 - C_{3\max,m}} \right)^2 \quad m = 0, 1, \text{ and } 2 \dots\dots\dots (B2)$$

The value of m of 0, 1 and 2 represents zero salinity, optimum salinity and twice optimum salinity conditions. $C_{3\max}$ is the height of binodal curve. The parameter A is related to salinity through the equation given below

$$\begin{aligned} A &= (A_o - A_1) \left(1 - \frac{C_{SE}}{C_{SEOP}} \right) + A_1 && \text{for } C_{SE} \leq C_{SEOP} \\ A &= (A_2 - A_1) \left(\frac{C_{SE}}{C_{SEOP}} - 1 \right) + A_1 && \text{for } C_{SE} > C_{SEOP} \end{aligned} \dots\dots\dots (B3)$$

where, CSE is the effective salinity and CSEOP is the optimum salinity. Solving A1, A2 and A3 in terms of $C_{2\ell}$ is given by

$$C_{3\ell} = \frac{1}{2} \left[-AC_{2\ell} + \sqrt{AC_{2\ell}^2 + 4AC_{2\ell}(1 - C_{2\ell})} \right] \quad \ell = 1, 2, \text{ or } 3 \quad \dots (B4)$$

We know that the sum of the concentration of all the components in a phase is equal to one.

$$C_{1\ell} = 1 - C_{2\ell} - C_{3\ell} \quad \dots\dots\dots (B5)$$

Figure B1 shows ternary diagrams for a surfactant-oil-water mixture at various salinities. The binodal curve and corresponding tie lines are seen in the figure for various ternary plots. As the salinity increases, the mixture shows a transition for Type II- to Type III. Along with this transition the height of binodal curve also changes. The height of the curve decreases when the system goes from Type II- to Type III. Further increase in salinity causes the mixture to go from Type III to Type II+.

There are only two phases below the binodal curve for Type II (–) and Type II(+) phase behavior,. The following equation defines the tie lines when two phases exist.

$$\frac{C_{3\ell}}{C_{2\ell}} = E \left(\frac{C_{3\ell'}}{C_{1\ell'}} \right)^F \quad \dots\dots\dots (B6)$$

where ℓ and ℓ' are the two phases. In the absence of available data for tie lines, F is calculated from $F = -1/B$. For a symmetric binodal curve ($B=-1$), F is equal to 1.

Because the component concentrations are in volume fractions, they must add up to one; therefore, imposing the constraint equations gives:

$$C_{1\ell'} + C_{2\ell'} + C_{3\ell'} = 1 \dots\dots\dots (B7)$$

There are 5 equations and 6 unknowns. The equations could be solved by choosing any phase concentration of a component between 0 and 1 to sweep the phase diagram.

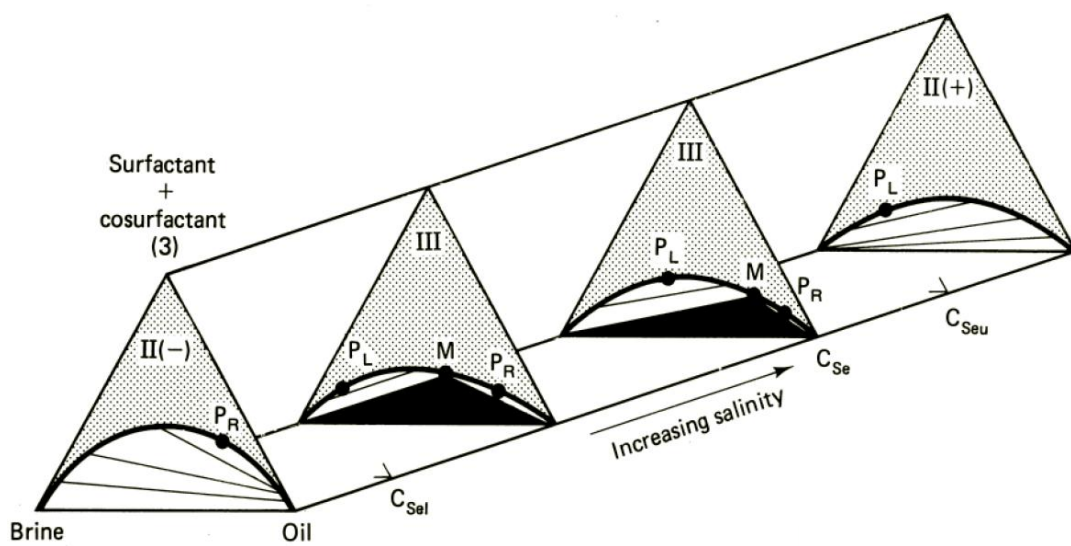


Figure B1: Ternary diagrams for surfactant-water-oil mixture at different salinities

Appendix C: Guidelines for Selection of phase behavior parameters for Alkaline/Surfactant/Polymer (ASP) flooding.

This appendix gives guidelines to obtain the input parameters for UTCHEM to model physical and chemical phenomenon such as microemulsion phase behavior, surfactant adsorption, micro emulsion viscosity, IFT, capillary desaturation and physical dispersion.

The physics and chemistry of the ASP process can be quite complicated, and simulation of such processes demands that the user specify more data than are normally required for the simulation of other primary and secondary recovery processes. For example, the presence of surfactant causes multiple phases of liquid to be present, and each has its own flow properties. The viscosity and density of a given phase, properties which affect the fluid flow behavior, are functions of the composition of that phase, the temperature, salinity and the pH. To model all of these phenomena, the surfactant/water/oil phase behavior, interfacial tension, viscosity, and density must be known. Other critical data that involve the interaction between the surfactant solution and the reservoir rock include the surfactant adsorption and cation exchange. These phenomenon are modeled through equations which are matched with the experimental data available using input parameters (UTCHEM technical documentation, 2000).

The following sections describe procedures to obtain the input parameters to model the processes which are most important in terms of ASP flooding.

Phase Behavior

Phase behavior experiments identify surfactants with acceptably high oil solubilization, rapid coalescence times, and minimal tendency to form liquid crystals, gels, and emulsions. Solubilization ratio diagram, volume fraction diagram and ternary

diagrams commonly represent the phase behavior. The solubilization ratio diagram provides an understanding of the sensitivity of the surfactant solution behavior to additional electrolyte. Solubilization ratio diagrams provide information on the electrolyte concentrations at which a transition from Winsor Type I to Type III to Type II is observed (Figure C1). The salinity at which the transition occurs from Type I to Type III is called lower critical salinity (CSEL) and the salinity at which transition occurs from Type III to Type II is called upper critical salinity (CSEU). In addition, these diagrams provide information on the solubilization of the oil in the microemulsion and the optimum salinity. Ternary phase diagrams represent surfactant phase behavior as a function of varying concentrations of surfactant, oil, and water.

Phase Behavior data from laboratory

The factors which affect the phase behavior of a water/surfactant/oil system are oil concentration, surfactant concentration and electrolyte concentration. Laboratory phase behavior studies are done by varying one of these parameters keeping all the other fixed. Figure C2 shows the data of phase behavior experiment done on a system where the oil concentration is fixed at a WOR of 4 (20 % oil and 80 % water containing 0.5 % surfactant). The type of surfactants used is shown in the figure.

The electrolyte concentration (salinity) is varied from 20,000 ppm Na_2CO_3 to 45,000 ppm Na_2CO_3 . The salinity at which the oil solubilization ratio and water solubilization ratio are equal is called the optimum salinity. The optimum salinity occurs at an electrolyte concentration of 32,500 ppm Na_2CO_3 and an optimum solubilization ratio of 9 is observed (figure C2). Lower and upper critical salinity is denoted by dashed lines and the phase regions are marked.

Background salinity

One of the things to be noted about the phase behavior plot shown in Figure C2 is that the salinity in terms of ppm Na₂CO₃ is the salinity added to brine, which already has some salinity. Usually the phase behavior experiments are performed with the formation water from the reservoir. In such cases the background salinity is the formation water salinity. The salinity of certain formation water is very high thus it is important to consider that background salinity in modeling phase behavior of such brine.

Phase Behavior Match

The phase behavior is modeled in UTCHEM using Hand's rule of binodal curve and is explained in Appendix B. The equations derived from Hand's model for phase behavior calculations are solved using the height of binodal curve as input parameters. The input parameters in UTCHEM which represent the height of binodal curve are HBNC70, HBNC71 and HBNC72, which are the height of binodal curve at zero, optimum and twice optimum salinity conditions (C_{3max}, m). The values of these parameters are obtained by matching the laboratory measured phase behavior data. It is important to match the phase behavior measured in the lab to get the Height of Binodal Curve (HBNC) parameters and the salinity window (CSEL and CSEU) which are to be used for core flood matching and further to a field scale simulations.

1) Phase Behavior Match using UTCHEM in Batch Mode

UTCHEM can be used to predict the phase behavior of a surfactant oil system by performing a batch mode simulation. Here the idea is to depict the experiment done in the lab. The phase behavior is modeled in UTCHEM using Hand's rule. The following caveats are to be kept in mind while running the simulation in batch mode.

- ✚ The permeability value is kept extremely high ($> 100000\text{md}$) and the porosity values are given a value of 1 to depict a pipette used in the experiment.
- ✚ The initial water saturation tab in UTCHEM (ISWI) is kept as the volume fraction of initial water in the phase behavior experiment for example if a WOR of 1 is used in the experiment then ISWI of 0.5 is to be used.
- ✚ Straight line relative permeability is used. The end points and exponents are kept as unity
- ✚ The viscosity of water and oil is kept as 1.
- ✚ The parameters for capillary pressure, dispersion and adsorption are zero.
- ✚ The phase behavior parameters (HBNC) are given an initial guess value for the first run. HBNC 71 is taken as $\frac{1}{2*\sigma}$ where σ is the solubilization ratio at optimum salinity. The values of HBNC70 and HBNC72 are kept at values higher than HBNC71. A value of 1.5 times HBNC71 can be used as an initial value for HBNC70 and HBNC72. For example, for a phase behavior data shown in Figure C2, the optimum solubilization ratio is around 9. Thus the initial approximation for HBNC71 would be $\frac{1}{2*9} = 0.055$ and the initial approximation for HBNC70 and HBNC71 are taken as 0.08.
- ✚ CSEL and CSEU are read from lab data and given as input in UTCHEM. These values could be fine tuned for better match of solubilization parameters over the entire range of salinities.
- ✚ The injection data in the well data section of the UTCHEM input file has to be entered carefully. Two wells are initially assigned in the well data (1 constant rate injector and 1 constant pressure producer). The injection well ID is kept as 1 and the producer well ID is kept as 2. The injection well data consists mainly of three

lines of input where each line represents each phase (first line for aqueous phase, second line for oleic and third for microemulsion phase).

- ✚ As mentioned earlier, the idea of running UTCHEM in batch mode is to depict the phase behavior experiment done in the laboratory. For a fixed oil concentration, the salinity in the pipettes is varied and solubilization ratios for oil and water are measured and are plotted against salinity (Figure C2). A UTCHEM simulation is performed for each pipette. The only parameter changing in these pipettes is the salinity.
- ✚ The ratio of water and oil injection rates in the input file represents the WOR of the test tube experiments. The exact values of the well rates are irrelevant. For example, if the WOR is 1 the injection rates for water and oil phase can be entered a same value. If the WOR is different then the ratio of the value of water to oil rate should be equal to the WOR. For 20 % oil and 80 % water, the water rate can be given a value of 0.08 and thus the oil a value of 0.02. Figure C3 shows the details of well injection in UTCHEM input file.
- ✚ The concentration values of each component are then entered. In the phase behavior experiments, the surfactant and the salt are mixed in water thus the concentrations of these components are entered in the first line of the well injection data (Figure C3). The concentration of oil is kept as 1 in the second line and all other concentration in that line is kept as zero. The salinity or the chloride concentration is entered in meq/ml. Therefore, the commonly used laboratory unit of weight percent should be converted to meq/ml. One of the important things to note is that the salinity entered in this section should be a summation of background salinity, explained earlier, and the added salinity for the particular pipette. The conversions from commonly used units to meq/ml for two cases are

shown below. The first one is the conversion of 15000 ppm NaCl (1.5 % weight NaCl). The second case is the conversion from 32,500 ppm Na₂CO₃.

✚ 15000 ppm NaCl is converted to meq/ml as follows:

❖ First Calculate the concentration of Na⁺ ion in NaCl:

$$✚ 15000 \left| \text{ppm NaCl} \right| = 15000 \left| \frac{\text{mg}}{1} \text{NaCl} \right| * \frac{23 \left| \frac{\text{g}}{\text{mole}} \text{Na} + \right|}{58.5 \left| \frac{\text{g}}{\text{mole}} \text{NaCl} \right|} = 5897.53 \left| \frac{\text{mg}}{1} \text{Na} + \right|$$

❖ Calculate the equivalent weight of Na⁺ :

$$\frac{23 \left| \frac{\text{g}}{\text{mole}} \text{Na} + \right| * 1000 \left| \frac{\text{mg}}{\text{g}} \right|}{1 \left| \frac{\text{eq}}{\text{mole}} \right|} = 23000 \left| \frac{\text{mg}}{\text{eq}} \text{Na} + \right|$$

❖ Calculate concentration in meq/ml

Divide the concentration of Na⁺ calculated above by the equivalent weight

$$\frac{5897.53 \left| \frac{\text{mg}}{1} \text{Na} + \right|}{23000 \left| \frac{\text{meq}}{\text{eq}} \right|} = 0.2564 \left| \frac{\text{eq}}{1} \text{Na} + \right| = 0.2564 \left| \frac{\text{meq}}{\text{ml}} \text{Na} + \right|$$

The second case is 32,500 ppm Na₂CO₃ (the optimum salinity for the phase behavior shown in Figure C2).

✚ 32,500 ppm Na₂CO₃ is converted to meq/ml as follows:

❖ First Calculate the concentration of Na⁺ ion in Na₂CO₃:

$$32500 \left| \text{ppm Na}_2\text{CO}_3 \right| = 32500 \left| \frac{\text{mg}}{1} \text{Na}_2\text{CO}_3 \right| * \frac{23 \left| \frac{\text{g}}{\text{mole}} \text{Na} + \right|}{106 \left| \frac{\text{g}}{\text{mole}} \text{Na}_2\text{CO}_3 \right|} * 2 = 14103.77 \left| \frac{\text{mg}}{1} \text{Na} + \right|$$

It should be noted that there are 2 moles of Na⁺ ions for every mole of CO₃²⁻ ion in Na₂CO₃

❖ Calculate the equivalent weight of Na⁺ :

$$\frac{23 \left| \frac{\text{g}}{\text{mole}} \text{Na} + \right| * 1000 \left| \frac{\text{mg}}{\text{g}} \right|}{1 \left| \frac{\text{eq}}{\text{mole}} \right|} = 23000 \left| \frac{\text{mg}}{\text{eq}} \text{Na} + \right|$$

❖ Calculate concentration in meq/ml

Divide the concentration of Na⁺ calculated above by the equivalent weight

$$\frac{14103.77 \left| \frac{\text{mg}}{1} \text{Na} + \right|}{23000 \left| \frac{\text{meq}}{\text{eq}} \right|} = 0.6132 \left| \frac{\text{eq}}{1} \text{Na} + \right| = 0.6132 \left| \frac{\text{meq}}{\text{ml}} \text{Na} + \right|$$

The background salinity for the case shown in Figure C2 is 2865 ppm NaCl, which is equal to 0.0513 meq/ml. Thus to simulate the pipette with optimum salinity the anionic concentration entered in the input file will be a summation of 0.6132 and 0.0513 meq/ml which is 0.6645 meq/ml as seen in Figure C3.

✚ After simulating for a particular salinity, the solubilization ratio is calculated from the values given in the output file (history of the producer) by using the formula

$$R_{23} = \frac{C_{23}}{C_{33}}$$

$$C_{23} = \frac{\text{volume of dissolved Oil in microemulsion phase}}{\text{volume of microemulsion phase}}$$

$$C_{33} = \frac{\text{volume of added surfactant t in microemulsion phase}}{\text{volume of microemulsion phase}}$$

$$C_{13} = 1 - C_{23} - C_{33}$$

Where R_{23} -- oil solubilization ratio

C_{23} -- Concentration of oil solubilized in microemulsion

C_{33} -- Concentration of Surfactant solubilized in microemulsion

✚ The simulated values of oil and water solubilization ratio are matched with the measured lab data. If simulated value of solubilization ratio at that salinity is not matching with the lab data, then the values given as initial guess for HBNC70, HBNC71 and HBNC72 are changed and run the UTCHEM simulation again. This procedure is repeated until a good match for that salinity is achieved.

✚ The above discussion outlines a procedure to match the solubilization ratio at a particular salinity (solubilization ratio observed in one pipette). The above steps are repeated for all the salinity by only changing the salinity value in the input file. Figure C4 shows the match of UTCHEM batch results with lab data. The final values of HBNC s, CSEL and CSEU are given in Table C1.

2) Phase Behavior Match using spreadsheet

A spreadsheet was developed to match the phase behavior data from the laboratory. The equations of Hand's model explained in Appendix B are solved for the values of compositions of different components (water, oil and surfactant) in different phases (aqueous, oleic and microemulsion). These compositions are solved for the entire range of salinities indicated in the phase behavior experiments. Solubilization ratio are calculated from the compositions solved and are matched with the lab data. The initial guess for input parameters such as HBNC70, HBNC71 and HBNC72 are entered in the spreadsheet. CSEL, CSEU, the background salinity and the surfactant concentration are also entered as input to the spreadsheet. Figure C5 shows the part of the spreadsheet where the input parameters are entered. Input parameters are entered in the cells colored in yellow. Figure C5 shows the input parameters used to match the phase behavior data shown in Figure C2. The laboratory data are also entered as input to the spreadsheet. Figure C6 shows the part of spreadsheet where the lab data should be entered. As said earlier, the input data are entered in cells colored in yellow.

After all the input values, described earlier, are lab entered, the PLOT tab shown in Figure C6 should be clicked. This will plot the solubilization ratio values from the equations described in Appendix B. The solubilization ratios are plotted with the lab data to compare the values. Figure C7 shown the result of the match using spreadsheet. A good match is observed between the lab data and that calculated by the spreadsheet. Figure C8 shows the match of the lab data with both UTCHEM and the Spreadsheet.

The input values of HBNC s, CSEL and CSEU are then used in core flood and field scale simulations.

Table C1: Phase behavior parameters used to match the phase behavior data shown in figure C3

Height of binodal curve at zero salinity, HBNC 70	0.06
Height of binodal curve at optimum salinity, HBNC 71	0.05
Height of binodal curve at twice optimum salinity, HBNC 72	0.06
Lower critical salinity window, CSEL, meq/ml	0.5
Upper critical salinity window, CSEU, meq/ml	0.85

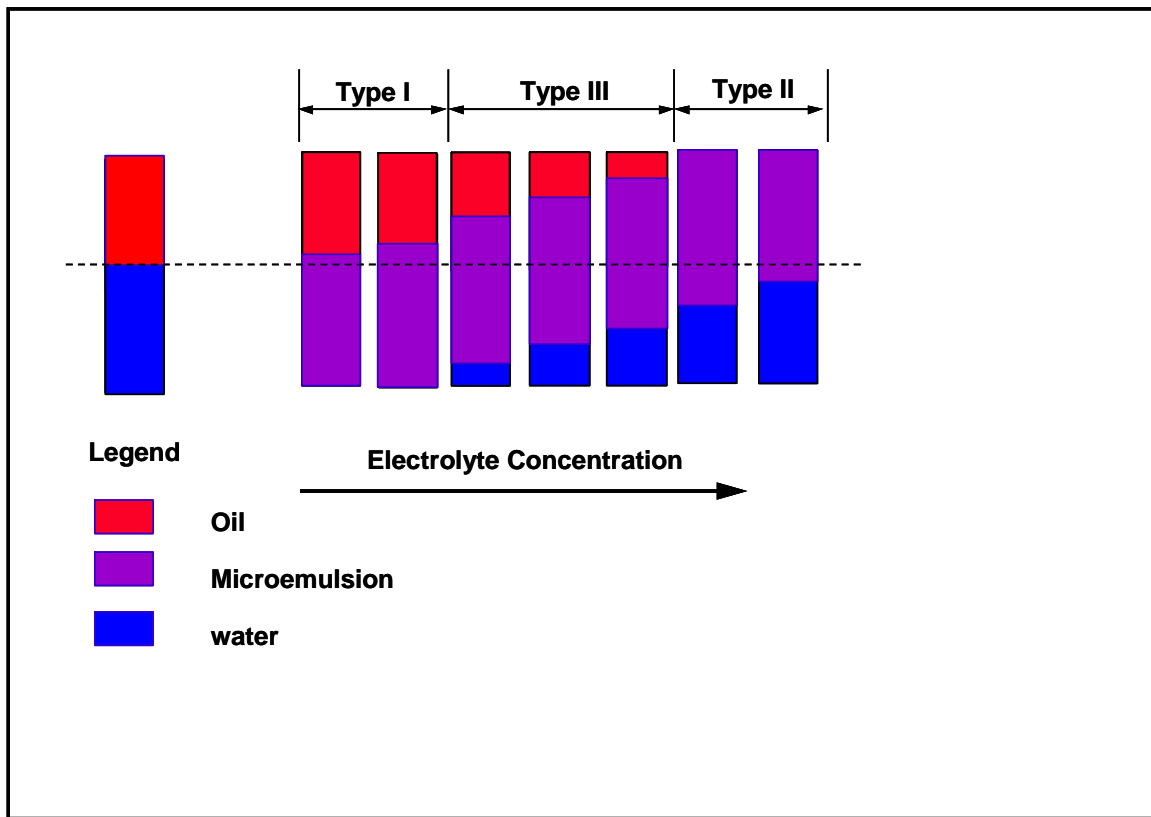


Figure C1: The effect of salinity on microemulsion phase behavior. Winsor type regions are also marked

0.25 % ISOFOL (C32-7PO-6EO-SULFATE) + 0.25 % PETROSTEP S3A ; 0.25 % TEGBE +
0.4 % MA 80 I (SODIUM DIHEXYL SULFOSUCCINATE)

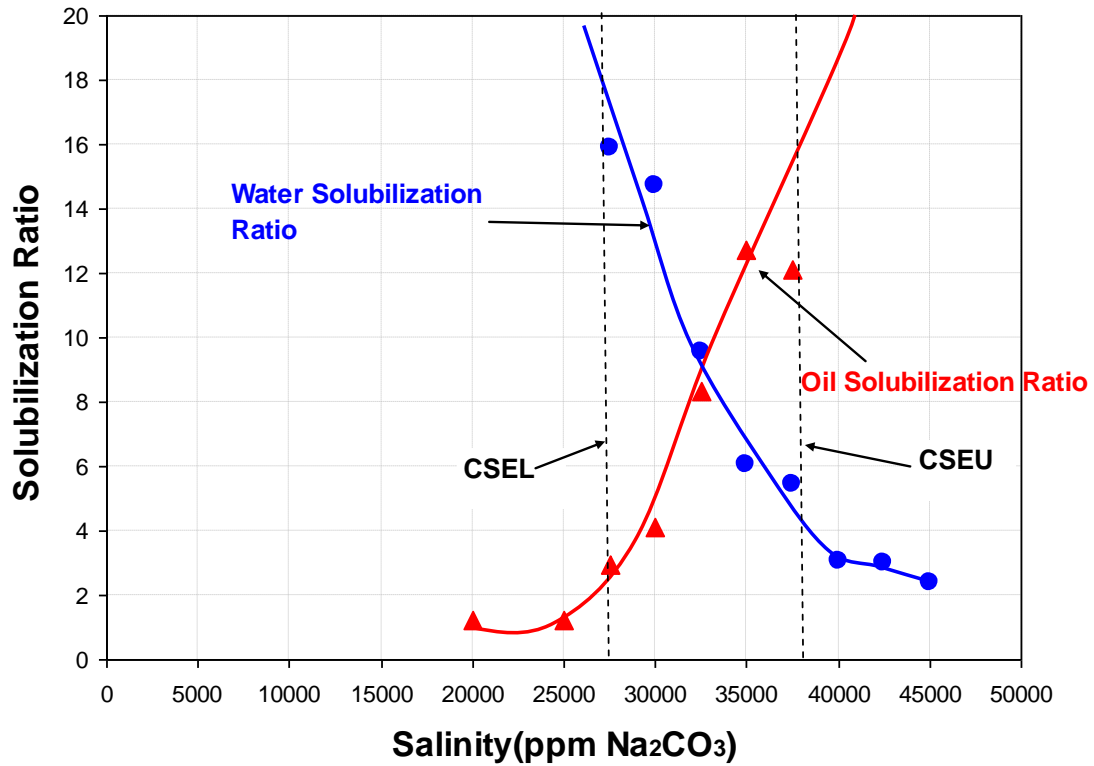


Figure C2: Phase behavior laboratory data

CC

CC

*----	ID	Injection rate (QI)	Water	Oil	Surfactant	Polymer	Chloride	Calcium	Alcohol 1
	1	0.08	0.995	0	0.005	0	0.664508	0	0
	1	0.02	0	1	0	0	0	0	0
	1	0	0	0	0	0	0	0	0

WOR (80 % Water and 20 % Oil)

Surfactant Concentration

Chloride Concentration (Salinity)

Figure C3: Data which are entered in the injection details of the input file to match the laboratory phase behavior data

0.25 % ISO FOL (C32-7PO-6EO-SULFATE) + 0.25 % PETROSTEP S3A ; 0.25 % TEGBE + 0.4 % MA 80 I (SODIUM DIHEXYL SULFOSUCCINATE)

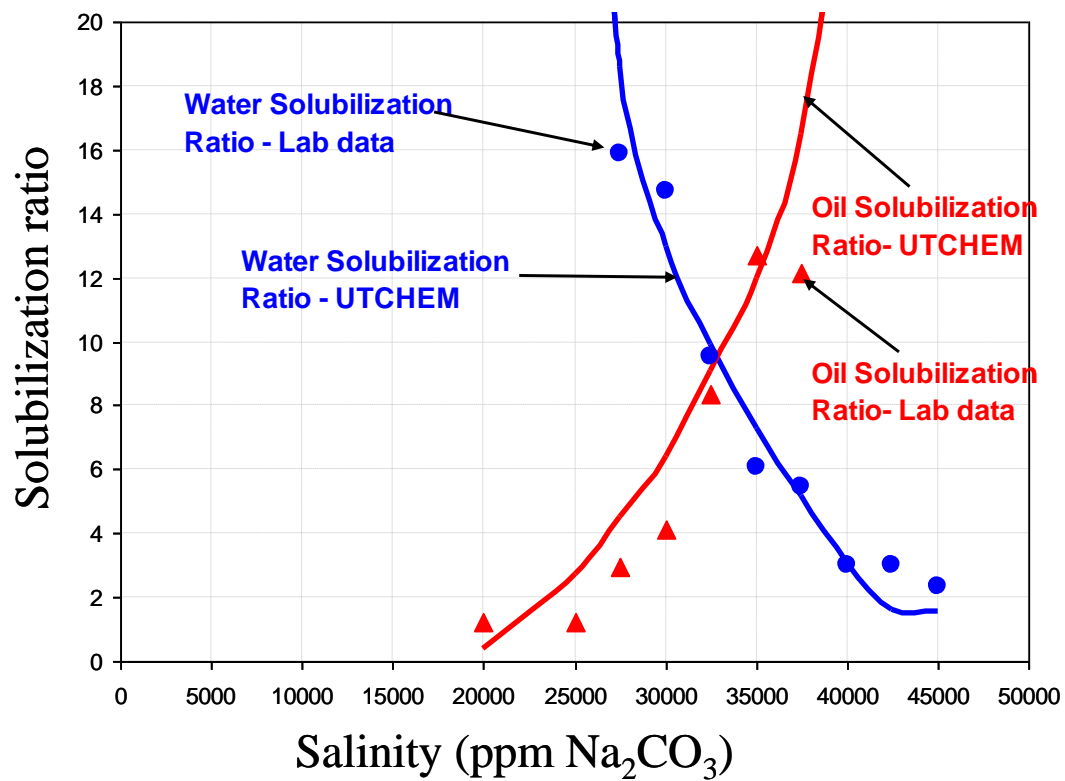


Figure C4: Phase behavior match with laboratory data using UTCHEM in batch mode

ENTER THE OPTIMUM SOLUBILIZATION RATIO		9.4
INITIAL GUESS FOR HBNC 71		0.051
ENTER VALUES OF INPUT PARAMETERS		
HBNC70	0.0600	Height of binodal curve at zero salinity
HBNC71	0.0500	Height of binodal curve at optimal salinity
HBNC72	0.0600	Height of binodal curve at twice optimal salinity
CSEL7	0.5000	Minimum effective salinity for type III systems
CSEU7	0.8500	Maximum effective salinity for type III systems
CSOPT	0.6750	Optimal salinity
CPRC	1.0000	Right hand plait point
CPLC	0.0000	Left hand plait point
DENSITY	0.7300	oil density, mg/L
	4.5	
CSE	0.0513	Enter Background Salinity Here
	0.9004	Salinity, meq/ml
Surfactant	0.50	Surfactant Concentration in Water, % Volume

Figure C5: Input parameters entered in the spreadsheet to match the phase behavior data



enter salinity here salinity wt %	TDS, ppm	SOLUBILIZATION VALUES FROM LAB		SPREADSHEET	
		R13	R23	R13	R23
2	20000		1.2121	225.9242	0.3409
2.5	25000		1.2308	37.59703	2.1703
2.75	27500	15.88235	2.9412	19.10561	4.4014
3	30000	14.70588	4.1176	13.3717	6.4880
3.25	32500	9.552239	8.3582	10.0834	8.8853
3.5	35000	6.060606	12.7273	7.490121	11.7427
3.75	37500	5.454545	12.1212	5.294111	16.0512
4	40000	3.030303		3.205001	25.5215
4.25	42500	2.985075		0.402088	199.6417
4.5	45000	2.366864		0.27991	278.6297

Figure C6: A screen shot of the spreadsheet which was developed to match the phase behavior data. The picture shows the input salinity values and solubilization ratios from lab and also from the spreadsheet

0.25 % ISO FOL (C32-7PO-6EO-SULFATE) + 0.25 % PETROSTEP S3A ; 0.25 % TEGBE + 0.4 % MA 80 I (SODIUM DIHEXYL SULFOSUCCINATE)

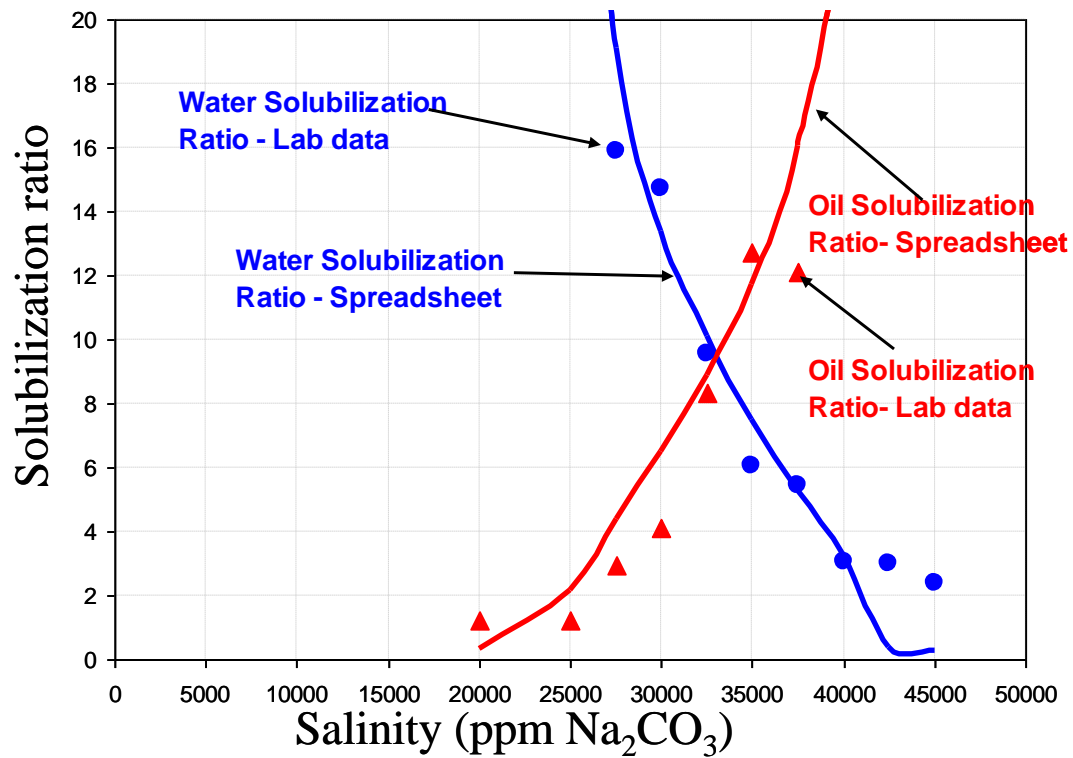


Figure C7: Phase behavior match with laboratory data using the spreadsheet developed

0.25 % ISO FOL (C32-7PO-6EO-SULFATE) + 0.25 % PETROSTEP S3A ; 0.25 % TEGBE + 0.4 % MA 80 I (SODIUM DIHEXYL SULFOSUCCINATE)

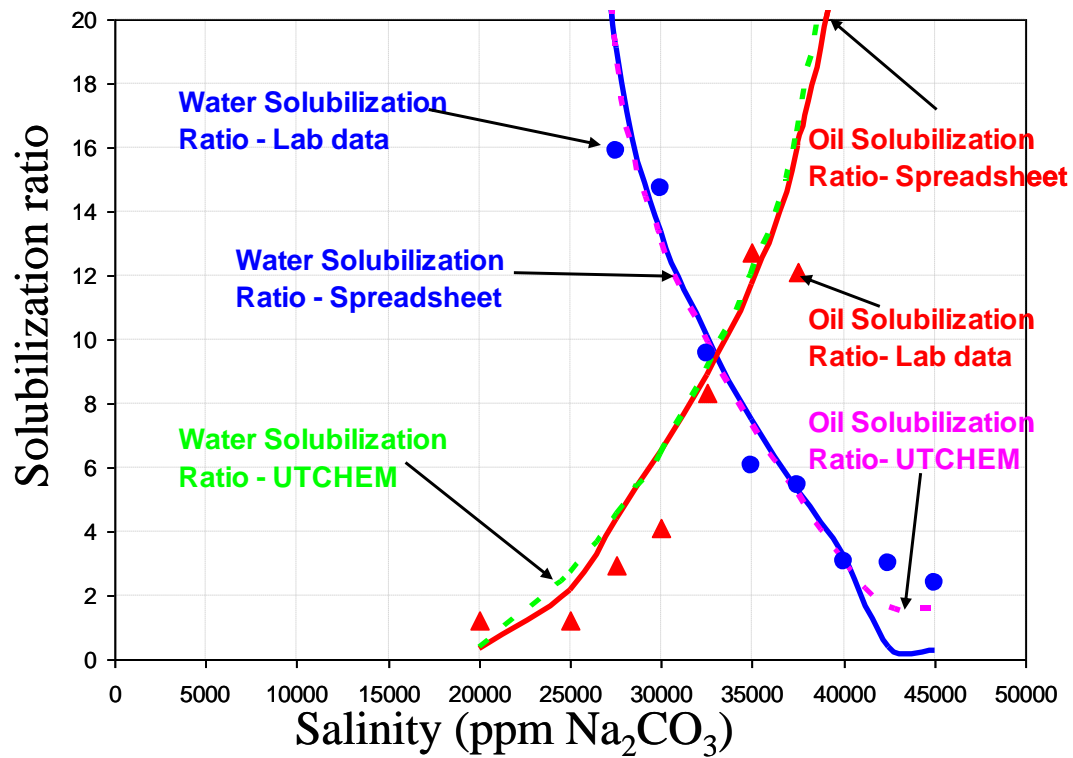


Figure C8: Phase behavior match with laboratory data using UTCHEM in batch mode as well as spreadsheet developed

Appendix D: UTCHEM INPUT FILES

D1: INPUT FILE FOR 43 X 47 X 19 MODEL FOR THE CASE DESCRIBE IN CHAPTER 2:

```

CC*****
**
CC
CC          *
CC  BRIEF DESCRIPTION OF DATA SET : UTCHEM9p97          *
CC          *
CC*****
**
CC
CC          *
CC          *
CC          *
CC  LENGTH (FT) : 2100      PROCESS:          *
CC  THICKNESS (FT) : 37 ft    INJ. RATE (FT3/DAY) :          *
CC  WIDTH (FT) : 2400      COORDINATES : CARTESIAN          *
CC  POROSITY : variable      PROD. RATE (FT3/DAY):          *
CC  GRID BLOCKS : 43x47x19    1BBL=5.615 cubic feet          *
CC  DATE :          A1 Sand - original grid size          *
CC          *
CC*****
**
CC          *
CC*****
**
CC          *
CC  RESERVOIR DESCRIPTION          *
CC          *
CC*****
**
CC
CC
*----RUNNO (title)
UTMIN6
CC
CC
*----HEADER (need 3 lines)
UTMIN6
SP Flood
water flood till 56 % oil recovery
CC
CC SIMULATION FLAGS
*---- IMODE IMES IDISPC ICWM ICAP IREACT IBIO ICOORD ITREAC ITC IGAS ieng idual itens
1 2 3 0 0 0 0 1 0 0 0 0 0 0
CC
CC NUMBER OF GRID BLOCKS AND FLAG SPECIFIES CONSTANT OR VARIABLE GRID SIZE
*----NX NY NZ IDXYZ IUNIT
43 47 19 2 0
CC
CC CONSTANT GRID BLOCK SIZE IN X, Y, AND Z (in ft)
*----DX
75 75 75.00002 74.99998 75 75.00003 37.49997 37.5 37.5 37.5
37.5 37.5 37.5 37.5 37.5 37.5 37.50006 37.5 37.49994
37.5
37.50006 37.49994 37.5 37.5 37.50012 37.49988 37.5 37.5 37.50012
37.49988

```



```

37.5      37.5  37.50012      37.49988 37.5      37.5      75      75.00012 75      74.99988
75      75.00012      74.99988
CC
CC CONSTANT GRID BLOCK SIZE IN X, Y, AND Z (in ft)
*----DY
75      75      75.00002      74.99998      75      75.00003      74.99997      75
      37.5      37.5
37.5      37.5      37.5      37.5      37.50006 37.5      37.49994      37.5 37.50006 37.49994
37.5      37.5      37.50012      37.49988      37.5 37.5      37.50012      37.49988
      37.5      37.5
37.50012 37.49988 37.5      37.5      37.50012 37.49988      37.50012      37.5 75
74.99988
75      75.00012 74.99988      75      75      75.00024      74.99976
CC
CC
*----DZ (this is mean from NET from ecl2gocad) total thickness is about 37 ft
2 2 2 2 2 2 2 2 2 2 2 2 2 2 2 2 1
CC
CC TOTAL NO. OF COMPONENTS, NO. OF TRACERS, NO. OF GEL COMPONENTS
*----N no NTw nta ngc ng noth
      7 0 0 0 0 0 0
CC
CC All species must be present even for standard waterflood.
*---- species name
water
oil
surf(M3+IOS)
poFlymer(AN-125)
anion
calcium
alc(EGBE+t-Pent)
CC
CC FLAG INDICATING IF THE COMPONENT IS INCLUDED IN CALCULATIONS OR NOT
*----ICF(KC) FOR KC=1,N
      1 1 1 1 1 0 1
CC
CC*****
CC
CC      *
CC OUTPUT OPTIONS      *
CC      *
CC*****
CC
CC ICOPSM=0==>ECHO TO UNIT 5; ICUMTM=0==>TIME PRINTING;istop=1==>PV SPEC
CC FLAG TO ECHO THE INPUT, FLAG TO WRITE TO UNIT 5, FLAG FOR PV OR DAYS
*----ICUMTM ISTOP IOUTGMS
      1 1 0
CC
CC FLAG INDICATING IF THE PROFILE OF KCTH COMPONENT SHOULD BE WRITTEN
*----IPRFLG(KC),KC=1,N
      1 1 1 1 1 0 1
CC
CC FLAG FOR PRES,SAT.,TOTAL CONC.,TRACER CONC.,CAP.,GEL, ALKALINE PROFILES
*----IPPRES IPSAT IPCTOT IPBIO IPCAP IPGEL IPALK IPTEMP IPOBS
      1 1 1 0 0 0 0 0 0
CC ICKL is phase conc. (K is component and L is phase)
CC FLAG FOR WRITING SEVERAL PROPERTIES TO UNIT 6 (PROFIL)
*----ICKL IVIS IPER ICNM ICSE IHYSTP IFOAMP INONEQ
      1 1 1 1 1 0 0 0
CC
CC FLAG FOR WRITING SEVERAL PROPERTIES TO UNIT 6 (PROFIL)

```

```

*----IADS IVEL IRKF IPHSE
1 0 1 1
CC
CC*****
CC
CC RESERVOIR PROPERTIES
CC
CC*****
CC
CC
CC MAX. SIMULATION TIME
*---- TMAX 3.4 PV water
6.1
CC
CC ROCK COMPRESSIBILITY (1/PSI), STAND. PRESSURE(PSIA)
*----COMPR PSTAND
0.000008 14.7
CC Porosity Values For Each Grid Input Given Through Include Files
CC FLAGS INDICATING CONSTANT OR VARIABLE POROSITY, X,Y,AND Z PERMEABILITY
*----IPOR1 IPERMX IPERMY IPERMZ IMOD ITRANZ INTG
4 4 4 4 1 0 0
CC Depth To The Top Layer Input Given Through Include Files
CC FLAG FOR CONSTANT OR VARIABLE DEPTH, PRESSURE, WATER SATURATION
*----IDEPH IPRESS ISWI ICWI
4 1 0 -1
CC
CC
*----IPRESS DEPTH
550. 1965.77185
CC
CC WATER SATURATION
*----ISWI
0.2
CC
CC FLAG FOR RESERVOIR PROPERTY MODIFICATION
*----IMPOR IMKX IMKY IMKZ IMSW
0 1 1 1 0
CC
CC NUMBER OF REGIONS WITH MODIFIED X PERMEABILITY
*---- NMOD1
17
CC
CC FIRST AND LAST INDEX IN X,Y,Z DIRECTION,MODIFIED METHOD,CONSTANT VALUE.
*---- IMIN IMAX JMIN JMAX KMIN KMAX IFACT FACTX
16 16 13 13 19 19 2 0.4968
30 30 13 13 19 19 2 0.4968
36 36 25 25 19 19 2 0.5001
30 30 37 37 19 19 2 0.4995
16 16 37 37 19 19 2 0.4968
10 10 25 25 19 19 2 0.4968
10 10 5 5 19 19 2 0.5001
36 36 5 5 19 19 2 0.4968
36 36 44 44 19 19 2 0.5002
10 10 44 44 19 19 2 0.4968
22 22 25 25 19 19 2 0.4968
22 22 5 5 19 19 2 0.4968
40 40 13 13 19 19 2 0.5007
40 40 37 37 19 19 2 0.4968
22 22 44 44 19 19 2 0.4968
4 4 37 37 19 19 2 0.4968

```

4	4	13	13	19	19	2	0.4968
---	---	----	----	----	----	---	--------

CC
CC NUMBER OF REGIONS WITH MODIFIED Y PERMEABILITY
*---- NMOD2
17
CC
CC FIRST AND LAST INDEX IN X,Y,Z DIRECTION,MODIFIED METHOD,CONSTANT VALUE.
*---- IMIN IMAX JMIN JMAX KMIN KMAX IFACT FACTX

16	16	13	13	19	19	2	0.4968
30	30	13	13	19	19	2	0.4968
36	36	25	25	19	19	2	0.5001
30	30	37	37	19	19	2	0.4995
16	16	37	37	19	19	2	0.4968
10	10	25	25	19	19	2	0.4968
10	10	5	5	19	19	2	0.5001
36	36	5	5	19	19	2	0.4968
36	36	44	44	19	19	2	0.5002
10	10	44	44	19	19	2	0.4968
22	22	25	25	19	19	2	0.4968
22	22	5	5	19	19	2	0.4968
40	40	13	13	19	19	2	0.5007
40	40	37	37	19	19	2	0.4968
22	22	44	44	19	19	2	0.4968
4	4	37	37	19	19	2	0.4968
4	4	13	13	19	19	2	0.4968

CC
CC NUMBER OF REGIONS WITH MODIFIED Z PERMEABILITY
*---- NMOD3
17
CC
CC FIRST AND LAST INDEX IN X,Y,Z DIRECTION,MODIFIED METHOD,CONSTANT VALUE.
*---- IMIN IMAX JMIN JMAX KMIN KMAX IFACT FACTX

16	16	13	13	19	19	2	0.4968
30	30	13	13	19	19	2	0.4968
36	36	25	25	19	19	2	0.5001
30	30	37	37	19	19	2	0.4995
16	16	37	37	19	19	2	0.4968
10	10	25	25	19	19	2	0.4968
10	10	5	5	19	19	2	0.5001
36	36	5	5	19	19	2	0.4968
36	36	44	44	19	19	2	0.5002
10	10	44	44	19	19	2	0.4968
22	22	25	25	19	19	2	0.4968
22	22	5	5	19	19	2	0.4968
40	40	13	13	19	19	2	0.5007
40	40	37	37	19	19	2	0.4968
22	22	44	44	19	19	2	0.4968
4	4	37	37	19	19	2	0.4968
4	4	13	13	19	19	2	0.4968

CC formation water
CC CONSTANT CHLORIDE AND CALCIUM CONCENTRATIONS (MEQ/ML)
*----C50 C60
0.0513 0.0
CC
CC*****
CC utchem requires 2 alcohols
CC PHYSICAL PROPERTY DATA
CC
CC*****
CC

```

CC
CC OIL CONC. AT PLAIT POINT FOR TYPE II(+) AND TYPE II(-), CMC (do not change)
*---- C2PLC C2PRC EPSME IHAND
    0. 1. 0.0001 0
CC
CC
*---- IFGHBN
    0
CC SLOPE AND INTERCEPT OF BINODAL CURVE AT ZERO, OPT., AND 2XOPT SALINITY
CC
*----HBNS70 HBNC70 HBNS71 HBNC71 HBNS72 HBNC72
    0.0 0.055 0 0.035 0. 0.055
CC SLOPE AND INTERCEPT OF BINODAL CURVE AT ZERO, OPT., AND 2XOPT SALINITY
CC FOR ALCOHOL 2
*----HBNS80 HBNC80 HBNS81 HBNC81 HBNS82 HBNC82
    0. 0. 0. 0. 0. 0.
CC D
CC LOWER AND UPPER EFFECTIVE SALINITY FOR ALCOHOL 1(7) AND ALCOHOL 2 (8)
*----CSEL7 CSEU7 CSEL8 CSEU8
    0.5 0.85 0. 0.
CC
CC THE CSE SLOPE PARAMETER FOR CALCIUM AND ALCOHOL 1 AND ALCOHOL 2
*----BETA6 BETA7 BETA8
    0.0 0 0.0
CC
CC FLAG FOR ALCOHOL PART. MODEL AND PARTITION COEFFICIENTS
*----IALC OPSK7O OPSK7S OPSK8O OPSK8S
    0 0.0 0 0. 0.
CC
CC NO. OF ITERATIONS, AND TOLERANCE
*----NALMAX EPSALC
    20 .0001
CC
CC ALCOHOL 1 PARTITIONING PARAMETERS IF IALC=1 (leave as is)
*----AKWC7 AKWS7 AKM7 AK7 PT7
    4.671 1.79 48 35.31 0.222
CC
CC ALCOHOL 2 PARTITIONING PARAMETERS IF IALC=1
*----AKWC8 AKWS8 AKM8 AK8 PT8
    0. 0. 0. 0. 0.
CC
CC 0 = Healy and Reed and 1 is Chun-Huh
*--- ift
    1
CC
CC INTERFACIAL TENSION PARAMETERS
*----CHUH AHUH
    0.3 10.
CC
CC LOG10 OF OIL/WATER INTERFACIAL TENSION
*----XIFTW
    1.48
CC
CC mass transfer flag
*----imass ICOR
    0 0
cc
cc
*--- IWALT IWALF
    0 0

```

```

CC
CC CAPILLARY DESATURATION PARAMETERS FOR PHASE 1, 2, AND 3
*----ITRAP T11 T22 T33
2 2000. 75000. 365.
CC
CC relative perm. flag (0:imbibition corey,1:first drainage corey)
*----iperm IRTYPE
0 0
CC RESIDUAL SATURATION FOR EACH PHASE INPUT GIVEN THROUGH INCLUDE FILES
CC FLAG FOR CONSTANT OR VARIABLE REL. PERM. PARAMETERS
*----ISRW IPRW IEW
4 0 0
CC
CC CONSTANT ENDPOINT REL. PERM. OF PHASES 1,2,AND 3 AT LOW CAPILLARY NO.
*----PIRW P2RWZ P3RW
.30 0.7 0.30
CC
CC VARIABLE REL. PERM. EXPONENT OF PHASES 1,2,AND 3 AT LOW CAPILLARY NO.
*----E1W E2W E3W
2 2 2
CC
CC RES. SATURATION OF PHASES 1,2,AND 3 AT HIGH CAPILLARY NO.
*----SIRC(=SWIR) S2RC(=SORCHEM) S3RC(SMER=SWIR)
0.0001 0.0001 0.0001
CC
CC ENDPOINT REL. PERM. OF PHASES 1,2,AND 3 AT HIGH CAPILLARY NO.
*----PIRC P2RC P3RC
1. 1. 1.
CC
CC REL. PERM. EXPONENT OF PHASES 1,2,AND 3 AT HIGH CAPILLARY NO.
*----E13CW E23C E31C
1 1 1
CC
CC WATER AND OIL VISCOSITY at reference temperature, RESERVOIR TEMPERATURE (leave zero)
*----VIS1 VIS2 TEMPV
0.37 3.4 0.
CC
CC MICROEMULSION VISCOSITY PARAMETERS
*----ALPHA1 ALPHA2 ALPHA3 ALPHA4 ALPHA5
.1 2.5 0.1 0.1 0.1
CC
CC PARAMETERS TO CALCULATE POLYMER VISCOSITY AT ZERO SHEAR RATE
*----AP1 AP2 AP3
45 625 1000
CC
CC PARAMETER TO COMPUTE CSEP,MIN. CSEP, AND SLOPE OF LOG VIS. VS. LOG CSEP
*----BETAP CSE1 SSLOPE
1. .01 -0.377
CC
CC PARAMETER FOR SHEAR RATE DEPENDENCE OF POLYMER VISCOSITY
*----GAMMAC GAMHF POWN IPMOD ISHEAR RWEFF GAMHF2
4 30 1.8 0 1 0.4 0.0
CC
CC FLAG FOR POLYMER (4) PARTITIONING, PERM. REDUCTION PARAMETERS
*----IPOLYM EPHI3 EPHI4 BRK CRK rkcut
1 1. 1 100 0.04 10
CC
CC SPECIFIC WEIGHT FOR COMPONENTS 1,2,3,7,AND 8 , AND GRAVITY FLAG
*----DEN1 DEN2 den23 DEN3 DEN7 DEN8 IDEN
.433 .377 0.377 .433 .346 0. 2

```

```

CC
CC FLAG FOR CHOICE OF UNITS ( 0:BOTTOMHOLE CONDITION , 1: STOCK TANK)
*----ISTB
1
CC
CC FVF FOR PHASE 1,2,3
*----(FVF(L),L=1,NPHAS)
1 1.083 1
CC
CC COMPRESSIBILITY FOR VOL. OCCUPYING COMPONENTS 1,2,3,7,AND 8
*----COMPC(1) COMPC(2) COMPC(3) COMPC(7) COMPC(8)
0.000003 0.00001 0. 0. 0.
CC
CC CONSTANT OR VARIABLE PC PARAM., WATER-WET OR OIL-WET PC CURVE FLAG
*----ICPC IEPC IOW
0 0 0
CC
CC CAPILLARY PRESSURE PARAMETERS, CPC
*----CPC
0.
CC
CC CAPILLARY PRESSURE PARAMETERS, EPC
*---- EPC
2.
CC
CC MOLECULAR DIFFUSIVITY OF KCTH COMPONENT IN PHASE 1 (D(KC),KC=1,N)
*----D(1) D(2) D(3) D(4) D(5) D(6) D(7) D(8) D(9) D(10) D(11)
0. 0. 0. 0. 0. 0. 6*0
CC
CC MOLECULAR DIFFUSIVITY OF KCTH COMPONENT IN PHASE 2 (D(KC),KC=1,N)
*----D(1) D(2) D(3) D(4) D(5) D(6) D(7) D(8) D(9) D(10) D(11)
0. 0. 0. 0. 0. 0. 6*0
CC
CC MOLECULAR DIFFUSIVITY OF KCTH COMPONENT IN PHASE 3 (D(KC),KC=1,N)
*----D(1) D(2) D(3) D(4) D(5) D(6) D(7) D(8) D(9) D(10) D(11)
0. 0. 0. 0. 0. 0. 6*0
CC
CC LONGITUDINAL AND TRANSVERSE DISPERSIVITY (ft) OF PHASE 1
*----ALPHAL(1) ALPHAT(1)
4 0.4
CC
CC LONGITUDINAL AND TRANSVERSE DISPERSIVITY OF PHASE 2
*----ALPHAL(2) ALPHAT(2)
4 0.4
CC
CC LONGITUDINAL AND TRANSVERSE DISPERSIVITY OF PHASE 3
*----ALPHAL(3) ALPHAT(3)
4 0.4
CC
CC
*--- IADSO
0
CC
CC SURFACTANT AND POLYMER ADSORPTION PARAMETERS
*----AD31 AD32 B3D AD41 AD42 B4D iadk iads1 fads refk(mD)
0.125 0.0 1000. 1 0. 100. 0 0 0 0.
CC
CC PARAMETERS FOR CATION EXCHANGE OF CLAY AND SURFACTANT MW (needed for cation exch)
*----QV XKC XKS EQW
0.0 0.0 0.0 429.

```

```

CC
CC*****
CC
CC WELL DATA
CC
CC*****
CC
CC
CC flag for right and left boundary
*---- ibound  IZONE
      0      0
CC
CC TOTAL NUMBER OF WELLS, WELL RADIUS FLAG, FLAG FOR TIME OR COURANT NO.
*----NWELL  IRO  ITIME  NWELR
      17   2   1   17
CC
CC WELL ID,LOCATIONS,AND FLAG FOR SPECIFYING WELL TYPE, WELL RADIUS, SKIN
*----IDW IW JW IFLAG  RW  SWELL IDIR IFIRST ILAST IPRF
      1 16 13  1  0.4  0  3  1  19  1
cc
cc
*---KPRF
111111110111111111
CC
CC WELL NAME
*---- WELNAM
S1_I1
CC
CC MAX. AND MIN. ALLOWABLE BOTTOMHOLE PRESSURE AND RATE
*----ICHEK  PWFMIN  PWFMAX  QTMIN  QTMAX
      0    300.0  1300.0  0.0   14036.5
CC
CC WELL ID,LOCATIONS,AND FLAG FOR SPECIFYING WELL TYPE, WELL RADIUS, SKIN
*----IDW IW JW IFLAG  RW  SWELL IDIR IFIRST ILAST IPRF
      2 30 13  1  0.4  0  3  1  19  1
cc
cc
*---KPRF
111101011111111111
CC
CC WELL NAME
*---- WELNAM
S1_I2
CC
CC MAX. AND MIN. ALLOWABLE BOTTOMHOLE PRESSURE AND RATE
*----ICHEK  PWFMIN  PWFMAX  QTMIN  QTMAX
      0    300.0  1300.0  0.0   14036.5
CC
CC WELL ID,LOCATIONS,AND FLAG FOR SPECIFYING WELL TYPE, WELL RADIUS, SKIN
*----IDW IW JW IFLAG  RW  SWELL IDIR IFIRST ILAST IPRF
      3 36 25  1  0.4  0  3  1  19  1
cc
cc
*---KPRF
000101111111111111
CC
CC WELL NAME
*---- WELNAM
S1_I3
CC

```

```

CC MAX. AND MIN. ALLOWABLE BOTTOMHOLE PRESSURE AND RATE
*---ICHEK PWFMIN PWFMAX QTMIN QTMAX
  0   300.0 1300.0 0.0 14036.5
CC
CC WELL ID,LOCATIONS,AND FLAG FOR SPECIFYING WELL TYPE, WELL RADIUS, SKIN
*---IDW IW JW IFLAG RW SWELL IDIR IFIRST ILAST IPRF
  4 30 37 1 0.4 0 3 1 19 1
cc
cc
*---KPRF
11010011111111111111
CC
CC WELL NAME
*--- WELNAM
S1_I4
CC
CC MAX. AND MIN. ALLOWABLE BOTTOMHOLE PRESSURE AND RATE
*---ICHEK PWFMIN PWFMAX QTMIN QTMAX
  0   300.0 1300.0 0.0 14036.5
CC
CC WELL ID,LOCATIONS,AND FLAG FOR SPECIFYING WELL TYPE, WELL RADIUS, SKIN
*---IDW IW JW IFLAG RW SWELL IDIR IFIRST ILAST IPRF
  5 16 37 1 0.4 0 3 1 19 1
cc
cc
*---KPRF
11111111111111111111
CC
CC WELL NAME
*--- WELNAM
S1_I5
CC
CC MAX. AND MIN. ALLOWABLE BOTTOMHOLE PRESSURE AND RATE
*---ICHEK PWFMIN PWFMAX QTMIN QTMAX
  0   300.0 1300.0 0.0 14036.5
CC
CC WELL ID,LOCATIONS,AND FLAG FOR SPECIFYING WELL TYPE, WELL RADIUS, SKIN
*---IDW IW JW IFLAG RW SWELL IDIR IFIRST ILAST IPRF
  6 10 25 1 0.4 0 3 1 19 1
cc
cc
*---KPRF
11111111111111111111
CC
CC WELL NAME
*--- WELNAM
S1_I6
CC
CC MAX. AND MIN. ALLOWABLE BOTTOMHOLE PRESSURE AND RATE
*---ICHEK PWFMIN PWFMAX QTMIN QTMAX
  0   300.0 1300.0 0.0 14036.5
CC
CC WELL ID,LOCATIONS,AND FLAG FOR SPECIFYING WELL TYPE, WELL RADIUS, SKIN
*---IDW IW JW IFLAG RW SWELL IDIR IFIRST ILAST IPRF
  7 10 5 1 0.4 0 3 1 19 1
cc
cc
*---KPRF
11111111111111111111
CC

```



```

CC WELL NAME
*---- WELNAM
S1_I7
CC
CC MAX. AND MIN. ALLOWABLE BOTTOMHOLE PRESSURE AND RATE
*----ICHEK PWFMIN PWFMAX QTMIN QTMAX
      0    300.0  1400.0 0.0  7018.25
CC
CC WELL ID,LOCATION,AND FLAG FOR SPECIFYING WELL TYPE, WELL RADIUS, SKIN
*----IDW IW JW IFLAG RW  SWELL IDIR IFIRST ILAST IPRF
      8 36 5  1  0.4  0  3  1  19  1
cc
cc
*---KPRF
11111001111111111111
CC
CC WELL NAME
*---- WELNAM
S1_I8
CC
CC MAX. AND MIN. ALLOWABLE BOTTOMHOLE PRESSURE AND RATE
*----ICHEK PWFMIN PWFMAX QTMIN QTMAX
      0    300.0  1400.0 0.0  7018.25
CC
CC WELL ID,LOCATION,AND FLAG FOR SPECIFYING WELL TYPE, WELL RADIUS, SKIN
*----IDW IW JW IFLAG RW  SWELL IDIR IFIRST ILAST IPRF
      9 36 44 1  0.4  0  3  1  19  1
cc
cc
*---KPRF
00111111111111111111
CC
CC WELL NAME
*---- WELNAM
S1_I9
CC
CC MAX. AND MIN. ALLOWABLE BOTTOMHOLE PRESSURE AND RATE
*----ICHEK PWFMIN PWFMAX QTMIN QTMAX
      0    300.0  1400.0 0.0  7018.25
CC
CC WELL ID,LOCATION,AND FLAG FOR SPECIFYING WELL TYPE, WELL RADIUS, SKIN
*----IDW IW JW IFLAG RW  SWELL IDIR IFIRST ILAST IPRF
     10 10 44 1  0.4  0  3  1  19  1
cc
cc
*---KPRF
11111111111111111111
CC
CC WELL NAME
*---- WELNAM
S1_I10
CC
CC MAX. AND MIN. ALLOWABLE BOTTOMHOLE PRESSURE AND RATE
*----ICHEK PWFMIN PWFMAX QTMIN QTMAX
      0    300.0  1400.0 0.0  7018.25
CC
CC WELL ID,LOCATION,AND FLAG FOR SPECIFYING WELL TYPE, WELL RADIUS, SKIN
*----IDW IW JW IFLAG RW  SWELL IDIR IFIRST ILAST IPRF
     11 22 25 2  0.4  0  3  1  19  1
cc

```

```

cc
*---KPRF
0011111111110011111
CC
CC WELL NAME
*---- WELNAM
S1_P1
CC
CC MAX. AND MIN. ALLOWABLE BOTTOMHOLE PRESSURE AND RATE
*----ICHEK PWFMIN PWFMAX QTMIN QTMAX
0 300.0 1300. 0.0 56146.0
CC
CC WELL ID,LOCATIONS,AND FLAG FOR SPECIFYING WELL TYPE, WELL RADIUS, SKIN
*----IDW IW JW IFLAG RW SWELL IDIR IFIRST ILAST IPRF
12 22 5 2 0.4 0 3 1 19 1
cc
cc
*---KPRF
1101111111111111111
CC
CC WELL NAME
*---- WELNAM
S1_P2
CC
CC MAX. AND MIN. ALLOWABLE BOTTOMHOLE PRESSURE AND RATE
*----ICHEK PWFMIN PWFMAX QTMIN QTMAX
0 300.0 1400. 0.0 28073
CC
CC WELL ID,LOCATIONS,AND FLAG FOR SPECIFYING WELL TYPE, WELL RADIUS, SKIN
*----IDW IW JW IFLAG RW SWELL IDIR IFIRST ILAST IPRF
13 40 13 2 0.4 0 3 1 19 1
cc
cc
*---KPRF
0000010111111111111
CC
CC WELL NAME
*---- WELNAM
S1_P3
CC
CC MAX. AND MIN. ALLOWABLE BOTTOMHOLE PRESSURE AND RATE
*----ICHEK PWFMIN PWFMAX QTMIN QTMAX
0 300.0 1400. 0.0 28073
CC
CC WELL ID,LOCATIONS,AND FLAG FOR SPECIFYING WELL TYPE, WELL RADIUS, SKIN
*----IDW IW JW IFLAG RW SWELL IDIR IFIRST ILAST IPRF
14 40 37 2 0.4 0 3 1 19 1
cc
cc
*---KPRF
0110011111111111111
CC
CC WELL NAME
*---- WELNAM
S1_P4
CC
CC MAX. AND MIN. ALLOWABLE BOTTOMHOLE PRESSURE AND RATE
*----ICHEK PWFMIN PWFMAX QTMIN QTMAX
0 300.0 1400. 0.0 28073
CC

```

```

CC WELL ID,LOCATIONS,AND FLAG FOR SPECIFYING WELL TYPE, WELL RADIUS, SKIN
*----IDW IW JW IFLAG RW SWELL IDIR IFIRST ILAST IPRF
    15 22 44 2 0.4 0 3 1 19 1
cc
cc
*---KPRF
11110111111111111111
CC
CC WELL NAME
*---- WELNAM
S1_P5
CC
CC MAX. AND MIN. ALLOWABLE BOTTOMHOLE PRESSURE AND RATE
*----ICHEK PWFMIN PWFMAX QTMIN QTMAX
    0 300.0 1400. 0.0 28073
CC
CC WELL ID,LOCATIONS,AND FLAG FOR SPECIFYING WELL TYPE, WELL RADIUS, SKIN
*----IDW IW JW IFLAG RW SWELL IDIR IFIRST ILAST IPRF
    16 4 37 2 0.4 0 3 1 19 1
cc
cc
*---KPRF
11110111111111111111
CC
CC WELL NAME
*---- WELNAM
S1_P6
CC
CC MAX. AND MIN. ALLOWABLE BOTTOMHOLE PRESSURE AND RATE
*----ICHEK PWFMIN PWFMAX QTMIN QTMAX
    0 300.0 1400. 0.0 28073
CC
CC WELL ID,LOCATIONS,AND FLAG FOR SPECIFYING WELL TYPE, WELL RADIUS, SKIN
*----IDW IW JW IFLAG RW SWELL IDIR IFIRST ILAST IPRF
    17 4 13 2 0.4 0 3 1 19 1
cc
cc
*---KPRF
11111111111111111111
CC
CC WELL NAME
*---- WELNAM
S1_P7
CC
CC MAX. AND MIN. ALLOWABLE BOTTOMHOLE PRESSURE AND RATE
*----ICHEK PWFMIN PWFMAX QTMIN QTMAX
    0 300.0 1400. 0.0 28073
CC
CC Pressure constrained producer
*----WELL ID PWF
    1 44916.8 1. 0. 0. 0. 0.05130 0. 2*0 4*0
    1 0. 0. 0. 0. 0. 0. 0. 6*0
    1 0. 0. 0. 0. 0. 0. 0. 6*0
CC
CC Pressure constrained producer
*----WELL ID PWF
    2 44916.8 1. 0. 0. 0. 0.05130 0. 2*0 4*0
    2 0. 0. 0. 0. 0. 0. 0. 6*0
    2 0. 0. 0. 0. 0. 0. 0. 6*0
CC

```

CC Pressure constrained producer

*----WELL ID PWF

3 44916.8 1. 0. 0. 0. 0.05130 0. 2*0 4*0

3 0. 0. 0. 0. 0. 0. 0. 6*0

3 0. 0. 0. 0. 0. 0. 0. 6*0

CC

CC id,INJ. RATE AND INJ. COMP. FOR RATE CONS. WELLS FOR EACH PHASE(L=1,3)

*----id QI(M,L) C(M,KC,L) (need to keep 2nd and 3rd lines for oil and ME)

4 44916.8 1. 0. 0. 0. 0.05130 0. 2*0 4*0

4 0. 0. 0. 0. 0. 0. 0. 6*0

4 0. 0. 0. 0. 0. 0. 0. 6*0

CC

CC

*----id QI(M,L) C(M,KC,L) (need to keep 2nd and 3rd lines for oil and ME)

5 44916.8 1. 0. 0. 0. 0.05130 0. 2*0 4*0

5 0. 0. 0. 0. 0. 0. 0. 6*0

5 0. 0. 0. 0. 0. 0. 0. 6*0

CC

CC id,INJ. RATE AND INJ. COMP. FOR RATE CONS. WELLS FOR EACH PHASE(L=1,3)

*----id QI(M,L) C(M,KC,L) (need to keep 2nd and 3rd lines for oil and ME)

6 44916.8 1. 0. 0. 0. 0.05130 0. 2*0 4*0

6 0. 0. 0. 0. 0. 0. 0. 6*0

6 0. 0. 0. 0. 0. 0. 0. 6*0

CC

CC id,INJ. RATE AND INJ. COMP. FOR RATE CONS. WELLS FOR EACH PHASE(L=1,3)

*----id QI(M,L) C(M,KC,L) (need to keep 2nd and 3rd lines for oil and ME)

7 22458.4 1. 0. 0. 0. 0.05130 0. 2*0 4*0

7 0. 0. 0. 0. 0. 0. 0. 6*0

7 0. 0. 0. 0. 0. 0. 0. 6*0

CC

CC

*----id QI(M,L) C(M,KC,L) (need to keep 2nd and 3rd lines for oil and ME)

8 22458.4 1. 0. 0. 0. 0.05130 0. 2*0 4*0

8 0. 0. 0. 0. 0. 0. 0. 6*0

8 0. 0. 0. 0. 0. 0. 0. 6*0

CC

CC id,INJ. RATE AND INJ. COMP. FOR RATE CONS. WELLS FOR EACH PHASE(L=1,3)

*----id QI(M,L) C(M,KC,L) (need to keep 2nd and 3rd lines for oil and ME)

9 22458.4 1. 0. 0. 0. 0.05130 0. 2*0 4*0

9 0. 0. 0. 0. 0. 0. 0. 6*0

9 0. 0. 0. 0. 0. 0. 0. 6*0

CC

CC id,INJ. RATE AND INJ. COMP. FOR RATE CONS. WELLS FOR EACH PHASE(L=1,3)

*----id QI(M,L) C(M,KC,L) (need to keep 2nd and 3rd lines for oil and ME)

10 22458.4 1. 0. 0. 0. 0.05130 0. 2*0 4*0

10 0. 0. 0. 0. 0. 0. 0. 6*0

10 0. 0. 0. 0. 0. 0. 0. 6*0

CC

CC Pressure constrained producer

*----WELL ID PWF

11 300.0

CC

CC Pressure constrained producer

*----WELL ID PWF

12 300.0

CC

CC Pressure constrained producer

*----WELL ID PWF

13 300.0

CC

```

CC Pressure constrained producer
*----WELL ID PWF
14 300.0
CC
CC Pressure constrained producer
*----WELL ID PWF
15 300.0
CC
CC Pressure constrained producer
*----WELL ID PWF
16 300.0
CC
CC Pressure constrained producer
*----WELL ID PWF
17 300.0
CC waterflood to 56 % cum oil recovery
CC CUM. INJ. TIME , AND INTERVALS (PV OR DAY) FOR WRITING TO OUTPUT FILES (3.7.8)
*----TINJ CUMPR1 CUMHI2 WRHPV(HIST) WRPRF(PLOT) RSTC
3.8 0.2 0.2 0.2 0.2 0.2
CC
CC FOR IMES=2 ,THE INI. TIME STEP,CONC. TOLERANCE,MAX.,MIN. time steps
*----DT DCLIM CNMAX CNMIN
0.00001 0.01 0.3 0.01
CC
CC
*----IBMOD
0
CC
CC IRO, ITIME, NEW FLAGS FOR ALL THE WELLS
*----IRO ITSTEP IFLAG
2 1 10*1 7*2
CC
CC NUMBER OF WELLS CHANGES IN LOCATION OR SKIN OR PWF
*----NWEL1
0
CC
CC NUMBER OF WELLS WITH RATE CHANGES, ID - SURFACTANT FLOOD INTO 10 INJECTORS
*----NWEL2 ID
10 1 2 3 4 5 6 7 8 9 10
CC
CC id,INJ. RATE AND INJ. COMP. FOR RATE CONS. WELLS FOR EACH PHASE(L=1,3)
*----id QI(M,L) C(M,KC,L) (need to keep 2nd and 3rd lines for oil and ME)
1 14036.5 0.995 0. 0.005 .2 0.7116 0 0
1 0. 0. 0. 0. 0. 0. 0. 6*0
1 0. 0. 0. 0. 0. 0. 0. 6*0
CC
CC id,INJ. RATE AND INJ. COMP. FOR RATE CONS. WELLS FOR EACH PHASE(L=1,3)
*----id QI(M,L) C(M,KC,L) (need to keep 2nd and 3rd lines for oil and ME)
2 14036.5 0.995 0. 0.005 .2 0.7116 0 0
2 0. 0. 0. 0. 0. 0. 0. 6*0
2 0. 0. 0. 0. 0. 0. 0. 6*0
CC
CC
*----id QI(M,L) C(M,KC,L) (need to keep 2nd and 3rd lines for oil and ME)
3 14036.5 0.995 0. 0.005 .2 0.7116 0 0
3 0. 0. 0. 0. 0. 0. 0. 6*0
3 0. 0. 0. 0. 0. 0. 0. 6*0
CC
CC
*----id QI(M,L) C(M,KC,L) (need to keep 2nd and 3rd lines for oil and ME)

```

```

4 14036.5 0.995 0. 0.005 .2 0.7116 0 0
4 0. 0. 0. 0. 0. 0. 0. 6*0
4 0. 0. 0. 0. 0. 0. 0. 6*0
CC
CC id,INJ. RATE AND INJ. COMP. FOR RATE CONS. WELLS FOR EACH PHASE(L=1,3)
*----id QI(M,L) C(M,KC,L) (need to keep 2nd and 3rd lines for oil and ME)
5 14036.5 0.995 0. 0.005 .2 0.7116 0 0
5 0. 0. 0. 0. 0. 0. 0. 6*0
5 0. 0. 0. 0. 0. 0. 0. 6*0
CC
CC id,INJ. RATE AND INJ. COMP. FOR RATE CONS. WELLS FOR EACH PHASE(L=1,3)
*----id QI(M,L) C(M,KC,L) (need to keep 2nd and 3rd lines for oil and ME)
6 14036.5 0.995 0. 0.005 .2 0.7116 0 0
6 0. 0. 0. 0. 0. 0. 0. 6*0
6 0. 0. 0. 0. 0. 0. 0. 6*0
CC
CC id,INJ. RATE AND INJ. COMP. FOR RATE CONS. WELLS FOR EACH PHASE(L=1,3)
*----id QI(M,L) C(M,KC,L) (need to keep 2nd and 3rd lines for oil and ME)
7 7018.25 0.995 0. 0.005 .2 0.7116 0 0
7 0. 0. 0. 0. 0. 0. 0. 6*0
7 0. 0. 0. 0. 0. 0. 0. 6*0
CC
CC id,INJ. RATE AND INJ. COMP. FOR RATE CONS. WELLS FOR EACH PHASE(L=1,3)
*----id QI(M,L) C(M,KC,L) (need to keep 2nd and 3rd lines for oil and ME)
8 7018.25 0.995 0. 0.005 .2 0.7116 0 0
8 0. 0. 0. 0. 0. 0. 0. 6*0
8 0. 0. 0. 0. 0. 0. 0. 6*0
CC
CC id,INJ. RATE AND INJ. COMP. FOR RATE CONS. WELLS FOR EACH PHASE(L=1,3)
*----id QI(M,L) C(M,KC,L) (need to keep 2nd and 3rd lines for oil and ME)
9 7018.25 0.995 0. 0.005 .2 0.7116 0 0
9 0. 0. 0. 0. 0. 0. 0. 6*0
9 0. 0. 0. 0. 0. 0. 0. 6*0
CC
CC id,INJ. RATE AND INJ. COMP. FOR RATE CONS. WELLS FOR EACH PHASE(L=1,3)
*----id QI(M,L) C(M,KC,L) (need to keep 2nd and 3rd lines for oil and ME)
10 7018.25 0.995 0. 0.005 .2 0.7116 0 0
10 0. 0. 0. 0. 0. 0. 0. 6*0
10 0. 0. 0. 0. 0. 0. 0. 6*0
CC
CC CUM. INJ. TIME , AND INTERVALS (PV OR DAY) FOR WRITING TO OUTPUT FILES (3.7.8)
*----TINJ CUMPR1 CUMHI2 WRHPV(HIST) WRPRF(PLOT) RSTC
4.1 0.05 0.05 0.05 0.05 0.05
CC Surf Inj
CC FOR IMES=2 ,THE INI. TIME STEP,CONC. TOLERANCE,MAX.,MIN. time steps
*----DT DCLIM CNMAX CNMIN
0.00001 0.001 0.01 0.001
CC
CC No changes in the boundary condition
*--- IBMOD
0
CC
CC IRO, ITIME, NEW FLAGS FOR ALL THE WELLS
*---- IRO ITIME IFLAG
2 1 10*1 7*2
CC
CC NUMBER OF WELLS changes IN LOCATION OR SKIN OR PWF
*----NWEL1
0
CC

```

CC NUMBER OF WELLS WITH RATE changes, id

*----NWEL2 Id

10 1 2 3 4 5 6 7 8 9 10

CC

CC id,INJ. RATE AND INJ. COMP. FOR RATE CONS. WELLS FOR EACH PHASE(L=1,3)

*----id QI(M,L) C(M,KC,L) (need to keep 2nd and 3rd lines for oil and ME)

1 14036.5 1 0.0 0. .115 0.0513 0 0

1 0. 0. 0. 0. 0. 0. 0. 6*0

1 0. 0. 0. 0. 0. 0. 0. 6*0

CC

CC id,INJ. RATE AND INJ. COMP. FOR RATE CONS. WELLS FOR EACH PHASE(L=1,3)

*----id QI(M,L) C(M,KC,L) (need to keep 2nd and 3rd lines for oil and ME)

2 14036.5 1 0.0 0. .115 0.0513 0 0

2 0. 0. 0. 0. 0. 0. 0. 6*0

2 0. 0. 0. 0. 0. 0. 0. 6*0

CC

CC id,INJ. RATE AND INJ. COMP. FOR RATE CONS. WELLS FOR EACH PHASE(L=1,3)

*----id QI(M,L) C(M,KC,L) (need to keep 2nd and 3rd lines for oil and ME)

3 14036.5 1 0.0 0. .115 0.0513 0 0

3 0. 0. 0. 0. 0. 0. 0. 6*0

3 0. 0. 0. 0. 0. 0. 0. 6*0

CC

CC id,INJ. RATE AND INJ. COMP. FOR RATE CONS. WELLS FOR EACH PHASE(L=1,3)

*----id QI(M,L) C(M,KC,L) (need to keep 2nd and 3rd lines for oil and ME)

4 14036.5 1 0.0 0. .115 0.0513 0 0

4 0. 0. 0. 0. 0. 0. 0. 6*0

4 0. 0. 0. 0. 0. 0. 0. 6*0

CC

CC id,INJ. RATE AND INJ. COMP. FOR RATE CONS. WELLS FOR EACH PHASE(L=1,3)

*----id QI(M,L) C(M,KC,L) (need to keep 2nd and 3rd lines for oil and ME)

5 14036.5 1 0.0 0. .115 0.0513 0 0

5 0. 0. 0. 0. 0. 0. 0. 6*0

5 0. 0. 0. 0. 0. 0. 0. 6*0

CC

CC id,INJ. RATE AND INJ. COMP. FOR RATE CONS. WELLS FOR EACH PHASE(L=1,3)

*----id QI(M,L) C(M,KC,L) (need to keep 2nd and 3rd lines for oil and ME)

6 14036.5 1 0.0 0. .115 0.0513 0 0

6 0. 0. 0. 0. 0. 0. 0. 6*0

6 0. 0. 0. 0. 0. 0. 0. 6*0

CC

CC id,INJ. RATE AND INJ. COMP. FOR RATE CONS. WELLS FOR EACH PHASE(L=1,3)

*----id QI(M,L) C(M,KC,L) (need to keep 2nd and 3rd lines for oil and ME)

7 7018.25 1 0.0 0. .115 0.0513 0 0

7 0. 0. 0. 0. 0. 0. 0. 6*0

7 0. 0. 0. 0. 0. 0. 0. 6*0

CC

CC id,INJ. RATE AND INJ. COMP. FOR RATE CONS. WELLS FOR EACH PHASE(L=1,3)

*----id QI(M,L) C(M,KC,L) (need to keep 2nd and 3rd lines for oil and ME)

8 7018.25 1 0.0 0. .115 0.0513 0 0

8 0. 0. 0. 0. 0. 0. 0. 6*0

8 0. 0. 0. 0. 0. 0. 0. 6*0

CC

CC id,INJ. RATE AND INJ. COMP. FOR RATE CONS. WELLS FOR EACH PHASE(L=1,3)

*----id QI(M,L) C(M,KC,L) (need to keep 2nd and 3rd lines for oil and ME)

9 7018.25 1 0.0 0. .115 0.0513 0 0

9 0. 0. 0. 0. 0. 0. 0. 6*0

9 0. 0. 0. 0. 0. 0. 0. 6*0

CC

CC id,INJ. RATE AND INJ. COMP. FOR RATE CONS. WELLS FOR EACH PHASE(L=1,3)

*----id QI(M,L) C(M,KC,L) (need to keep 2nd and 3rd lines for oil and ME)

```

10 7018.25 1 0.0 0. .115 0.0513 0 0
10 0. 0. 0. 0. 0. 0. 0. 6*0
10 0. 0. 0. 0. 0. 0. 0. 6*0
CC
CC CUM. INJ. TIME , AND INTERVALS (PV OR DAY) FOR WRITING TO OUTPUT FILES (3.7.8)
*----TINJ CUMPR1 CUMHI2 WRHPV(HIST) WRPRF(PLOT) RSTC
5.1 0.1 0.1 0.1 0.1 0.05
CC
CC FOR IMES=2 ,THE INI. TIME STEP,CONC. TOLERANCE,MAX.,MIN. time steps
*----DT DCLIM CNMAX CNMIN
0.00001 0.001 0.1 0.01
CC
CC No changes in the boundary condition
*--- IBMOD
0
CC
CC IRO, ITIME, NEW FLAGS FOR ALL THE WELLS
*---- IRO ITIME IFLAG
2 1 10*1 7*2
CC
CC NUMBER OF WELLS changes IN LOCATION OR SKIN OR PWF
*----NWEL1
0
CC
CC NUMBER OF WELLS WITH RATE changes, id
*----NWEL2 Id
10 1 2 3 4 5 6 7 8 9 10
CC
CC id,INJ. RATE AND INJ. COMP. FOR RATE CONS. WELLS FOR EACH PHASE(L=1,3)
*----id QI(M,L) C(M,KC,L) (need to keep 2nd and 3rd lines for oil and ME)
1 14036.5 1. 0. 0. 0.0 0.0513 0. 0
1 0. 0. 0. 0. 0. 0. 0. 6*0
1 0. 0. 0. 0. 0. 0. 0. 6*0
CC
CC id,INJ. RATE AND INJ. COMP. FOR RATE CONS. WELLS FOR EACH PHASE(L=1,3)
*----id QI(M,L) C(M,KC,L) (need to keep 2nd and 3rd lines for oil and ME)
2 14036.5 1. 0. 0. 0.0 0.0513 0. 0
2 0. 0. 0. 0. 0. 0. 0. 6*0
2 0. 0. 0. 0. 0. 0. 0. 6*0
CC
CC id,INJ. RATE AND INJ. COMP. FOR RATE CONS. WELLS FOR EACH PHASE(L=1,3)
*----id QI(M,L) C(M,KC,L) (need to keep 2nd and 3rd lines for oil and ME)
3 14036.5 1. 0. 0. 0.0 0.0513 0. 0
3 0. 0. 0. 0. 0. 0. 0. 6*0
3 0. 0. 0. 0. 0. 0. 0. 6*0
CC
CC id,INJ. RATE AND INJ. COMP. FOR RATE CONS. WELLS FOR EACH PHASE(L=1,3)
*----id QI(M,L) C(M,KC,L) (need to keep 2nd and 3rd lines for oil and ME)
4 14036.5 1. 0. 0. 0.0 0.0513 0. 0
4 0. 0. 0. 0. 0. 0. 0. 6*0
4 0. 0. 0. 0. 0. 0. 0. 6*0
CC
CC id,INJ. RATE AND INJ. COMP. FOR RATE CONS. WELLS FOR EACH PHASE(L=1,3)
*----id QI(M,L) C(M,KC,L) (need to keep 2nd and 3rd lines for oil and ME)
5 14036.5 1. 0. 0. 0.0 0.0513 0. 0
5 0. 0. 0. 0. 0. 0. 0. 6*0
5 0. 0. 0. 0. 0. 0. 0. 6*0
CC
CC id,INJ. RATE AND INJ. COMP. FOR RATE CONS. WELLS FOR EACH PHASE(L=1,3)
*----id QI(M,L) C(M,KC,L) (need to keep 2nd and 3rd lines for oil and ME)

```



```

6 14036.5 1. 0. 0. 0.0 0.0513 0. 0
6 0. 0. 0. 0. 0. 0. 0. 6*0
6 0. 0. 0. 0. 0. 0. 0. 6*0
CC
CC id,INJ. RATE AND INJ. COMP. FOR RATE CONS. WELLS FOR EACH PHASE(L=1,3)
*----id QI(M,L) C(M,KC,L) (need to keep 2nd and 3rd lines for oil and ME)
7 7018.25 1. 0. 0. 0.0 0.0513 0. 0
7 0. 0. 0. 0. 0. 0. 0. 6*0
7 0. 0. 0. 0. 0. 0. 0. 6*0
CC
CC id,INJ. RATE AND INJ. COMP. FOR RATE CONS. WELLS FOR EACH PHASE(L=1,3)
*----id QI(M,L) C(M,KC,L) (need to keep 2nd and 3rd lines for oil and ME)
8 7018.25 1. 0. 0. 0.0 0.0513 0. 0
8 0. 0. 0. 0. 0. 0. 0. 6*0
8 0. 0. 0. 0. 0. 0. 0. 6*0
CC
CC id,INJ. RATE AND INJ. COMP. FOR RATE CONS. WELLS FOR EACH PHASE(L=1,3)
*----id QI(M,L) C(M,KC,L) (need to keep 2nd and 3rd lines for oil and ME)
9 7018.25 1. 0. 0. 0.0 0.0513 0. 0
9 0. 0. 0. 0. 0. 0. 0. 6*0
9 0. 0. 0. 0. 0. 0. 0. 6*0
CC
CC id,INJ. RATE AND INJ. COMP. FOR RATE CONS. WELLS FOR EACH PHASE(L=1,3)
*----id QI(M,L) C(M,KC,L) (need to keep 2nd and 3rd lines for oil and ME)
10 7018.25 1. 0. 0. 0.0 0.0513 0. 0
10 0. 0. 0. 0. 0. 0. 0. 6*0
10 0. 0. 0. 0. 0. 0. 0. 6*0
CC post flush formation water injection
CC CUM. INJ. TIME , AND INTERVALS (PV OR DAY) FOR WRITING TO OUTPUT FILES (3.7.8)
*----TINJ CUMPR1 CUMHI2 WRHPV(HIST) WRPRF(PLOT) RSTC
6.1 0.5 0.5 0.1 0.3 0.3
CC
CC FOR IMES=2 ,THE INI. TIME STEP,CONC. TOLERANCE,MAX.,MIN. time steps
*----DT DCLIM CNMAX CNMIN
0.000001 0.001 0.2 0.01

```

D2: INPUT FILE FOR 43 X 47 X 19 MODEL FOR THE CASE DESCRIBE IN CHAPTER 3:

```

CC*****
**
CC
CC          *
CC BRIEF DESCRIPTION OF DATA SET : UTCHEM9p97 *
CC          *
CC*****
**
CC ASP SCALE-UP *
CC          *
CC          *
CC LENGTH (FT) : 2100 PROCESS: *
CC THICKNESS (FT) : 37 ft INJ. RATE (FT3/DAY) : *
CC WIDTH (FT) : 2400 COORDINATES : CARTESIAN *
CC POROSITY : variable PROD. RATE (FT3/DAY): *
CC GRID BLOCKS : 43x47x19 1BBL=5.615 cubic feet *
CC DATE : 06/16/2008 A1 Sand - original grid size *
CC          *
CC*****
**

```

```

CC
CC*****
**
CC
CC RESERVOIR DESCRIPTION
CC
CC*****
**
CC
CC
*----RUNNO (title)
UTASP3
CC
CC
*----HEADER (need 3 lines)
UTMIN3
ASP SCALE-UP
RESTART FOR ASP
CC
CC SIMULATION FLAGS
*---- IMODE IMES IDISPC ICWM ICAP IREACT IBIO ICOORD ITREAC ITC IGAS ieng idual itens
      2 2 3 0 0 5 0 1 0 0 0 0 0 0
CC
CC NUMBER OF GRID BLOCKS AND FLAG SPECIFIES CONSTANT OR VARIABLE GRID SIZE
*----NX NY NZ IDXYZ IUNIT
      43 47 19 2 0
CC
CC CONSTANT GRID BLOCK SIZE IN X, Y, AND Z (in ft)
*----DX
75 75 75.00002 74.99998 75 75.00003 37.49997 37.5 37.5 37.5
37.5 37.5 37.5 37.5 37.5 37.5 37.50006 37.5 37.49994
37.5
37.50006 37.49994 37.5 37.5 37.50012 37.49988 37.5 37.5 37.50012
37.49988
37.5 37.5 37.50012 37.49988 37.5 37.5 75 75.00012 75 74.99988
75 75.00012 74.99988
CC
CC CONSTANT GRID BLOCK SIZE IN X, Y, AND Z (in ft)
*----DY
75 75 75.00002 74.99998 75 75.00003 74.99997 75
37.5 37.5 37.5
37.5 37.5 37.5 37.5 37.50006 37.5 37.49994 37.5 37.50006 37.49994
37.5 37.5 37.50012 37.49988 37.5 37.5 37.50012 37.49988
37.5 37.5
37.50012 37.49988 37.5 37.5 37.50012 37.49988 37.50012 37.5 75
74.99988
75 75.00012 74.99988 75 75 75.00024 74.99976
CC
CC
*----DZ (this is mean from NET from ecl2gocad) total thickness is about 37 ft
2 2 2 2 2 2 2 2 2 2 2 2 2 2 2 2 1
CC
CC TOTAL NO. OF COMPONENTS, NO. OF TRACERS, NO. OF GEL COMPONENTS
*----N no NTw nta ngc ng noth
      12 0 0 0 4 0 0
CC
CC All species must be present even for standard waterflood.
*---- species name (total 9)
water
oil

```

```

surf(M3+IOS)
polymer(AN-125)
ANION
CALCIUM
alc1
alc2
SODIUM
hydrogen
alkali
HAo
CC
CC FLAG INDICATING IF THE COMPONENT IS INCLUDED IN CALCULATIONS OR NOT
*----ICF(KC) FOR KC=1,N
  1 1 1 1 1 1 0 0 1 1 1 1
CC
CC*****
CC
CC          *
CC  OUTPUT OPTIONS          *
CC          *
CC*****
CC ICUM=0 for output in days, =1 for PV
CC ISTOP=0 for TMAX & TINJ in days, =1 for PV
CC 3.2.1 FLAG TO WRITE TO UNIT 3,FLAG FOR PV OR DAYS TO PRINT OR TO STOP THE RUN
*---- ICUMTM ISTOP IOUTGMS
  1 1 0
CC
CC 3.2.2 FLAG INDICATING IF THE PROFILE OF KCTH COMPONENT SHOULD BE WRITTEN
*---- IPRFLG(KC),KC=1,N
  1 1 1 1 1 1 0 0 1 1 1 1
CC
CC 3.2.3 FLAG FOR PRES.,SAT.,TOTAL CONC.,TRACER CONC.,CAP.,GEL, ALKALINE PROFILES
*---- IPPRES IPSAT IPTOT IPBIO IPCAP IPGEL IPALK IPTEMP IPOBS
  1 1 1 0 0 0 1 0 0
CC
CC 3.2.4 FLAG FOR WRITING SEVERAL PROPERTIES TO UNIT 4 (Prof)
*---- ICKL IVIS IPER ICNM ICSE IHYSTP IFOAMP INONEQ
  1 1 0 1 1 0 0 0
CC
CC 3.2.5 FLAG for variables to PROF output file
*---- IADS IVEL IRKF IPHSE
  1 0 1 0
CC
CC*****
CC
CC          *
CC  RESERVOIR PROPERTIES          *
CC          *
CC*****
CC
CC
CC MAX. SIMULATION TIME
*---- TMAX 3.4 PV water
  9.3
CC
CC ROCK COMPRESSIBILITY (1/PSI), STAND. PRESSURE(Psia)
*----COMPR PSTAND
  0.000008 14.7
CC Porosity Values For Each Grid Input Given Through Include Files
CC FLAGS INDICATING CONSTANT OR VARIABLE POROSITY, X,Y,AND Z PERMEABILITY
*----IPOR1 IPERMX IPERMY IPERMZ IMOD ITRANZ INTG
  4 4 4 4 1 0 0

```

CC Depth To The Top Layer Input Given Through Include Files
CC FLAG FOR CONSTANT OR VARIABLE DEPTH, PRESSURE, WATER SATURATION
*----DEPTH IPRESS ISWI ICWI
4 1 0 -1
CC
CC 4/10/2009- Chevron
*----IPRESS DEPTH
550. 1965.77185
CC 4/10/2009- Chevron
CC WATER SATURATION
*----ISWI
0.2
CC
CC FLAG FOR RESERVOIR PROPERTY MODIFICATION
*----IMPOR IMKX IMKY IMKZ IMSW
0 1 1 1 0
CC
CC NUMBER OF REGIONS WITH MODIFIED X PERMEABILITY
*---- NMOD1
17
CC
CC FIRST AND LAST INDEX IN X,Y,Z DIRECTION,MODIFIED METHOD,CONSTANT VALUE.
*---- IMIN IMAX JMIN JMAX KMIN KMAX IFACT FACTX
16 16 13 13 19 19 2 0.4968
30 30 13 13 19 19 2 0.4968
36 36 25 25 19 19 2 0.5001
30 30 37 37 19 19 2 0.4995
16 16 37 37 19 19 2 0.4968
10 10 25 25 19 19 2 0.4968
10 10 5 5 19 19 2 0.5001
36 36 5 5 19 19 2 0.4968
36 36 44 44 19 19 2 0.5002
10 10 44 44 19 19 2 0.4968
22 22 25 25 19 19 2 0.4968
22 22 5 5 19 19 2 0.4968
40 40 13 13 19 19 2 0.5007
40 40 37 37 19 19 2 0.4968
22 22 44 44 19 19 2 0.4968
4 4 37 37 19 19 2 0.4968
4 4 13 13 19 19 2 0.4968
CC
CC NUMBER OF REGIONS WITH MODIFIED Y PERMEABILITY
*---- NMOD2
17
CC
CC FIRST AND LAST INDEX IN X,Y,Z DIRECTION,MODIFIED METHOD,CONSTANT VALUE.
*---- IMIN IMAX JMIN JMAX KMIN KMAX IFACT FACTX
16 16 13 13 19 19 2 0.4968
30 30 13 13 19 19 2 0.4968
36 36 25 25 19 19 2 0.5001
30 30 37 37 19 19 2 0.4995
16 16 37 37 19 19 2 0.4968
10 10 25 25 19 19 2 0.4968
10 10 5 5 19 19 2 0.5001
36 36 5 5 19 19 2 0.4968
36 36 44 44 19 19 2 0.5002
10 10 44 44 19 19 2 0.4968
22 22 25 25 19 19 2 0.4968
22 22 5 5 19 19 2 0.4968
40 40 13 13 19 19 2 0.5007

40	40	37	37	19	19	2	0.4968
22	22	44	44	19	19	2	0.4968
4	4	37	37	19	19	2	0.4968
4	4	13	13	19	19	2	0.4968

CC
 CC NUMBER OF REGIONS WITH MODIFIED Z PERMEABILITY
 *---- NMOD3
 17
 CC
 CC FIRST AND LAST INDEX IN X,Y,Z DIRECTION,MODIFIED METHOD,CONSTANT VALUE.
 *---- IMIN IMAX JMIN JMAX KMIN KMAX IFACT FACTX

16	16	13	13	19	19	2	0.4968
30	30	13	13	19	19	2	0.4968
36	36	25	25	19	19	2	0.5001
30	30	37	37	19	19	2	0.4995
16	16	37	37	19	19	2	0.4968
10	10	25	25	19	19	2	0.4968
10	10	5	5	19	19	2	0.5001
36	36	5	5	19	19	2	0.4968
36	36	44	44	19	19	2	0.5002
10	10	44	44	19	19	2	0.4968
22	22	25	25	19	19	2	0.4968
22	22	5	5	19	19	2	0.4968
40	40	13	13	19	19	2	0.5007
40	40	37	37	19	19	2	0.4968
22	22	44	44	19	19	2	0.4968
4	4	37	37	19	19	2	0.4968
4	4	13	13	19	19	2	0.4968

CC formation water
 CC CONSTANT CHLORIDE AND CALCIUM CONCENTRATIONS (MEQ/ML)
 *----C50 C60
 0.1323 0.03391
 CC
 CC*****
 CC *
 CC PHYSICAL PROPERTY DATA *
 CC *
 CC*****
 CC
 CC 3.4.1 OIL CONC. AT PLAIT POINT FOR TYPE II(+)AND TYPE II(-), CMC
 CC CMC
 *---- c2plc c2prc epsme ihand
 0 1 0.001 0
 CC
 CC 3.4.2 flag indicating type of phase behavior parameters
 *---- ifghbn=0 for input height of binodal curve; =1 for input sol. ratio
 0
 CC 3.4.3 SLOPE AND INTERCEPT OF BINODAL CURVE AT ZERO, OPT., AND 2XOPT SALINITY
 CC FOR ALCOHOL 1
 *---- hbns70 hbnc70 hbns71 hbnc71 hbns72 hbnc72
 0 0.03 0 0.015 0 0.03
 CC 3.4.5 SLOPE AND INTERCEPT OF BINODAL CURVE AT ZERO, OPT., AND 2XOPT SALINITY
 CC FOR ALCOHOL 2
 *---- hbns80 hbnc80 hbns81 hbnc81 hbns82 hbnc82
 0 0 0 0 0 0
 CC
 CC 3.4.6 LOWER AND UPPER EFFECTIVE SALINITY FOR ALCOHOL 1 AND ALCOHOL 2
 *---- csel7 cseu7 csel8 cseu8
 0.55 1.1 0 0
 CC 3.4.7 THE CSE SLOPE PARAMETER FOR CALCIUM AND ALCOHOL 1 AND ALCOHOL 2

```

CC Ca Alcohol#1 Alcohol#2
*---- beta6 beta7 beta8
      0 0 0
CC
CC 3.4.8 FLAG FOR ALCOHOL PART. MODEL AND PARTITION COEFFICIENTS
*---- ialc opsk7o opsk7s opsk8o opsk8s
      0 0 0 0 0
CC these are used only for alcohol partitioning in a two alcohol system:
CC 3.4.9 NO. OF ITERATIONS, AND TOLERANCE
*---- nalmax epsalc
      20 0.0001
CC 3.4.10 ALCOHOL 1 PARTITIONING PARAMETERS IF IALC=1
CC aq-oleic aq-oleic surf-oleic
*---- akwc7 akws7 akm7 ak7 pt7
      4.671 1.79 48 35.31 0.222
CC
CC 3.4.11 ALCOHOL 2 PARTITIONING PARAMETERS IF IALC=1
*---- akwc8 akws8 akm8 ak8 pt8
      0 0 0 0 0
CC
CC 3.4.22 ift model flag
*---- ift=0 for Healy&Reed; =1 for Chun Huh correl.
      1
CC 3.4.24 INTERFACIAL TENSION PARAMETERS
CC typ=.1-.35 typ=5-20
*---- chuh ahuh
      0.3 10
CC 14 dynes/cm
CC units of log 10 dynes/cm = mN/m
*---- xifw
      1.146
CC 3.4.26 ORGANIC MASS TRANSFER FLAG
CC imass=0 for no oil sol. in water. icorr=0 for constant MTC
*---- imass icor
      0 0
CC 3.4.31 CAPILLARY DESATURATION PARAMETERS FOR PHASE 1, 2, AND 3
CC diff. from core AQ OLEIC ME
*---- itrap t11 t22 t33
      1 1865 59074 364
CC
CC 3.4.32 FLAG FOR RELATIVE PERMEABILITY AND CAPILLARY PRESSURE MODEL
*---- iperm=0 irtype
      0 0
CC RESIDUAL SATURATION FOR EACH PHASE INPUT GIVEN THROUGH INCLUDE FILES
CC FLAG FOR CONSTANT OR VARIABLE REL. PERM. PARAMETERS
*---- ISRW IPRW IEW
      0 0 0
CC
CC CONSTANT RES. SATURATION OF PHASES 1,2,AND 3 AT LOW CAPILLARY NO.
*---- S1RWC S2RWC S3RWC
      0.2 0.35 0.2
CC
CC CONSTANT ENDPOINT REL. PERM. OF PHASES 1,2,AND 3 AT LOW CAPILLARY NO.
*---- P1RW P2RW P3RW
      0.06 0.93 0.06
CC
CC CONSTANT REL. PERM. EXPONENT OF PHASES 1,2,AND 3 AT LOW CAPILLARY NO.
*---- E1W E2W E3W
      2.5 2.0 2.5
CC

```

```

CC RES. SATURATION OF PHASES 1,2,AND 3 AT HIGH CAPILLARY NO.
*----S1RC S2RC S3RC
    .0 .0 .0
CC
CC ENDPOINT REL. PERM. OF PHASES 1,2,AND 3 AT HIGH CAPILLARY NO.
*----P1RC P2RC P3RC
    1.0 1.0 1.0
CC
CC REL. PERM. EXPONENT OF PHASES 1,2,AND 3 AT HIGH CAPILLARY NO.
*----E13CW E23C E31C
    1.0 1.0 1.0
CC Stars 19 cp
CC water oil =0 for isothermal modeling
*----VIS1 VIS2 TSTAND
    0.48 17 0
CC
CC 3.4.80 COMPOSITIONAL PHASE VISCOSITY PARAMETERS for microemulsion
*----ALPHAV1 ALPHAV2 ALPHAV3 ALPHAV4 ALPHAV5
    1.0 2.0 0.5 0.5 0.5
CC
CC 3.4.81 PARAMETERS TO CALCULATE POLYMER VISCOSITY AT ZERO SHEAR RATE
*----AP1 AP2 AP3
    27.4 1 3172
CC
CC 3.4.82 PARAMETER TO COMPUTE CSEP,MIN. CSEP, AND SLOPE OF LOG VIS. VS. LOG CSEP
*----BETAP CSE1 SSLOPE
    1 0.01 -0.78
CC
CC 3.4.83 PARAMETER FOR SHEAR RATE DEPENDENCE OF POLYMER VISCOSITY
*----GAMMAC GAMHF POWN ipmod
    16.0 3.1 1.8 0
CC
CC 3.4.84 FLAG FOR POLYMER PARTITIONING, PERM. REDUCTION PARAMETERS
*----IPOLYM EPHI3 EPHI4 BRK CRK rkcut
    1 1.0 1.0 100 0.015 10
CC
CC if IDEN=1 ignore gravity effect; =2 then include gravity effect
*----DEN1 DEN2 DEN23 DEN3 DEN7 DEN8 IDEN
    0.44 0.4065 0.4065 0.42 0.346 0 2
CC ISTB=0:BOTTOMHOLE CONDITION , 1: STOCK TANK
CC 3.4.93 FLAG FOR CHOICE OF UNITS when printing
*-----ISTB
    1
CC 3.4.94 FORMATION VOLUME FACTOR - may set all these to 1.0 and just factor in post-proc
CC water oil me
*-----FVF(I), I=1 TO MXP (IGAS=0 MXP=3,IGAS=1 MXP=4)
    1.00265 1.057 1
CC
CC 3.4.95 COMPRESSIBILITY FOR VOL. OCCUPYING COMPONENTS 1,2,3,7,AND 8
*----COMPC(1) COMPC(2) COMPC(3) COMPC(7) COMPC(8)
    2.7e-6 4.96e-5 0 0 0
CC
CC CONSTANT OR VARIABLE PC PARAM., WATER-WET OR OIL-WET PC CURVE FLAG
*----ICPC IEPC IOW
    0 0 0
CC
CC CAPILLARY PRESSURE PARAMETERS, CPC
*----CPC
    0.
CC

```

```

CC CAPILLARY PRESSURE PARAMETERS, EPC
*---- EPC
2.
CC
CC 3.4.117 MOLECULAR DIFFUSION COEF. KCTH COMPONENT IN PHASE 1
*---- D(KC,1),KC=1,N
0 0 0 0 0 0 0 0 0 0 0 0
CC
CC 3.4.118 MOLECULAR DIFFUSION COEF. KCTH COMPONENT IN PHASE 2
*---- D(KC,2),KC=1,N
0 0 0 0 0 0 0 0 0 0 0 0
CC
CC 3.4.119 MOLECULAR DIFFUSION COEF. KCTH COMPONENT IN PHASE 3
*---- D(KC,3),KC=1,N
0 0 0 0 0 0 0 0 0 0 0 0
CC modify disperivities
CC 3.4.121 LONGITUDINAL AND TRANSVERSE DISPERSIVITY OF PHASE 1
*---- ALPHAL(1) ALPHAT(1)
0.02 0.00
CC
CC 3.4.122 LONGITUDINAL AND TRANSVERSE DISPERSIVITY OF PHASE 2
*---- ALPHAL(2) ALPHAT(2)
0.02 0.00
CC
CC 3.4.124 LONGITUDINAL AND TRANSVERSE DISPERSIVITY OF PHASE 3
*---- ALPHAL(3) ALPHAT(3)
0.02 0.00
CC
CC 3.4.125 flag to specify organic adsorption calculation
*---- iadso=0 if organic adsorption is not considered
0
CC
CC 3.4.130 SURFACTANT AND POLYMER ADSORPTION PARAMETERS
*---- AD31 AD32 B3D AD41 AD42 B4D IADK IADS1 FADS REFK
1.7 0.05 1000 2 0.1 100 0 0 0 50
CC
CC 3.4.131 PARAMETERS FOR CATION EXCHANGE OF CLAY AND SURFACTANT
*---- QV XKC XKS EQW
0 0 0 400
cc
cc
*--- acid number EQW phtol soapk
0.5 400 8.5 1
cc
cc
*--- cselp, cseup, EQWSP
0.06 0.12 500
cc
cc
*--- imix
0
cc
cc
*--- c160 iphad
8 1
cc
cc
*--- HPHAD
0.1
cc

```



```

cc
*--- cna   calk   calcrit
      0.087   0.002   0.01
cc
cc Need to estimate for carbonate adsorption
*--- alkad  alkbd
      4    100
cc
cc
*---- icatex
      0
CC
CC*****
CC
CC WELL DATA
CC
CC*****
CC
CC
CC flag for right and left boundary
*---- ibound  IZONE
      0      0
CC
CC TOTAL NUMBER OF WELLS, WELL RADIUS FLAG, FLAG FOR TIME OR COURANT NO.
*----NWELL  IRO  ITIME  NWELR
      17    2    1    17
CC 4/10/2009
CC WELL ID,LOCATIONS,AND FLAG FOR SPECIFYING WELL TYPE, WELL RADIUS, SKIN
*----IDW IW  JW  IFLAG  RW  SWELL IDIR IFIRST ILAST  IPRF
      1 16  13  1  0.4  0  3  1  19  1
cc
cc
*---KPRF
1111111101111111111
CC
CC WELL NAME
*---- WELNAM
S1_I1
CC
CC MAX. AND MIN. ALLOWABLE BOTTOMHOLE PRESSURE AND RATE
*----ICHEK  PWFMIN  PWFMAX  QTMIN  QTMAX
      0    300.0  1300.0  0.0  14036.5
CC
CC WELL ID,LOCATIONS,AND FLAG FOR SPECIFYING WELL TYPE, WELL RADIUS, SKIN
*----IDW IW  JW  IFLAG  RW  SWELL IDIR IFIRST ILAST  IPRF
      2 30 13  1  0.4  0  3  1  19  1
cc
cc
*---KPRF
1111010111111111111
CC
CC WELL NAME
*---- WELNAM
S1_I2
CC
CC MAX. AND MIN. ALLOWABLE BOTTOMHOLE PRESSURE AND RATE
*----ICHEK  PWFMIN  PWFMAX  QTMIN  QTMAX
      0    300.0  1300.0  0.0  14036.5
CC
CC WELL ID,LOCATIONS,AND FLAG FOR SPECIFYING WELL TYPE, WELL RADIUS, SKIN

```

```

*---IDW IW JW IFLAG RW SWELL IDIR IFIRST ILAST IPRF
  3 36 25 1 0.4 0 3 1 19 1
cc
cc
*---KPRF
00010111111111111111
CC
CC WELL NAME
*--- WELNAM
S1_I3
CC
CC MAX. AND MIN. ALLOWABLE BOTTOMHOLE PRESSURE AND RATE
*---ICHEK PWFMIN PWFMAX QTMIN QTMAX
  0 300.0 1300.0 0.0 14036.5
CC
CC WELL ID,LOCATIONS,AND FLAG FOR SPECIFYING WELL TYPE, WELL RADIUS, SKIN
*---IDW IW JW IFLAG RW SWELL IDIR IFIRST ILAST IPRF
  4 30 37 1 0.4 0 3 1 19 1
cc
cc
*---KPRF
11010011111111111111
CC
CC WELL NAME
*--- WELNAM
S1_I4
CC
CC MAX. AND MIN. ALLOWABLE BOTTOMHOLE PRESSURE AND RATE
*---ICHEK PWFMIN PWFMAX QTMIN QTMAX
  0 300.0 1300.0 0.0 14036.5
CC
CC WELL ID,LOCATIONS,AND FLAG FOR SPECIFYING WELL TYPE, WELL RADIUS, SKIN
*---IDW IW JW IFLAG RW SWELL IDIR IFIRST ILAST IPRF
  5 16 37 1 0.4 0 3 1 19 1
cc
cc
*---KPRF
11111111111111111111
CC
CC WELL NAME
*--- WELNAM
S1_I5
CC
CC MAX. AND MIN. ALLOWABLE BOTTOMHOLE PRESSURE AND RATE
*---ICHEK PWFMIN PWFMAX QTMIN QTMAX
  0 300.0 1300.0 0.0 14036.5
CC
CC WELL ID,LOCATIONS,AND FLAG FOR SPECIFYING WELL TYPE, WELL RADIUS, SKIN
*---IDW IW JW IFLAG RW SWELL IDIR IFIRST ILAST IPRF
  6 10 25 1 0.4 0 3 1 19 1
cc
cc
*---KPRF
11111111111111111111
CC
CC WELL NAME
*--- WELNAM
S1_I6
CC
CC MAX. AND MIN. ALLOWABLE BOTTOMHOLE PRESSURE AND RATE

```

```

*----ICHEK PWFMIN PWFMAX QTMIN QTMAX
0 300.0 1300.0 0.0 14036.5
CC
CC WELL ID,LOCATIONS,AND FLAG FOR SPECIFYING WELL TYPE, WELL RADIUS, SKIN
*----IDW IW JW IFLAG RW SWELL IDIR IFIRST ILAST IPRF
7 10 5 1 0.4 0 3 1 19 1
cc
cc
*---KPRF
11111111111111111111
CC
CC WELL NAME
*---- WELNAM
S1_I7
CC
CC MAX. AND MIN. ALLOWABLE BOTTOMHOLE PRESSURE AND RATE
*----ICHEK PWFMIN PWFMAX QTMIN QTMAX
0 300.0 1400.0 0.0 7018.25
CC
CC WELL ID,LOCATIONS,AND FLAG FOR SPECIFYING WELL TYPE, WELL RADIUS, SKIN
*----IDW IW JW IFLAG RW SWELL IDIR IFIRST ILAST IPRF
8 36 5 1 0.4 0 3 1 19 1
cc
cc
*---KPRF
11111001111111111111
CC
CC WELL NAME
*---- WELNAM
S1_I8
CC
CC MAX. AND MIN. ALLOWABLE BOTTOMHOLE PRESSURE AND RATE
*----ICHEK PWFMIN PWFMAX QTMIN QTMAX
0 300.0 1400.0 0.0 7018.25
CC
CC WELL ID,LOCATIONS,AND FLAG FOR SPECIFYING WELL TYPE, WELL RADIUS, SKIN
*----IDW IW JW IFLAG RW SWELL IDIR IFIRST ILAST IPRF
9 36 44 1 0.4 0 3 1 19 1
cc
cc
*---KPRF
00111111111111111111
CC
CC WELL NAME
*---- WELNAM
S1_I9
CC
CC MAX. AND MIN. ALLOWABLE BOTTOMHOLE PRESSURE AND RATE
*----ICHEK PWFMIN PWFMAX QTMIN QTMAX
0 300.0 1400.0 0.0 7018.25
CC
CC WELL ID,LOCATIONS,AND FLAG FOR SPECIFYING WELL TYPE, WELL RADIUS, SKIN
*----IDW IW JW IFLAG RW SWELL IDIR IFIRST ILAST IPRF
10 10 44 1 0.4 0 3 1 19 1
cc
cc
*---KPRF
11111111111111111111
CC
CC WELL NAME

```

```

*---- WELNAM
S1_I10
CC
CC MAX. AND MIN. ALLOWABLE BOTTOMHOLE PRESSURE AND RATE
*----ICHEK PWFMIN PWFMAX QTMIN QTMAX
0 300.0 1400.0 0.0 7018.25
CC
CC WELL ID,LOCATIONS,AND FLAG FOR SPECIFYING WELL TYPE, WELL RADIUS, SKIN
*----IDW IW JW IFLAG RW SWELL IDIR IFIRST ILAST IPRF
11 22 25 2 0.4 0 3 1 19 1
cc
cc
*---KPRF
0011111111110011111
CC
CC WELL NAME
*---- WELNAM
S1_P1
CC DW, max 10000 bbls/d
CC MAX. AND MIN. ALLOWABLE BOTTOMHOLE PRESSURE AND RATE
*----ICHEK PWFMIN PWFMAX QTMIN QTMAX
0 300.0 1300. 0.0 56146.0
CC
CC WELL ID,LOCATIONS,AND FLAG FOR SPECIFYING WELL TYPE, WELL RADIUS, SKIN
*----IDW IW JW IFLAG RW SWELL IDIR IFIRST ILAST IPRF
12 22 5 2 0.4 0 3 1 19 1
cc
cc
*---KPRF
1101111111111111111
CC
CC WELL NAME
*---- WELNAM
S1_P2
CC
CC MAX. AND MIN. ALLOWABLE BOTTOMHOLE PRESSURE AND RATE
*----ICHEK PWFMIN PWFMAX QTMIN QTMAX
0 300.0 1400. 0.0 28073
CC
CC WELL ID,LOCATIONS,AND FLAG FOR SPECIFYING WELL TYPE, WELL RADIUS, SKIN
*----IDW IW JW IFLAG RW SWELL IDIR IFIRST ILAST IPRF
13 40 13 2 0.4 0 3 1 19 1
cc
cc
*---KPRF
0000010111111111111
CC
CC WELL NAME
*---- WELNAM
S1_P3
CC
CC MAX. AND MIN. ALLOWABLE BOTTOMHOLE PRESSURE AND RATE
*----ICHEK PWFMIN PWFMAX QTMIN QTMAX
0 300.0 1400. 0.0 28073
CC
CC WELL ID,LOCATIONS,AND FLAG FOR SPECIFYING WELL TYPE, WELL RADIUS, SKIN
*----IDW IW JW IFLAG RW SWELL IDIR IFIRST ILAST IPRF
14 40 37 2 0.4 0 3 1 19 1
cc
cc

```

```

*---KPRF
01100111111111111111
CC
CC WELL NAME
*---- WELNAM
S1_P4
CC
CC MAX. AND MIN. ALLOWABLE BOTTOMHOLE PRESSURE AND RATE
*----ICHEK PWFMIN PWFMAX QTMIN QTMAX
0 300.0 1400. 0.0 28073
CC
CC WELL ID,LOCATIONS,AND FLAG FOR SPECIFYING WELL TYPE, WELL RADIUS, SKIN
*----IDW IW JW IFLAG RW SWELL IDIR IFIRST ILAST IPRF
15 22 44 2 0.4 0 3 1 19 1
cc
cc
*---KPRF
11110111111111111111
CC
CC WELL NAME
*---- WELNAM
S1_P5
CC
CC MAX. AND MIN. ALLOWABLE BOTTOMHOLE PRESSURE AND RATE
*----ICHEK PWFMIN PWFMAX QTMIN QTMAX
0 300.0 1400. 0.0 28073
CC
CC WELL ID,LOCATIONS,AND FLAG FOR SPECIFYING WELL TYPE, WELL RADIUS, SKIN
*----IDW IW JW IFLAG RW SWELL IDIR IFIRST ILAST IPRF
16 4 37 2 0.4 0 3 1 19 1
cc
cc
*---KPRF
11101111111111111111
CC
CC WELL NAME
*---- WELNAM
S1_P6
CC
CC MAX. AND MIN. ALLOWABLE BOTTOMHOLE PRESSURE AND RATE
*----ICHEK PWFMIN PWFMAX QTMIN QTMAX
0 300.0 1400. 0.0 28073
CC
CC WELL ID,LOCATIONS,AND FLAG FOR SPECIFYING WELL TYPE, WELL RADIUS, SKIN
*----IDW IW JW IFLAG RW SWELL IDIR IFIRST ILAST IPRF
17 4 13 2 0.4 0 3 1 19 1
cc
cc
*---KPRF
11111111111111111111
CC
CC WELL NAME
*---- WELNAM
S1_P7
CC
CC MAX. AND MIN. ALLOWABLE BOTTOMHOLE PRESSURE AND RATE
*----ICHEK PWFMIN PWFMAX QTMIN QTMAX
0 300.0 1400. 0.0 28073
CC
CC Pressure constrained producer

```

*----WELL ID QI(M,L) water oil surf polymer anion cation alc1 alc2 sodium hyd Alkali HA0
 1 44916.8 1. 0. 0. 0. 0.0842 0.001 0 0 0.087 8 0.0043 0
 1 0. 0. 0. 0. 0. 0. 0. 6*0
 1 0. 0. 0. 0. 0. 0. 0. 6*0

CC

CC Pressure constrained producer

*----WELL ID QI(M,L) water oil surf polymer anion cation alc1 alc2 sodium hyd Alkali HA0
 2 44916.8 1. 0. 0. 0. 0.0842 0.001 0 0 0.087 8 0.0043 0
 2 0. 0. 0. 0. 0. 0. 0. 6*0
 2 0. 0. 0. 0. 0. 0. 0. 6*0

CC

CC Pressure constrained producer

*----WELL ID QI(M,L) water oil surf polymer anion cation alc1 alc2 sodium hyd Alkali HA0
 3 44916.8 1. 0. 0. 0. 0.0842 0.001 0 0 0.087 8 0.0043 0
 3 0. 0. 0. 0. 0. 0. 0. 6*0
 3 0. 0. 0. 0. 0. 0. 0. 6*0

CC

CC id,INJ. RATE AND INJ. COMP. FOR RATE CONS. WELLS FOR EACH PHASE(L=1,3)

*----id QI(M,L) water oil surf polymer anion cation alc1 alc2 sodium hyd Alkali HA0
 4 44916.8 1. 0. 0. 0. 0.0842 0.001 0 0 0.087 8 0.0043 0
 4 0. 0. 0. 0. 0. 0. 0. 6*0
 4 0. 0. 0. 0. 0. 0. 0. 6*0

CC

CC

*----id QI(M,L) water oil surf polymer anion cation alc1 alc2 sodium hyd Alkali HA0
 5 44916.8 1. 0. 0. 0. 0.0842 0.001 0 0 0.087 8 0.0043 0
 5 0. 0. 0. 0. 0. 0. 0. 6*0
 5 0. 0. 0. 0. 0. 0. 0. 6*0

CC

CC id,INJ. RATE AND INJ. COMP. FOR RATE CONS. WELLS FOR EACH PHASE(L=1,3)

*----id QI(M,L) water oil surf polymer anion cation alc1 alc2 sodium hyd Alkali HA0
 6 44916.8 1. 0. 0. 0. 0.0842 0.001 0 0 0.087 8 0.0043 0
 6 0. 0. 0. 0. 0. 0. 0. 6*0
 6 0. 0. 0. 0. 0. 0. 0. 6*0

CC

CC id,INJ. RATE AND INJ. COMP. FOR RATE CONS. WELLS FOR EACH PHASE(L=1,3)

*----id QI(M,L) water oil surf polymer anion cation alc1 alc2 sodium hyd Alkali HA0
 7 22458.4 1. 0. 0. 0. 0.0842 0.001 0 0 0.087 8 0.0043 0
 7 0. 0. 0. 0. 0. 0. 0. 6*0
 7 0. 0. 0. 0. 0. 0. 0. 6*0

CC

CC

*----id QI(M,L) water oil surf polymer anion cation alc1 alc2 sodium hyd Alkali HA0
 8 22458.4 1. 0. 0. 0. 0.0842 0.001 0 0 0.087 8 0.0043 0
 8 0. 0. 0. 0. 0. 0. 0. 6*0
 8 0. 0. 0. 0. 0. 0. 0. 6*0

CC

CC id,INJ. RATE AND INJ. COMP. FOR RATE CONS. WELLS FOR EACH PHASE(L=1,3)

*----id QI(M,L) water oil surf polymer anion cation alc1 alc2 sodium hyd Alkali HA0
 9 22458.4 1. 0. 0. 0. 0.0842 0.001 0 0 0.087 8 0.0043 0
 9 0. 0. 0. 0. 0. 0. 0. 6*0
 9 0. 0. 0. 0. 0. 0. 0. 6*0

CC

CC id,INJ. RATE AND INJ. COMP. FOR RATE CONS. WELLS FOR EACH PHASE(L=1,3)

*----id QI(M,L) water oil surf polymer anion cation alc1 alc2 sodium hyd Alkali HA0
 10 22458.4 1. 0. 0. 0. 0.0842 0.001 0 0 0.087 8 0.0043 0
 10 0. 0. 0. 0. 0. 0. 0. 6*0
 10 0. 0. 0. 0. 0. 0. 0. 6*0

CC

CC Pressure constrained producer

```

*----WELL ID PWF
11      300.0
CC
CC Pressure constrained producer
*----WELL ID PWF
12      300.0
CC
CC Pressure constrained producer
*----WELL ID PWF
13      300.0
CC
CC Pressure constrained producer
*----WELL ID PWF
14      300.0
CC
CC Pressure constrained producer
*----WELL ID PWF
15      300.0
CC
CC Pressure constrained producer
*----WELL ID PWF
16      300.0
CC
CC Pressure constrained producer
*----WELL ID PWF
17      300.0
CC
CC CUM. INJ. TIME , AND INTERVALS (PV OR DAY) FOR WRITING TO OUTPUT FILES (3.7.8)
*----TINJ CUMPR1 CUMHI2 WRHPV(HIST) WRPRF(PLOT) RSTC
7      4.9 4.9 0.2 0.5 4.9
CC
CC FOR IMES=2 ,THE INI. TIME STEP,CONC. TOLERANCE,MAX.,MIN. time steps
*----DT DCLIM CNMAX CNMIN
0.00001 0.001 0.2 0.01
CC
CC
*----IBMOD
0
CC
CC IRO, ITIME, NEW FLAGS FOR ALL THE WELLS
*----IRO ITSTEP IFLAG
2 1 10*1 7*2
CC
CC NUMBER OF WELLS CHANGES IN LOCATION OR SKIN OR PWF
*----NWEL1
0
CC
CC NUMBER OF WELLS WITH RATE CHANGES, ID - SURFACTANT FLOOD INTO 10 INJECTORS
*----NWEL2 ID
10 1 2 3 4 5 6 7 8 9 10
CC
CC Pressure constrained producer
*----WELL ID QI(M,L) water oil surf polymer anion cation alc1 alc2 sodium hyd Alkali HA0
1 44916.8 0.998 0. 0.002 0.30 0.0839 0.00 0. 0. 0.606 10 0.5214 0.00001
1 0. 0. 0. 0. 0. 0. 0. 6*0
1 0. 0. 0. 0. 0. 0. 0. 6*0
CC
CC Pressure constrained producer
*----WELL ID QI(M,L) water oil surf polymer anion cation alc1 alc2 sodium hyd Alkali HA0
2 44916.8 0.998 0. 0.002 0.30 0.0839 0.00 0. 0. 0.606 10 0.5214 0.00001

```

```

2      0.      0.      0.      0.      0.      0.      0.      6*0
2      0.      0.      0.      0.      0.      0.      0.      6*0
CC
CC Pressure constrained producer
*----WELL ID QI(M,L) water oil surf polymer anion cation alc1 alc2 sodium hyd Alkali HA0
3 44916.8 0.998 0. 0.002 0.30 0.0839 0.00 0. 0. 0.606 10 0.5214 0.00001
3 0. 0. 0. 0. 0. 0. 0. 0. 6*0
3 0. 0. 0. 0. 0. 0. 0. 0. 6*0
CC
CC id,INJ. RATE AND INJ. COMP. FOR RATE CONS. WELLS FOR EACH PHASE(L=1,3)
*----id QI(M,L) water oil surf polymer anion cation alc1 alc2 sodium hyd Alkali HA0
4 44916.8 0.998 0. 0.002 0.30 0.0839 0.00 0. 0. 0.606 10 0.5214 0.00001
4 0. 0. 0. 0. 0. 0. 0. 0. 6*0
4 0. 0. 0. 0. 0. 0. 0. 0. 6*0
CC
CC
*----id QI(M,L) water oil surf polymer anion cation alc1 alc2 sodium hyd Alkali HA0
5 44916.8 0.998 0. 0.002 0.30 0.0839 0.00 0. 0. 0.606 10 0.5214 0.00001
5 0. 0. 0. 0. 0. 0. 0. 0. 6*0
5 0. 0. 0. 0. 0. 0. 0. 0. 6*0
CC
CC id,INJ. RATE AND INJ. COMP. FOR RATE CONS. WELLS FOR EACH PHASE(L=1,3)
*----id QI(M,L) water oil surf polymer anion cation alc1 alc2 sodium hyd Alkali HA0
6 44916.8 0.998 0. 0.002 0.30 0.0839 0.00 0. 0. 0.606 10 0.5214 0.00001
6 0. 0. 0. 0. 0. 0. 0. 0. 6*0
6 0. 0. 0. 0. 0. 0. 0. 0. 6*0
CC
CC id,INJ. RATE AND INJ. COMP. FOR RATE CONS. WELLS FOR EACH PHASE(L=1,3)
*----id QI(M,L) water oil surf polymer anion cation alc1 alc2 sodium hyd Alkali HA0
7 22458.4 0.998 0. 0.002 0.30 0.0839 0.00 0. 0. 0.606 10 0.5214 0.00001
7 0. 0. 0. 0. 0. 0. 0. 0. 6*0
7 0. 0. 0. 0. 0. 0. 0. 0. 6*0
CC
CC
*----id QI(M,L) water oil surf polymer anion cation alc1 alc2 sodium hyd Alkali HA0
8 22458.4 0.998 0. 0.002 0.30 0.0839 0.00 0. 0. 0.606 10 0.5214 0.00001
8 0. 0. 0. 0. 0. 0. 0. 0. 6*0
8 0. 0. 0. 0. 0. 0. 0. 0. 6*0
CC
CC id,INJ. RATE AND INJ. COMP. FOR RATE CONS. WELLS FOR EACH PHASE(L=1,3)
*----id QI(M,L) water oil surf polymer anion cation alc1 alc2 sodium hyd Alkali HA0
9 22458.4 0.998 0. 0.002 0.30 0.0839 0.00 0. 0. 0.606 10 0.5214 0.00001
9 0. 0. 0. 0. 0. 0. 0. 0. 6*0
9 0. 0. 0. 0. 0. 0. 0. 0. 6*0
CC
CC id,INJ. RATE AND INJ. COMP. FOR RATE CONS. WELLS FOR EACH PHASE(L=1,3)
*----id QI(M,L) water oil surf polymer anion cation alc1 alc2 sodium hyd Alkali HA0
10 22458.4 0.998 0. 0.002 0.30 0.0839 0.00 0. 0. 0.606 10 0.5214 0.00001
10 0. 0. 0. 0. 0. 0. 0. 0. 6*0
10 0. 0. 0. 0. 0. 0. 0. 0. 6*0
CC
CC CUM. INJ. TIME , AND INTERVALS (PV OR DAY) FOR WRITING TO OUTPUT FILES (3.7.8)
*----TINJ CUMPR1 CUMHI2 WRHPV(HIST) WRPRF(PLOT) RSTC
7.3 0.1 0.1 0.01 0.1 0.05
CC
CC FOR IMES=2 ,THE INI. TIME STEP,CONC. TOLERANCE,MAX.,MIN. time steps
*----DT DCLIM CNMAX CNMIN
0.00001 0.005 0.05 0.001
CC
CC

```



```

*----IBMOD
0
CC
CC IRO, ITIME, NEW FLAGS FOR ALL THE WELLS
*----IRO ITSTEP IFLAG
2 1 10*1 7*2
CC
CC NUMBER OF WELLS CHANGES IN LOCATION OR SKIN OR PWF
*----NWEL1
0
CC
CC NUMBER OF WELLS WITH RATE CHANGES, ID - SURFACTANT FLOOD INTO 10 INJECTORS
*----NWEL2 ID
10 1 2 3 4 5 6 7 8 9 10
CC
CC Pressure constrained producer
*----WELL ID QI(M,L) water oil surf polymer anion cation alc1 alc2 sodium hyd Alkali HA0
1 44916.8 1.00 0. 0.000 0.2 0.0842 0.013 0. 0. 0.087 8 0.0043 0.00
1 0. 0. 0. 0. 0. 0. 0. 6*0
1 0. 0. 0. 0. 0. 0. 0. 6*0
CC
CC Pressure constrained producer
*----WELL ID QI(M,L) water oil surf polymer anion cation alc1 alc2 sodium hyd Alkali HA0
2 44916.8 1.00 0. 0.000 0.2 0.0842 0.013 0. 0. 0.087 8 0.0043 0.00
2 0. 0. 0. 0. 0. 0. 0. 6*0
2 0. 0. 0. 0. 0. 0. 0. 6*0
CC
CC Pressure constrained producer
*----WELL ID QI(M,L) water oil surf polymer anion cation alc1 alc2 sodium hyd Alkali HA0
3 44916.8 1.00 0. 0.000 0.2 0.0842 0.013 0. 0. 0.087 8 0.0043 0.00
3 0. 0. 0. 0. 0. 0. 0. 6*0
3 0. 0. 0. 0. 0. 0. 0. 6*0
CC
CC id,INJ. RATE AND INJ. COMP. FOR RATE CONS. WELLS FOR EACH PHASE(L=1,3)
*----id QI(M,L) water oil surf polymer anion cation alc1 alc2 sodium hyd Alkali HA0
4 44916.8 1.00 0. 0.000 0.2 0.0842 0.013 0. 0. 0.087 8 0.0043 0.00
4 0. 0. 0. 0. 0. 0. 0. 6*0
4 0. 0. 0. 0. 0. 0. 0. 6*0
CC
CC
*----id QI(M,L) water oil surf polymer anion cation alc1 alc2 sodium hyd Alkali HA0
5 44916.8 1.00 0. 0.000 0.2 0.0842 0.013 0. 0. 0.087 8 0.0043 0.00
5 0. 0. 0. 0. 0. 0. 0. 6*0
5 0. 0. 0. 0. 0. 0. 0. 6*0
CC
CC id,INJ. RATE AND INJ. COMP. FOR RATE CONS. WELLS FOR EACH PHASE(L=1,3)
*----id QI(M,L) water oil surf polymer anion cation alc1 alc2 sodium hyd Alkali HA0
6 44916.8 1.00 0. 0.000 0.2 0.0842 0.013 0. 0. 0.087 8 0.0043 0.00
6 0. 0. 0. 0. 0. 0. 0. 6*0
6 0. 0. 0. 0. 0. 0. 0. 6*0
CC
CC id,INJ. RATE AND INJ. COMP. FOR RATE CONS. WELLS FOR EACH PHASE(L=1,3)
*----id QI(M,L) water oil surf polymer anion cation alc1 alc2 sodium hyd Alkali HA0
7 22458.4 1.00 0. 0.000 0.2 0.0842 0.013 0. 0. 0.087 8 0.0043 0.00
7 0. 0. 0. 0. 0. 0. 0. 6*0
7 0. 0. 0. 0. 0. 0. 0. 6*0
CC
CC
*----id QI(M,L) water oil surf polymer anion cation alc1 alc2 sodium hyd Alkali HA0
8 22458.4 1.00 0. 0.000 0.2 0.0842 0.013 0. 0. 0.087 8 0.0043 0.00

```

```

      8 0. 0. 0. 0. 0. 0. 0. 6*0
      8 0. 0. 0. 0. 0. 0. 0. 6*0
CC
CC id,INJ. RATE AND INJ. COMP. FOR RATE CONS. WELLS FOR EACH PHASE(L=1,3)
*----id QI(M,L) water oil surf polymer anion cation alc1 alc2 sodium hyd Alkali HA0
      9 22458.4 1.00 0. 0.000 0.2 0.0842 0.013 0. 0. 0.087 8 0.0043 0.00
      9 0. 0. 0. 0. 0. 0. 0. 6*0
      9 0. 0. 0. 0. 0. 0. 0. 6*0
CC
CC id,INJ. RATE AND INJ. COMP. FOR RATE CONS. WELLS FOR EACH PHASE(L=1,3)
*----id QI(M,L) water oil surf polymer anion cation alc1 alc2 sodium hyd Alkali HA0
      10 22458.4 1.00 0. 0.000 0.2 0.0842 0.013 0. 0. 0.087 8 0.0043 0.00
      10 0. 0. 0. 0. 0. 0. 0. 6*0
      10 0. 0. 0. 0. 0. 0. 0. 6*0
CC
CC CUM. INJ. TIME , AND INTERVALS (PV OR DAY) FOR WRITING TO OUTPUT FILES (3.7.8)
*----TINJ CUMPR1 CUMHI2 WRHPV(HIST) WRPRF(PLOT) RSTC
      8.3 0.1 0.1 0.01 0.1 0.05
CC
CC FOR IMES=2 ,THE INI. TIME STEP,CONC. TOLERANCE,MAX.,MIN. time steps
*----DT DCLIM CNMAX CNMIN
      0.00001 0.005 0.05 0.001
CC
CC
*----IBMOD
      0
CC
CC IRO, ITIME, NEW FLAGS FOR ALL THE WELLS
*---- IRO ITSTEP IFLAG
      2 1 10*1 7*2
CC
CC NUMBER OF WELLS CHANGES IN LOCATION OR SKIN OR PWF
*----NWEL1
      0
CC
CC NUMBER OF WELLS WITH RATE CHANGES, ID - SURFACTANT FLOOD INTO 10 INJECTORS
*----NWEL2 ID
      10 1 2 3 4 5 6 7 8 9 10
CC
CC Pressure constrained producer
*----WELL ID QI(M,L) water oil surf polymer anion cation alc1 alc2 sodium hyd Alkali HA0
      1 44916.8 1 0. 0.0 0.0 0.05130 0.001 0 0 0.0513 8 0.001 0
      1 0. 0. 0. 0. 0. 0. 6*0
      1 0. 0. 0. 0. 0. 0. 6*0
CC
CC Pressure constrained producer
*----WELL ID QI(M,L) water oil surf polymer anion cation alc1 alc2 sodium hyd Alkali HA0
      2 44916.8 1 0. 0.0 0.0 0.05130 0.001 0 0 0.0513 8 0.001 0
      2 0. 0. 0. 0. 0. 0. 6*0
      2 0. 0. 0. 0. 0. 0. 6*0
CC
CC Pressure constrained producer
*----WELL ID QI(M,L) water oil surf polymer anion cation alc1 alc2 sodium hyd Alkali HA0
      3 44916.8 1 0. 0.0 0.0 0.05130 0.001 0 0 0.0513 8 0.001 0
      3 0. 0. 0. 0. 0. 0. 6*0
      3 0. 0. 0. 0. 0. 0. 6*0
CC
CC id,INJ. RATE AND INJ. COMP. FOR RATE CONS. WELLS FOR EACH PHASE(L=1,3)
*----id QI(M,L) water oil surf polymer anion cation alc1 alc2 sodium hyd Alkali HA0
      4 44916.8 1 0. 0.0 0.0 0.05130 0.001 0 0 0.0513 8 0.001 0

```

```

4 0. 0. 0. 0. 0. 0. 0. 6*0
4 0. 0. 0. 0. 0. 0. 0. 6*0
CC
CC
*----id QI(M,L) water oil surf polymer anion cation alc1 alc2 sodium hyd Alkali HA0
5 44916.8 1 0. 0.0 0.0 0.05130 0.001 0 0 0.0513 8 0.001 0
5 0. 0. 0. 0. 0. 0. 0. 6*0
5 0. 0. 0. 0. 0. 0. 0. 6*0
CC
CC id,INJ. RATE AND INJ. COMP. FOR RATE CONS. WELLS FOR EACH PHASE(L=1,3)
*----id QI(M,L) water oil surf polymer anion cation alc1 alc2 sodium hyd Alkali HA0
6 44916.8 1 0. 0.0 0.0 0.05130 0.001 0 0 0.0513 8 0.001 0
6 0. 0. 0. 0. 0. 0. 0. 6*0
6 0. 0. 0. 0. 0. 0. 0. 6*0
CC
CC id,INJ. RATE AND INJ. COMP. FOR RATE CONS. WELLS FOR EACH PHASE(L=1,3)
*----id QI(M,L) water oil surf polymer anion cation alc1 alc2 sodium hyd Alkali HA0
7 22458.4 1 0. 0.0 0.0 0.05130 0.001 0 0 0.0513 8 0.001 0
7 0. 0. 0. 0. 0. 0. 0. 6*0
7 0. 0. 0. 0. 0. 0. 0. 6*0
CC
CC
*----id QI(M,L) water oil surf polymer anion cation alc1 alc2 sodium hyd Alkali HA0
8 22458.4 1 0. 0.0 0.0 0.05130 0.001 0 0 0.0513 8 0.001 0
8 0. 0. 0. 0. 0. 0. 0. 6*0
8 0. 0. 0. 0. 0. 0. 0. 6*0
CC
CC id,INJ. RATE AND INJ. COMP. FOR RATE CONS. WELLS FOR EACH PHASE(L=1,3)
*----id QI(M,L) water oil surf polymer anion cation alc1 alc2 sodium hyd Alkali HA0
9 22458.4 1 0. 0.0 0.0 0.05130 0.001 0 0 0.0513 8 0.001 0
9 0. 0. 0. 0. 0. 0. 0. 6*0
9 0. 0. 0. 0. 0. 0. 0. 6*0
CC
CC id,INJ. RATE AND INJ. COMP. FOR RATE CONS. WELLS FOR EACH PHASE(L=1,3)
*----id QI(M,L) water oil surf polymer anion cation alc1 alc2 sodium hyd Alkali HA0
10 22458.4 1 0. 0.0 0.0 0.05130 0.001 0 0 0.0513 8 0.001 0
10 0. 0. 0. 0. 0. 0. 0. 6*0
10 0. 0. 0. 0. 0. 0. 0. 6*0
CC
CC CUM. INJ. TIME , AND INTERVALS (PV OR DAY) FOR WRITING TO OUTPUT FILES (3.7.8)
*----TINJ CUMPR1 CUMHI2 WRHPV(HIST) WRPRF(PLOT) RSTC
9.3 0.1 0.1 0.01 0.1 0.05
CC
CC FOR IMES=2 ,THE INI. TIME STEP,CONC. TOLERANCE,MAX.,MIN. time steps
*----DT DCLIM CNMAX CNMIN
0.00001 0.005 0.1 0.001

```

D3: INPUT FILE FOR PHASE BEHAVIOR MATCH USING UTCHEM IN BATCH MODE:

```
CC*****
CC                                     *
CC  BRIEF DESCRIPTION OF DATA SET : UTCHEM (VERSION 9.0 )      *
CC                                     *
CC*****
CC                                     *
CC  batch calculation to obtain UTCHEM phase behavior          *
CC                                     *
CC  LENGTH (FT) :          PROCESS : SURFACTANT                *
CC  THICKNESS (FT) :          INJ. RATE (FT3/DAY) : 0.05        *
CC  WIDTH (FT) :          COORDINATES : CARTESIAN              *
CC  POROSITY :          *
CC  GRID BLOCKS : 5x 1x1          *
CC  DATE : 5/14/2000          *
CC                                     *
CC*****
CC                                     *
CC  RESERVOIR DESCRIPTION          *
CC                                     *
CC*****
CC
CC Run number
*---- RUNNO
UTBATC
CC
CC Title and run description
*---- title(i)
get the hand's parameter from batch samples
one test tube with certain salinity of 0.66 meq/ml and WOR =4
NO Correct fluid properties, only match of phase behavior parameters
CC
CC SIMULATION FLAGS
*---- IMODE IMES IDISPC ICWM ICAP IREACT IBIO ICOORD ITREAC ITC IGAS IENG
      1  2  0  0  0  0  0  1  0  0  0  0
CC
CC no. of gridblocks,flag specifies constant or variable grid size,unit
*---- NX  NY  NZ  IDXYZ  IUNIT
      5  1  1  0  0
CC
CC constant grid block size in x,y,and z
*---- dx1      dy1      dz1
      1        1        1
CC
CC total no. of components,no. of tracers,no. of gel components
*----n  no  ntw  nta  ngc  ng  noth
      7  0  0  0  0  0  0
CC
CC Name of the components
*----spname(i) for i=1 to n
Water
Oil
Surf.
Polymer
Chloride
Calcium
```

```

Alcohol 1
CC
CC flag indicating if the component is included in calculations or not
*----icf(kc) for kc=1,n
  1 1 1 0 1 1 1
CC
CC*****
CC
CC      *
CC  OUTPUT OPTIONS      *
CC      *
CC*****
CC
CC
CC FLAG TO WRITE TO UNIT 3,FLAG FOR PV OR DAYS TO PRINT OR TO STOP THE RUN
*---- ICUMTM ISTOP IOUTGMS
  0  0  0
CC
CC FLAG INDICATING IF THE PROFILE OF KCTH COMPONENT SHOULD BE WRITTEN
*---- IPRFLG(KC),KC=1,N
  1 1 1 0 1 1 1
CC
CC FLAG FOR PRES.,SAT.,TOTAL CONC.,TRACER CONC.,CAP.,GEL, ALKALINE PROFILES
*---- IPPRES IPSAT IPTOT IPBIO IPCAP IPGEL IPALK IPTEMP IPOBS
  0  0  0  0  0  0  0  0  0
CC
CC FLAG FOR WRITING SEVERAL PROPERTIES TO UNIT 4 (Prof)
*---- ICKL IVIS IPER ICNM ICSE IHYSTP IFOAMP INONEQ
  0  0  0  0  0  0  0  0
CC
CC FLAG for variables to PROF output file
*---- IADS IVEL IRKF IPHSE
  0  0  0  0
CC
CC*****
CC
CC      *
CC  RESERVOIR PROPERTIES      *
CC      *
CC*****
CC
CC
CC MAX. SIMULATION TIME ( DAYS)
*---- TMAX
  300
CC
CC ROCK COMPRESSIBILITY (1/PSI), STAND. PRESSURE(PSIA)
*---- COMPR      PSTAND
  0      0
CC
CC FLAGS INDICATING CONSTANT OR VARIABLE POROSITY, X,Y,AND Z PERMEABILITY
*---- IPOR1 IPERMX IPERMY IPERMZ IMOD
  0  1  1  0  0
CC
CC CONSTANT POROSITY FOR WHOLE RESERVOIR
*---- PORC1
  1
CC
CC CONSTANT X-PERMEABILITY (MILIDARCY) FOR LAYER K = 1,NZ
*---- PERMX(K),K=1,NZ
  1000000
CC

```

```

CC CONSTANT Y-PERMEABILITY (MILIDARCY) FOR LAYER K = 1,NZ
*---- PERMY(K),K=1,NZ
      1000000
CC
CC CONSTANT Z-PERMEABILITY FOR WHOLE RESERVOIR
*---- PERMZC
      1000000
CC
CC FLAG FOR CONSTANT OR VARIABLE DEPTH, PRESSURE, WATER SATURATION,INITIAL AQUEOUS
PHASE cOMPOSITIONS
*----IDEPth IPRESS ISWI ICWI
      0    0    0  -1
CC
CC CONSTANT DEPTH (FT)
*---- D111
      0
CC
CC CONSTANT PRESSURE (PSIA)
*---- PRESS1
      1
CC
CC CONSTANT INITIAL WATER SATURATION
*---- SWI
      1
CC
CC BRINE SALINITY AND DIVALENT CATION CONCENTRATION (MEQ/ML)
*---- C50    C60
      0.0513  0.0
CC
CC*****
CC                                     *
CC  PHYSICAL PROPERTY DATA                                     *
CC                                     *
CC*****
CC
CC
CC OIL CONC. AT PLAIT POINT FOR TYPE II(+)AND TYPE II(-), CMC
*---- c2plc c2prc epsme ihand
      0    1    0.001  0
CC
CC flag indicating type of phase behavior parameters
*---- ifghbn
      0
CC SLOPE AND INTERCEPT OF BINODAL CURVE AT ZERO, OPT., AND 2XOPT SALINITY
CC FOR ALCOHOL 1
*---- hbns70 hbnc70 hbns71 hbnc71 hbns72 hbnc72
      0 .06  0  0.05  0  0.060
CC SLOPE AND INTERCEPT OF BINODAL CURVE AT ZERO, OPT., AND 2XOPT SALINITY
CC FOR ALCOHOL 2(AAY: if add Alkaline, these are for soap Binodal curves"
*---- hbns80 hbnc80 hbns81 hbnc81 hbns82 hbnc82
      0    0    0    0    0    0
CC
CC LOWER AND UPPER EFFECTIVE SALINITY FOR ALCOHOL 1 AND ALCOHOL 2
*---- csel7 cseu7 csel8 cseu8
      0.5  0.85  0    0
CC
CC THE CSE SLOPE PARAMETER FOR CALCIUM AND ALCOHOL 1 AND ALCOHOL 2
*---- beta6 beta7 beta8
      0    0    0
CC

```

CC FLAG FOR ALCOHOL PART. MODEL AND PARTITION COEFFICIENTS

*---- ialc opsk7o opsk7s opsk8o opsk8s
0 0.04 2.8 0 0

CC

CC NO. OF ITERATIONS, AND TOLERANCE

*---- nalmax epsalc
20 0.0001

CC

CC ALCOHOL 1 PARTITIONING PARAMETERS IF IALC=1

*---- akwc7 akws7 akm7 ak7 pt7
4.671 1.79 48 35.31 0.222

CC

CC ALCOHOL 2 PARTITIONING PARAMETERS IF IALC=1

*---- akwc8 akws8 akm8 ak8 pt8
0 0 0 0 0

CC

CC ift model flag

*---- ift
1

CC

CC INTERFACIAL TENSION PARAMETERS

*---- chuh ahuh
0.3 13

CC

CC LOG10 OF OIL/WATER INTERFACIAL TENSION

*---- xifw
1.65

CC

CC ORGANIC MASS TRANSFER FLAG

*---- imass icor
0 0

CC

CC CAPILLARY DESATURATION PARAMETERS FOR PHASE 1, 2, AND 3

*---- itrap t11 t22 t33
0 1865 59074 364.2

CC

CC FLAG FOR RELATIVE PERMEABILITY AND CAPILLARY PRESSURE MODEL

*---- iperm
0

CC

CC FLAG FOR CONSTANT OR VARIABLE REL. PERM. PARAMETERS

*---- isrw iprw iew
0 0 0

CC

CC CONSTANT RES. SATURATION OF PHASES 1,2,AND 3 AT LOW CAPILLARY NO.

*---- s1rwc s2rwc s3rwc
0 0 0

CC

CC CONSTANT ENDPOINT REL. PERM. OF PHASES 1,2,AND 3 AT LOW CAPILLARY NO.

*---- p1rwc p2rwc p3rwc
1 1 1

CC

CC CONSTANT REL. PERM. EXPONENT OF PHASES 1,2,AND 3 AT LOW CAPILLARY NO.

*---- e1wc e2wc e3wc
1 1 1

CC

CC WATER AND OIL VISCOSITY , RESERVOIR TEMPERATURE

*---- VIS1 VIS2 TSTAND
1 1 0

CC

```

CC COMPOSITIONAL PHASE VISCOSITY PARAMETERS
*---- ALPHAV1 ALPHAV2 ALPHAV3 ALPHAV4 ALPHAV5
      0      0      0      0      0
CC
CC PARAMETERS TO CALCULATE POLYMER VISCOSITY AT ZERO SHEAR RATE
*---- AP1   AP2   AP3
      81   2700  2500
CC
CC PARAMETER TO COMPUTE CSEP,MIN. CSEP, AND SLOPE OF LOG VIS. VS. LOG CSEP
*---- BETAP CSE1 SSLOPE
      10   0.01  0.17
CC
CC PARAMETER FOR SHEAR RATE DEPENDENCE OF POLYMER VISCOSITY
*---- GAMMAC GAMHF POWN
      20   10   1.8
CC
CC CC FLAG FOR POLYMER PARTITIONING, PERM. REDUCTION PARAMETERS
*---- IPOLYM EPHI3 EPHI4 BRK  CRK
      1     1     0.8  1000  0.0186
CC
CC SPECIFIC WEIGHT FOR COMPONENTS 1,2,3,7,8 ,Coefficient of oil and GRAVITY FLAG
*---- DEN1  DEN2  DEN23  DEN3  DEN7  DEN8  IDEN
      0.433  0.433  0.433  0.433  0.433  0    2
CC
CC FLAG FOR CHOICE OF UNITS ( 0:BOTTOMHOLE CONDITION , 1: STOCK TANK)
*----- ISTB
      0
CC
CC COMPRESSIBILITY FOR VOL. OCCUPYING COMPONENTS 1,2,3,7,AND 8
*---- COMPC(1) COMPC(2) COMPC(3) COMPC(7) COMPC(8)
      0      0      0      0      0
CC
CC CONSTANT OR VARIABLE PC PARAM., WATER-WET OR OIL-WET PC CURVE FLAG
*---- ICPC IEPC IOW
      0      0      0
CC
CC CAPILLARY PRESSURE PARAMETER, CPC0
*---- CPC0
      0
CC
CC CAPILLARY PRESSURE PARAMETER, EPC0
*---- EPC0
      2
CC
CC MOLECULAR DIFFUSION COEF. KCTH COMPONENT IN PHASE 1
*---- D(KC,1),KC=1,N
      0      0      0      0      0      0      0
CC
CC MOLECULAR DIFFUSION COEF. KCTH COMPONENT IN PHASE 2
*---- D(KC,2),KC=1,N
      0      0      0      0      0      0      0
CC
CC MOLECULAR DIFFUSION COEF. KCTH COMPONENT IN PHASE 3
*---- D(KC,3),KC=1,N
      0      0      0      0      0      0      0
CC
CC LONGITUDINAL AND TRANSVERSE DISPERSIVITY OF PHASE 1
*---- ALPHAL(1)  ALPHAT(1)
      0          0
CC

```



```

CC LONGITUDINAL AND TRANSVERSE DISPERSIVITY OF PHASE 2
*---- ALPHAL(2)  ALPHAT(2)
      0      0
CC
CC LONGITUDINAL AND TRANSVERSE DISPERSIVITY OF PHASE 3
*---- ALPHAL(3)  ALPHAT(3)
      0      0
CC
CC flag to specify organic adsorption calculation
*---- iadso
      0
CC
CC SURFACTANT AND POLYMER ADSORPTION PARAMETERS
*---- AD31  AD32  B3D  AD41  AD42  B4D  IADK  IADS1  FADS  REFK
      0  0 1000 0.7  0  100  0  0  0  0
CC
CC PARAMETERS FOR CATION EXCHANGE OF CLAY AND SURFACTANT
*---- QV  XKC  XKS  EQW
      0  0  0  419
CC
CC*****
CC                                  *
CC  WELL DATA                                  *
CC                                  *
CC*****
CC
CC
CC FLAG FOR SPECIFIED BOUNDARY AND ZONE IS MODELED
*---- IBOUND  IZONE
      0  0
CC
CC TOTAL NUMBER OF WELLS, WELL RADIUS FLAG, FLAG FOR TIME OR COURANT NO.
*---- NWELL  IRO  ITIME  NWREL
      2  2  1  2
CC
CC WELL ID,LOCATIONS,AND FLAG FOR SPECIFYING WELL TYPE, WELL RADIUS, SKIN
*---- IDW  IW  JW  IFLAG  RW  SWELL  IDIR  IFIRST  ILAST  IPRF
      1  1  1  1  0.5  0  3  1  1  0
CC
CC WELL NAME
*---- WELNAM
INJECTOR
CC
CC ICHEK , MAX. AND MIN. ALLOWABLE BOTTOMHOLE PRESSURE AND RATE
*---- ICHEK  PWFMIN  PWFMAX  QTMIN  QTMAX
      0  0  5000  0  1000
CC
CC WELL ID,LOCATIONS,AND FLAG FOR SPECIFYING WELL TYPE, WELL RADIUS, SKIN
*---- IDW  IW  JW  IFLAG  RW  SWELL  IDIR  IFIRST  ILAST  IPRF
      2  5  1  2  0.5  0  3  1  1  0
CC
CC WELL NAME
*---- WELNAM
PRODUCER
CC
CC ICHEK , MAX. AND MIN. ALLOWABLE BOTTOMHOLE PRESSURE AND RATE
*---- ICHEK  PWFMIN  PWFMAX  QTMIN  QTMAX
      0  0  5000  0  50000
CC
CC ID,INJ. RATE AND INJ. COMP. FOR RATE CONS. WELLS FOR EACH PHASE (L=1,3)

```

```

*---- ID Injection rate (QI)  Water  Oil  Surfactant Polymer Chloride Calcium Alcohol 1
1      0.08      0.995  0  0.005  0  0.664508  0.0  0.0
1      0.02  0  1  0  0  0  0  0
1      0  0  0  0  0  0  0  0  0
CC
CC ID, BOTTOM HOLE PRESSURE FOR PRESSURE CONSTRAINT WELL (IFLAG=2 OR 3)
*---- ID  PWF
2  1
CC
CC CUM. INJ. TIME , AND INTERVALS (PV OR DAY) FOR WRITING TO OUTPUT FILES
*---- TINJ  CUMPR1  CUMHI1  WRHPV  WRPRF  RSTC
500  20  20  20  20  50
CC
CC FOR IMES=2 ,THE INI. TIME STEP,CONC. TOLERANCE,MAX.,MIN. courant numbers
*---- DT  DCLIM  CNMAX  CNMIN
0.05  0.003  0.2  0.01

```

References

- Anderson, G. A., Delshad, M., King, C. B., Mohammadi, H., Pope, G. A., "Optimization of Chemical Flooding in a Mixed-Wet Dolomite Reservoir," SPE 100082, paper presented at the 2006 SPE/DOE Symposium on Improved Oil Recovery held in Tulsa, Oklahoma, April 2006.
- Atkinson, H.: "Recovery of Petroleum from Oil Bearing Sands," U.S. Patent No. 1,651,311 (Nov. 29, 1927).
- Bhuyan, D.: "Development of an Alkaline/Surfactant/Polymer Compositional Reservoir Simulator," PhD Dissertation, The University of Texas at Austin 1989.
- Brownell, L.E. and Katz, D.L.: "Flow of Fluids Through Porous Media—Part II," Chem. Eng. Prog. (1947) 43, No. 11, 601.
- Christie, M. A., Mansfield, M., King, P. R., Barker, J. W., Culverwell, I. D., "A Renormalization Based Upscaling Technique for WAG Floods in Heterogeneous Reservoirs", SPE 29127, February 1995.
- Delshad, M., Delshad, M., Bhuyan, D., Pope, G. A., Lake, L. W., "Effect of Capillary Number on the Residual Saturation of Three-Phase Micellar Solution", SPE 14911, paper presented at the SPE/DOE 5th Symposium on Enhanced Oil Recovery held in Tulsa, Oklahoma, April 1986.
- Delshad, M., Pope, G.A., and Sepehrnoori, K., "A Compositional Simulator for Modeling Surfactant Enhanced Aquifer Remediation, 1. Formulation," J. of Contaminant Hydrology **23**, 303-327, November 1996.
- Durlofsky, L. A., "Upscaling of Geocellular Models for Reservoir Flow Simulation: A Review of Recent Progress", paper presented at 7th International Forum on Reservoir Simulation, Germany, June 23-27, 2003.
- Dwarakanath, V., Chaturvedi, T., Jackson, A.C., Malik, T., Siregar, A., and Zhao, P.: "Using Co-solvents to Provide Gradients and Improve Oil Recovery during Chemical Flooding in a Light Oil Reservoir," Paper SPE 113965 presented at the SPE Improved Oil Recovery Symposium, Tulsa, OK, April 2008.
- Garmeh, G., Johns, R. T., "Upscaling of Miscible Floods in Heterogeneous Reservoirs Considering Reservoir Mixing", SPE 124000, paper presented at the 2009 SPE Annual Technical Conference and Exhibition held in New Orleans, Louisiana, October 2009.

- Green, D. W., Willhite, G.P.: "Enhanced Oil Recovery", Society of Petroleum Engineers, Richardson, Texas, 1998.
- Healy, R. N., Reed, R. L., Stenmark, D.G., "Multiphase Microemulsion Systems", SPE 5565, paper presented at the SPE-AIME 50th Annual Fall Meeting held in Dallas, Texas, October 1975.
- Healy, R. N., Reed, R. L., "Physicochemical Aspects of Microemulsion Flooding", SPE 4583, paper presented at the SPE-AIME 48th Annual Fall Meeting held in Las Vegas, Nevada, October 1973.
- Hirasaki, G. J., van Domselaar, H.R., Nelson, R.C., "Evaluation of the Salinity Gradient Concept in Surfactant Flooding", SPEJ June, 486-500, June 1983.
- Huh, C.: "Interfacial Tension and Solubilizing Ability of a Microemulsion Phase That Coexists With Oil and Brine," J. Colloid Interface Sci., Volume 71, 1979, p. 408-428.
- Jackson, A.C.: "Experimental Study of the Benefits of Sodium Carbonate on Surfactants for Enhanced Oil Recovery", M.S Thesis, University of Texas at Austin, December 2006.
- Jakupstovu, S., Zhou, D., Kamath, J., Durlofsky, L.A., Stenby, E.H., "Upscaling of Miscible Displacement Processes", proceedings of the 6th Nordic Symposium on Petrophysics, Norway, May 2001.
- Jennings, H. Y. Jr.: "A Study of Caustic Solution-Crude Oil Interracial Tensions," SPEJ (June 1975) 197-202.
- Jin, M.: "A Study of Non-Aqueous Phase Liquid Characterization and Surfactant Remediation," PhD dissertation, The University of Texas, Austin, Texas (1995).
- Leung, J., Srinivasan, S., Huh, C., "Accounting for Heterogeneity in Scale-Up of Apparent Polymer Viscosity for Field Scale Application", paper presented at the 2010 SPE Improved Oil Recovery Symposium held in Tulsa, Oklahoma, April 2010.
- Levitt, D.B. et al. "Identification and Evaluation of High Performance EOR Surfactants," SPE 100089, presented at SPE IOR Symposium, Tulsa, OK, April 2006.
- Mohammadi, H.: "Mechanistic Modeling, Design, and Optimization of Alkaline/Surfactant/Polymer Flooding", PhD Dissertation, University of Texas at Austin, August 2008.
- Nelson, R.C., Lawson, Thigpen, and Stegemeier, G.L.: "Cosurfactant-Enhanced Alkaline Flooding", SPE/DOE 12672, April 1984.

- Nelson, R. C., Pope, G.A., "Phase Relationship in Chemical Flooding", SPE 6773, paper presented at the SPE- AIME 52nd Annual Fall Technical Conference and Exhibition held in Denver, October 1977.
- Pope, G A, Wu, W, Narayanaswamy, G, Delshad, M, Sharma, M M, Wang, P, "Modeling Relative Permeability Effects in Gas Condensate Reservoirs with a new Trapping Model". SPE Reservoir Eval. and Eng., 3(2), April 2000, p. 171-8.
- Rosen, Milton J, "Surfactants and Interfacial Phenomena", John Wiley & Sons Inc., Hoboken, N.J, Third Edition (2004)
- Salager, J.L., Bourrel, M., Schechter, R.S., and Wade, W.H.: "Mixing Rules for Optimum Phase-Behavior Formulations of Surfactant/Oil/Water Systems," SPEJ, October issue, 1979, p. 271-278.
- UTCHEM-9, Volume II: Technical Documentation for UTCHEM 9.0, "A Three-Dimensional Chemical Flooding Simulator," The University of Texas at Austin, Texas, 2000.
- Winsor, P.A.: "Solvent Properties of Amphiphilic Compounds," Butterworths, London, 1954.
- Wu, Wei-Jr, "Optimum Design of Field-Scale Chemical Flooding Using Reservoir Simulation", PhD Dissertation, University of Texas at Austin, Austin, Texas, 1996.
- Yuan, C., Delshad, M., and Wheeler, M.F., "Parallel Simulations of Commercial-Scale Polymer Floods," SPE 132441 prepared for the SPE Western Regional Meeting, Anaheim, CA, May 27-29, 2010.
- Zhang, D.L., Liu, S., Yan, W., Puerto, M. and Hirasaki, G.J.: "Favorable attributes of Alkali-Surfactant-Polymer Flooding", SPE 99744, paper presented in SPE Improved oil recovery Symposium Tulsa, OK, April 2006.

Vitae

Faiz Koyassan Veedu was born in Calicut, India on 21 August 1984 to Mr. Abdul Kader Maliyackel and Naseema K.V. After finishing his high school in 2002 from Al-farook high school, Calicut, India, he entered Bharati Vidyapeeth University, Pune. He earned a Bachelor Degree from there in the field of Chemical Engineering in June 2006. After his graduation, he worked as chemical engineer at Travancore Titanium Products Limited, Trivandrum, India for one year. In January 2008, he joined graduate school at The University of Texas at Austin in the field of petroleum engineering.

Permanent Address: 23/1633 B, Faaz

Thiruvannur Road, Panniyankara

Calicut, 673003

This thesis was typed by the author.